University of Alberta

Organometallic Chemistry of Methylene–Bridged Rh/Os and Ir/Ru Complexes

by

Steven James Trepanier Ⓒ

A thesis submitted to the Faculty of Graduate Studies and Research in partial fulfillment of the requirements for the degree of Doctor of Philosophy

Department of Chemistry

Edmonton, Alberta
Fall, 2002

University of Alberta

Release Form

Name of Author:	Steven James Trepanier
Title of Thesis:	Organometallic Chemistry of Methylene-Bridged Rh/Os and Ir/Ru Complexes
Degree:	Doctor of Philosophy
Year this Degree Granted:	2002

Permission is hereby granted to the University of Alberta Library to reproduce single copies of this thesis and to lend or sell such copies for private, scholarly or scientific research purposes only.

The author reserves all other publication rights, and neither the thesis nor extensive extracts from it may be printed or otherwise reproduced without the author's prior written permission.

Steven Trepanier

Steven James Trepanier
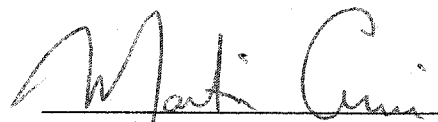
R.R. #2, Maidstone
Ontario, Canada
N0R 1K0

Date _Sept 30_ 2002

University of Alberta
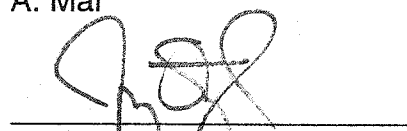
Faculty of Graduate Studies and Research

The undersigned certify that they have read, and recommend to the Faculty of Graduate Studies and Research for acceptance, a thesis entitled **Organometallic Chemistry of Rh/Os and Ir/Ru Methylene-bridged Complexes** submitted by Steven James Trepanier in partial fulfillment of the requirements for the degree of Doctor of Philosophy.

_____

M. Cowie (Supervisor)

_____

R. B. Jordan

_____

A. Mar

_____

J. M. Stryker

_____

P. Y. K. Choi

_____

D. M. Heinekey

Date: Sept. 16/2002

Abstract

The binuclear complex $[RhOs(CO)_4(dppm)_2][BF_4]$ (1) (dppm = $Ph_2PCH_2PPh_2$) reacts with diazomethane to give three products depending on temperature. At -80°C the methylene-bridged product $[RhOs(CO)_3(\mu\text{-}CH_2)(\mu\text{-}CO)(dppm)_2][BF_4]$ (2) is obtained. Warming this complex to -40°C in the presence of diazomethane yields the butanediyl species $[RhOs(C_4H_8)(CO)_3(dppm)_2][BF_4]$ (3). If either 1 or 2 is treated with diazomethane at ambient temperature, the sole product obtained is $[RhOs(CH_2CH=CH_2)(CH_3)(CO)_3(dppm)_2][BF_4]$ (4) in which the allyl group is bound to Rh and the methyl group is bound to Os. Attempts to model the above processes by reaction of a number of substrates with 2 support our assumption of substrate coordination at Rh and insertion into the $Rh\text{-}CH_2$ bond.

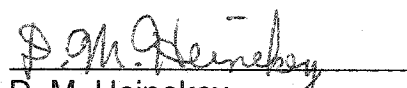The heterobinuclear complexes $[IrRu(CO)_3(\mu\text{-}H)(dppm)_2]$ and $[IrRuH(CO)_3(\mu\text{-}CO)(dppm)_2]$ are prepared from the reactions of $[PPN][HRu(CO)_4]$ with $[IrCl(dppm)_2]$ and $[Ir(CO)(dppm)_2][Cl]$, respectively (PPN = $(Ph_3P)_2N$; dppm = $Ph_2PCH_2PPh_2$). Protonation of each monohydride species yields $[IrRu(CO)_3(\mu\text{-}H)_2(dppm)_2][BF_4]$, which under an atmosphere of carbon monoxide gives $[IrRu(CO)_4(dppm)_2][BF_4]$ (5). The complex $[IrRu(CO)_3(\mu\text{-}CH_2)\text{-}(\mu\text{-}CO)(dppm)_2][BF_4]$ (6) is obtained by the reaction of compound $[IrRu(CO)_4(dppm)_2][BF_4]$ with diazomethane. Although $[IrRu(CO)_3(\mu\text{-}CH_2)(\mu\text{-}CO)(dppm)_2][BF_4]$ does not react further with diazomethane under these

conditions, carbonyl abstraction using trimethylamine oxide in the presence of CH_2N_2 yields the methylene-bridged, ethylene adduct, $[IrRu(C_2H_4)(CO)_3(\mu\text{-}CH_2)\text{-}(dppm)_2][BF_4]$ (7). The compounds $[IrRuL(CO)_3(\mu\text{-}CH_2)(dppm)_2][BF_4]$ (L = NCMe, PMe_3, CH_2CHCN) can also be prepared from 6 in the presence of Me_3NO or by ethylene displacement from 7.

Protonation of $[RhOs(CO)_3(\mu\text{-}CH_2)(\mu\text{-}CO)(dppm)_2][CF_3SO_3]$ (2) with triflic acid at -80°C yields the methyl complex $[RhOs(CO)_4(\mu\text{-}CH_3)(dppm)_2]\text{-}[CF_3SO_3]_2$ in which the methyl group is primarily bound to Os while involved in an agostic interaction with Rh. Warming this species to -20°C results in methyl migration to a terminal site on Rh yielding $[RhOs(CH_3)(CO)_2(\mu\text{-}CO)_2(dppm)_2]\text{-}[CF_3SO_3]_2$ and subsequent warming to ambient temperature results in migratory insertion to yield the acetyl-bridged $[RhOs(CF_3SO_3)(CO)_2(\mu\text{-}C(CH_3)O)(\mu\text{-}CO)(dppm)_2][CF_3SO_3]$. The coordinated triflate anion can be replaced at low temperature by CO and PMe_3 to give $[RhOs(L)(CO)_2(\mu\text{-}C(CH_3)O)(\mu\text{-}CO)(dppm)_2][CF_3SO_3]_2$ (L = CO, PMe_3). Spectroscopic and structural evidence suggests an oxycarbene formulation for the acetyl group. Warming the PMe_3 adduct results in isomerization involving the acetyl bridging group, which is C-bound to Rh, to a group which is C-bound to Os. Similar acetyl complexes have been obtained with the analogous Ir/Ru system.

Acknowledgments

I would like to thank my supervisor, Dr. Marty Cowie, for his assistance and support throughout the production of this thesis. I also thank all the other Cowie group members who have helped out with things in the lab. Dr. Bob McDonald and Dr. Mike Ferguson are thanked for their friendship and for conducting the X-ray crystallography studies. The NMR staff, particularly Glen and Gerdy, are recognized for performing many laborious NMR experiments. I would also like to acknowledge everyone from Spectral Services, Elemental Analysis, the Machine Shop, the Electronics Shop, the General Office and the Store Room for their assistance.

Finally, I would like to thank my family and friends for all their support during my graduate existence.

Table of Contents

List of Tables

Appendix 1

List of Figures

List of Schemes

Chapter 1

Chapter 2

Chapter 3

Chapter 4

Appendix 1

List of Abbreviations and Symbols

anal.	analysis
approx.	approximately
ca.	circa (approximately)
calcd	calculated
dppm	bis(diphenylphosphino)methane
equiv	equivalent
Et	ethyl
h	hour
IR	infrared
Me	methyl
MeOH	methanol
mg	milligram
min	minute
mL	millilitres
mmol	millimoles
MHz	megahertz
MS	mass spectrometry
NMR	nuclear magnetic resonance
Ph	phenyl
THF	tetrahydrofuran
μL	microlitres

Chapter 1

Introduction

The formation of carbon-carbon bonds is probably the most important transformation in synthetic chemistry, being necessary for the conversion of simple organic molecules into larger, more complex ones. Examples of such transformations that are industrially important include hydroformylation, methanol carbonylation, olefin polymerization and the Fischer-Tropsch reaction.[1] Although the first three of these processes have demonstrated spectacular successes of well-defined homogeneous metal catalysts,[1c] the majority of industrial catalysts are heterogeneous, in which the catalyst involves either a metal surface or metals absorbed on a solid support,[2] and the chemical substrates (usually gases or liquids) are passed over the catalyst at elevated temperatures and pressures. This method is highly effective from a practical standpoint since the newly synthesized products can be easily separated from the solid catalyst. However, the harsh conditions employed and the catalyst itself, which can have a number of different types of active sites, usually give rise to a range of products, including some which are undesirable. The lack of knowledge about the structure of the active sites of the catalyst makes it difficult to obtain a thorough chemical understanding of the processes occurring on the catalyst surface; therefore, few heterogeneously-catalyzed reactions are fully understood.[3] Without a better understanding of the process of interest it is not possible to rationally modify the catalyst performance to optimize product yields and distributions. Instead, the approach to catalyst modification is empirical, in which systematic changes in the reaction conditions are correlated with the resultant product distributions.

One means of gaining insight into heterogeneously-catalyzed reactions involves the use of well-behaved, soluble metal complexes that can mimic the transformations occurring on the catalyst surface.[4] These complexes can then be

carefully studied by a variety of spectroscopic techniques under homogeneous conditions to obtain detailed information about the catalyst system. While there will certainly be differences in the behaviour of soluble metal complexes and heterogeneous metal catalysts in a given transformation, the elementary chemical steps should be similar. Well-behaved metal complexes also have the advantage of being capable of essentially infinite modification so that they can be systematically altered either by modifying the ligand environment or by changing the metals. The effects of these modifications can be examined with respect to the activity and selectivity of the reaction. There are many examples of such modifications leading to significant changes in homogeneous transition-metal-catalyzed reactions.[5] For example, the use of $Co_2(CO)_8$ as an olefin hydroformylation catalyst yields a mixture of linear and branched aldehydes, whereas the addition of bulky phosphines to the catalyst, under comparable conditions, gives primarily straight-chain alcohols.[6] Also, the use of rhodium instead of cobalt in these hydroformylation catalysts results in higher activity and thus the reactions can be performed at lower temperatures and pressures.[7]

The simplest mononuclear complexes, containing only a single metal centre, while most easily understood, are not ideal models for surface reactivity since they are unable to mimic the effects of adjacent metal centres. Aggregates of metal atoms, or clusters, in which there are a number of metals in close proximity can be more representative of a metal surface.[4,8] The presence of two or more adjacent metals allows new types of binding modes and reactivities of substrate molecules due to the availability of multisite interactions, and also allows for metal-metal interactions. The bridging mode of a substrate or ligand, which is unavailable in mononuclear chemistry, can facilitate the activation of various substrates. For example, activation of the CO bond by metal clusters appears to be facilitated by coordination of each end of the CO to a different metal, similar to that which is presumed to occur on catalyst surfaces.[9] Other key hydrocarbyl fragments such as the carbide, methyne, and methylene groups have also been

isolated in metal clusters,[10] whereas they are less frequently observed in mononuclear complexes.

The presence of adjacent metals also allows for the migration of hydride, alkyl, and CO groups between metals, which is a common surface characteristic.[11] When two different metals are being used in heterogeneous systems this migration is known as the "spillover effect".[12] An adjacent metal can therefore act as a source of molecular fragments needed in the catalytic cycle. Thus a ligand is able to bind to one of the metals under one set of conditions and then be transferred to the other metal under modified conditions. For example, in a heterogeneous bimetallic Cu-Ru system, activation of dihydrogen occurs first at ruthenium followed by hydride transfer to copper at elevated temperatures. In this system, copper addition results in an increased selectivity for CH_4 formation during CO hydrogenation.[13]

The presence of a coordinatively unsaturated metal can also affect the reactivity of a bimetallic system by providing a site for ligands to associate. Unsaturation is a key element of the high reactivity of such mononuclear compounds as Vaska's complex ($[IrCl(CO)(PPh_3)_2]$) and Wilkinson's catalyst ($[RhCl(PPh_3)_3]$). In the bimetallic complex $[RhRe(CO)_4(dppm)_2]$ (dppm = $Ph_2PCH_2PPh_2$), in which there is coordinative unsaturation at rhodium, reaction with H_2 occurs at -80 °C.[14] By comparison, the dirhenium analog $[Re_2(CO)_6(dppm)_2]$, containing two saturated metal centres, only reacts with H_2 at 172 °C;[15] in this latter case, reaction occurs only after elimination of a carbonyl ligand.

Although larger clusters more closely resemble heterogeneous metal surfaces and would therefore serve as better models than smaller analogues, experimentally, their study can suffer from solubility problems and increased difficulty in characterizing the complexes due to the large number of ligands associated with the complex. A simple binuclear complex, containing two metals, can be used as a minimal, yet effective model for adjacent metal involvement in

catalyst surface reactions. Although such over-simplified models vary significantly in most respects from an actual catalyst surface, they do allow us to obtain a better understanding of how adjacent metals interact with and transform substrate molecules.

Sabatier and Senderens first produced methane by reacting hydrogen and carbon monoxide over a nickel catalyst in 1902.[16] Fischer and Tropsch reported the synthesis of various hydrocarbons using iron and cobalt catalysts in 1923,[17] and today the term Fischer-Tropsch (FT) synthesis is used to describe the catalytic hydrogenation of carbon monoxide to form higher hydrocarbons or oxygenates. The Fischer-Tropsch (FT) reaction, shown in a simplified (unbalanced) form in equation (1), is a fascinating and important reaction in which synthesis gas, also referred to as syn-gas, ($CO + H_2$) is converted into a variety of products including linear alkanes, α-olefins, and oxygen-containing products such as ethanol. In this reaction the carbon monoxide is converted into hydrocarbons by C-C bond

$$CO + H_2 \implies C_nH_{2n+2} + C_mH_{2m} + \text{oxygenates} + H_2O \qquad (1)$$
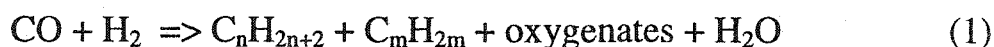
formation. This reaction was first used industrially in Germany during the Second World War for the conversion of coal into diesel fuel. Syn-gas can be prepared from a variety of fossil fuels and is thus important to countries with little oil but plenty of cheap coal or natural gas. The FT synthesis is also of use in tapping "stranded" natural gas reserves, where the gas is located in a remote location. Gas-to-liquid conversion via the FT reaction allows the resulting liquid hydrocarbons to be more readily and more economically shipped.[18]

Although currently only the government-backed SASOL (South African Synthetic Oil Limited) of South Africa, and Shell, which has recently brought on-stream a plant in Malaysia, are involved in industrial-scale FT synthesis,

companies such as Exxon, Syntroleum, and Rentech are now involved in FT chemistry either through research, pilot plants or planned large-scale plants.[19]

Although fuel produced by the FT process cannot currently compete economically with that derived from conventional oil reserves, it is viable when these reserves are not readily available, and will certainly become competitive as oil reserves become depleted.[20] Fuels derived from the FT process also benefit from the absence of harmful impurities such as aromatics and sulfur-containing compounds.

The applicability of the Fischer-Tropsch reaction is diverse. Its usefulness lies in the fact that the products of the FT reaction are dependent upon the reaction conditions and the catalyst employed. Iron-based catalysts yield mainly linear alkenes and oxygenates while cobalt produces mostly linear alkanes. Ruthenium catalysts give high molecular-weight hydrocarbons while rhodium yields oxygenates and hydrocarbons.[21] Given the ability of all Group 8 and 9 metals to function as FT catalysts, and the differing product distributions obtained with each metal, a logical extension of the studies of monometallic catalysts is to investigate *combinations* of these metals as catalysts. It is of interest to determine how combinations of metals influence catalytic activity and product distribution. It is well-known that incorporating a different metal into a metal catalyst composed of only one type of metal can lead to new reactivities.[22] This cooperativity can result from the different properties of the two metals. Indeed, increased selectivities have been observed with some of the bimetallic catalysts investigated. For example, the combination of ruthenium and cobalt gives an FT catalyst with an increased turnover rate and selectivity for C_5 and higher products with respect to those of the monometallic catalysts.[23] Cobalt-ruthenium catalysts also demonstrate enhanced ethylene hydroformylation activity,[24] and a rhodium-ruthenium catalyst has been developed which has a higher selectivity, compared to the respective monometallic catalyst systems, for the production of ethylene glycol from syngas.[25] Although there have been successful investigations into the

usefulness of bimetallic **FT** catalysts, there continues to be little understanding of the roles of the different metals.

The generally accepted initial mechanism of the **FT** reaction is show below (Scheme 1.1). Carbon monoxide is adsorbed by the catalyst where it is dissociated into surface-bound carbide and oxide units. The resulting carbide moiety then reacts with surface hydrides (derived from H_2) to subsequently form methyne, methylene, and methyl groups. It is important to note that all of these hydrocarbyl groups have been observed in organometallic complexes, demonstrating the similarity between the chemistry which occurs in homo and heterogeneous systems.
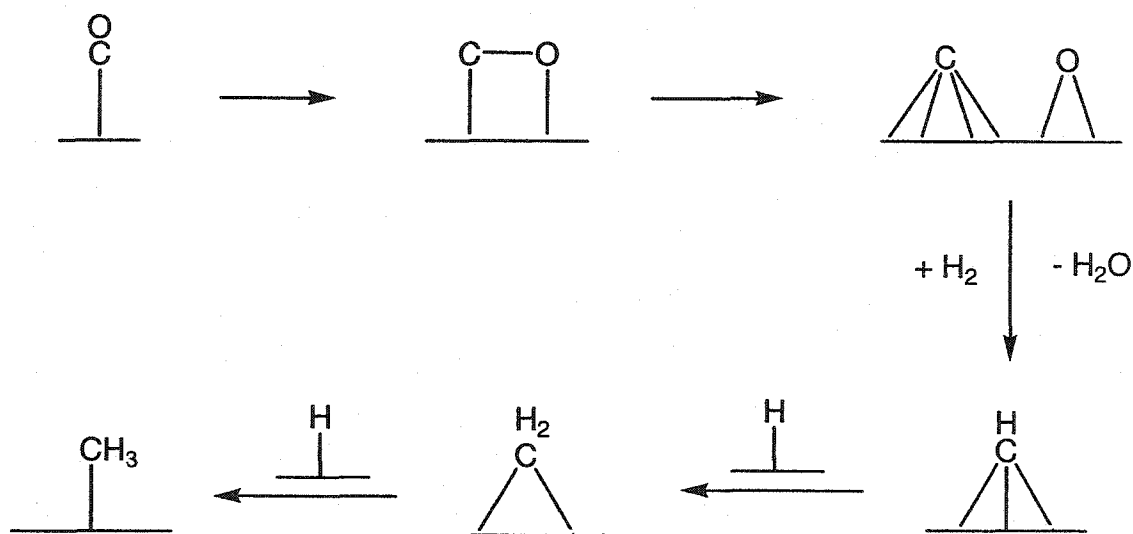
Scheme 1.1. A simplified diagram for the conversion of syn gas into hydrocarbyl groups. The metal surface is designated by a horizontal line.

There are various theories on how these groups associate to form the observed organic products. The earliest mechanism, proposed by Fischer and

Tropsch, suggested that carbon-carbon bonds are formed via polymerization of methylene groups on the metal surface.[26] This simple, stepwise coupling of methylene groups was disproved by Brady and Pettit who showed, using diazomethane over the catalyst metals, that only ethylene was produced.[27] However, if the same reaction was carried out in the presence of H_2, the normal distribution of **FT** products resulted. The need for H_2 in addition to the methylene groups led to the idea that conversion of methylene groups into methyl groups occurred and that C-C bond formation occurred by sequential alkyl migration to bridging methylene groups yielding ethyl, propyl, butyl, etc. fragments (see Scheme 1.2). The resulting alkyl group can then be released by coupling with an adjacent hydride group to form linear hydrocarbons or undergo β-hydride elimination yielding α-olefins.
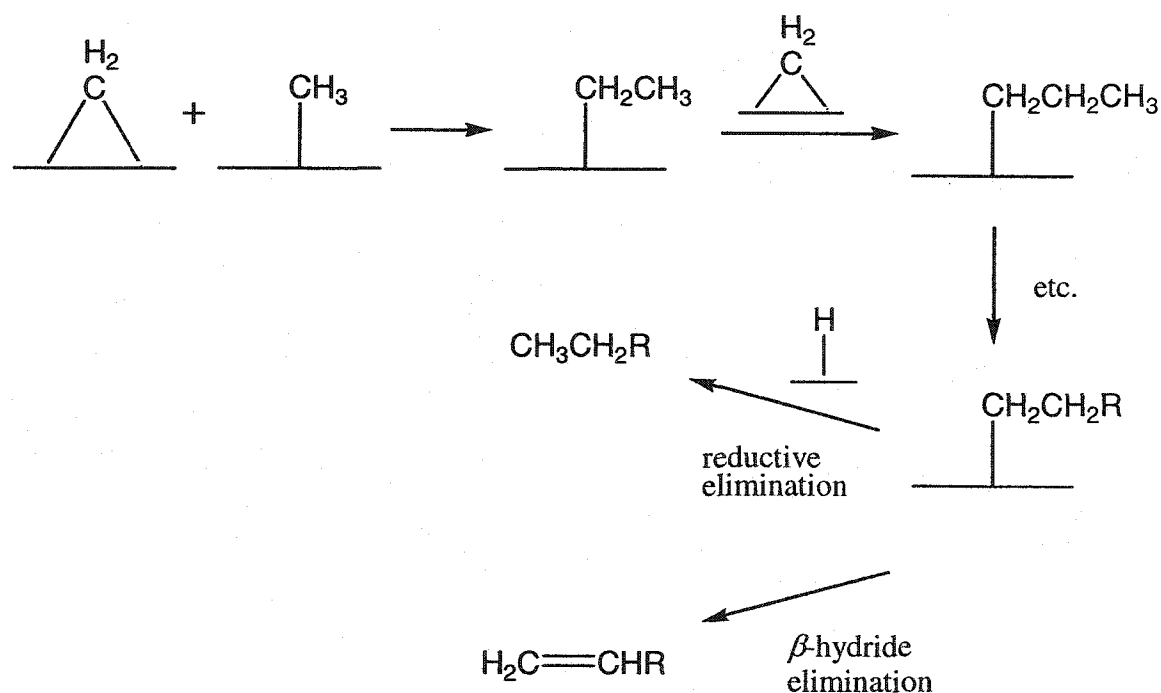
Scheme 1.2. The Brady-Pettit mechanism for chain growth and formation of linear alkanes and α–olefins in the **FT** reaction.

Although the Brady-Pettit mechanism still finds widespread acceptance, it fails to offer satisfactory explanations for several observations which may limit the general scope of this mechanism. First, there is an unusually low amount of C_2 hydrocarbons produced in the FT reaction, suggesting a mechanistic difference between C_2 fragment formation and the formation of subsequent C_n fragments. In addition, small but significant amounts of branched hydrocarbons are produced which can not be accommodated by this mechanism. Although the reductive elimination step, forming alkanes, is a reasonable termination step, α-olefins are known to be the primary products, which subsequently are hydrogenated to alkanes by the hydrogen present. Formation of α-olefins by this mechanism would result from β-hydride elimination, however there should be a low tendency for the alkyl chain to eliminate a hydride group on a surface already covered with hydride fragments.

On the basis of studies on model methylene-bridged Rh_2 complexes, Maitlis proposed the involvement of vinyl or alkenyl groups in carbon chain growth in FT reactions.[28] In this "alkenyl" mechanism, shown in Scheme 1.3, it is proposed that methylene and methyne groups couple to form a surface vinyl group, which subsequently couples with an adjacent methylene group to form an allyl fragment. Isomerization of the allyl group by a 1,3 hydrogen shift generates a substituted vinyl group which can lead to long-chain hydrocarbons by subsequent insertion and isomerization steps. It is noted that this mechanism differentiates the formation of C_2 products from subsequent steps which involve vinyl/methylene coupling. This mechanism is also supported by the fact that a vinyl/methylene coupling is more kinetically favoured than an alkyl/methylene coupling[29] and has been supported by the use of labelled vinyl probes under FT conditions over a variety of heterogeneous catalysts.

As a demonstration of the use of binuclear complexes as models for the heterogeneous FT reaction, we draw attention to the work of Maitlis in which he
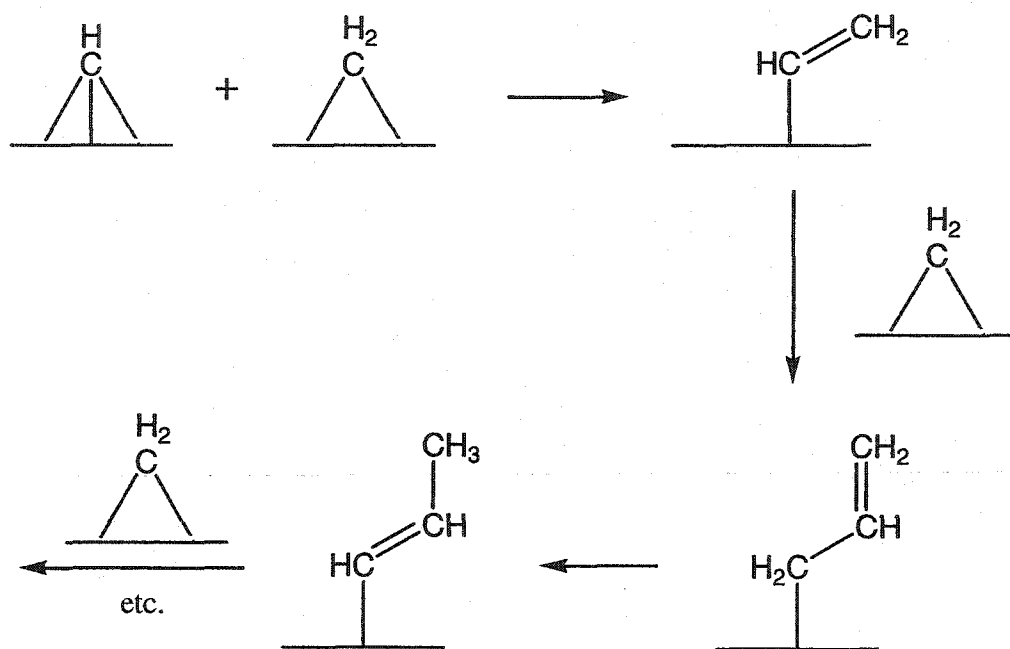
Scheme 1.3. Maitlis' "alkenyl" mechanism for initiation and chain growth in the **FT** reaction.

used the dirhodium complex $[Cp^*RhCH_3(\mu\text{-}CH_2)]_2$ (**1**) as a model of a surface containing adjacent methylene and methyl groups. Upon heating, complex **1** yields propene and methane (see Scheme 1.4).[28] Although this complex appears to be well-suited as a model for the Pettit mechanism, labeling studies of this reaction indicate that the C_3 product does not result simply from the coupling of methylene and methyl groups, followed by a β-elimination step. Instead, Maitlis has proposed a mechanism involving: (a) formation of a bridging methyne; (b) coupling of a methyl group with the methyne; (c) β-elimination from this group to form a vinyl-hydride; and (d) and coupling of the vinyl group with the remaining $\mu\text{-}CH_2$ to give an allyl moiety which then eliminates with the hydride to yield propene.

(1)
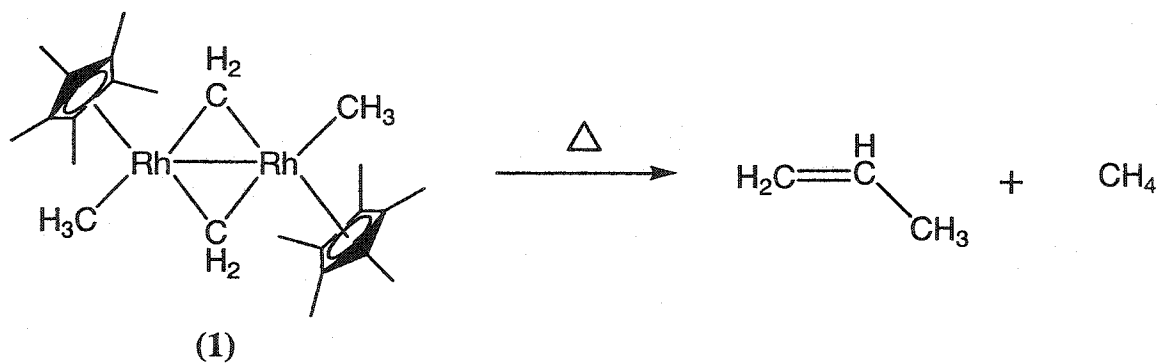
Scheme 1.4. Formation of propene and methane from Maitlis' dirhodium complex **(1)**.

To support his "alkenyl" mechanism, Maitlis has synthesized a divinyl-di-μ-methylene complex [Cp*Rh(CH=CH$_2$)(μ-CH$_2$)]$_2$ **(2)**. Oxidation of **2**, yields the allylic cation **3**, shown in Scheme 1.5, demonstrating the facile coupling of the vinyl and methylene groups.

(2)   **(3)**
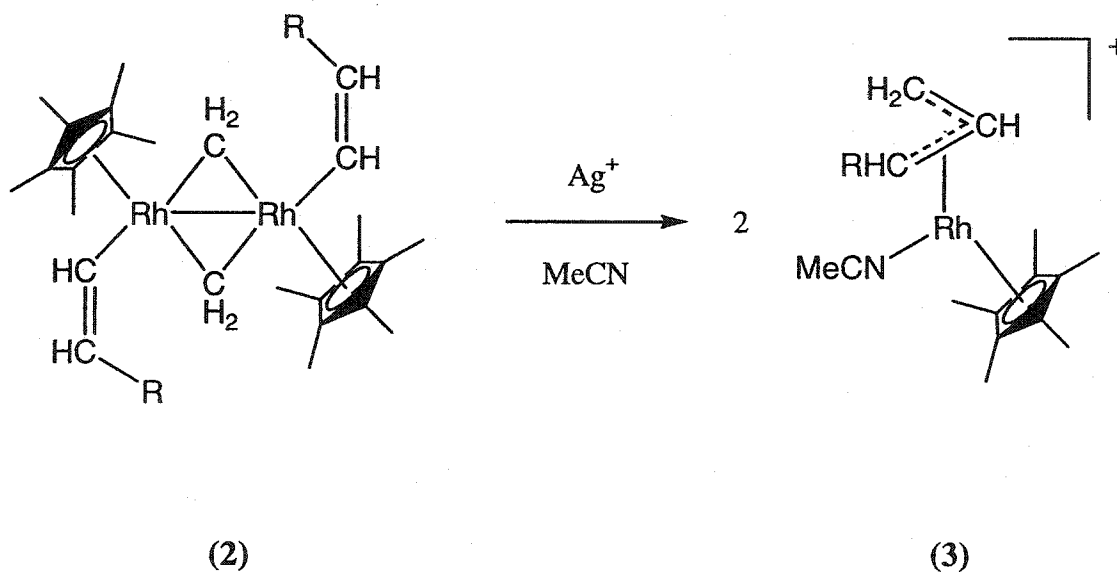
Scheme 1.5. Coupling of vinyl and methylene groups to yield an allyl complex. Oxidation of **2** in acetonitrile yields the allylic complex **3**.

Only a few other bimetallic systems have been investigated with the goal of mimicing **FT** reaction steps. Pettit has synthesized a methylene-bridged diiron complex $[Fe_2(CO)_8(\mu\text{-}CH_2)]$ (**4**) from the reaction of $[Fe_2(CO)_8]^{2-}$ with CH_2I_2.[30] When a benzene solution of **4** is heated to 55 °C under 400 psi of ethylene, propylene (>90 %) and $(C_2H_4)Fe(CO)_4$ are produced, as shown in Scheme 1.6.

(4)
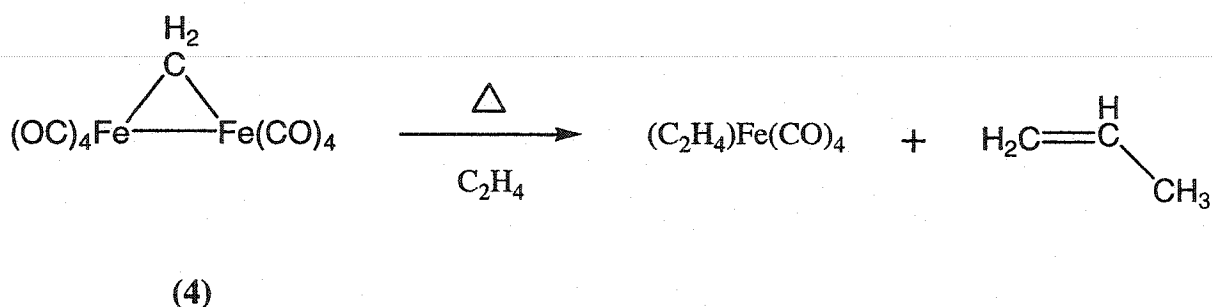
Scheme 1.6. Formation of propene from the thermolysis of the methylene-bridged diiron complex (**4**) in the presence of ethylene.

Pettit proposed the following mechanism to rationalize the observed C-C bond formation: (a) loss of a CO ligand and coordination of ethylene; (b) insertion of the olefin into an Fe-CH$_2$ bond; and (c) β-hydride elimination to form an allyl-hydride complex which then reductively eliminates to form propene. However, none of these intermediates were observed.

Knox has conducted more extensive investigations of carbon-carbon bond formation on diruthenium systems.[31] The compound $[Cp_2Ru_2(C_2H_4)(CO)(\mu\text{-}CO)(\mu\text{-}CH_2)]$ (**5**) was generated by passing ethylene through a solution of $[Cp_2Ru_2(CO)(CH_3CN)(\mu\text{-}CH_2)(\mu\text{-}CO)]$ as shown in Scheme 1.7. Heating **5** at 250 °C for three hours again yielded propene (29 %) together with several other organic products.

Another attempt to induce methylene-ethylene coupling involved the reaction of **5** with the oxidant AgBF$_4$. Instead of a carbon-carbon bond forming reaction, the complex [Cp$_2$Ru$_2$(CO)$_2$(μ-C$_2$H$_3$)(μ-CO)]$^+$ (**6**), containing a μ-vinyl ligand, was generated. Knox suggests that olefin C-H activation may be a way of generating the vinyl groups which are important **FT** species in Maitlis' alkenyl mechanism for hydrocarbon formation.
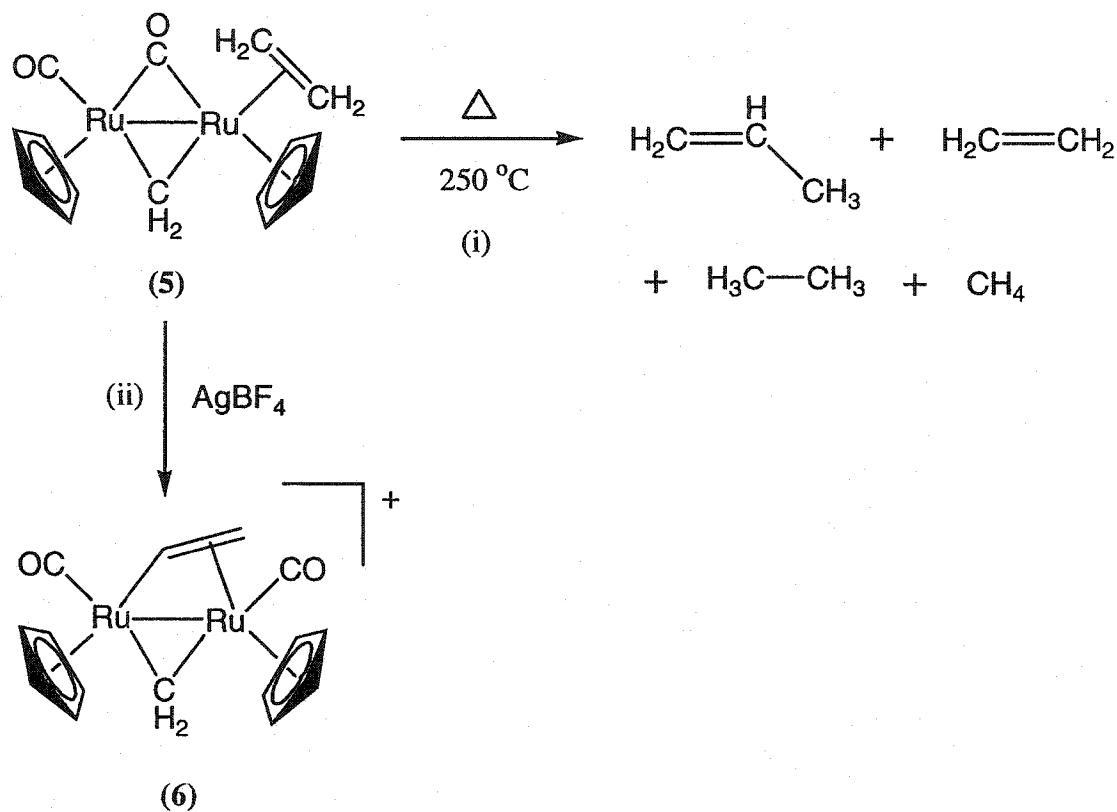
Scheme 1.7. (i) Thermolysis of **5** yields several organic products, including propene. (ii) Oxidation of **5** leads to C-H activation of the ethylene group yielding **6** which contains a μ-vinyl group.

In addition to olefins and alkanes, oxygenates such as alcohols and aldehydes are often obtained in the FT reaction; the selective formation of ethanol and ethylene glycol is of particular current interest. Very little has been done in modeling the synthesis of oxygenates in FT chemistry; hence, little is known about the processes involved in their formation. However, the incorporation of oxygen in these products indicates that their formation must proceed by a different mechanism than that of the alkanes or olefins. One obvious proposal for the production of oxygenates is based upon the carbonyl migratory insertion reaction which is frequently observed in organometallic chemistry. This mechanism for FT oxygenate formation was first proposed by Pichler and Schultz in 1970 [32] and has subsequently undergone variations by later workers in this area.[33] After alkyl migration to a metal-bound carbonyl, the acyl-CO can then reductively eliminate with a metal-bound hydride group to form an aldehyde or be reduced by hydrogen to form a hydroxymethyl moiety. Elimination of the latter hydroxymethyl group with a surface hydride results in alcohol formation. Both routes are shown in Scheme 1.8. Several complexes, with FT-active metals, and containing acyl groups have been synthesized and reduced. In the compound $CpFe(CH_3CO)(CO)_2$, the acyl group can be selectively reduced by hydrosilanes to yield either a siloxyalkyl or an alkyl group.[34] In a bimetallic Rh_2 example, the compound $[Rh_2(CH_3CO)(CO)_3(dppm)_2][CF_3SO_3]$ reacts with H_2 to produce acetaldehyde.[35]

In this thesis, a series of heterobinuclear complexes containing one Group 8 and one Group 9 metal will be used to model aspects of bimetallic FT catalysts. In order to assure that the metals remain together during the chemistry of interest, and are therefore able to display cooperative effects that we assume might be significant in subsequent chemistry, we have used the diphosphine ligand bis(diphenylphosphino)methane (dppm) (Figure 1.1) to hold the metals in close proximity. The strong metal-phosphorus bonds of these late-metal complexes
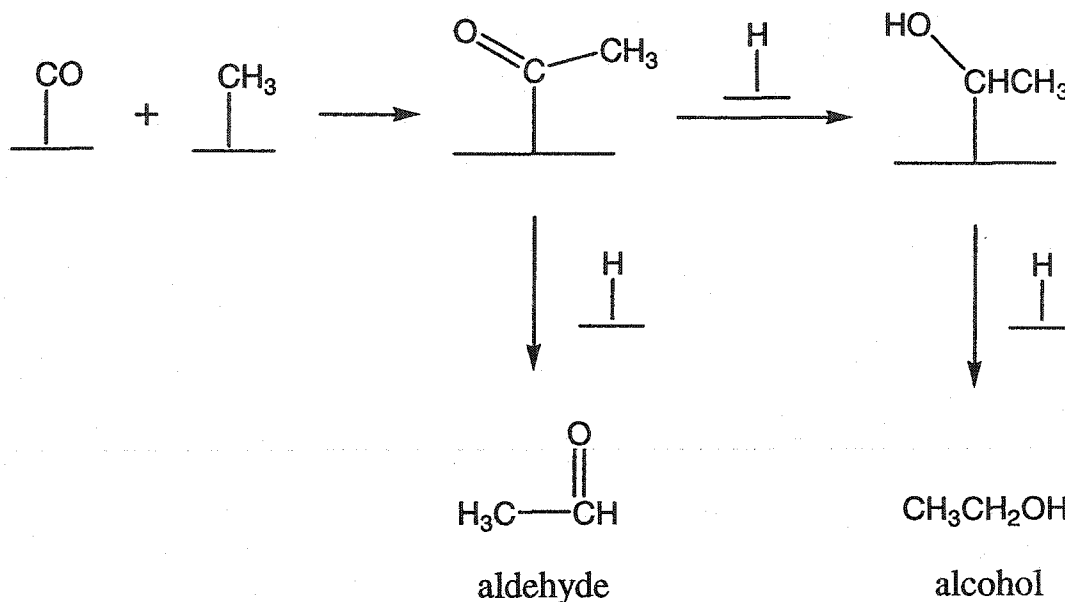
Scheme 1.8. The Pichler and Schultz mechanism for oxygenate formation in the **FT** synthesis.

create a stable framework for the study of reactions with various organic substrates. In addition, the presence of NMR active ^{1}H and ^{31}P nuclei in this ligand, as well as the ^{1}H and ^{13}C nuclei in the other ligands of the complexes, are of immense importance to the spectroscopic characterization of these complexes.

$$P \diagdown P \quad = \quad Ph_2PCH_2PPh_2$$

$$M \quad = \quad Rh, Ir$$

$$M' \quad = \quad Ru, Os$$
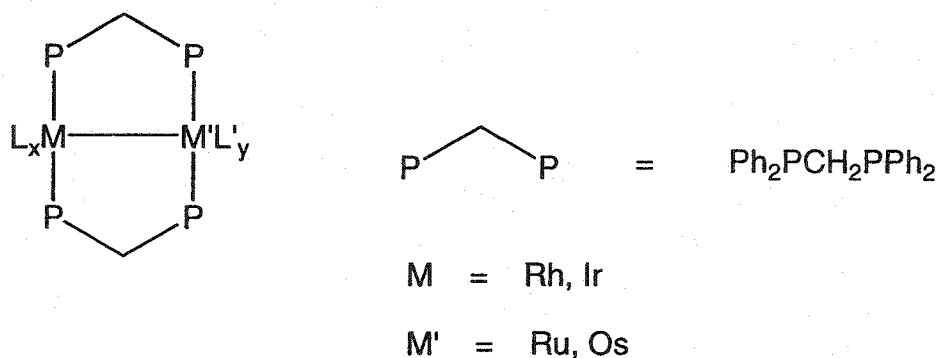
Figure 1.1. The basic dppm-bridged framework of the bimetallic complexes studied in this thesis.

The ligands L and L' are groups such as hydride, carbonyl or hydrocarbyl moieties, which are relevant in Fischer-Tropsch chemistry. Group 8 and 9 metal combinations (Rh/Os, Ir/Ru) are investigated since they have demonstrated high FT activity in a variety of catalytic systems. Our investigations into this chemistry began with the Rh/Os combination of metals since our research group already had extensive experience with these complexes, and the preparations of the precursor compounds were well-established.[36] The basic route to the formation of Rh/Os complexes containing the framework shown in Figure 1.1 involves the reaction of $[HOs(CO)_4]^-$ with $[RhCl(dppm)_2]$. Displacement of the chloride ligand, facilitated by the anionic osmium complex, is followed by unwinding of the chelating rhodium-bound dppm ligands which then occupy positions bridging both metals. Although the analogous Ir/Ru complexes had not been reported at the time this work was initiated, we anticipated that they should be accessible using a similar strategy, and a portion of this thesis involves studies of this combination of metals.

It is generally accepted that the methylene group (CH_2) is of fundamental importance in FT chemistry. Our goal in this thesis is to synthesize bimetallic group 8/9 metal complexes containing bridging methylene groups and examine their reactivity with a variety of organic substrates which may have relevance in the Fischer-Tropsch reaction. This may lead to a better understanding of the types of carbon-carbon bond forming reactions which can occur on metal surfaces and the roles of the different metals in the transformations.

References and Notes

1. (a) Collman, J. P.; Hegedus, L.S.; Norton, J.R.; Finke, R.G. *Principles and Applications of Organotransition Metal Chemistry* University Science Books: Mill Valley California, **1987**, pp. 523-660. (b) Huheey, J. E.; Keiter, E. A.; Keiter, R. L. *Inorganic Chemistry – Principles of Structure and Reactivity 4th*

Ed. HarperCollins College Publishers: New York, **1993**. pp. 705-723. (c)

Parshall, G. W.; Ittel, S. D. *Homogeneous Catalysis* John Wiley & Sons Inc.:

New York, **1992**. pp.10-47, 96-99.

2. Bond, G. C. *Heterogeneous Catalysis* Clarendon: Oxford, **1987**.

3. (a) Niemantsverdriet, J. W. *Catalysis*; Moulijin, J. A.; van Leeuwen, P. W.;

Santen, R. A., eds.; Elsevier: Netherlands, **1993**, Chapter 10. (b) Campbell,

I.M. *Catalysis at Surfaces* Chapman and Hall: New York, **1988**, Chapter 4.

4. Muetterties, E. L. *Pure Appl. Chem.* **1982**, *25*, 57.

5. Shrauzer, G. N. ed. *Transition Metals in Homogeneous Catalysis* Dekker:

New York, **1971**.

6. Evans, D.; Osborn, J. A.; and Wilkinson, G. *J. Chem. Soc. (A)* **1968**, 3133.

7. *Chem. Eng. News* **1988**, *66*, 27.

8. (a) Muetterties, E. L. *Science* **1977**, *196*, 839. (b) Muetterties, E. L. *Chem.

Soc. Rev.* **1982**, *11*, 283.

9. Herrmann, W. A. *Angew. Chem., Int. Ed. Engl.* **1982**, *21*, 117.

10. (a) Tachikawa, M.; Muetterties, E. L. *J. Am. Chem. Soc.* **1980**, *102*, 4541.

(b) Beno, M. A.; Williams, J. M.; Tachikawa, M.; Muetterties, E. L. *J. Am.

Chem. Soc.* **1980**, *102*, 4542. (c) Davies, D. L.; Gracey, B. P.; Guerchais, V.;

Knox, S. A.; Orpen, A. G. *J. Chem. Soc. Chem. Commun.* **1984**, 841. (d)

Dutta, T. K.; Vites, J. C.; Jacobsen, G. B.; Fehlner, T. P. *Organometallics*

1987, *6*, 842. (e) Calvert, R. B.; Shapley, J. R. *J. Am. Chem. Soc.* **1978**, *100*,

7726.

11. Gates, B. C.; Guczi, L. and Knoezinger, H. eds. *Metal Clusters in Catalysis* Elsevier: Amsterdam, **1986**.

12. (a) van't Blik, H. F. J.; Koningsberger, D. C.; Prins, R. *J. Catal.* **1986**, *97*, 210. (b) Hurst, N. W.; Gentry, S. J.; Jones, A.; McNicol, B. D. *Catal. Rev. Sci. Eng.* **1982**, *24*, 233.

13. Bond, G. C.; Yide, X. *J. Mol. Catal.* **1984**, *25*, 141.

14. Antonelli, D. M.; Cowie, M. *Organometallics* **1990**, *29*, 4039.

15. Lee, K. W.; Brown, T. L. *Organometallics* **1985**, *4*, 1025.

16. Sabatier, P.; Senderens, J. B. *Hebd. Seances Acad. Sci.* **1902**, *134*, 514.

17. Fischer, F.; Tropsch, H. *Brennst. Chem.* **1923**, *4*, 276.

18. Schulz, H. *Appl. Cat. A* **1999**, *186*, 3.

19. Overett, M. J.; Hill, O.; Moss, J. R. *Coord. Chem. Rev.* **2000**, *206*, 581.

20. *Chem. & Eng. News* **1998**, March 23, 18.

21. Vannice, M. A. *J. Catal.* **1975**, *37*, 449.

22. Sinfelt, J. H. *Bimetallic Catalysts* **1983**, John Wiley & Sons, New York, NY.

23. Iglesia, E.; Soled, S. L.; Fiato, R.; Via, G. H. *J. Catal.* **1993**, *143*, 345.

24. Huang, L.; Xu, Y. *Catalysis Letters* **2000**, *69*, 145.

25. Dombek, B. D. *Organometallics* **1985**, *4*, 1707.

26. Fischer, F.; Tropsch, H. *Brennst. Chem.* **1926**, *7*, 97.

27. Brady, R. C.; Pettit, R. *J. Am. Chem. Soc.* **1981**, *103*, 1287.

28. Maitlis, P. M.; Long, H. C.; Quyoum, R.; Turner, M. L.; Wang, Z-Q. *Chem. Commun.* **1996**, 1.

29. Calhorda, M. J.; Brown, J. M.; Cooley, N. A. *Organometallics* **1991**, *10*, 1431.

30. Sumner, C. E.; Riley, P. E.; Davis, R. E.; Pettit, R. *J. Am. Chem. Soc.* **1980**, *102*, 1752.

31. Doherty, N. M.; Howard, J.A.; Knox, S. A. R.; Terrill, N. J.; Yates, M. I. *J. Chem. Soc., Chem. Commun.* **1989**, 638.

32. Pichler, H.; Schultz, H. *Chem. Ing. Tech.* **1970**, *12*, 1160.

33. (a) Masters, C. *Adv. Organomet. Chem.* **1979**, *17*, 61. (b) Henrici-Olive, G.; Olive, S. *Angew. Chem., Int. Ed. Engl.* **1976**, *15*, 136.

34. (a) Akita, M.; Mitani, O.; Moro-oka, Y. *J. Chem. Soc., Chem. Commun.* **1989**, 527. (b) Akita, M.; Mitani, O.; Sayama, M.; Moro-oka, Y. *Organometallics* **1991**, *10*, 1394.

35. Eisenberg, R.; Shafiq, F.; Kramarz, K. W. *Inorg. Chim. Acta* **1993**, *213*, 111.

36. (a) Antonelli, D. M.; Cowie, M. *Organometallics* **1990**, *9*, 1818. (b) Hilts, R.; Franchuk, R.; Cowie, M. *Organometallics* **1991**, *10*, 304.

Chapter 2

The Coupling of Methylene Groups at Rh/Os Centres

Introduction

In spite of the industrial successes of the Fischer-Tropsch (FT) reaction[1] since its discovery over 75 years ago,[2] the process is still not well understood and its lack of selectivity continues to be a drawback. Although there is general agreement that the reaction is a result of the stepwise polymerization of methylene groups,[3] how this polymerization occurs is unknown and a number of mechanisms have been proposed, the most prominent of which involve either: (1) the direct polymerization of methylene units (Fischer and Tropsch);[2] (2) the coupling of methylene and alkyl fragments (Brady and Pettit; Biloen and Sachtler)[4] or (3) the coupling of methylene and vinyl groups (Maitlis et al.).[5] The observation that even within the closely related group 8 and 9 transition-metal catalysts, the different metals give substantially different products and product distributions,[6] suggested to us that some control over product distributions might be achieved by the use of combinations of these metals. We are interested in synthesizing bimetallic complexes of the Group 8 and 9 metals, containing methylene groups and studying their reactivity with other organic substrates in order to mimic possible reaction pathways in FT synthesis particularly as it relates to the involvement of different adjacent metals in carbon-carbon bond formation.

Experimental

General Comments

All solvents were dried (using appropriate drying agents), distilled before use, and stored under nitrogen. Reactions were performed under an argon atmosphere using standard Schlenk techniques. $RhCl_3 \cdot xH_2O$ was purchased from Strem Chemicals, $Os_3(CO)_{12}$ was purchased from Colonial Metals Inc., and Diazald (including ^2H and ^{13}C enriched) was purchased from Aldrich. ^{13}C-

enriched CO (99.4% enrichment) was purchased from Isotec Inc. and Cambridge Isotope Laboratories (99% enrichment). The compound [RhOs(CO)$_4$(dppm)$_2$][BF$_4$] (1) was prepared by the published procedure.[7]

NMR spectra were recorded on a Bruker AM-400 or Varian iNova-400 spectrometer operating at 400.1 MHz for ^{1}H, 161.9 MHz ^{31}P, and 100.6 MHz for ^{13}C nuclei. Infrared spectra were obtained on a Nicolet Magna 750 FTIR spectrometer with a NIC-Plan IR microscope. Spectroscopic data for all compounds described in this chapter appear in Table 2.1. The elemental analyses were performed by the microanalytical service within the department. Electrospray ionization mass spectra were run on a Micromass Zabspec spectrometer. In all cases the distribution of isotope peaks for the appropriate parent ion matched very closely that calculated from the formulation given.

Preparation of Compounds

(a) **[RhOs(CO)$_4$(μ-CH$_2$)(dppm)$_2$][BF$_4$] (2).** The compound [RhOs(CO)$_4$(dppm)$_2$]-[BF$_4$] (1) (100 mg, 0.079 mmol) was dissolved in 15 mL of CH$_2$Cl$_2$ and the solution cooled to -78 °C. Diazomethane (ca. 18 equiv.), generated from 300 mg (1.4 mmol) of Diazald, was passed through the solution for 30 min. The solution was kept at -78 °C and put under dynamic vacuum for another 30 min. The cold bath was then removed and the reaction mixture was pumped to dryness, yielding a yellow residue. This residue was dissolved in 5 mL of CH$_2$Cl$_2$ and 30 mL of ether was added to precipitate a yellow solid. The solid was washed with 3 x 5 mL of ether and dried in vacuo (92 % yield). Anal. Calcd. for RhOsP$_4$F$_4$BO$_4$C$_{55}$H$_{46}$: C, 51.81; H, 3.64. Found: C, 51.63; H, 3.67. MS m/z 1188 (M$^+$ - BF$_4$)

Table 2.1 Spectroscopic Data for Compounds

Compound	IR $(cm^{-1})^{a,b}$	NMR^{c,d}		
		$\delta\ ^{31}P\{^1H\}^e$ (ppm)	$\delta\ ^1H$ (ppm)^{f,g}	$\delta\ ^{13}C\{^1H\}$ (ppm)^g
[RhOs(CO)$_4$(μ-CH$_2$)-(dppm)$_2$][BF$_4$] (2)	2043 (s) 1970(s) 1798 (m)	P(Rh): 33.7 (dm, $^1J_{RhP}$ = 157 Hz) P(Os): -2.8 (m)	μ-CH$_2$: 2.25 (m, 2H) dppm: 3.75 (m, 2H); 2.80 (m, 2H)	μ-CH$_2$: 32.8 (d, $^1J_{RhC}$ = 15 Hz) CO(Os): 176.3 (br); 176.6 (t); μ-CO: 210.5 (dm, $^1J_{RhC}$ = 26 Hz) CO(Rh): 195.0 (dt, $^1J_{RhC}$ = 57 Hz)
[RhOs(C$_4$H$_8$)(CO)$_3$-(dppm)$_2$][BF$_4$] (3)	1970 (s) 1850 (m)	P(Rh): 22.2 (dm, $^1J_{RhP}$ = 106 Hz) P(Os): -6.7 (m)	C$_4$H$_8$: 0.67 (m, 2H$_4$); 1.06 (m, 2H$_5$); 2.09 (br, 2H$_6$); 1.18 (br, 2H$_7$) dppm: 3.80 (m, 2H); 3.93 (m, 2H)^h	C$_4$H$_8$: 24.6 (d, $^1J_{CC}$ = 31 Hz, C$_4$); 36.2 (t, $^1J_{CC}$ = 34 Hz, C$_5$); 37.8 ($^1J_{CC}$ = 33 Hz, C$_6$); -0.3 (d, $^1J_{CC}$ = 30 Hz, C$_7$) CO(Os): 182.4 (dt, $^2J_{PC}$ = 9 Hz, $^2J_{CC}$ = 2 Hz); 191.1 (m) CO(Rh): 186.4 (ddt, $^1J_{RhC}$ = 81 Hz, $^2J_{CC}$ = 5 Hz, $^2J_{PC}$ = 17 Hz)
[RhOs(CO)$_3$(PMe$_3$)(μ-CH$_2$)(dppm)$_2$][BF$_4$] (5)	1976 (s) 1960 (s) 1907 (s)	P(Rh): 18.2 (dm, $^1J_{RhP}$ = 104 Hz) P(Os): -10.8 (m) PMe$_3$: -56.2 (dm, $^1J_{RhP}$ = 117 Hz)	Me$_3$P: 0.75 (d, 9H, $^2J_{PH}$ = 8 Hz) dppm: 3.53 (m, 2H); 4.31 (m, 2H) μ-CH$_2$: 4.88 (m, 2H)	Me$_3$P: 18.02 (d, 3C, $^1J_{PC}$ = 20 Hz) dppm: 26.1 (m, 2C) μ-CH$_2$: 75.9 (m, 1C) CO(Os): 181.4 (dt, $^3J_{CPMe3}$ = 18 Hz, $^2J_{CP(Os)}$ = 14 Hz); 189.1 (dt, $^3J_{CPMe3}$ = 2 Hz, $^2J_{CP(Os)}$ = 4 Hz) CO(Rh): 199.6 (ddt, $^1J_{RhC}$ = 51 Hz $^2J_{CPMe3}$ = 4 Hz, $^2J_{CP(Rh)}$ = 20 Hz)

[RhOs(CO)$_3$(C$_2$H$_4$)-(dppm)$_2$][BF$_4$] (6)		P(Rh): 33.1 (m) P(Os): -7.1 (m)	C$_2$H$_4$ (Rh): 2.76 (m, 4H, $^2J_{RhH}$ = 2 Hz) dppm: 4.04 (m, 4H)	
[RhOs(CO)$_2$(C$_2$H$_4$)$_2$-(dppm)$_2$][BF$_4$] (7)	1858 (s)	P(Rh): 32.7 (dm, $^1J_{RhP}$ = 154 Hz) P(Os): 1.8 (m)	C$_2$H$_4$ (Os): 0.90 (t, 4H, $^3J_{PH}$ = 6 Hz) C$_2$H$_4$ (Rh): 2.89 (m, 4H, $^2J_{RhH}$ = 2 Hz) dppm: 3.76 (m, 4H)	C$_2$H$_4$ (Os): 23.5 (s, 2C) C$_2$H$_4$ (Rh): 64.6 (d, 2C, $^1J_{RhC}$ = 11 Hz) dppm: 34.5 (m, 2C) CO(Os): 195.5 (dt,
[RhOs(CO)$_3$(μ-CH$_2$)-(dppm)$_2$][BF$_4$] (8)	1994 (s) 1937 (s)	P(Rh): 27.0 (m) P(Os): 2.1 (m)	6.38 (tt, $^3J_{P(Os)H}$ = 13 Hz, $^3J_{P(Rh)H}$ = 8 Hz) 4.25 (m, 2H) 3.82 (m, 2H)	dppm: 22.4 (m, 2C) μ-CH$_2$: 93.9 (s, br, 1C) CO(Os): 177.4 (dt, $^2J_{RhC}$ = 4 Hz, $^2J_{CP(Os)}$ = 9 Hz); 186.7 (t, $^2J_{CP(Os)}$ = 5 Hz) CO(Rh): 189.7 (dt, $^1J_{RhC}$ = 63 Hz, $^2J_{CP(Rh)}$ = 14 Hz)

[a] IR abbreviations: s = strong, m = medium. [b] Powder microscope. [c] NMR abbreviations: s = singlet, d = doublet, t = triplet, m = multiplet, br = broad. [d] NMR data at 25 °C in CD$_2$Cl$_2$. [e] ^{31}P chemical shifts referenced to external 85% H$_3$PO$_4$. [f] Chemical shifts for the phenyl hydrogens not given. [g] ^{1}H and ^{13}C chemical shifts referenced to TMS. [h] Labeling of the hydrogen and carbon atoms of the C$_4$H$_8$ unit is as shown in Figure 2.3

(b) [RhOs(C₄H₈)(CO)₃(dppm)₂][BF₄] (3). Method (i). The compound [RhOs(CO)₄(μ-CH₂)(dppm)₂][BF₄] (2) (50 mg, 0.039 mmol) was dissolved in 20 mL of CH_2Cl_2 and the solution cooled to -60 °C. Diazomethane (ca. 15 equiv.), generated from 500 mg (2.3 mmol) of Diazald, was passed through the solution for 1 h and the solution was stirred for an additional hour. The solution was then put under dynamic vacuum at -60°C for 1 h. The cold bath was then removed and the reaction mixture was pumped to dryness, yielding a yellow residue. This residue was dissolved in 5 mL of CH_2Cl_2 and 40 mL of ether was added to precipitate a yellow solid. The solid was washed with 3 x 5 mL of ether and dried in vacuo (85 % yield). Anal. Calcd. for $RhOsP_4F_4BO_3C_{57}H_{52}$: C, 53.12; H, 4.07. Found: C, 52.81; H, 3.92. MS m/z 1202 (M^+ - BF_4).

Method (ii). The compound [RhOs(CO)₄(dppm)₂][BF₄] (1) (50 mg, 0.040 mmol) was dissolved in 20 mL of CH_2Cl_2 and the solution cooled to -60°C. Diazomethane (ca. 15 equiv.), generated from 500 mg (2.3 mmol) of Diazald, was passed through the solution for 1 h and the solution was stirred for an additional hour. The solution was then put under dynamic vacuum for 1 h. The cold bath was then removed and the reaction was pumped to dryness, yielding a yellow residue. This residue was dissolved in 5 mL of CH_2Cl_2 and 40 mL of ether was added to precipitate a yellow solid. The solid was washed with 3 x 5 mL of ether and dried in vacuo (82 % yield).

(c) [RhOs(C₃H₅)(CH₃)(CO)₃(dppm)₂][BF₄] (4). The compound [RhOs(CO)₄(μ-CH₂)(dppm)₂][BF₄] (2) (50 mg, 0.039 mmol) was dissolved in 5 mL of THF. Diazomethane (ca. 12 equiv.), generated from 100 mg (0.47 mmol) of Diazald, was passed through the solution for 15 minutes. 30 mL of ether was then added resulting in the precipitation of a yellow solid, which was washed with 3 x 5 mL of ether and dried in vacuo (87 % yield). Compound 4 was previously prepared

from the reaction of [RhOs(CO)$_4$(dppm)$_2$][BF$_4$] with CH$_2$N$_2$ and was completely characterized at that time.[8]

(d) Reaction of Compound 3 with H$_2$. Dihydrogen was passed through an NMR tube containing [RhOs(C$_4$H$_8$)(CO)$_3$(dppm)$_2$][BF$_4$] (3) (10 mg, 0.008 mmol) dissolved in 0.7 mL of THF-d$_8$ for 30 seconds and the solution was left under an H$_2$ atmosphere. After approximately 8 h, 10% of the starting material had reacted, yielding the products [RhOs(μ-H)$_2$(CO)$_3$(dppm)$_2$][BF$_4$] and butane; as was observed by NMR spectroscopy. After 72 h, 3 had completely reacted, yielding these products.

(e) Reaction of Compound 4 with H$_2$. Dihydrogen was passed through an NMR tube containing [RhOs(C$_3$H$_5$)(CH$_3$)(CO)$_3$(dppm)$_2$][BF$_4$] (4) (10 mg, 0.008 mmol) dissolved in 0.7 mL of THF-d$_8$ for 30 seconds. After approximately 8 h, 15% of the starting material had reacted, yielding the products [RhOs(μ-H)$_2$(CO)$_3$-(dppm)$_2$][BF$_4$], propene, and methane; as was observed by NMR spectroscopy. After 72 h, compound 4 had completely reacted, yielding these products.

(f) [RhOs(CO)$_3$(PMe$_3$)(μ-CH$_2$)(dppm)$_2$][BF$_4$] (5). The compound [RhOs(CO)$_4$(μ-CH$_2$)(dppm)$_2$][BF$_4$] (2) (40 mg, 0.031 mmol) was dissolved in 5 mL of CH$_2$Cl$_2$ and 31 μL of a 1.0 M solution of PMe$_3$ in THF (0.031 mmol), was then added to the solution. The resulting yellow solution was stirred for 15 min and then concentrated to 3 mL under an argon stream. Ether (20 mL) was then added to precipitate a yellow solid which was washed with 3 x 10 mL of ether and dried in vacuo (yield 92 %). Satisfactory elemental analysis has not yet been obtained. MS m/z 1236 (- BF$_4$).

(g) [RhOs(C$_2$H$_4$)(CO)$_3$(dppm)$_2$][BF$_4$] (6). The compound [RhOs(CO)$_4$(dppm)$_2$]-[BF$_4$] **(1)** (80 mg, 0.064 mmol) was dissolved in 10 mL of CH$_2$Cl$_2$ and the solution placed under an ethylene atmosphere. Me$_3$NO (4.8 mg, 0.064 mmol), dissolved in 5 mL of CH$_2$Cl$_2$, was then added to the solution. The solution immediately became orange but after several minutes changed to yellow. After stirring for 30 min, the solution was concentrated to 5 mL under an argon stream and 30 mL of ether was added to precipitate a yellow solid. The solid was then washed with 3 x 5 mL of ether and dried in vacuo. The ^{31}P NMR spectrum of this sample shows a mixture of compounds **1**, **6**, and **7**. A pure sample of **6** has not yet been isolated.

(h) [RhOs(C$_2$H$_4$)$_2$(CO)$_2$(dppm)$_2$][BF$_4$] (7). The compound [RhOs(CO)$_4$-(dppm)$_2$][BF$_4$] **(1)** (80 mg, 0.064 mmol) was dissolved in 10 mL of CH$_2$Cl$_2$ and the solution placed under an ethylene atmosphere. Me$_3$NO (9.6 mg, 0.13 mmol), dissolved in 5 mL of CH$_2$Cl$_2$, was then added to the solution. The solution immediately became orange but after several minutes changed to yellow. After stirring for 30 min, the solution was concentrated to 5 mL under an argon stream and 30 mL of ether was added to precipitate a yellow solid. The solid was then washed with 3 x 5 mL of ether and dried in vacuo (91 % yield). Anal. Calcd. for RhOsP$_4$F$_4$BO$_2$C$_{56}$H$_{52}$: C, 53.34; H, 4.16. Found: C, 53.08; H, 3.89. MS m/z 1174 (M$^+$ - BF$_4$).

(i) Reaction of (2) with ethyldiazoacetate and trimethylsilyldiazomethane. To an NMR tube containing [RhOs(CO)$_4$(μ-CH$_2$)(dppm)$_2$][BF$_4$] **(2)** (10 mg, 0.008 mmol) dissolved in 0.5 mL of CD$_2$Cl$_2$, was added N$_2$C(H)CO$_2$Et (1 μL, 0.02 mmol). After approximately 8 h, a small amount of the compound [RhOs(CO)$_4$(dppm)$_2$][BF$_4$] **(1)** was observed by NMR spectroscopy. After another 72 h, ^{1}H and ^{31}P NMR spectroscopy indicated that **2** had completely disappeared yielding [RhOs(CO)$_4$(dppm)$_2$][BF$_4$] **(1)** and the olefin

$H_2C=C(H)CO_2Et$, which was characterized by matching the ^1H NMR spectrum of this compound with a pure sample of ethyl acrylate.

The reaction of **2** with $N_2C(H)SiMe_3$ was conducted in a similar manner. However, in this case the products obtained were $H_2C=C(H)SiMe_3$ and complex **1**, as identified by ^1H and ^{31}P NMR spectroscopy.

(j) Reaction of Compound 2 with dimethylallene. To an NMR tube containing $[RhOs(CO)_4(\mu\text{-}CH_2)(dppm)_2][BF_4]$ (**2**) (10 mg, 0.008 mmol) dissolved in 0.5 mL of CD_2Cl_2, was added $Me_2C=C=CH_2$ (4 μL, 0.04 mmol). After approximately 12 h, a small amount of the compound $[RhOs(CO)_4(dppm)_2][BF_4]$ (**1**) was observed by NMR spectroscopy. After three days all of **2** had disappeared leaving **1** as the only phosphorus-containing product observed. 1,1-dimethyl-1,3 butadiene was also identified on the basis of its ^1H NMR spectrum.

(k) $[RhOs(CO)_3(\mu\text{-}CH_2)(dppm)_2][BF_4]$ (8). The compound $[RhOs(CO)_4(\mu\text{-}CH_2)(dppm)_2][BF_4]$ (**2**) (50 mg, 0.039 mmol) was dissolved in 4 mL of CH_2Cl_2 and Me_3NO (3.0 mg, 0.039 mmol), dissolved in 4 mL of CH_2Cl_2, was then added to the solution. The solution immediately became orange. After stirring for 30 min the solution was concentrated to 4 mL under an argon stream, and 30 mL of ether was added to precipitate an orange solid. The solid was then washed with 3 x 5 mL of ether, recrystallized from CH_2Cl_2/ether, and dried in vacuo (yield 77 %). Satisfactory elemental analysis has not yet been obtained. MS m/z 1160 (- BF_4).

(l) Reaction of Compound 8 with CH_2N_2. $[RhOs(CO)_3(\mu\text{-}CH_2)(dppm)_2][BF_4]$ (**8**) (10 mg, 0.008 mmol) was dissolved in 0.7 mL of CD_2Cl_2 in an NMR tube and cooled to -78°C. Diazomethane (ca. 10 equiv.) was passed through the solution for 2 min. The reaction mixture was analyzed by ^{31}P and ^1H NMR spectroscopy. Due to the many products obtained, characterization was not possible.

(m) Reaction of Compound 8 with H₂C=CH₂. [RhOs(CO)₃(μ-CH₂)(dppm)₂]-[BF₄] (**8**) (10 mg, 0.008 mmol) was dissolved in 0.7 mL of CD₂Cl₂ in an NMR tube and cooled to -78°C. Ethylene (ca. 20 equiv.) was passed through the solution for 1 min. The reaction mixture was analyzed by ^{31}P and ^{1}H NMR spectroscopy. Several products were present but not characterized.

X-ray Data Collection and Structure Solution

X-ray data collection and structure solutions were carried out by Dr. R. McDonald in the departmental X-ray Structure Determination Laboratory.

Yellow-orange crystals of [RhOs(CO)₃(μ-CO)(μ-CH₂)(dppm)₂][BF₄] (**2**) were obtained via slow diffusion of diethyl ether into a dichloromethane solution of the compound. Data were collected on a Bruker P4/RA/SMART 1000 CCD diffractometer[9] using Mo Kα radiation at -80 °C. The data were corrected for absorption through use of the SADABS procedure. Unit cell parameters were obtained from a least-squares refinement of the setting angles of 5792 reflections from the data collection, and the space group was determined to be I2/a (an alternate setting of C2/c [No. 15]). See Table 2.2 for a summary of crystal data and X-ray data collection information.

Pale yellow crystals of [RhOs(CO)₃(C₄H₈)(dppm)₂][BF₄] (**3**) were obtained via slow diffusion of diethyl ether into a dichloromethane solution of the compound. Data were collected and corrected for absorption as for **2** above. Unit cell parameters were obtained from a least-squares refinement of the setting angles of 7295 reflections from the data collection. The space group was determined to be P2₁/n (an alternate setting of P2₁/c [No. 14]).

The structure of **2** was solved using the direct-methods program SHELXS–86,[10] and refinement was completed using the program SHELXL-93.[11] Hydrogen

atoms were assigned positions based on the geometries of their attached carbon atoms, and were given thermal parameters 20% greater than those of the attached carbons. For **2** the boron and two fluorine atom positions for the tetrafluoroborate anion were found to be disordered; each of these atoms was split into two positions, which were assigned occupancy factors of 0.5 and were allowed to refine independently. The final model for **2** was refined to values of $R_1(F) = 0.0329$ (for 8578 data with $F_O^2 \geq 2\sigma(F_O^2)$) and $wR_2(F^2) = 0.0744$ (for all 10519 independent data).

The structure of **3** was solved using direct methods (SHELXS–86[10]), and refinement was completed using the program SHELXL-93,[11] during which the hydrogen atoms were treated as for **2**. The final model for **3** was refined to values of $R_1(F) = 0.0675$ (for 4930 data with $F_O^2 \geq 2\sigma(F_O^2)$) and $wR_2(F^2) = 0.1869$ (for all 9864 independent data).

Table 2.2 Crystallographic Data for Compounds 2 and 3

	[RhOs(CO)$_4$(CH$_2$)(dppm)$_2$][BF$_4$] (2)	[RhOs(CO)$_3$(CH$_2$)$_4$(dppm)$_2$][BF$_4$] (3)
formula	C$_{55}$H$_{46}$BF$_4$O$_4$OsP$_4$Rh	C$_{57}$H$_{52}$BF$_4$O$_3$OsP$_4$Rh
formula weight	1274.72	1288.79
crystal dimensions (mm)	0.54 × 0.11 × 0.07	0.41 × 0.06 × 0.02
crystal system	monoclinic	monoclinic
space group	I2/a (an alternate setting of C2/c [No. 15])	P2$_1$/n (a non-standard setting of P2$_1$/c [No. 14])
a (Å)	42.751 (3)[a]	17.1806 (12)[b]
b (Å)	10.2233 (6)	12.1815 (7)
c (Å)	23.5803 (12)	26.533 (2)
β (deg)	90.4321 (11)	103.1770 (10)
V (Å^3)	10305.7 (10)	5406.7 (6)
Z	8	4
ρ_{calcd} (g cm^{-3})	1.643	1.583
μ (mm^{-1})	2.968	2.828
diffractometer	Bruker P4/RA/SMART 1000 CCD	Bruker P4/RA/SMART 1000 CCD
Radiation (λ [Å])	graphite-monochromated Mo Kα (0.71073)	graphite-monochromated Mo Kα (0.71073)
temperature (°C)	–80	–80
scan type	φ rotations (0.3°) / ω scans (0.3°) (30 s exposures)	φ rotations (0.3°) / ω scans (0.3°) (20 s exposures)
data collection 2θ limit (deg)	52.76	50.74
total data collected	24873 (-52 ≤ h ≤ 53, -12 ≤ k ≤ 12, -29 ≤ l ≤ 10)	30774 (-20 ≤ h ≤ 20, -14 ≤ k ≤ 5, -31 ≤ l ≤ 31)
independent reflections	10519 (R$_{int}$ = 0.0409)	9864
number of observed reflections (NO)	8578 (F$_o^2$ ≥ 2σ(F$_o^2$))	4930 (F$_o^2$ ≥ 2σ(F$_o^2$))
Structure solution method	direct methods (SHELXS–86)	direct methods (SHELXS–86)
refinement method	full-matrix least-squares on F^2 (SHELXL–93)	full-matrix least-squares on F^2 (SHELXL–93)
absorption correction method	empirical (SADABS)	Gaussian integration (face-indexed)
range of transmission factors	0.8192–0.2971	0.9452–0.8285
data/restraints/parameters	10519 [F$_o^2$ ≥ –3σ(F$_o^2$)] / 0/ 658	9864 [F$_o^2$ ≥ –3σ(F$_o^2$)] / 7/ 641
goodness-of-fit (S)	0.996 [F$_o^2$ ≥ –3σ(F$_o^2$)]	0.925 [F$_o^2$ ≥ –3σ(F$_o^2$)]
R$_1$ [F$_o^2$ ≥ 2σ(F$_o^2$)]	0.0329	R$_1$ = 0.0675
wR$_2$ (all data)	0.0744	wR$_2$ = 0.1869
largest difference peak and hole	1.631 and –0.741 e Å^{-3}	3.891 and –1.530 e Å^{-3}

[a]Obtained from least-squares refinement of 5792 centered reflections.

[b]Obtained from least-squares refinement of 7295 centered reflections.

Results

(a) C_1, C_2, C_3, and C_4 Product Formation.

(i) Methylene Coupling.

The mixed-metal complex $[RhOs(CO)_4(dppm)_2][BF_4]$ (**1**) (dppm =

$Ph_2PCH_2PPh_2$) reacts with excess diazomethane at ambient temperature, yielding

essentially quantitatively $[RhOs(\eta^1\text{-}CH_2CH=CH_2)(CH_3)(CO)_3(dppm)_2][BF_4]$ (**4**),[8]

in which the allyl group is η^1-bound to Rh and the methyl group is bound to Os

(see Scheme 2.1). Compound **2** (as the triflate salt) has been prepared

independently by the reaction of the η^3-allyl complex $[RhOs(\eta^3\text{-}C_3H_5)(CO)_3\text{-}$

$(dppm)_2]$[7] with methyl triflate, and has very similar spectral parameters to a

number of related compounds having an alkenyl group bound to Rh and a methyl

ligand bound to Os, one of which was characterized by an X-ray structure.[12] The

η^1 bonding mode of the allyl ligand is established by NMR spectroscopy for which

the ^1H NMR spectrum shows ^{31}P coupling of the Rh-bound phosphines to only the

hydrogens on the α-carbon, and the $^{13}C\{^1H\}$ NMR spectrum which also shows Rh

coupling (24 Hz) to only the α-carbon. However, spin-saturation-transfer

experiments (via irradiation of the rhodium-bound methylene protons) at room

temperature indicate that the allyl group is fluxional, alternating coordination to

the rhodium between the α and γ carbons. The methyl group is identified as being

bound to Os by selective $^1H\{^{31}P\}$ experiments, in which coupling of the methyl

hydrogens to only the Os-bound phosphorus nuclei is observed. The complete

characterization of **4** is not described herein since this compound was previously

characterized. Spectroscopic data for **4** is given in References and Notes.[13]

In an attempt to learn more about this unprecedented conversion of

diazomethane-generated methylene groups to an allyl and a methyl ligand, we

attempted to observe intermediates in this transformation by carrying out the

reaction at low temperatures. At -80°C, the above reaction yields the methylene-

Scheme 2.1
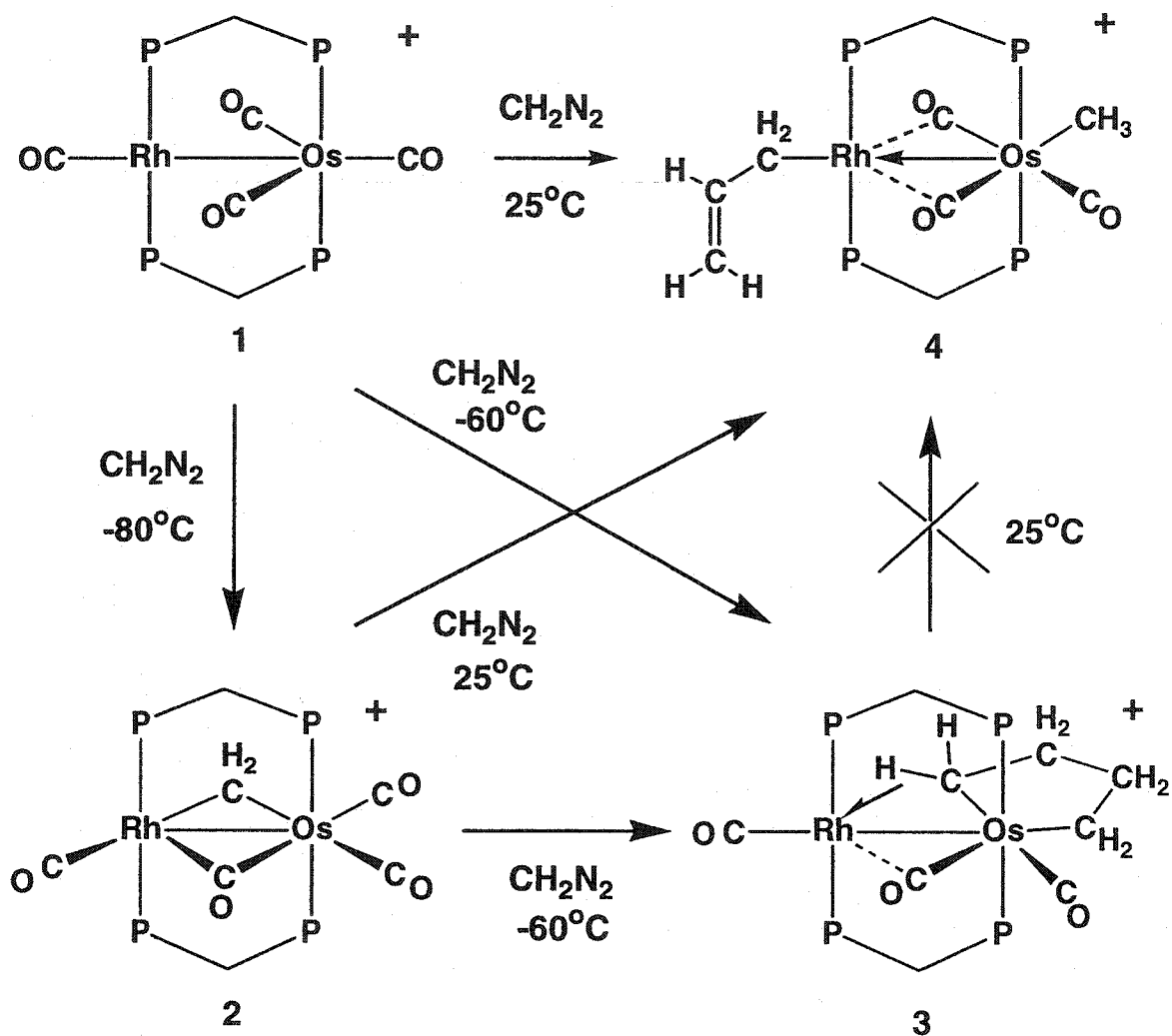
bridged complex [RhOs(CO)$_4$(μ-CH$_2$)(dppm)$_2$][BF$_4$] (2),[14] which can be isolated in high yield by first removing the excess diazomethane before warming to ambient temperature. The ^{13}C{^{1}H} NMR spectrum of 2 shows four carbonyl resonances. Two of these resonances, at 176.3 and 176.6 ppm, are in the characteristic range for carbonyls terminally bound to osmium and this has been confirmed by selective ^{31}P NMR decoupling experiments in which selective decoupling of the Os-bound ^{31}P nuclei results in collapse of the Os-bound carbonyl resonances from triplets to singlets. The signal at 195.0 ppm represents a rhodium-bound carbonyl as determined by selective ^{31}P NMR decoupling experiments and by the Rh-C coupling constant ($^1J_{Rh-C}$ = 57 Hz) which is typical of such groups. The resonance at 210.5 ppm is in the characteristic range for bridging or semi-bridging carbonyls, and ^{13}C{^{31}P} NMR spectroscopy which shows coupling of this carbonyl to all ^{31}P nuclei allows us to confirm the bridging mode of this group. The 26 Hz coupling of this carbonyl carbon to Rh is also typical of bridging carbonyls. The bridging nature of this carbonyl is also confirmed by the IR spectrum which shows a low-frequency peak at 1798 cm^{-1}.

In the ^{1}H NMR spectrum, the methylene group appears as a pseudo-quintet at 2.25 ppm having essentially equal coupling to all four ^{31}P nuclei, confirming that it bridges the metals. No coupling of the methylene protons to Rh is evident. In the ^{13}C{^{1}H} NMR spectrum this methylene carbon appears at 32.8 ppm and displays a coupling of 15 Hz to Rh. In this case no coupling between the Rh-bound phosphines and the methylene carbon is observed.

The structure of 2 was confirmed by an X-ray structure determination and a representation of the cation (with only the ipso carbons of the phenyl groups drawn) is shown in Figure 2.1 with important bond lengths and angles given in Table 2.3. The structure is typical of bis-dppm-bridged binuclear complexes, having both diphosphines in essentially trans arrangements at each metal, although the phosphines on Rh are bent back significantly (P(2)-Rh-P(4) = 156.69(4)°) compared to those on Os (P(1)-Os-P(3) = 174.42(3)°).
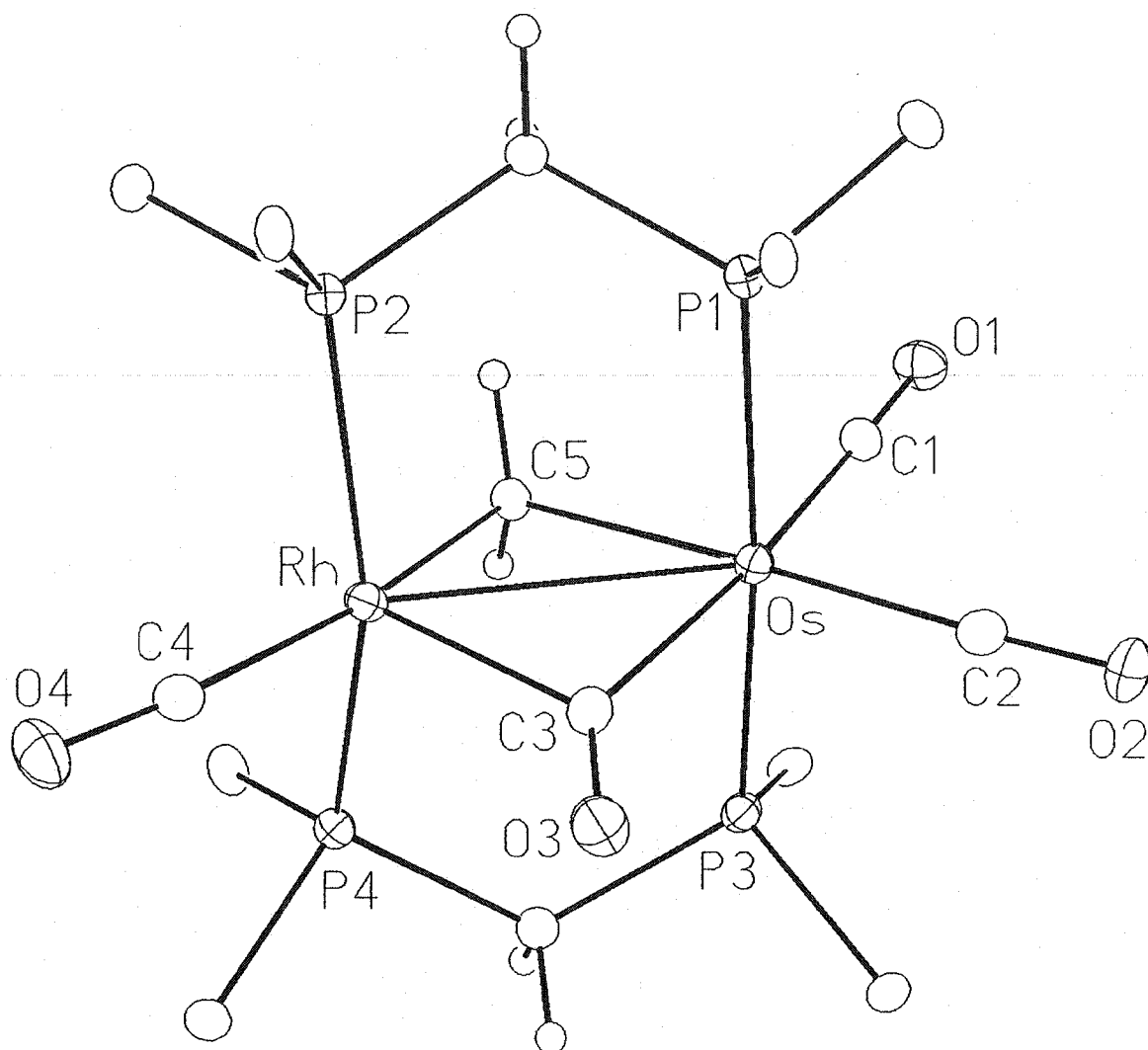
Figure 2.1. Perspective view of the cation of [RhOs(CO)$_3$(μ-CH$_2$)(μ-CO)-

(dppm)$_2$][BF$_4$] (2) showing the atom-labeling scheme. Non-hydrogen atoms are

represented by Gaussian ellipsoids at the 20% probability level. Hydrogen atoms

are shown with arbitrarily small thermal parameters. Only the ipso carbons of the

dppm phenyl groups are shown for clarity.

Table 2.3 Selected Distances and Angles for Compound 2

(a) Distance

b) Angles

Atom 1	Atom 2	Distance (Å)
Os	Rh	2.9413(4)
Os	P(1)	2.3867(9)
Os	P(3)	2.3891(10)
Os	C(1)	1.907(4)
Os	C(2)	1.917(4)
Os	C(3)	2.157(4)
Os	C(5)	2.210(4)
Rh	P(2)	2.3483(9)
Rh	P(4)	2.3014(10)
Rh	C(3)	2.027(4)
Rh	C(4)	1.895(4)
Rh	C(5)	2.088(4)
O(1)	C(1)	1.150(5)
O(2)	C(2)	1.143(5)
O(3)	C(3)	1.163(5)
O(4)	C(4)	1.144(5)

Atom 1	Atom 2	Atom 3	Angle (°)
P(1)	Os	P(3)	174.42(3)
C(1)	Os	C(2)	94.43(17)
C(1)	Os	C(3)	173.61(16)
C(1)	Os	C(5)	85.62(15)
C(2)	Os	C(3)	91.96(16)
C(2)	Os	C(5)	177.83(14)
C(3)	Os	C(5)	87.98(14)
P(2)	Rh	P(4)	156.69(4)
C(3)	Rh	C(4)	95.50(17)
C(3)	Rh	C(5)	94.92(16)
C(4)	Rh	C(5)	169.13(16)
Os	C(3)	Rh	89.28(16)
Os	C(3)	O(3)	141.7(3)
Rh	C(3)	O(3)	128.9(3)
Os	C(5)	Rh	86.32(14)
P(1)	C(6)	P(2)	110.00(18)
P(3)	C(7)	P(4)	121.2(2)

If the metal-metal bond is ignored, the geometry about Rh can be described as a tetragonal pyramid having the phosphines, the methylene, and the terminal carbonyl group in the basal sites, with the bridging carbonyl in the apical site. This description of Rh as a tetragonal pyramid is consistent with the bending back of the phosphines as described earlier. Similarly, the other atoms in the basal plane, C(4) and C(5), are also bent away from the apical site (C(4)-Rh-C(5) = 169.1(2)°). The geometry at Os (also ignoring the metal-metal bond) is pseudo-octahedral with all angles between adjacent ligands close to 90°. The Rh-Os separation (2.9413(4) Å) is intermediate between what one would expect for a normal single bond (ca. 2.7-2.8 Å)[7,15] and a non-bonded separation (>3.1Å)[15] and leaves some uncertainty in the nature of this interaction. Two valence bond extremes can be proposed for a compound having the formulation of **2** as shown in Figure 2.2. In the one extreme (**I**) the carbonyl labeled C(3)O(3) in Figure 2.2 is terminally bound to Os giving a 16-electron configuration at Rh and an 18-electron count at Os. This formulation would not be expected to have a Rh-Os bond. In the second extreme (**II**) carbonyl C(3)O(3) has a conventional bridging geometry and an accompanying Rh-Os bond, giving both metals an 18-electron configuration. The observed geometry appears to fall somewhere between the

(I)   (II)
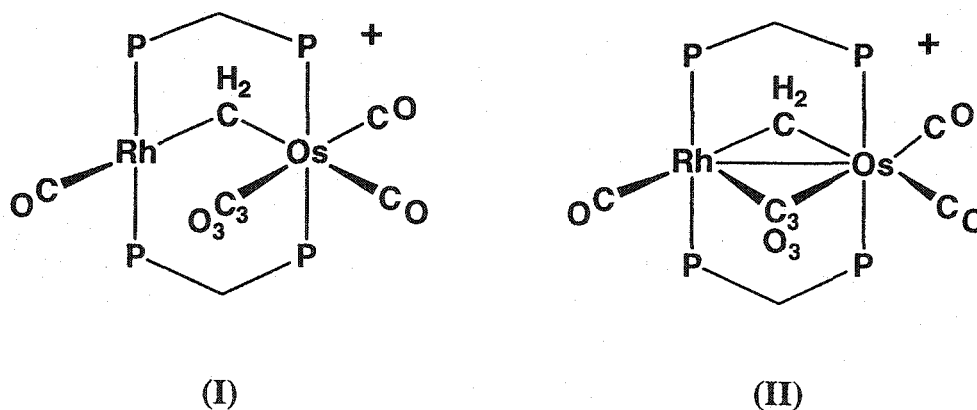
Figure 2.2 Bonding Extremes for Compound 2

two. This also shows up in the geometry at the carbonyl C(3)O(3) which is reminiscent of a semi-bridging carbonyl in which this group is more linear with respect to the metal (Os) to which it is σ-bound (Os-C(3)-O(3) = 141.7(3)°; Rh-C(3)-O(3) =128.9(3)°). Surprisingly, both bonds involving the bridging methylene and carbonyl groups (C(5) and C(3)) and Rh are shorter than the respective bonds to Os (Rh-C(5) = 2.088(4) , Os-C(5) = 2.210(4) Å; Rh-C(3) = 2.027(4) Å, Os-C(3) = 2.157(4) Å. Certainly for the carbonyl group, this is the opposite of what is usually observed in which a semibridging CO is more tightly bound to the metal with which it is σ-bound. It may be that the shorter bonds involving Rh reflect the lower steric repulsions at this metal, by virtue of its lower coordination number, and this is supported by the shorter Rh-P distances compared to Os-P (see Table 2.3).

It had earlier been discovered that the reaction of $[RhOs(CO)_4(dppm)_2]$-$[BF_4]$ (1) with diazomethane at ambient temperature yielded the unusual allyl/methyl complex $[RhOs(C_3H_5)(CH_3)(CO)_3(dppm)_2][BF_4]$ (4).[8] We find that this product is also obtained from the methylene-bridged compound $[RhOs(CO)_4$-$(\mu$-$CH_2)(dppm)_2][BF_4]$ (2) under identical reaction conditions, suggesting that 2 could be an intermediate in the formation of 4. This has been confirmed by subsequent labeling studies (vide infra).

If either compound 1 or 2 is reacted with excess diazomethane at between -60°C and -40°C a third product of methylene incorporation, $[RhOs(C_4H_8)(CO)_3$-$(dppm)_2][BF_4]$ (3) results, in which the condensation of four methylene units has occurred forming an osmacyclopentane moiety (Scheme 2.1). The structure of 3 has been established by an X-ray structure determination and a representation of the complex cation (in which only the ipso carbons of the phenyl groups are shown) is presented in Figure 2.3. Important bond lengths and angles are given in Table 2.4. The structure of 3 is related to that of the methylene-bridged precursor 2 by replacement of the bridging methylene group and the adjacent Os-bound
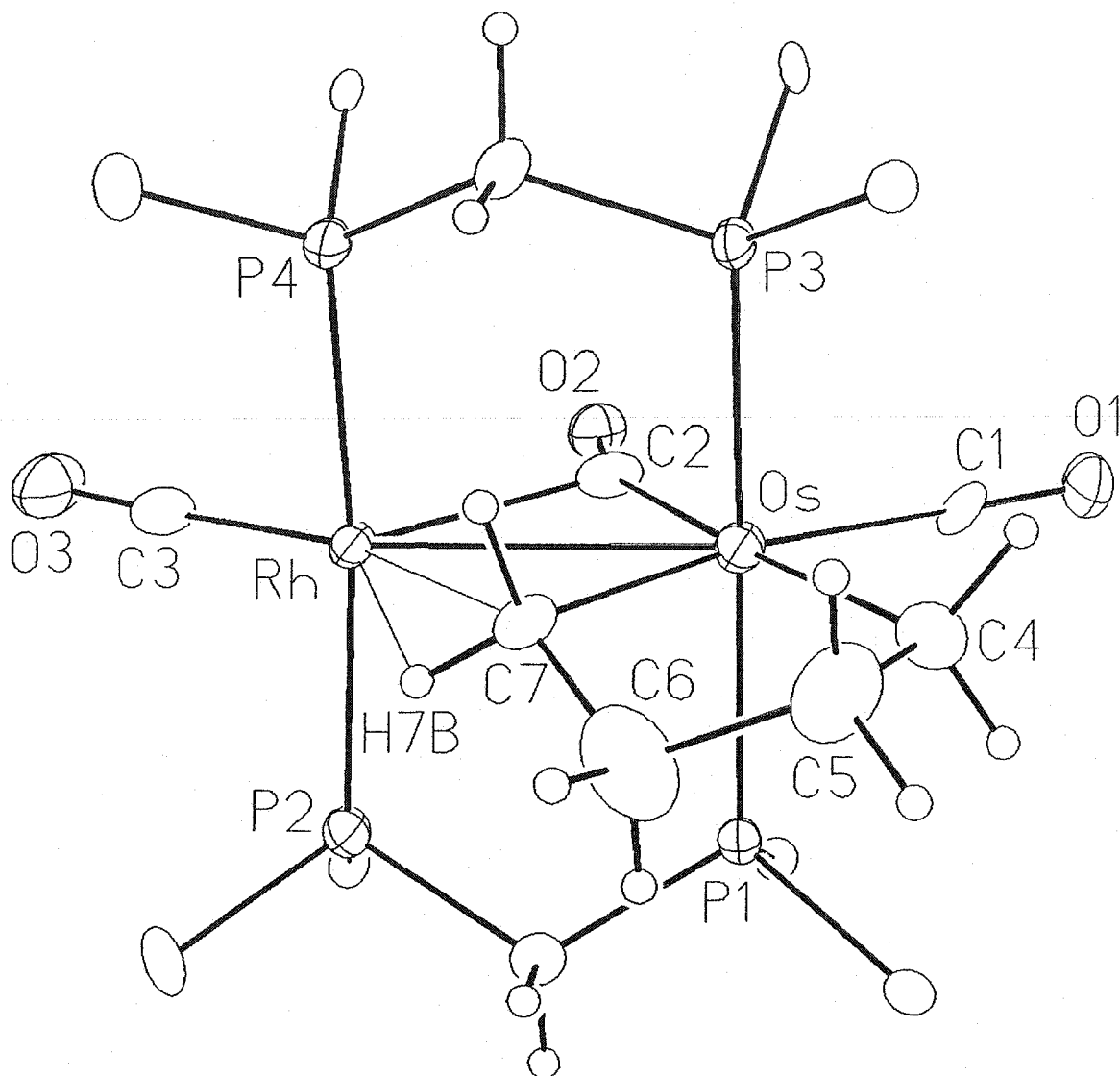
Figure 2.3. Perspective view of the cation of [RhOs(C₄H₈)(CO)₃(dppm)₂][BF₄]
(**3**) showing the atom-labeling scheme. Non-hydrogen atoms are represented by
Gaussian ellipsoids at the 20% probability level. Hydrogen atoms are shown with
arbitrarily small thermal parameters. Only the ipso carbons of the dppm phenyl
rings are shown for clarity.

Table 2.4 Selected Bond Distances and Angles of Compound 3

(a) Distances   (b) Angles

Atom 1	Atom 2	Distance (Å)	Atom 1	Atom 2	Atom 3	Angle (°)
Os	Rh	2.9420(14)	P(1)	Os	P(3)	176.14(14)
Os	P(1)	2.385(4)	C(1)	Os	C(2)	94.2(7)
Os	P(3)	2.384(4)	C(1)	Os	C(4)	78.2(7)
Os	C(1)	1.89(2)	C(1)	Os	C(7)	156.9(6)
Os	C(2)	2.02(2)	C(2)	Os	C(4)	172.4(6)
Os	C(4)	2.22(2)	C(2)	Os	C(7)	108.6(6)
Os	C(7)	2.29(2)	C(4)	Os	C(7)	79.0(5)
Rh	P(2)	2.331(4)	P(2)	Rh	P(4)	174.4(2)
Rh	P(4)	2.329(4)	Os	C(2)	Rh	82.8(6)
Rh	O(5)	2.240(5)	Os	C(2)	O(2)	155.6(14)
Rh	C(2)	2.41(2)	Rh	C(2)	O(2)	121.3(13)
Rh	C(3)	1.83(2)	Os	C(4)	C(5)	111.8(11)
Rh	C(7)	2.466(13)	C(4)	C(5)	C(6)	110.4(15)
Rh	H(7B)	1.95	C(5)	C(6)	C(7)	112.1(17)
O(1)	C(1)	1.11(2)	Os	C(7)	Rh	76.3(4)
O(2)	C(2)	1.12(2)	Os	C(7)	C(6)	103.0(12)
O(3)	C(3)	1.14(2)	Rh	C(7)	C(6)	153.6(10)
C(4)	C(5)	1.47(2)				
C(5)	C(6)	1.48(3)				
C(6)	C(7)	1.52(2)				

carbonyl by a C_4H_8 fragment. The bridging methylene goup of **2** has been replaced by the Os-C(7) linkage of the butanediyl fragment and by an agostic interaction involving C(7)H(7B) (vide infra), and one terminal Os-CO linkage (C(1)O(1)) has been replaced by the Os-C(4) linkage at the other end of the butanediyl fragment. Again, as in compound **2**, the Rh-Os separation is long (2.942(1) Å) and suggests a weak interaction between the metals. The butanediyl fragment chelates to Os, having normal Os-C distances (Os-C(4) = 2.22(2)Å, Os-C(7) = 2.29(2)Å) and a bite angle of 79.0(5)°. Within this hydrocarbyl fragment the C-C distances (1.47(2) - 1.52(2)Å) are normal for single bonds between sp^3-hybridized carbons, as are the angles at these carbons (103(1)°-112(2)°). Although the hydrogen atoms were not located in this X-ray study, their positions have been idealized based on the geometries about their attached carbon atoms. This places H(7B) in close proximity to Rh (ca. 1.93 Å), suggesting an agostic interaction of C(7)H(7B) with Rh. This interaction is supported by the Rh-C(7) distance (2.47(1)Å) which is typical of such an interaction[16] and has been confirmed in solution by NMR studies (vide infra).

The carbonyl C(2)O(2) bridges the two metals asymmetrically with a more linear arrangement towards osmium (Rh-C(2)-O(2) = 121.3(13)°, Os-C(2)-O(2) = 155.6(14)°). This semi-bridging interaction with Rh results in a longer Rh-C(2) distance (2.41(2) Å) compared to Os-C(2) (2.02(2) Å), and this bonding assignment is also supported by the IR spectrum showing a low-frequency band at 1850 cm^{-1}.

NMR characterization of **3** confirms that the geometry observed in the crystal is maintained in solution. The ^{1}H NMR spectrum of **3** displays four methylene resonances for the osmacyclopentane group. The connectivity of the methylenes has been established using selective ^{1}H{^{31}P} NMR spectroscopy and ^{1}H/^{1}H HMQC experiments. Unlike the solid-state structure, in which the agostic interaction involving H(7B) is clearly different from uncoordinated H(7A), the solution NMR study shows only one broad resonance for both hydrogens

suggesting that a fluxional process interchanges them. Surprisingly, these hydrogens which are assumed to be involved in an agostic interaction, as shown in the solid-state structure, do not give rise to the highest-field resonance. However, labeling studies are strongly supportive of this interaction. If compound **3** is generated from **1** by reaction with $^{13}CH_2N_2$, the ^1H NMR resonance at 1.18 ppm shows a carbon-hydrogen coupling of 112 Hz. This is significantly less than that observed for the other methylenes of the butanediyl group, which have C-H coupling constants from 127 to 133 Hz. If, as suggested, both hydrogens of the "agostic" methylene group are alternating between an agostic and a terminal C-H bond, the average C-H coupling constant that would be observed is an average of the normal terminal C-H bond and the agostic C-H bond, which will have a reduced value by virtue of the 3-centre interaction involving Rh. Assuming a value of $^1J_{CH}$ = 130 Hz for the terminal bond, the value for the agostic C-H bond is calculated from the average to be 94 Hz, consistent with previous reports.[17] Compound **3** does not convert to **4** upon warming to ambient temperature, thus the two compounds are apparently derived by independent paths.

Further evidence for the agostic interaction comes from the ^{13}C NMR spectrum, where the resonance for C(7) appears at -0.3 ppm (the ^{13}C resonances are correlated to their attached protons using $^1H/^{13}C$ HMQC spectroscopy.) which is considerably upfield from the other ring carbons (24.6, 36.2, 37.8 ppm) possibly indicating an additional interaction with the electron-rich rhodium centre. Surprisingly, no coupling of this carbon to Rh is observed. Also observed in the ^{13}C NMR spectrum are three carbonyl resonances. The resonance at 186.4 ppm is assigned to a Rh-bound carbonyl based on selective $^{13}C\{^{31}P\}$ spectroscopy and a strong coupling of this carbon to rhodium ($^1J_{Rh-C}$ = 81 Hz). The signal at 182.4 ppm is due to a terminally bound osmium carbonyl, and the remaining resonance at 191.1 ppm is due to a semi-bridging carbonyl (no Rh coupling was observed due to the complexity of the signal). This is confirmed by a band at 1850 cm^{-1} in the IR spectrum.

At -40°C and above, the reaction of **2** with CH_2N_2 yields an increasing ratio of **4** to **3**. At -40°C the ratio is 1:50; at -20°C, 1:10; at 0°C, 3:1; until at room temperature only **4** is produced.

(ii) Labeling Studies.

In an effort to determine mechanistic information on the transformations of **2** to either **3** or **4**, the reactions of $[RhOs(CO)_4(\mu\text{-}CD_2)(dppm)_2][BF_4]$ (**2-D$_2$**) and $[RhOs(CO)_4(\mu\text{-}^{13}CH_2)(dppm)_2][BF_4]$ (**2-^{13}C**) with unlabeled CH_2N_2 have been monitored. In compound **3**, synthesized from either **2-^{13}C** or **2-D$_2$** at -60°C, the ^{13}C or deuterium label is scrambled equally between the two adjacent sites remote from Rh, with none appearing in the other sites, as shown in Scheme 2.2. The reaction of CH_2N_2 with (**2-^{13}C**) at ambient temperature yields **4**, in which the allyl group is ^{13}C enriched in a 1:2:1 proportion at the α, β and γ positions, with no ^{13}C incorporation into the methyl group (see Scheme 2.3). In the reaction of **2-D$_2$** with unlabeled CH_2N_2, deuterium incorporation into all four sites of **4** is observed (vide infra). There is no evidence of deuterium incorporation into the dppm ligand of either product **3** or **4**. In Schemes 2.2 and 2.3 only the metals and the relevant hydrocarbyl fragments are shown. Note also that ^{13}C- and ^{2}H- enriched ethylene is observed in all reactions. Based on the labeling studies, a reaction sequence that rationalizes the selective formation of products **3** or **4** is proposed and will be explained in the Discussion section.

(iii) Hydrogenolysis of Compounds 3 and 4.

Both complexes **3** and **4** react slowly with H_2 and undergo hydrogenolysis of the metal-alkyl bonds as shown in Scheme 2.4. In the reaction of **3** with H_2 the products obtained are the known dihydride complex $[RhOs(CO)_3(\mu\text{-}H)_2(dppm)_2]$-$[BF_4]^7$ together with butane, whereas the reaction of **4** yields the same dihydride complex along with propene and methane. Interestingly, $[RhOs(CO)_3(\mu\text{-}H)_2$-
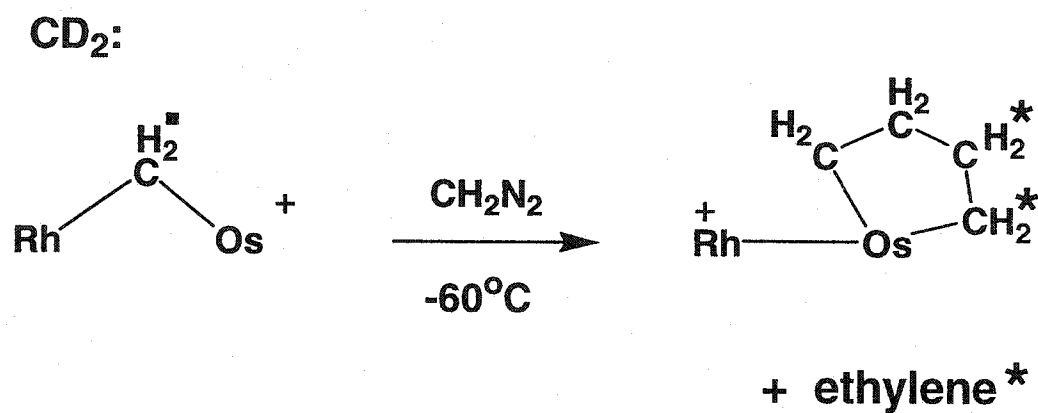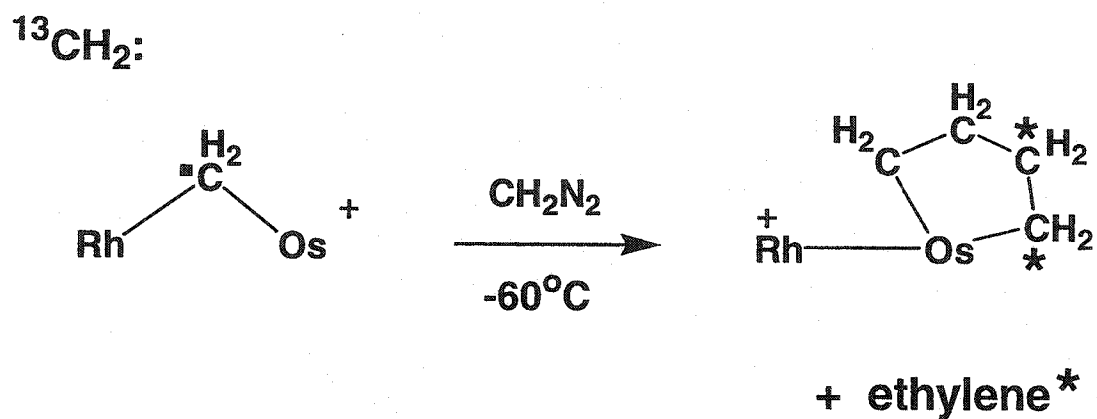
Scheme 2.2 Label Incorporation into Compound **3**
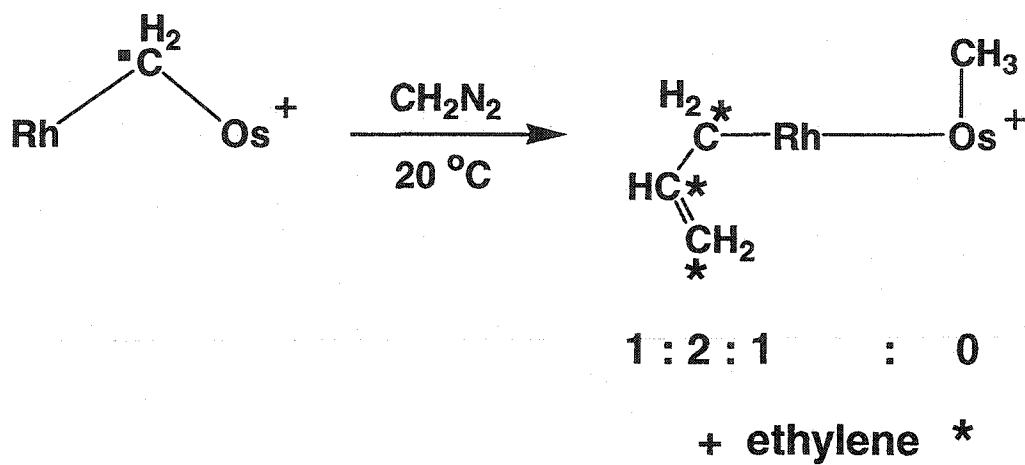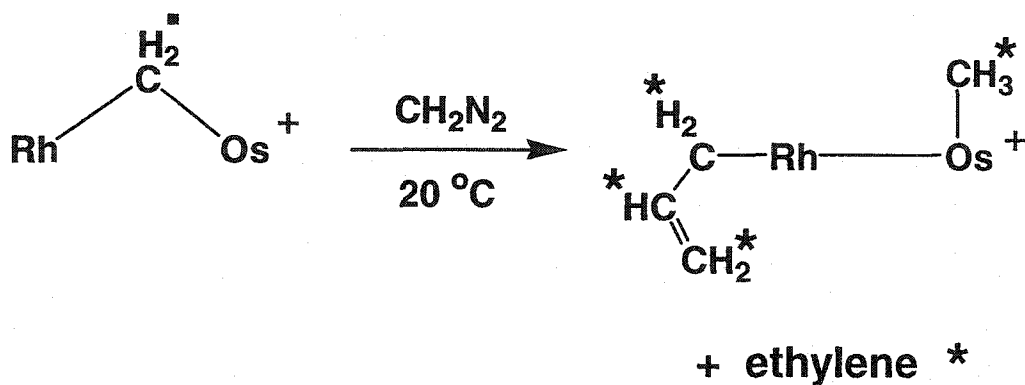
Scheme 2.3 Label Incorporation into Compound **4**

Scheme 2.4
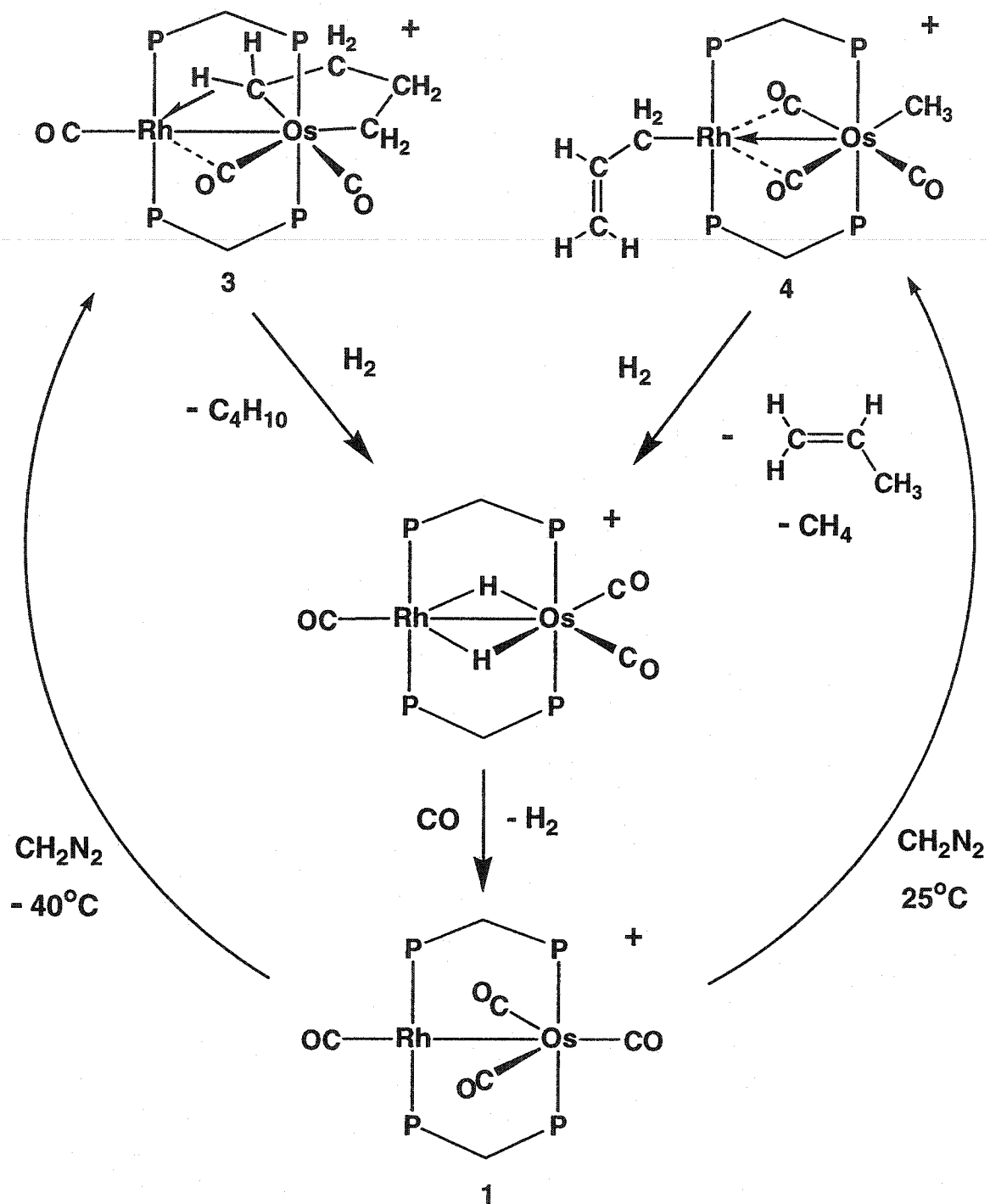
-(dppm)$_2$][BF$_4$] can be converted to the complex [RhOs(CO)$_4$(dppm)$_2$][BF$_4$] via addition of CO, and this complex can be converted back to either the osma-cyclopentane complex (3) or allyl/methyl complex (4) by addition of CH$_2$N$_2$ at the appropriate temperatures. Regeneration of the starting hydrocarbyl species 3 and 4 allows us to construct a pseudo-catalytic cycle for the selective formation of butane, or methane and propene, from diazomethane.

(iv) Ethylene Complexes

The transformation of the methylene-bridged species 2 into the allyl- and butanediyl- containing products, on reaction with diazomethane presumably proceeds through an ethylene or related C$_2$ intermediate. Clearly such a species could also be generated directly from a reaction involving ethylene. Although the reaction of [RhOs(CO)$_4$(dppm)$_2$][BF$_4$] (1) with ethylene does not occur, the addition of one equivalent of Me$_3$NO results in an instantaneous reaction yielding a mixture of compounds: the mono-ethylene complex [RhOs(C$_2$H$_4$)(CO)$_3$-(dppm)$_2$][BF$_4$] (6), the bis-ethylene complex [RhOs(C$_2$H$_4$)$_2$(CO)$_2$(dppm)$_2$][BF$_4$] (7), and the starting material (1) (Scheme 2.5). Unfortunately, instead of removing only one carbonyl from 1, yielding solely the mono-ethylene tricarbonyl compound (6), this mono-ethylene adduct is susceptible to removal of another CO under these reaction conditions, resulting in the formation of the bis-ethylene dicarbonyl compound (7) and unreacted starting material. As a result, we have been unable to obtain a pure sample of 6 without contamination by 7, and characterization is currently incomplete. The ^{31}P NMR spectrum of 6 displays a pattern that is characteristic for complexes in this system. The downfield multiplet at approximately 33.1 ppm represents the Rh-bound dppm phosphines but is superimposed over the similar resonance of compound 7, and the upfield multiplet at -7.1 ppm is from the Os-bound dppm phosphines.

The ^{13}C NMR spectrum of 6 has not yet been obtained and thus the location of the carbonyl groups on this bimetallic framework cannot be unequivocally

Scheme 2.5
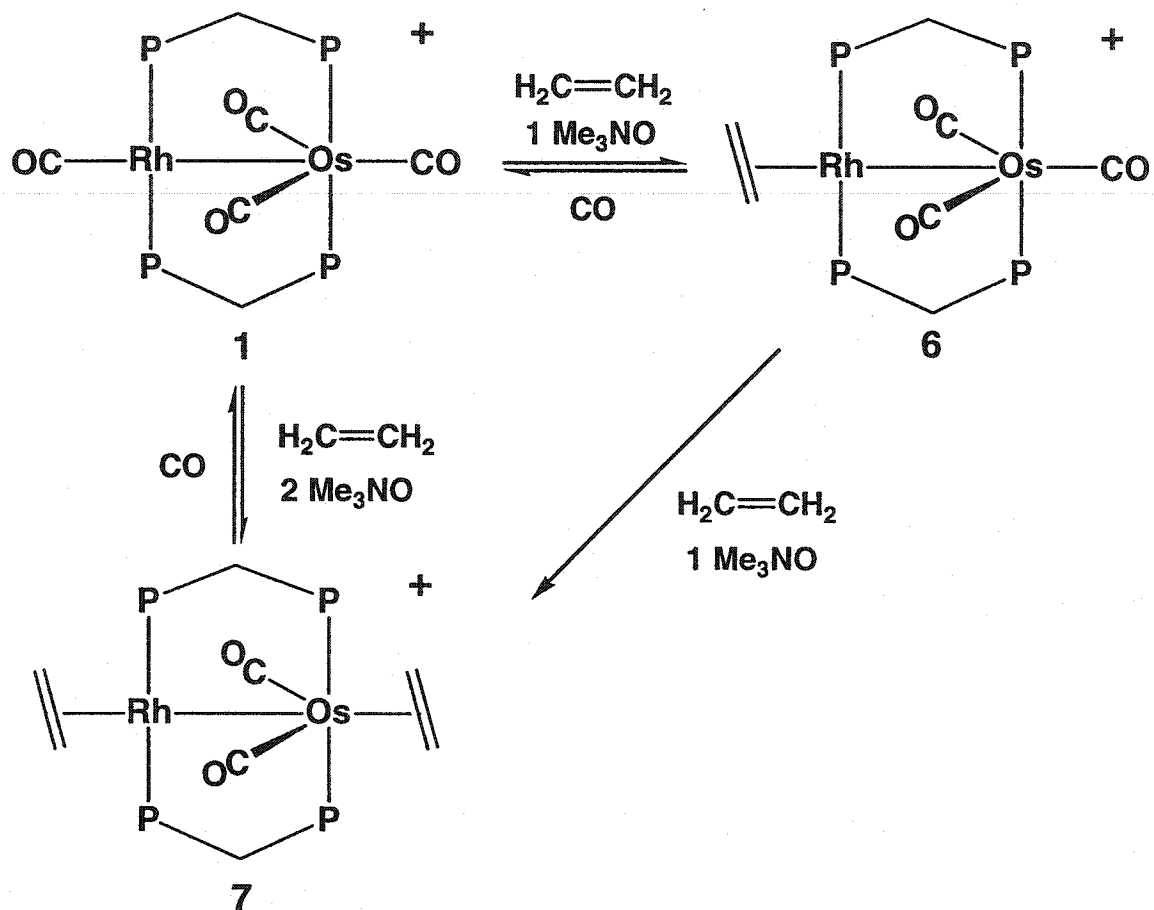
assigned. However, the very close similarity of the osmium-bound phosphine chemical shifts in the ^{31}P NMR spectrum of [RhOs(CO)$_4$(dppm)$_2$][BF$_4$] (**1**) and **6** (-7.6 and -7.1 ppm respectively) suggests that the coordination sphere of Os in both compounds is similar, suggesting that **6** also has three terminal carbonyl groups bound to osmium. In addition, the ^{31}P resonance for the Rh-bound phosphines of **6** is very similar to that of **7** (33.1 and 32.7 ppm respectively), which is proposed to have an identical geometry at Rh (vide infra). The ^{1}H NMR spectrum of **6** shows a multiplet at 4.04 ppm for the dppm-methylene protons, indicating back/front symmetry in the molecule, and a doublet at 2.76 ppm ($^2J_{Rh-H}$ = 2 Hz) for the ethylene group, which is rhodium-bound. Although **6** fails to react further with ethylene, a bis-ethylene complex can be obtained by the reaction of **1** with excess C$_2$H$_4$ in the presence of two equivalents of Me$_3$NO. This product, [RhOs(C$_2$H$_4$)$_2$(CO)$_2$(dppm)$_2$][BF$_4$] (**7**), has been shown by selective ^{1}H{^{31}P} NMR experiments to have an η^2-bound ethylene group on each metal. In the ^{1}H NMR spectrum, one ethylene group appears as a triplet at 0.90 ppm due to coupling of the protons to the osmium-bound phosphines and the other appears as a broad multiplet at 2.89 ppm due to coupling to both the rhodium-bound phosphines and to rhodium ($^2J_{Rh-H}$ = 2 Hz). The dppm methylene protons appear as a multiplet at 3.76 ppm indicating front/back symmetry in the molecule.

In the ^{13}C{^{1}H} NMR spectrum of **7**, a multiplet at 195.5 ppm represents two equivalent carbonyl groups which show coupling to the osmium-bound ^{31}P nuclei, suggesting that they are coordinated to osmium, and an 8 Hz coupling to Rh indicating a probable weak semi-bridging interaction with this metal. The semi-bridging nature of these carbonyls is further supported by the IR spectrum which shows a band at 1858 cm^{-1}. The rhodium-bound ethylene carbons are observed as a doublet at 64.6 ppm ($^1J_{Rh-C}$ = 11 Hz) while those bound to osmium appear as a singlet at 23.5 ppm. The dppm methylene carbons are represented by a multiplet at 34.5 ppm. As noted above, the ^{31}P NMR spectrum of the Rh-bound phosphines of **6** are almost superimposable with that of **7** while replacement of an

Os-bound carbonyl in **6** by the second ethylene has resulted in a significant shift of the Os-bound ^{31}P nuclei. Addition of CO to **6** or **7** regenerates the tetracarbonyl compound **1**, liberating ethylene.

(b) Reactivity of Compound 2
(i) Reaction with Other Diazoalkanes

We have also investigated the reaction of [RhOs(CO)$_4$(μ-CH$_2$)(dppm)$_2$]-[BF$_4$] (**2**) with two other diazoalkanes in attempts to effect C-C bond formation and to model possible intermediates in the synthesis of **3** and **4**. The reaction of ethyldiazoacetate and trimethylsilyldiazomethane with **2** proceeds slowly but goes cleanly to completion after several days. In these reactions the exclusive metal-containing complex produced is **1**, as shown in Scheme 2.6, together with formation of the corresponding olefins ethylacrylate and trimethylsilylethylene, which are readily identified by comparison of their ^{1}H NMR spectra with those of the authentic samples.

Scheme 2.6
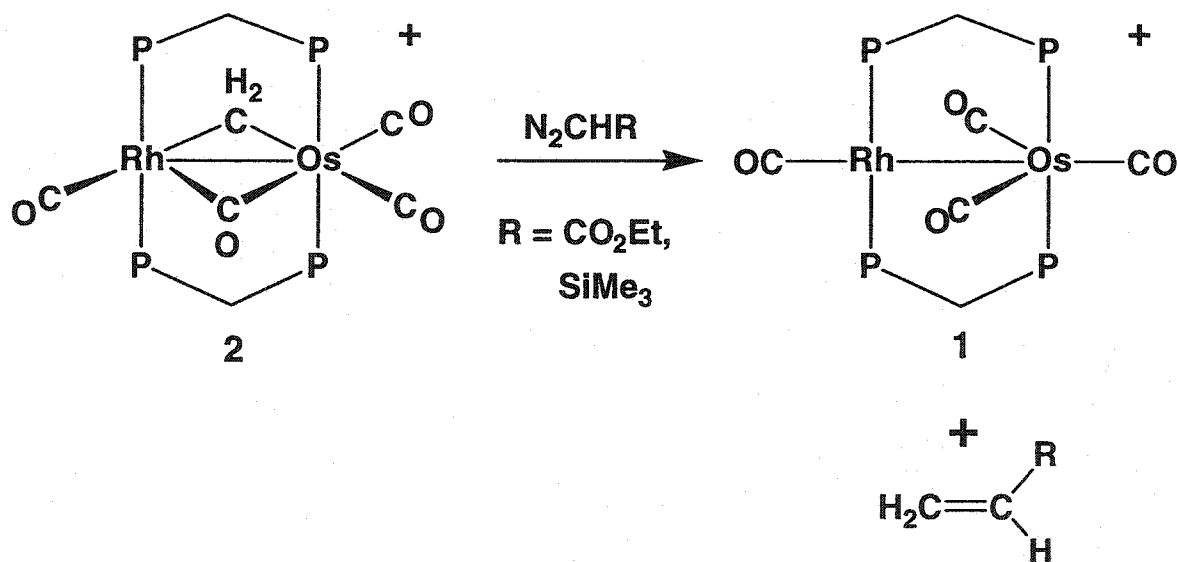
(ii) PMe₃ addition

The complex [RhOs(CO)$_3$(μ-CO)(μ-CH$_2$)(dppm)$_2$][BF$_4$] (**2**) reacts readily with PMe$_3$ yielding [RhOs(CO)$_3$(PMe$_3$)(μ-CH$_2$)(dppm)$_2$][BF$_4$] (**5**) quantitatively, accompanied by the loss of CO (Scheme 2.7). Compound **5** can also be effectively synthesized by the addition of PMe$_3$ to the tricarbonyl compound [RhOs(CO)$_3$(μ-CH$_2$)(dppm)$_2$][BF$_4$] (**8**). In the ^{31}P{^{1}H} NMR spectrum of **5** there are the typical low- and high-field multiplets at 18.2 and -10.8 ppm representing the rhodium and osmium-bound dppm phosphines, respectively, as well as a very high-field doublet of multiplets at -56.2 ppm due to the PMe$_3$ group. The large rhodium coupling ($^1J_{RhP}$ = 117 Hz) to this phosphine clearly indicates that the PMe$_3$ group is bound to rhodium. In the ^{1}H NMR spectrum, a doublet at 0.75 ppm ($^2J_{PH}$ = 8 Hz) represents the methyl protons of the PMe$_3$ group, while the bridging methylene group appears as a multiplet at 4.88 ppm, showing coupling to all five ^{31}P nuclei. Also bound to rhodium is a carbonyl which resonates at 199.6 ppm in the ^{13}C NMR spectrum ($^1J_{RhP}$ = 51 Hz). Two other carbonyls, terminally bound to osmium, are observed at 181.4 and 189.1 ppm. It is significant that all carbonyls in **5** are terminally bound. Similar structures have been observed in the analogous Ir/Ru (see Chapter 3) and Rh/Ru[24] compounds; the structures of which have been confirmed by X-ray crystallography. Although **5** is isoelectronic with **2** (a CO replaced by a PMe$_3$), the structures are significantly different with **5** having a PMe$_3$ group bound at the previously vacant site on Rh. The presence of two terminal ligands on rhodium in **5** is unexpected based on steric arguments since the larger PMe$_3$ group should favour the carbonyl group being pushed towards Os, resulting in a bridging configuration as seen in **2**. However, it appears that the terminal carbonyl may be favoured electronically since it can more effectively remove electron density on Rh, which is increased by the electron-donating PMe$_3$ group. While **2** rapidly reacts with diazomethane, the isoelectronic species **5**, is unreactive.

Scheme 2.7
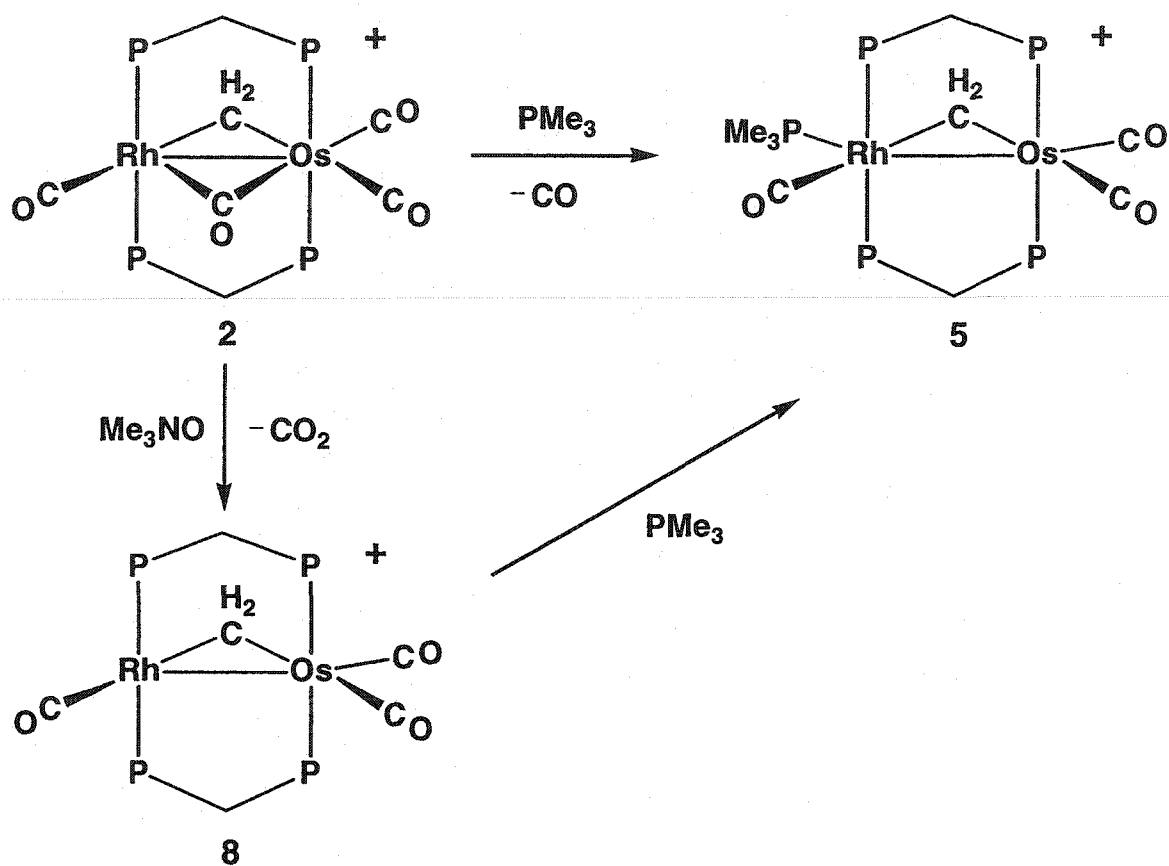
(iii) Reaction of 2 with dimethylallene

In order to investigate the reactivity of the methylene-bridged complexes with other unsaturated substrates, the compound $[RhOs(CO)_4(\mu\text{-}CH_2)(dppm)_2]$-$[BF_4]$ (2) was treated with dimethylallene. When a solution of 2 is combined with an excess of dimethylallene (5 equiv), a small amount of the compound $[RhOs(CO)_4(dppm)_2][BF_4]$ (1) is observed after several hours. After several days complete conversion to 1 and 1,1-dimethyl-1,3-butadiene has occurred. No additional products were observed when this reaction was carried out at lower

temperatures. Identification of the butadiene was accomplished by comparison of the ^{1}H NMR spectrum with that of an authentic sample.

(iv) CO Removal from 2 and Subsequent Reactivity

The observation that many of the reactions of 2 with substrates result in CO loss, suggested that the tricarbonyl analogue might show enhanced reactivity. One carbonyl of the compound $[RhOs(CO)_4(\mu-CH_2)(dppm)_2][BF_4]$ (2) can be removed using Me_3NO yielding $[RhOs(CO)_3(\mu-CH_2)(dppm)_2][BF_4]$ (8) (Scheme 2.7). While the tetracarbonyl complex (2) can be left under air for months without any decomposition, the tricarbonyl complex (8) decomposes after only a few days in the air; illustrating its increased reactivity. The ^{1}H NMR spectrum of 8 shows the bridging methylene group as a triplet of triplets at 6.38 ppm with coupling to both sets of dppm phosphines, indicating the bridging mode of this group. No coupling to rhodium is observed. In the ^{13}C NMR spectrum three carbonyl resonances are observed and are assigned on the basis of their coupling to rhodium or to the different ^{31}P nuclei. The resonance at 189.7 ppm represents a carbonyl bound to rhodium ($^1J_{Rh-C} = 63$ Hz), and peaks at 186.7 and 177.4 ppm which show coupling to only the osmium-bound phosphine ligands, indicate that there are two osmium-bound carbonyls. The osmium-bound carbonyl at 177.4 ppm also shows a small Rh coupling of 4 Hz which is probably due to two-bond coupling through the metal-metal bond. Although this carbonyl is attached to osmium, similar small rhodium couplings have been observed in this system when a carbonyl is located trans to a Rh-Os bond.[8a,b]

Not unexpectedly, the tricarbonyl complex 8 reacts with PMe_3, as observed with 2, yielding the PMe_3 adduct 5 instantly. In other chemistry, however, the two methylene-bridged complexes display different reactivities. Although the methylene-bridged tetracarbonyl complex 2 does not react with ethylene, the tricarbonyl complex 8 reacts readily with ethylene even at -78°C. However, several products are observed which have not yet been characterized. Compound

8 also reacts with CH_2N_2 at -78°C however, again, a mixture of products was obtained and these have not yet been characterized. Due to the large number of peaks present in the ^1H and ^{31}P NMR spectra, and the small quanitities of these many products, it is unclear as to whether compounds 3 and 4 are among the species present since the resonances for these species could not be unequivocally identified.

Discussion

(a) Mechanisms of Methylene Coupling

The observation that $[RhOs(CO)_4(dppm)_2][BF_4]$ (1) reacts with an excess of diazomethane at ambient temperature to give essentially quantitative conversion to $[RhOs(C_3H_5)(CH_3)(CO)_3(dppm)_2][BF_4]$ (4), in which an allyl group is bound to Rh with a methyl group bound to Os, is intriguing and led us to question how the transformation of four methylene groups into the allyl and methyl groups had occurred. We were also interested in establishing the functions of the two different metals in this process. We therefore reinvestigated the reaction of 1 with diazomethane at different temperatures in attempts to observe and characterize additional species that may help elucidate the methylene-coupling reaction. At the lowest temperature investigated (-80°C) the incorporation of only one methylene fragment occurred yielding the methylene-bridged product $[RhOs(CO)_3(\mu-CH_2)(\mu-CO)(dppm)_2][BF_4]$ (2). At temperatures between -60°C and -40°C a third species $[RhOs(C_4H_8)(CO)_3(dppm)_2][BF_4]$ (3), is observed in which the condensation of four methylene units to give a butanediyl fragment has occurred. Above -40°C, the allyl/methyl species $[RhOs(C_3H_5)(CH_3)(CO)_3(dppm)_2][BF_4]$ (4) begins to appear as a minor product, together with 3, although at temperatures approaching ambient it is the sole product. Compounds 3 and 4 do not interconvert at ambient temperature indicating that they are generated from 1 by

different reaction pathways. Compound **2** can also be used as the precursor of **3** and **4** by reaction with diazomethane at the temperatures given above. The isolation of **2** has allowed us to carry out isotope-labeling studies by generating the $^{13}CH_2$-labeled or CD_2-labeled compound, and following the distribution of the isotopes upon conversion to **3** and **4**. The incorporation of the labeled methylene group of **2** into the products **3** and **4** allows us to propose that **2** is involved as an intermediate in the formation of these products from **1**, and gives information on how these transformations occur. The sites of isotopic incorporation into these products were shown earlier in Schemes 2.2 and 2.3. In both cases some scrambling of the ^{13}C and ^{2}H occurred. In all insertion steps we assume that methylene insertion into the $Rh-CH_2$ bond rather than the $Os-CH_2$ bond occurs. This proposal is not only consistent with the results of the labeling study, but is also based on a predicted weaker Rh-C bond compared to Os-C bond,[18] and on the incipient coordinative unsaturation at Rh which allows for nucleophilic attack of diazomethane at this metal, followed by N_2 loss, generating a Rh-bound methylene group.

Although the X-ray structural details and spectroscopic parameters for **2** indicate a contribution from the carbonyl-bridged canonical form, which would give an 18-electron saturated configuration at both metals, nucleophilic displacement of a carbonyl by diazomethane is presumably favoured. The susceptibility of Rh to nucleophilic attack is demonstrated by the reaction of **2** with PMe$_3$ resulting in CO loss and coordination of PMe$_3$ to Rh, adjacent to the bridging methylene group. The failure of this PMe$_3$ adduct **5**, which is coordinatively saturated at both metals, to react with CH_2N_2 supports the idea that a vacant site at Rh is necessary. On the assumption that insertion occurs at Rh, the first product would be an ethylene-bridged structure **A**, shown in Scheme 2.8, in which the label (^{13}C or ^{2}H) has remained adjacent to Os. Conversion of a bridging ethylene group (μ-C_2H_4) into a terminally bound ethylene group (η^2-C_2H_4) has been demonstrated[19] and would yield the η^2-olefin product, **B**. η^2-olefin groups

Scheme 2.8
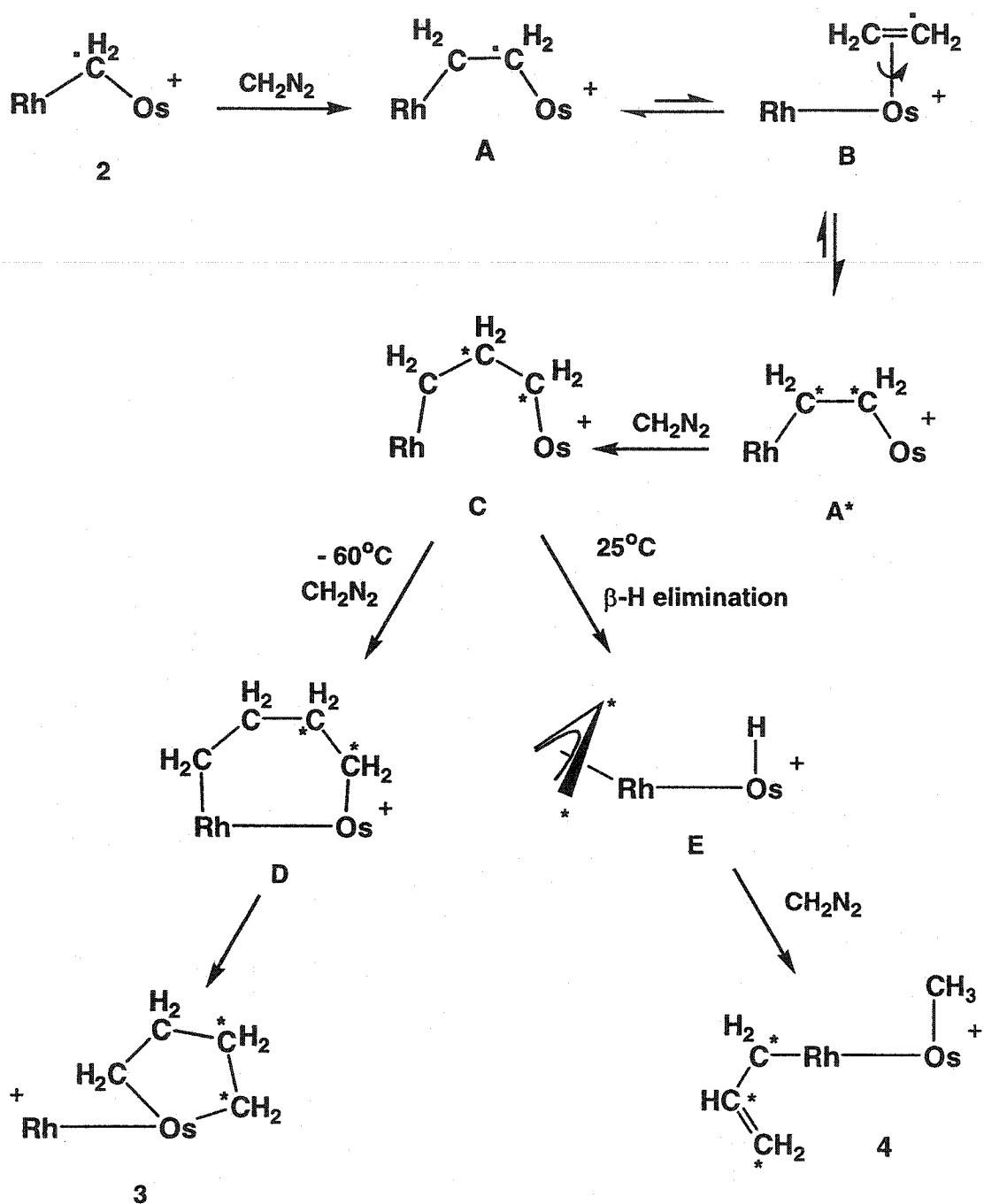
- ■ fully labeled
- * fractional enrichment

are known to undergo facile rotation about the metal-olefin bond[20] - a process that would scramble the label equally over the two CH_2 sites to give A* which shows the result of isotope scrambling upon movement of ethylene back to the bridging site. It is also worth noting at this stage that ethylene is always obtained in the reaction of either 1 or 2 with diazomethane. Presumably this occurs by ethylene loss from intermediate B, regenerating 1 which can react with CH_2N_2 to give 2. Methylene insertion into the $Rh-CH_2$ bond of A* would yield the propanediyl-bridged intermediate C, and subsequent insertion of another methylene group at Rh would yield D. The strained dimetallacycle D then presumably rearranges to the final product 3 which is favoured by formation of the unstrained 5-membered osmacycle. Note that stepwise insertion of methylene groups into the $Rh-CH_2$ bonds of the hydrocarbyl-bridged intermediates, together with ethylene rotation in B, rationalizes the sites of label incorporation in compound 3. The loss of the $Rh-CH_2$ bond upon alkyl migration from intermediate D to yield 3 is compensated for by the agostic interaction by this CH_2 group in the final product.

At higher temperatures, β-H elimination from the central carbon of the propanediyl-bridged fragment in C can occur to give an allyl/hydride complex, one possible isomer of which is shown as E, and subsequent methylene insertion into the Os-H bond could give the allyl/methyl complex 4. The sequence A*$\rightarrow$ C $\rightarrow$ E is not unlike that proposed by Pettit and coworkers, for the reaction of $[Fe_2(CO)_8(\mu-CH_2)]$ with ethylene,[21] in which a C_3H_6-bridged intermediate, analogous to C, is proposed to undergo β-hydride elimination to give an allyl/hydride complex, before elimination of propylene. Again, the proposal for the formation of 4 is consistent with the labeling study. β-H elimination from the ^{13}C-labeled C would give an allyl group having equal ^{13}C incorporation at one terminal CH_2 group and at the central carbon. Conversion to an η^1-allyl group would give a further dilution at the α and γ sites in 4 since there would be an equal probability of either end of the allyl group coordinating to the metal. According to

this scheme, no ^{13}C incorporation into the methyl group would occur since this carbon originates from unlabeled diazomethane. By arguments similar to those for ^{13}C scrambling, ^{2}H scrambling over the three allyl positions occurs. In addition, removal of one hydrogen from the central carbon in **C**, a site having ^{2}H incorporation, will incorporate some ^{2}H into the hydride group of **E** resulting in ^{2}H incorporation into the methyl group of **4**.

As the temperature is increased, the relative ratio of products **3**:**4** decreases. At -60°C only **3** is observed, whereas at -40°C the **3**:**4** ratio is 50:1, decreasing further to 10:1 at -20°C, and 1:3 at 0°C. At 25°C only **4** is observed. The slope of the Arrhenius plot (ln(k/T) vs (1/T)) for the formation of **4** from the proposed intermediate **C** would be steeper than that for the formation of **3**, indicating a greater $\Delta H^{\ddagger}$ value for **4** and a larger y-intercept indicating a greater $\Delta S^{\ddagger}$ value.

The greater $\Delta H^{\ddagger}$ for **4** is expected since this step involves the breaking of a C-H bond. The lower entropy of activation for **3** can be rationalized if we assume the formation of an intermediate diazomethane adduct resembling **F** (Scheme 2.9). This intermediate can then lose N_2 leading to incorporation of the fourth methylene unit and generating the osmacyclopentane complex **3**. However, at higher temperatures we suggest that formation of the diazomethane adduct becomes less favoured, favouring instead the propanediyl precursor **C**, which at these higher temperatures leads to β-hydride elimination yielding **E**. As noted earlier, this hydride subsequently reacts with diazomethane to give the methyl compound **4**. Unfortunately, the appropriate kinetic experiments to determine the activation enthalpy and entropy for the formation of **3** and **4** have not yet been carried out. One of the major problems in carrying out this study is the capricious nature of reactions involving diazomethane and transition metal complexes. We have found that under seemingly identical conditions the reaction of CH_2N_2 with **1** or **2** can lead to large amounts of polymethylene and ethylene in addition to the

Scheme 2.9
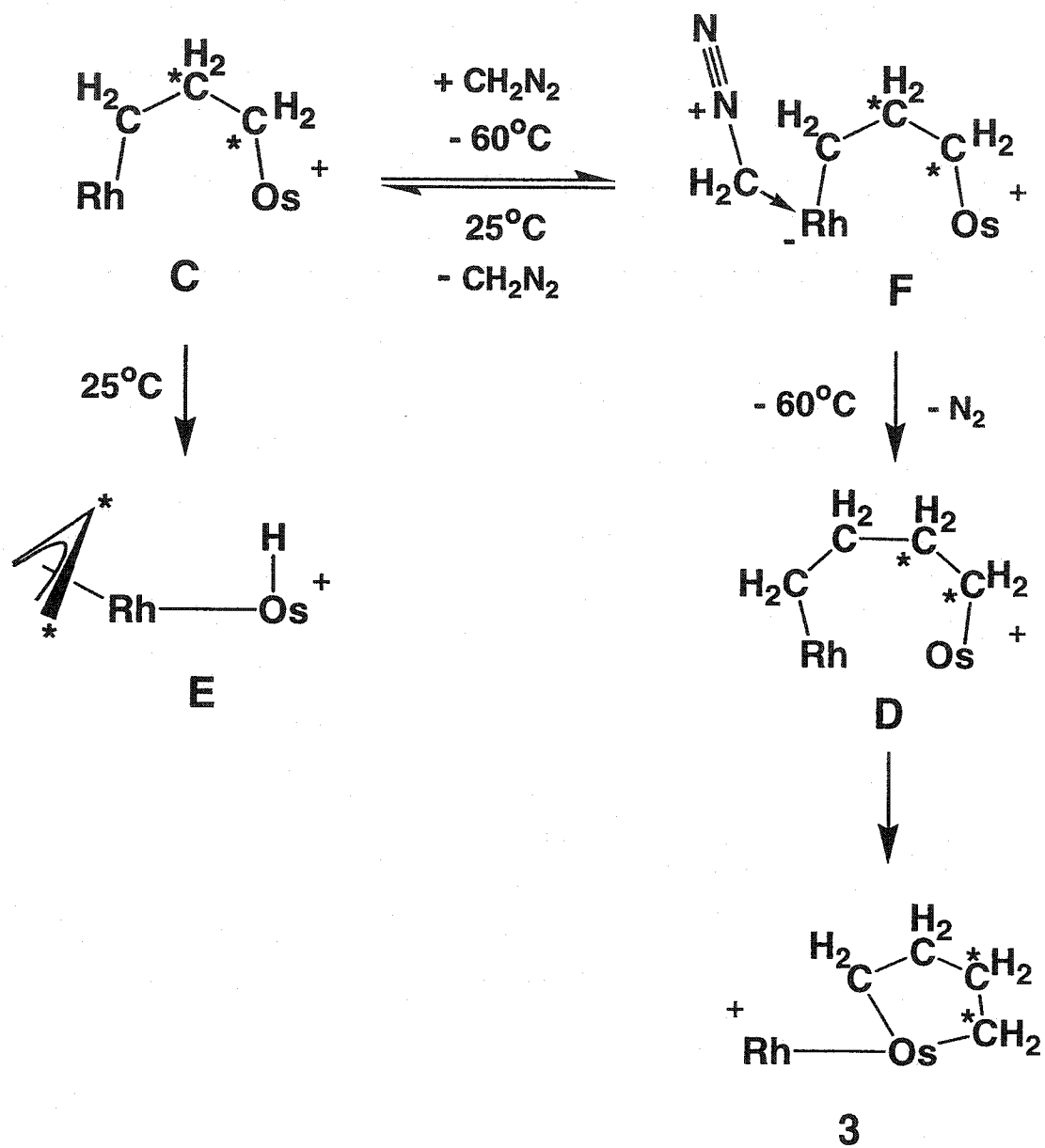
expected products (**3** or **4**). The formation of these organic products can result in incomplete formation of the complexes of interest, and difficulties in determining the concentration of diazomethane in solution during the reactions.

The exclusive formation of C_3(allyl) and C_4(butanediyl) complexes depending upon reaction temperature is unusual and suggests that the appropriate hydrocarbons could be formed in the presence of H_2, modeling another step in the Fischer-Tropsch reaction. Consequently both compounds **3** and **4** were reacted with H_2 and both proceeded slowly over a 48 hour period to generate the same hydride complex $[RhOs(CO)_3(\mu-H)_2(dppm)_2][BF_4]$. In the reaction of **4**, the hydrocarbon products obtained were propene and methane, as expected based on the hydrogenolysis of the rhodium-allyl and osmium-methyl bonds. Similarly, compound **3** yielded butane. The above dihydride complex is known to react with CO to yield the tetracarbonyl complex **1**[7] which as previously shown in this chapter, reacts with diazomethane to reform compound **3** or **4** depending upon the conditions. We have therefore modeled the selective conversion of methylene groups to these three hydrocarbons under H_2.

(b) Models for C_2 and C_3 Intermediates

In the conversion of methylene groups to larger hydrocarbyl fragments, a mechanism rationalizing the generation of the allyl/methyl complex **4** and the butanediyl product **3** and for the ultimate formation of propene, methane, and butane from the respective complexes under H_2, has been put forward. We were interested in modeling the individual steps to learn more about these trans- formations. The first step resulting in C-C bond formation involves the reaction of the methylene-bridged complex **2** with diazomethane, yielding an ethylene- bridged intermediate. In our proposal we assume nucleophilic attack of diazomethane at Rh. Such reactivity has been confirmed in the reaction of **2** with PMe_3 in which the PMe_3 adduct **5** is observed. This model supports our proposal

of nucleophilic attack at Rh initiating carbonyl displacement. It is also interesting that this PMe$_3$ adduct, having no vacant coordination site on Rh, does not undergo subsequent reaction with diazomethane, further illustrating the need for a vacant site on Rh to promote reactivity.

We have attempted to gain more direct support for diazoalkane coordination and activation at Rh by reacting 2 with other diazoalkanes such as N$_2$CH(CO$_2$Et) and N$_2$CHSiMe$_3$. In both cases, the respective olefins H$_2$C=C(H)R (R = CO$_2$Et, SiMe$_3$) and the complex [RhOs(CO)$_4$(dppm)$_2$][BF$_4$] (1) were obtained. We assume that the olefin-bridged species analogous to A (Scheme 2.5) was initially obtained, but was destabilized by repulsion between the dppm phenyls and the olefin substituents (CO$_2$Et, SiMe$_3$). A similar reactivity was observed by Knox in the reaction of the methylene-bridged diruthenium complex [(η-C$_5$H$_5$)$_2$Ru$_2$(μ-CH$_2$)(μ-CO)(CO)(MeCN)] with the sterically-demanding disubstituted diazoalkanes N$_2$=C(Ph)$_2$ and N$_2$=C(Ph)(C(O)Ph) where the olefins eliminated were H$_2$C=C(Ph)$_2$ and H$_2$C=C(Ph)(C(O)Ph).[23] Very few olefin adducts of these dppm-bridged complexes have been observed, probably because of the steric constraints involving the dppm phenyl groups which protrude into the area occupied by equatorially-bound olefin ligands, the substituents of which are directed above and below the equatorial plane and directed towards the bulky phenyl groups of the dppm ligands.

Another obvious route to an ethylene complex such as intermediate A in Scheme 2.8 is through the direct reaction of a suitable carbonyl precursor with ethylene. Therefore, the reaction of [RhOs(CO)$_4$(dppm)$_2$][BF$_4$] (1) with ethylene was conducted in the presence of Me$_3$NO, yielding a compound having the desired stoichiometry, namely, [RhOs(C$_2$H$_4$)(CO)$_3$(dppm)$_2$][BF$_4$] (6). However, this compound does not have the geometry suggested for A, which has an ethylene group bridging the metals, but instead has the ethylene group bound in a terminal η^2 coordination mode to Rh. Presumably 6 is the thermodynamic product while the ethylene-bridged intermediate A is a kinetic product in the methylene-coupling

reaction which is intercepted by reaction with diazomethane to eventually yield compounds **3** or **4**, before rearrangement to **6** is possible. The location of the ethylene group in this system appears to be important in the reaction with diazomethane. When **6** is treated with CH_2N_2 it forms neither the C_3 nor the C_4 condensation products, instead generating two other products which have not yet been characterized, but which will be the subject of further study.

Also produced in the above reaction, from removal of an additional CO and further reaction with ethylene is the bis-ethylene adduct $[RhOs(C_2H_4)_2(CO)_2(dppm)_2][BF_4]$ (**7**), which can be generated as the sole product by the reaction of $[RhOs(CO)_4(dppm)_2][BF_4]$ (**1**) with two equivalents of Me_3NO in the presence of ethylene. This bis-ethylene complex allows us the opportunity to test whether the C_4 species **3** may result from the coupling of two ethylene groups. Although the bis-ethylene compound **7** does not undergo an ethylene coupling reaction, the inability of this complex to generate the butanediyl fragment observed in **3** does not rule out an ethylene coupling mechanism for the synthesis of the C_4H_8 unit since the regiochemistry of the ethylene-coordination places them on opposite sides of the complex, preventing any coupling. Attempts to synthesize a tricarbonyl bis-ethylene complex, which would better represent a possible intermediate in the formation of the tricarbonyl complex **3**, by addition of CO led to the formation of **1** and the mono-ethylene complex **6**.

An important consideration in the synthesis of the *tricarbonyl* species **3** and **4** from the *tetracarbonyl* complex **2**, is the stage in the reaction at which CO loss occurs. This factor may dictate the course of the reaction and hence the products. A carbonyl can be removed from **2** yielding the tricarbonyl complex $[RhOs(CO)_3(\mu-CH_2)(dppm)_2][BF_4]$ (**8**), which was found to be very reactive with diazomethane producing several species even at $-78°C$. These products have not yet been characterized and the complexity of the resonances in the ^{31}P and ^{1}H NMR spectra prevent unequivocal identification of **3** and **4**. The mixture of products obtained in the low temperature CH_2N_2 reaction with **8** suggests that, in the

conversion of **2** to **3** and **4**, CO loss does not precede CH_2N_2 reaction with the complex. The presence of the fourth CO ligand of **2** somehow regulates the course of the reaction which selectively leads to the tricarbonyl complexes **3** and **4**. A similar reactivity has been observed in the analogous Rh/Ru tri- and tetra-carbonyl complexes.[24]

In our proposed mechanism to rationalize the formation of the C_3- and C_4-containing products **3** and **4**, the C_3 intermediate was proposed to result from CH_2 insertion into the Rh-C bond of an ethylene-bridged intermediate. Clearly the reverse process, ethylene insertion into the Rh-C bond of a bridging methylene species such as **2** or **8** should also give rise to C_3 species. Unfortunately, compound **2** proved to be unreactive towards all mono-olefin substrates, possibly due to the 18e configuration of Rh, where incoming substrates would coordinate. However, the tricarbonyl compound $[RhOs(CO)_3(\mu-CH_2)(dppm)_2][BF_4]$ (**8**) may be more susceptible to substrate addition due to the 16e configuration of Rh in this complex. The tricarbonyl analogue, **8**, is reactive but our investigation with this species is not complete. Compound **8** reacts with ethylene, however a mixture of products were obtained which have not yet been identified. Ethylene is an unfortunate choice because if insertion does occur, the initial product will contain a propanediyl-bridged group which should be susceptible to β-H elimination as proposed for the formation of **4** in Scheme 2.8. We therefore looked at other unsaturated substrates that would not contain β-hydrogens in the inserted product. Alkynes fit this description, and related work in the group with alkynes such as dimethyl acetylenedicarboxylate (DMAD) and hexafluorobutyne has led to the isolation and characterization of the C_3-bridged complex $[RhOs(MeO_2CC-CCO_2Me)CH_2)(CO)_3(dppm)_2][BF_4]$ in which the DMAD ligand has inserted into the Rh-CH_2 bond (Chart 2.1).[25] This complex has a C_3-bridged framework as proposed for intermediate **C** in Scheme 2.8, so may be a useful model for this intermediate.

Chart 2.1
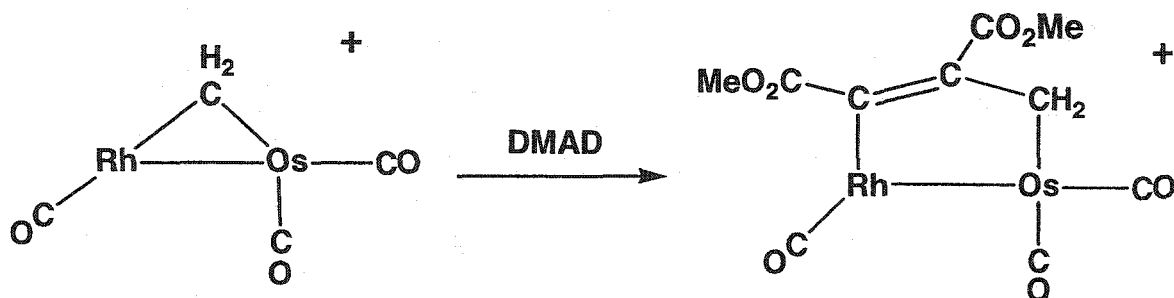
Allenes may also give rise to insertion products not having β-hydrogens, and dimethylallene is found to react cleanly with **2**. As shown in Scheme 2.10, dimethylallene might be expected to yield four possible products from insertion into the Rh-CH$_2$ bond. If the unsubstituted double bond of dimethylallene inserts into the Rh-CH$_2$ bond, two products are possible: (**a**) in which the "Me$_2$C=" moiety is adjacent to Rh or (**b**) in which this moiety is adjacent to the methylene group. Similarly, if the substituted double bond inserts into the Rh-CH$_2$ bond, species (**c**) or (**d**) are to be expected. Only (**a**) is susceptible to β-hydride elimination as proposed for intermediate **C**. Unfortunately, a product of insertion is not observed, and instead the reaction yields [RhOs(CO)$_4$(dppm)$_2$][BF$_4$] (**1**) and 1,1-dimethyl-1,3-butadiene. The CH$_2$ group of the butadiene presumably originates from coupling of the methylene-bridged group of **2** with the dimethylallene group, although labeling studies have not yet been conducted to confirm this.

We propose that formation of 1,1-dimethyl-1,3-butadiene proceeds (Scheme 2.11) via intermediate (**a**) in Scheme 2.10, by coordination of the dimethylallene group via the unsubstituted end of the dimethylallene to the vacant coordination site on rhodium with subsequent insertion of this end into the rhodium-methylene bond to form a C$_3$ bridging group (similar to intermediate **C** in the formation of **4**). β-hydride elimination of the central CH$_2$ group from this

Scheme 2.10
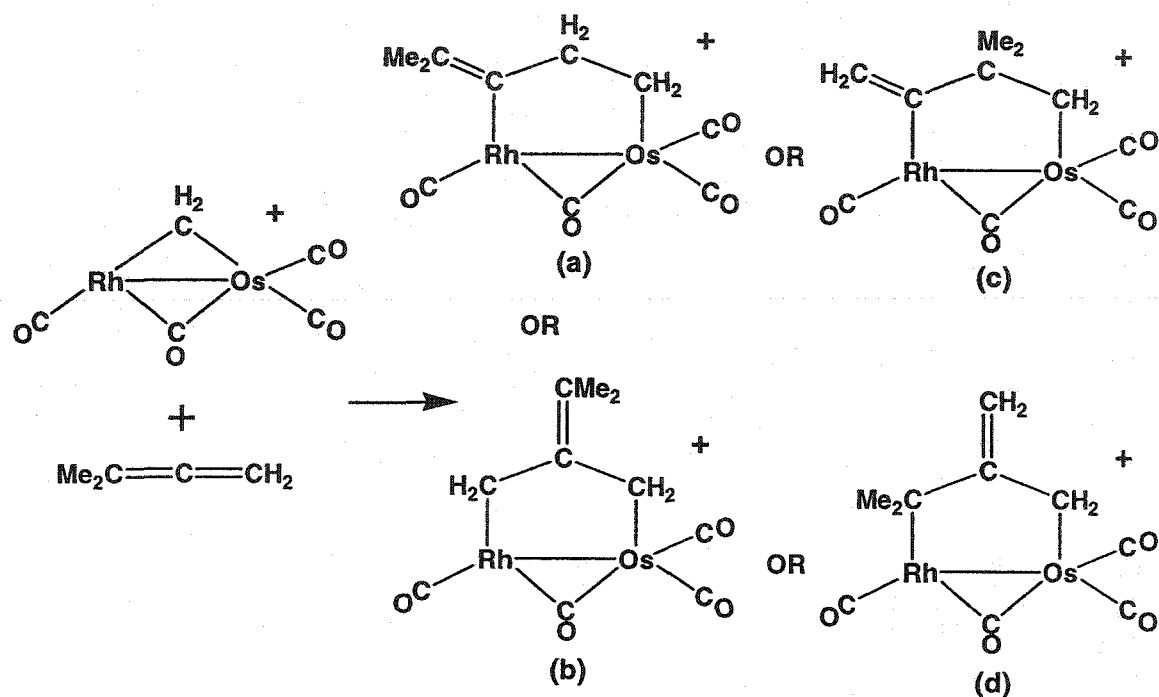
intermediate would form a hydride and an η^1-butadienyl group (analogous to **E** in the synthesis of **4**), and reductive elimination of the hydride and η^1-butadienyl group yields 1,1-dimethyl-1,3-butadiene and the complex [RhOs(CO)$_4$(dppm)$_2$]-[BF$_4$] (**1**). The major difference in the reactivity of dimethylallene and diazomethane (in the synthesis of **4**) with **2** is at the formation of the vinyl/hydride intermediate **E**. In our proposed mechanism for the formation of **4**, the hydride group of **E** reacts with diazomethane yielding a methyl group before reductive elimination of propene can occur.

Our proposal for 1,1-dimethylbutadiene formation from the reaction of **2** with 1,1-dimethylallene is supported by a related study involving the reaction of this substrate with the Rh/Ru analogue [RhRu(CO)$_3$(μ-CH$_2$)(dppm)$_2$][BF$_4$] in

Scheme 2.11
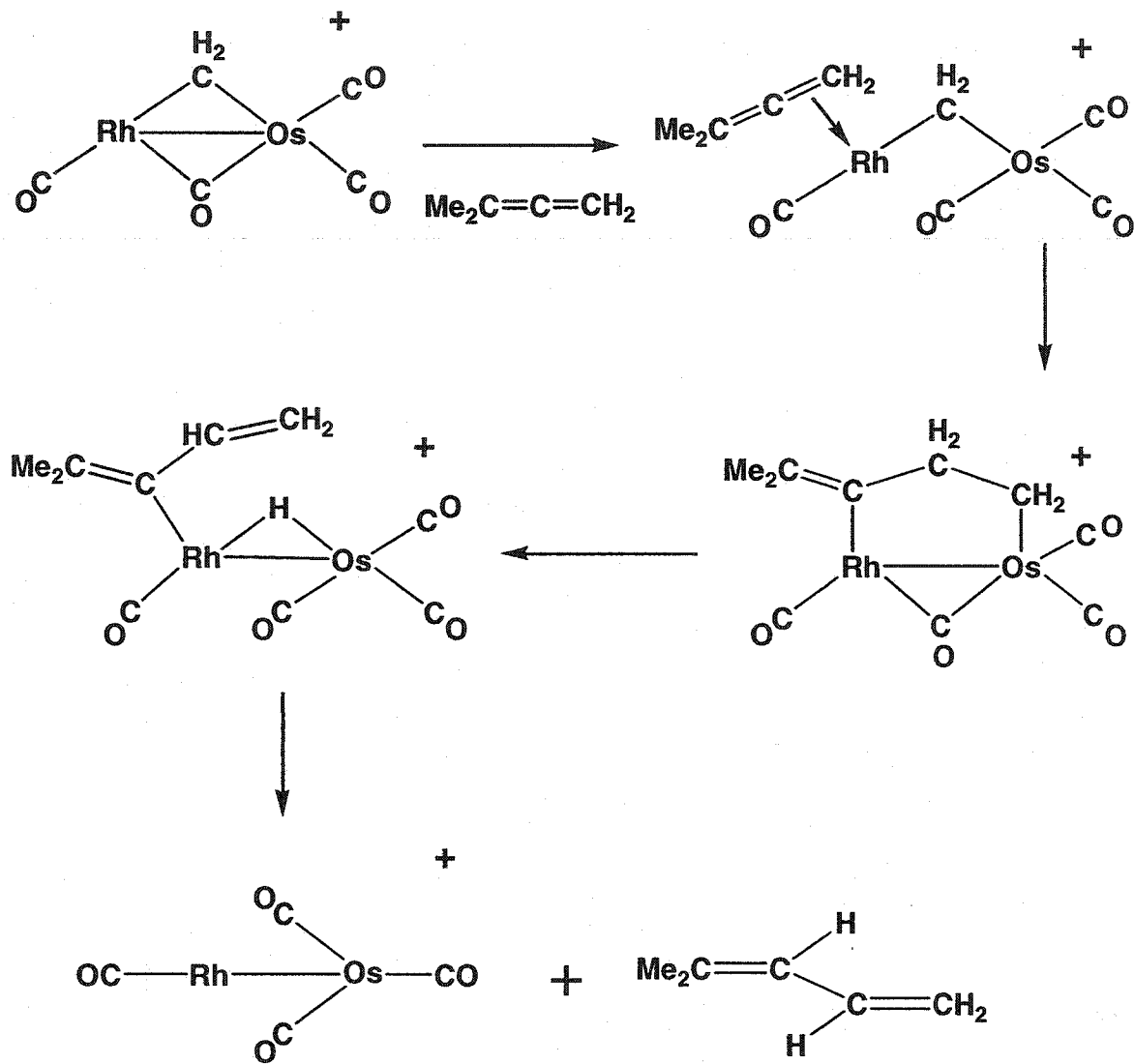
which the product diagrammed below (dppm groups omitted for clarity) is formed.[26] Clearly, this product has resulted from dimethylallene insertion with the Rh-CH$_2$ bond to yield structure (a) in Scheme 2.10. However, in this case, instead of β-hydride elimination as occurred for the Rh/Os complex, migration of the terminal CH$_2$ group to a carbonyl group occurred.
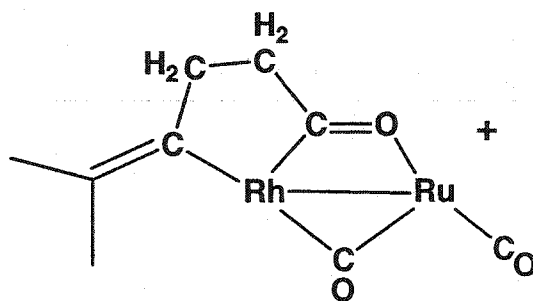
Conclusions

The *selective* coupling of methylene groups in this system to give either allyl (C$_3$) or metallacyclopentane (C$_4$) fragments on a mixed-metal core demonstrates how metals having different properties can have applications in Fischer-Tropsch chemistry. One goal of this research was to establish the roles of the different metals in the coupling of methylene fragments. Clearly in this homogeneous complex, the coordinative unsaturation of Rh coupled with the weaker Rh-C bond results in carbon-carbon bond formation at the Rh end of the bridging hydrocarbyl group. The greater strength of the Os-C bond serves to stabilize the intermediates, inhibiting hydrocarbon loss and thereby allowing subsequent increase in C-C chain length. Some hydrocarbon loss does occur as shown by the ethylene which is also formed in the diazomethane reactions with the methylene-bridged complex 2.

Currently, we are continuing in our attempts to synthesize stable analogues to the intermediates proposed in our mechanism for selective carbon-chain growth

shown in Scheme 2.8. In the next chapter, the effect of exchanging the Rh/Os core with Ir/Ru will be investigated.

References and Notes

1. (a) Pichler, *Adv. Catal.* **1952**, *4*, 271. (b) Jager, B.; Espinoza, R. *Catal. Today* **1995**, *23*, 17. (c) Van der Burgt, M.; van Klinken, J.; Sie, T. *The Shell Middle Distillate Synthesis Process*, 5th Synfuels Worldwide Symposium, Washington, DC, November 1985. (d) Haggin, J. *Chem. Eng. News*, 23rd July, 1990, p.27.

2. (a) Fischer, F.; Tropsch, H. *Brennst.-Chem.* **1926**, *7*, 97. *ibid. Chem. Ber.* **1926**, *59*, 830.

3. Kaminsky, M.P.; Winograd, N.; Geoffroy, G.L. and Vannice, M.A. *J. Am. Chem. Soc.* **1986**, *108*, 1315.

4. (a) Brady, R.C.; Pettit, R. *J. Am. Chem. Soc.* **1980**, *102*, 6181. (b) Brady, R.C.; Pettit, R.C. *J. Am. Chem. Soc.* **1981**, *103*, 1287. (c) Biloen, P.; Sachtler, W.M.H. *Adv. Catal.* **1980**, *30*, 165.

5. (a) Maitlis, P.M.; Lang, H.C.; Quyoum, R.; Turner, M.L.; Wang, Z.-Q. *Chem. Commun.* **1966**, 1. (b) Lang, H.C.; Turner, M.L.; Fornasiero, P.; Kaspar, J.; Graziani, M.; Maitlis, P.M. *J. Catal.* **1997**, *167*, 172.

6. Vannice, M.A. *J. Catal.* **1975**, *37*, 449.

7. Hilts, R.W.; Franchuk, R.A.; Cowie, M. *Organometallics*, **1991**, *10*, 304.

8. (a) Sterenberg, B. T. Ph.D. Thesis, **1997**. (b) Jenkins, J.A.; Cowie, M. *Organometallics* **1992**, *11*, 2767.

9. Programs for diffractometer operation, data collection, data reduction and absorption correction were those supplied by Bruker.

10. Sheldrick, G. M. Acta Crystallogr. **1990**, A46, 467–473.

11. Sheldrick, G. M. SHELXL-93. Program for crystal structure determination. University of Göttingen, Germany, **1993**.

12. Sterenberg, B.T.; McDonald, R.; Cowie, M. *Organometallics* **1997**, *16*, 2297.

13. Spectroscopic data for 4: ^{1}H NMR (400 MHz, CD2Cl2): δ 5.16 (ddt, $^3J_{HH}$ = 16, 10, 7 Hz, 1H), 3.70 (d, $^3J_{HH}$ = 10 Hz, 1H), 3.33 (m, 2H, dppm), 3.23 (m, 2H, dppm), 2.90, (d, $^3J_{HH}$ = 16 Hz, 1H), 2.60 (dm, $^3J_{HH}$ = 7 Hz, 2H), -0.26 (t, $^3J_{PH}$ = 7 Hz, 3H); $^{13}C\{^1H\}$ NMR (natural abundance): δ 232.6 (dt, $^1J_{RhC}$ = 27 Hz, CO), 203.5 (dt, $^1J_{RhC}$ = 12 Hz, CO), 179.0 (t, CO), 140.0 (s, CH), 111.0 (s, CH$_2$), 44.3 (d, $^1J_{RhC}$ = 24 Hz, CH$_2$), -17.7 (t, CH$_3$); $^{31}P\{^1H\}$ NMR: δ 27.2 (dm, $^1J_{RhP}$ = 148 Hz), -5.0 (m); IR: 2031, 1799 cm^{-1}. Anal. Calcd for RhOsP$_4$F$_4$BO$_3$C$_{57}$H$_{52}$: C, 51.99; H, 3.98. Found: C, 51.46; H, 3.35.

14. Trepanier, S. J.; Sterenberg, B. T.; McDonald, R.; Cowie, M. *J. Am. Chem. Soc.* **1999**, *121*, 2613.

15. Iggo, J. A.; Markham, D. P.; Shaw, B.L.; Thornton-Pett, M. *J. Chem. Soc., Chem. Commun.* **1985**, 432.

16. (a) *J. Am. Chem. Soc.* **1998**, *120*, 12539. (b) *Organometallics* **1985**, *4*, 1692. *Eur. J. Inorg. Chem.* **2000**, 753. *Acta. Cryst. Sec. C* **1991**, *C47*, 275. *Angew. Chem. Int. Ed.* **2001**, *40*, 781.

17. Brookhart, M.; Green, M.L.H.; Wong, L.-L. *Prog. Inorg. Chem.* **1988**, *36*, 1.

18. (a) Ziegler, T.; Tschinke, V. *Bonding Energetics in Organometallic Compounds*; Marks, T.J., Ed.; American Chemical Society: Washington, DC, 1990; Chapter 19. (b) Ziegler, T.; Tschinke, V.; Ursenbach, B. *J. Am. Chem. Soc.* **1987**, *109*, 4825. (c) Armentrout, P.B. *Bonding Energetics in Organometallic Compounds*; Marks, T.J., Ed.; American Chemical Society: Washington, DC, 1990; Chapter 2.

19. (a) Bender, B.R.; Ramage, D.L.; Norton, J.R.; Wiser, D.C.; Rappé, A.K. *J. Am. Chem. Soc.* **1997**, *119*, 5628. (b) Johnson, B.F.G.; Lewis, J.; Pippard, D.A. *J. Chem. Soc. Dalton* **1981**, 407.

20. Collman, J. P.; Hegedus, L.S.; Norton, J.R.; Finke, R.G. *Principles and Applications of Organotranstition Metal Chemistry* University Science Books: Mill Valley California, **1987**, pp. 523-660.

21. Sumner, C.E., Jr.; Riley, P.E.; Davis, R.E.; Pettit, R. *J. Am. Chem. Soc.* **1980**, *102*, 1752,

22. Herrmann, W. A. *Angew. Chem. Int. Ed.* **1978**, *17*, 800.

23. Akita, M.; Hua, R.; Knox, S. A. R.; Moro-oka, Y.; Nakanishi, S.; Yates, M. I. *Chem. Commun.* **1997**, 51.

24. Rowsell, B. D.; Trepanier, S. J.; Lam, R.; McDonald, R.; Cowie, M. *Organometallics* 2002, *21*, 3228.

25. Chokshi, A.; Graham, T.; Cowie, M. Unpublished results.

26. Rowsell, B.; Cowie, M. Unpublished results.

Chapter 3

Methylene-Bridged Ir/Ru Complexes

Introduction

The Fischer-Tropsch (FT) process, in which synthesis gas ($CO + H_2$) is converted into a variety of hydrocarbons, utilizes group 8 or 9 metals as catalysts.[1] Although all of the metals in these groups are active, only Co and Fe are widely used commercially. Ruthenium is actually the most active catalyst[2] but its greater expense limits its commercial utility. A comparison of these catalysts shows that the different metals give rise to substantially different product distributions.[3,4] For example, iron yields mainly linear alkenes and oxygenates, cobalt gives mostly linear alkanes, ruthenium gives high molecular-weight hydrocarbons, while rhodium yields oxygenates and hydrocarbons.

Reports of improved product selectivity in processes such as alkane isomerization and hydrogenolysis, when bimetallic catalysts were used instead of monometallic catalysts,[5] suggested to us that a similar approach might also be promising in FT chemistry. A few reports have already appeared on the use of mixed RuCo catalysts in FT chemistry, in which improved selectivity and activity were observed compared to the Co-supported catalysts alone.[6,7] In addition, improved activities and selectivities have been noted using combined Group 8/9 bimetallic catalysts in the formation of oxygenates from Syngas,[8] or in ethylene hydroformylation.[9]

Our interest in using heterobinuclear complexes of the groups 8 and 9 metals as models for bimetallic catalysts[10-13] led us to question whether combinations of these metals could lead to unusual examples of C-C bond formation of relevance to FT chemistry. In particular, we were interested in determining the functions of the different metals in such processes. In an earlier

study,[13] described in Chapter 2, we observed that a RhOs complex promoted facile coupling of diazomethane-generated methylene groups yielding either the allyl-methyl complex, [RhOs(η^1-C$_3$H$_5$)(CH$_3$)(CO)$_3$(dppm)$_2$][BF$_4$] (dppm = Ph$_2$PCH$_2$PPh$_2$), or a butanediyl-containing product, [RhOs(C$_4$H$_8$)(CO)$_3$(dppm)$_2$]-[BF$_4$], depending upon the temperature of the reaction. Labeling studies allowed us to suggest a mechanism, and a proposal was put forward rationalizing the functions of the different metals in these unusual transformations. An obvious extension of this study was to investigate other group 8/9 metal combinations for a comparison to the RhOs chemistry, and herein we present our initial findings on the related IrRu chemistry.

Experimental Section

General Comments

All solvents were dried (using appropriate drying agents), distilled before use, and stored under nitrogen. Reactions were performed under an argon atmosphere using standard Schlenk techniques. Ammonium hexachloroiridate(IV) was purchased from Vancouver Island Precious Metals and ruthenium trichloride hydrate was obtained from Colonial Metals Inc. Carbon-13 enriched CO (99.4% enrichment) was purchased from Isotec Inc. Diazomethane was generated from Diazald, which was purchased from Aldrich. The compounds Ru$_3$(CO)$_{12}$,[14] [PPN][HRu(CO)$_4$] (PPN = (Ph$_3$P)$_2$N)),[15] [IrCl(dppm)$_2$][16] and [Ir(CO)(dppm)$_2$]-[Cl][17] were prepared by the published procedures.

NMR spectra were recorded on a Bruker AM-400 spectrometer operating at 400.1 MHz for ^{1}H, 161.9 MHz for ^{31}P, and 100.6 MHz for ^{13}C nuclei. The ^{13}C{^{1}H}{^{31}P} NMR spectra were obtained on a Bruker WH-200 spectrometer operating at 50.3 MHz. Infrared spectra were obtained on a Nicolet Magna 750 FTIR Spectrometer with a NIC-Plan IR Microscope. The elemental analyses were

performed by the microanalytical service within the department. In cases where the analyses deviated significantly from the calculated values, the samples were also analyzed by Canadian Microanalytical Service Ltd. using V_2O_5, PbO_2, and Sn combustion catalysts. The values for the C analyses remained low presumably due to the formation of metal carbides. Spectroscopic data for the compounds prepared are presented in Table 3.1.

Electron ionization mass spectra were run on a Micromass ZabSpec. In all cases the distribution of isotope peaks for the appropriate parent ion matched very closely that calculated for the formulation given.

Preparation of Compounds

(a) [IrRu(CO)$_3$(μ-H)(dppm)$_2$] (1). The compound [PPN][HRu(CO)$_4$] (0.040 g, 0.06 mmol) was added to [IrCl(dppm)$_2$] (0.054 g, 0.06 mmol) dissolved in 5.0 mL of THF. The solution immediately turned green and a white precipitate formed (PPNCl). The green solution was concentrated under vacuum to *ca.* 2 mL and the solution allowed to slowly evaporate under an argon atmosphere. A green precipitate formed. Compound 1 is extremely air sensitive so all attempts to obtain elemental analyses resulted in sample decomposition; characterization was based on spectral methods, on the conversion of 1 to 2 by addition of carbon monoxide, and by the reverse transformation upon reaction of 2 with Me$_3$NO.

(b) [IrRu(H)(CO)$_3$(μ-CO)(dppm)$_2$] (2). The compound [Ir(CO)(dppm)$_2$][Cl] (1.026 g, 1.00 mmol) was suspended in 30 mL of THF, to which a suspension of [PPN][HRu(CO)$_4$] (0.753 g, 1.00 mmol) in 30 mL of THF was added by cannula. This mixture was stirred for 12 h resulting in an orange-brown solution and a white precipitate of [PPN][Cl]. The solution was concentrated under vacuum to ca. 10 mL, and 30 mL of ether was added to precipitate a yellow solid. The solid

Table 3.1 Spectroscopic Data For Compounds.

Compound	IR cm^{-1} [a,b]	NMR[c,d]		
		$^{31}P\{^1H\}$ (ppm)[e]	^1H (ppm)[f,g]	$^{13}C\{^1H\}$ (ppm)[g]
[IrRuH(CO)$_3$(dppm)$_2$] (1)	1926, 1835	48.4(m), 15.0(m)	-9.06(tt, $^2J_{PH}$ = 12,12 Hz, 1H), 3.87 (m, 4H),[d] -9.11(tt, $^2J_{PH}$ = 12,12 Hz, 1H), 4.13 (m, 2H), 3.75 (m, 2H)[h]	215.8(br, 2C), 185.6(t, $^2J_{PC}$ = 14 Hz, 1C),[d] 187.4(br, 1C), 212.0 (br, 1C), 223.5(br, 1C)[h]
[IrRuH(CO)$_4$(dppm)$_2$] (2)	1953(s), 1897(s), 1857(s), 1685(m)	40.3(m), 1.8(m)	5.85(m, 2H), 3.18(m, 2H), -9.95(t, $^2J_{PH}$ = 10 Hz, 1H)	262.7(m), 218.2(m), 207.8(t, $^2J_{PC}$ = 16.0 Hz), 189.1(m)[i]
[IrRu(CO)$_3$(μ-H)$_2$(dppm)$_2$]-[BF$_4$] (3)	2050(s), 2032(s), 1963(m)	34.6(m), 13.0(m)	4.14(m, 4H), -8.87 (tt, $^2J_{PH}$ = 13, 7 Hz, 2H)	198.3 (t, $^2J_{PC}$ = 11 Hz, 2C), 175.5 (t, $^2J_{PC}$ = 15 Hz, 1C)
[IrRu(CO)$_4$(dppm)$_2$][BF$_4$] (4)	1983(s), 1962(s)	30.0(m), -10.0(m)	4.30 (m, 4H)	206.7 (t, $^2J_{PC}$ = 13 Hz, 2C), 197.3 (t, $^2J_{PC}$ = 15 Hz, 1C), 172.2 (t, $^2J_{PC}$ = 10 Hz, 1C)

Compound	IR (ν_{CO})	^{31}P NMR	^{1}H NMR	^{13}C NMR
[IrRu(CO)$_4$(μ-CH$_2$)(dppm)$_2$]-[BF$_4$] (5)	2039(m), 1965(s), 1783(m)	30.2(m), 3.1(m)	3.87 (m, 2H), 3.57 (tt, $^3J_{PH}$ = 23, 11 Hz, 2H), 3.08 (m, 2H)	211.3 (dm, $^2J_{CC}$ = 23 Hz, 1C), 196.0 (t, $^2J_{PC}$ = 11 Hz, 1C), 191.7 (dt, $^2J_{PC}$ = 12 Hz, $^2J_{CC}$ = 23 Hz, 1C), 179.0 (t, $^2J_{PC}$ = 11 Hz, 1C)
[IrRu(C$_2$H$_4$)(CO)$_3$(μ-CH$_2$)(dppm)$_2$][BF$_4$] (6)	1962(ss), 2021(ss)	23.1(m), -5.3(m)	6.20 (tt, $^3J_{PH}$ = 10, 8 Hz, 2H), 4.46 (m, 2H), 3.28 (m, 2H), 1.73 (br, 2H), 0.54 (br, 2H)[h]	200.1 (t, $^2J_{PC}$ = 15 Hz, 1C), 195.8 (t, $^2J_{PC}$ = 11 Hz, 1C), 191.9 (t, $^2J_{PC}$ = 6 Hz, 1C), 64.3 (s, 1C), 22.6 (s), 26.4 (s)
[IrRu(PMe$_3$)(CO)$_3$(μ-CH$_2$)(dppm)$_2$][BF$_4$] (7)	2057(w), 1985(s), 1950(s), 1921(s)	24.8(m), -12.7(m), -59.1 (tt, $^2J_{PP}$ = 10, 9 Hz)	4.86 (m, 2H), 4.17 (ttd, $^3J_{PH}$ = 11, 7, 7 Hz, 2H), 3.44 (m, 2H), 0.95 (d, $^2J_{PH}$ = 10 Hz, 9H)	203.9 (t, $^2J_{PC}$ = 7 Hz, 1C), 198.9 (td, $^2J_{PC}$ = 18 Hz, $^3J_{PC}$ = 20 Hz, 1C), 183.3 (td, $^2J_{PC}$ = 15, 4 Hz, 1C)
[IrRu(NCMe)(CO)$_2$(μ-CH$_2$)(μ-CO)(dppm)$_2$][BF$_4$] (8)	1954(s), 1933(s,br), 1745(m)	37.9(m), 6.94(m)	3.97(m, 2H), 3.94(m, 2H), 2.88 (m, 2H), 1.14(s, 3H)	219.1 (br,t, $^2J_{PC}$ = 10 Hz, 1C), 195.6(t, $^2J_{PC}$ = 12 Hz, 1c), 182.5 (t, $^2J_{PC}$ = 11 Hz, 1C)

[IrRu(η^1-NC(H)C=CH$_2$)(CO)$_3$(μ-CH$_2$)(dppm)$_2$][BF$_4$] (9)	1965(s), 1948(s), 1755(m)	37.2(m), 6.6(m)	3.91 (m, 2H), 3.96 (m, 2H), 2.89 (m, 2H), 5.18 (d, $^3J_{HH}$ = 18 Hz, 1H), 5.68 (d, $^3J_{HH}$ = 11 Hz, 1H), 4.68 (dd, $^3J_{HH}$ = 18, 11 Hz, 1H)	218.8 (t, $^2J_{PC}$ = 10 Hz, 1C), 195.5 (t, $^2J_{PC}$ = 12 Hz, 1C), 182.2 (t, $^2J_{PC}$ = 11 Hz, 1C)

[a]IR abbreviations: s = strong, m = medium, w = weak. [b]Nujol mull or CH$_2$Cl$_2$ cast unless otherwise stated. [c]NMR abbreviations: m = multiplet, t = triplet, d = doublet, br = broad, tt = triplet of triplets, dt = doublet of triplets, ttd = triplet of triplets of doublets, td = triplet of doublets. [d]NMR data at 25 °C in CD$_2$Cl$_2$ unless otherwise stated. [e] ^{31}P chemical shifts referenced to external 85% H$_3$PO$_4$. [f]Chemical shifts for the phenyl hydrogens are not given. [g] ^{1}H and ^{13}C chemical shifts referenced to TMS. [h] -80 °C. [i] -60 °

was recrystallized from benzene/ether, and dried *in vacuo* (68% yield). Anal. Calcd for $C_{72}H_{63}O_4P_4IrRu$: C, 61.36; H, 4.51. Found: C, 61.79; H, 4.79%. This compound was found to have three molecules of benzene per complex molecule after drying *in vacuo*.

(c) **[IrRu(CO)₃(μ-H)₂(dppm)₂][BF₄] (3). Method (i).** Compound **1** (50 mg, 0.044 mmol) was dissolved in 5 mL of THF and $HBF_4 \cdot OMe_2$ (6 μL, 0.049 mmol) was added causing the solution to change from green to orange with the formation of a yellow precipitate. This precipitate was separated by filtration and washed with three 5 mL portions of diethylether (Yield = 74%). Anal. Calcd for $C_{53}H_{46}BF_4O_3P_4IrRu$: C, 51.55; H, 3.75. Found: C, 51.01; H, 3.65%. **Method (ii).** Compound **2** (300 mg, 0.255 mol) was dissolved in 15 mL of THF and $HBF_4 \cdot O(CH_3)_2$ (31 μL, 0.255 mmol) was added causing the solution to change immediately to orange. After 30 min a yellow precipitate formed. Ether (40 mL) was then added to precipitate the remaining solid. The solid obtained by this route was found to be a 1:1 mixture of **3** and **4**.

(d) **[IrRu(CO)₄(dppm)₂][BF₄] (4).** Compound **3** from method (i) part (c) or the mixture of solids from preparation (ii) part (c) was suspended in 20 mL of CH_2Cl_2 and stirred under a CO atmosphere for several hours after which a yellow slurry remained. Ether (40 mL) was then added to precipitate the remaining solid, which was then recrystallized from CH_2Cl_2/ether and dried *in vacuo* (82% yield based upon **1** or **2**). Anal. Calcd for $C_{54}H_{44}BF_4O_4P_4IrRu$: C, 51.44; H, 3.52. Found: C, 50.96; H, 3.65%. MS m/z 1175 ($M^+ - BF_4$).

(e) **[IrRu(CO)₄(μ-CH₂)(dppm)₂][BF₄] (5).** Compound **4** (100 mg, 0.079 mmol) was suspended in 15 mL of CH_2Cl_2. Diazomethane, generated from 300 mg of Diazald, was bubbled through this solution for 30 min after which the reaction

mixture became clear yellow. The solvent was evaporated to 5 mL under an argon stream and 30 mL of ether was added to precipitate a bright yellow solid. The solid was then recrystallized from CH_2Cl_2/ether and dried *in vacuo* (92% yield). Anal. Calcd for $C_{55}H_{46}BF_4O_4RuP_4Ir$: C, 51.81; H, 3.64. Found: C, 51.37; H, 3.84%. MS m/z 1189 ($M^+ - BF_4$).

(f) $[IrRu(C_2H_4)(CO)_3(\mu\text{-}CH_2)(dppm)_2][BF_4]$ (6). Method (i). Compound **5** (10 mg, 0.0078 mmol) and Me_3NO (0.60 mg, 0.0078 mmol) were placed in an NMR tube containing an ethylene atmosphere. Upon addition of CD_2Cl_2 (0.5 mL), the solution immediately changed to orange and then to yellow within 1 min. Elemental analyses were not performed due to facile loss of ethylene upon workup. **Method (ii).** Compound **5** (10 mg, 0.0078 mmol) and Me_3NO (0.6 mg, 0.0078 mmol) were placed in an NMR tube and CD_2Cl_2 (0.5 mL) was added. The solution was mixed for ca. 20 s, producing an orange-red solution, and then cooled to -78 °C. CH_2N_2 was then bubbled through the cold solution for 1 min resulting in a yellow solution. ^{31}P and ^1H NMR spectroscopy indicated that the product was compound **6**.

(g) $[IrRu(PMe_3)(CO)_3(\mu\text{-}CH_2)(dppm)_2][BF_4]$ (7). Method (i). Compound **5** (40 mg, 0.031 mmol) was dissolved in 2 mL of CH_2Cl_2 and PMe_3 (100 μL of a 1.0 M THF solution, 0.10 mmol) was added. The solution was stirred for 8 h. Ether (20 mL) was then added to precipitate a yellow solid. The solid was recrystallized from CH_2Cl_2/ether and dried *in vacuo* (48% yield). Anal. Calcd for $C_{57.2}H_{55.4}BCl_{0.4}F_4O_3P_5IrRu$: C, 51.27; H, 4.17; Cl, 1.05. Found: C, 51.12; H, 4.17; Cl, 0.57%. MS m/z 1237 ($M^+ - BF_4$). The fractional methylene chloride (0.2) of crystallization results because desolvation occurs readily upon removal of the crystals from the mother liquor. However, even storage under vacuum for extended periods does not result in complete solvent loss. The presence of

CH_2Cl_2 has been established by analysis for Cl and by ^1H NMR spectroscopy in chloroform.

Method (ii). Compound **6** (0.0078 mmol) was prepared *in situ* in an NMR tube containing 0.5 mL of CD_2Cl_2. 1 equiv of PMe_3 (7.8 µL of a 1.0 M THF solution, 0.0078 mmol) was added and the solution was mixed for 1 min. ^1H and ^{31}P NMR spectroscopy indicated complete conversion to **7**.

(h) $[IrRu(NCCH_3)(CO)_3(\mu-CH_2)(dppm)_2][BF_4]$ (8). Compound **5** (60.0 mg, 0.047 mmol), trimethylamine oxide (3.5 mg, 0.047 mmol) and acetonitrile (0.10 mL, 1.9 mmol) were placed into a flask and 3 mL of CH_2Cl_2 was added. The solution immediately turned orange. After stirring for 15 min 20 mL of ether was added, resulting in the precipitation of an orange solid. After filtering, this solid was recrystallized from CH_2Cl_2/ether and dried *in vacuo* (87% yield). Anal. Calcd for $C_{56}H_{49}NBF_4O_3P_4IrRu$: C, 52.22; H, 3.83; N, 1.09. Found: C, 51.52; H, 3.74; N, 1.29%. MS m/z 1161 ($M^+-BF_4-NCCH_3$).

(i) $[IrRu(\eta^1-NC(H)C=CH_2)(CO)_3(\mu-CH_2)(dppm)_2][BF_4]$ (9). Method (i). Compound **5** (60 mg. 0.047 mmol), Me_3NO (3.5 mg, 0.047 mmol) and acrylonitrile (0.1 mL, 1.5 mmol) were placed into a flask and 3 mL of CH_2Cl_2 were added. The solution immediately became orange. After stirring for 15 min, ether (20 mL) was added to precipitate an orange solid. The solid was then recrystallized from CH_2Cl_2/ether and dried *in vacuo* (85% yield). Anal. Calcd for $C_{57}H_{49}NBF_4O_3P_4IrRu$: C, 52.67; H, 3.80; N, 1.08%. Found: C, 51.65; H, 3.80; N, 1.34%.

Method (ii). Compound **6** (0.0078 mmol) was prepared *in situ* in an NMR tube as described in part (f) in 0.5 mL of CD_2Cl_2 and 1 equiv of acrylonitrile (0.5 µL) was added. ^1H and ^{31}P NMR spectroscopy indicated complete conversion to **9**.

X-ray Data Collection

X-ray data collection and structure solutions were carried out by Dr. R. McDonald in the departmental X-ray Structure Determination Laboratory. Yellow crystals of $[IrRuH(CO)_3(\mu\text{-}CO)(dppm)_2] \cdot 4.5C_6H_6$ (2) were obtained from slow diffusion of Et_2O into a benzene solution of the compound. Data were collected on a Bruker P4/RA/SMART 1000 CCD diffractometer[18] using Mo $K\alpha$ radiation at -80 °C. Unit cell parameters were obtained from a least-squares refinement of the setting angles of 6209 reflections from the data collection. The lack of systematic absences and the diffraction symmetry indicated that the space group was $P1$ or $P\bar{1}$; the latter was established by successful refinement of the structure. The data were corrected for absorption through use of Gaussian integration (indexing and measurement of crystal faces). See Table 3.2 for a summary of crystal data and X-ray data collection information.

Yellow crystals of $[IrRu(CO)_3(\mu\text{-}CH_2)(\mu\text{-}CO)(dppm)_2][BF_4] \cdot CH_2Cl_2$ (5) were obtained from slow evaporation of a dichloromethane solution of the compound. A suitable crystal was immediately transferred to the cold nitrogen stream after removal from the mother liquor. Others deteriorated noticeably owing to solvent loss after 10 min. Data were collected on a Bruker P4/RA/SMART 1000 CCD diffractometer using Mo $K\alpha$ radiation at -80 °C. Unit cell parameters were obtained from a least-squares refinement of the setting angles of 6519 reflections from the data collection. The space group was determined to be $P2_1/n$ (a nonstandard setting of $P2_1/c$ [No. 14]). The data were corrected for absorption through use of the *SADABS* procedure.

Light yellow crystals of $[IrRu(CO)_3(PMe_3)(\mu\text{-}CH_2)(dppm)_2][BF_4] \cdot 2CH_2Cl_2$ (8) were obtained from slow diffusion of Et_2O into a CH_2Cl_2 solution of the compound. Crystals again lost solvent quickly so they had to be mounted in the cold stream without delay. Data were collected on a Bruker P4/RA

Table 3.2 Crystallographic Data for Compounds **2**, **5** and **7**.

	[IrRuH(CO)$_4$(dppm)$_2$]•4.5C$_6$H$_6$ (2)	[IrRu(CO)$_4$(μ-CH$_2$)(dppm)$_2$]-[BF$_4$]•CH$_2$Cl$_2$ (5)	[IrRu(PMe$_3$)(CO)$_3$(μ-CH$_2$)-(dppm)$_2$][BF$_4$]•2CH$_2$Cl$_2$ (7)
formula	C$_{81}$H$_{72}$IrO$_4$P$_4$Ru	C$_{56}$H$_{48}$BCl$_2$F$_4$IrO$_4$P$_4$Ru	C$_{59}$H$_{59}$BCl$_4$F$_4$IrO$_3$P$_5$Ru
fw	1526.54	1359.80	1492.79
cryst dimens, mm	0.36x0.28x0.26	0.26x0.15x0.04	0.57x0.30x0.17
cryst syst	triclinic	monoclinic	monoclinic
space group	$P\bar{1}$ (No. 2)	$P2_1/n$ (non-standard setting of $P2_1/c$ (No. 14)	$P\,2_1/c$ (No. 14)
a, Å	14.0744(6)[a]	12.5470(7)[b]	20.356(2)[c]
b, Å	15.4510(7)	27.1409(13)	12.7687(11)
c, Å	17.6510(8)	15.9168(9)	23.221(2)
α, deg	89.8086(8)	90.0	90.0
β, deg	70.6204(8)	96.4809(10)	91.583(8)
γ, deg	74.9795(7)	90.0	90.0
V, Å^3	3482.8(3)	5385.6(5)	6033.2(9)
Z	2	4	4
d_{calcd}, g cm^{-3}	1.456	1.677	1.643
μ, mm^{-1}	2.267	3.027	9.583
diffractometer	Bruker P4/RA/SMART 1000 CCD[d]	Bruker P4/RA/SMART 1000 CCD[d]	Bruker P4/RA[d]
radiation (λ, Å)	graphite-monochromated Mo K$_\alpha$ (0.71073)	graphite-monochromated Mo K$_\alpha$ (0.71073)	graphite-monochromated Cu K$_\alpha$ (1.54178)
T, °C	-80	-80	-60

	ϕ rotations (0.3°)/ω scans (0.3°) (30 s exposures)	ϕ rotations (0.3°)/ω scans (0.3°) (30 s exposures)	ω
scan type			
2θ (max), deg	51.40	52.82	115.0
no. of unique refns	13178	11017	7345
no. of observns (NO)	11250 ($F_o^2 \geq 2\sigma$ (F_o^2))	6835 ($F_o^2 \geq 2\sigma$ (F_o^2))	6167 ($F_o^2 \geq 2\sigma$ (F_o^2))
range of abs corr factors	0.6416-0.4104	0.8943-0.5913	0.9873-0.3069
residual density e/Å^3	1.744 and -1.097	1.469 and -1.529	2.643 and - 2.124
R_1 ($F_o^2 > 2\sigma(F_o^2)$)[e]	0.0365	0.0549	0.0659
wR_2 (all data)	0.0973	0.1617	0.1739
GOF(S)[f]	1.040[$F_o^2 \geq -3\sigma$ (F_o^2)]	0.997 [$F_o^2 \geq -3\sigma$ (F_o^2)]	1.074 [$F_o^2 \geq -3\sigma(F_o^2)$]

[a]Cell parameters obtained from least-squares refinement of 6209 centered reflections.

[b]Cell parameters obtained from least-squares refinement of 6519 centered reflections.

[c]Cell parameters obtained from least-squares refinement of 44 reflections with $54.2 < 2\theta < 58.0°$.

[d]Programs for diffractometer operation, data reduction and absorption correction were those supplied by Bruker.

[e]$R_1 = \Sigma||F_o|-|F_c||/\Sigma|F_o|$; $wR_2 = [\Sigma w(F_o^2-F_c^2)^2/\Sigma w(F_o^4)]^{1/2}$.

[f]$S = [\Sigma w(F_o^2-F_c^2)^2/(n-p)]^{1/2}$ (n = number of data; p = number of parameters varied; $w = [\sigma^2(F_o^2) + (a_oP)^2 + a_1P]^{-1}$, where $P = [\max(F_o^2, 0) = 2F_c^2]/3)$. For 2 $a_o = 0.0494$, $a_1 = 1.1045$; for 5 $a_o = 0.0812$, $a_1 = 0.0$; for 7 $a_o = 0.1042$, $a_1 = 45.2444$.

diffractometer using Cu Kα radiation at -60 °C. Unit cell parameters were obtained from a least- squares refinement of the setting angles of 44 reflections with $54.2° < 2\theta < 58.0°$. The monoclinic diffraction symmetry and systematic absences indicated the space group to be $P2_1/c$ (No. 14). The data were corrected for absorption through use of a semiempirical method (ψ scans of several high-θ reflections).

Structure Solution and Refinement

The structure of **2** was solved using direct methods (*SHELXS-86*),[19a] and refinement was completed using the program *SHELXL-93*.[19b] Hydrogen atoms were assigned positions based on the geometries of their attached carbon atoms, and were given thermal parameters 20% greater than those of the attached carbons. The metal atom positions were disordered such that one position (Ir/Ru') was refined as an 85:15 combination of Ir and Ru, while the other (Ru/Ir') was refined with the reverse ratio (85% Ru and 15% Ir). This disorder of the metals is accompanied by a disorder of hydride and one carbonyl group (C(3)O(3)) such that the primed atoms (H(1'), C(3') and O(3')) have 15% occupancies while the related unprimed atoms have 85% occupancies. The iridium-hydride distances (Ir–H(1) and Ir'–H(1')) were fixed at 1.75 Å, and further restraints were applied to generate an idealized geometry for the hydride ligand H(1'): d(P(2)···H(1')) = d(P(4)···H(1')) = 2.75 Å; d(C(2)···H(1')) = d(C(4)···H(1')) = 3.00 Å. Distance restraints were also imposed upon the 15%-occupancy carbonyl group (C(3')O(3')) attached to Ir': d(Ir'–C(3')) = 1.92 Å; d(O(3')–C(3')) = 1.15 Å; d(Ir'···O(3')) = 3.07 Å. The final model for **2** refined to values of $R_1(F) = 0.0365$ (for 11250 data with $F_o^2 \geq 2\sigma(F_o^2)$) and $wR_2(F^2) = 0.0973$ (for all 13178 independent data).

The structure of **5** was solved using direct methods (*SHELXS-86*),[19a] and refinement was completed using the program *SHELXL-93*.[19b] Hydrogen atoms

were assigned positions based on the geometries of their attached carbon atoms, and were given thermal parameters 20% greater than those of the attached carbons. The metal atom positions were disordered such that one position (Ir/Ru') was refined as an 75:25 combination of Ir and Ru, while the other (Ru/Ir') was refined with the reverse ratio (75% Ru and 25% Ir). The bridging methylene group (C(5)) and one carbonyl (C(4)O(4)) were found to be disordered over two sites in the same 75:25 ratio. As a result there are two closely spaced positions for the methylene carbon with C(5) closer to Ir and C(5') closer to Ir'. The distances of C(5') to Ir' (2.05 Å) and Ru' (2.31 Å) were given fixed values based on the corresponding Ir–C(5) and Ru–C(5) distances. Distances within the BF_4^- ion (F–B = 1.35 A; F$\cdots$F = 2.20 Å) and the disordered solvent CH_2Cl_2 molecule (Cl–C = 1.80 Å; Cl$\cdots$Cl = 2.95 Å) were given fixed idealized values. The final model for **5** refined to values of $R_1(F)$ = 0.0549 (for 6835 data with $F_o^2 \geq 2\sigma(F_o^2)$) and $wR_2(F^2)$ = 0.0973 (for all 11017 independent data).

The structure of **7** was solved using direct methods (*SHELXS-86*),[19a] and refinement was completed using the program *SHELXL-93*.[19b] Hydrogen atoms were assigned positions based on the geometries of their attached carbon atoms, and were given thermal parameters 20% greater than those of the attached carbons. The final model for **7** refined to values of $R_1(F)$ = 0.0659 (for 6167 data with $F_o^2 \geq 2\sigma(F_o^2)$) and $wR_2(F^2)$ = 0.1739 (for all 7345 independent data).

Measurement of Exchange in Compound 6

The rate of rotation for the ethylene group of compound **6** was determined from the results of ^{1}H NMR selective inversion-recovery experiments. Data analysis was carried out according to the method of McClung and coworkers[20] (Mrs. G. Aarts is acknowledged for conducting the NMR experiments and interpretation of the results obtained.). The activation parameters for this process were calculated form the rate constants (k) at various temperatures (Dr. R. B.

Jordan is acknowledged for the calculation of the activation parameters.). Refer to Table 3.3 for results.

Table 3.3 Data for Variable-Temperature Line-Shape Analysis for Ethylene Rotation in Compound 6.

Temperature (^{o}C)	k(observed) (s^{-1})	k(calculated) (s^{-1})
-86.7	3.0	2.5
-81.6	5.5	5.8
-75.3	13	16
-69.6	40	36
-63.8	90	82

Using the Arrhenius equation,

$$\ln(k/T) = \ln(k_B/h) - \Delta H^{\ddagger}/RT + \Delta S^{\ddagger}/R$$

where: R = gas constant

k_B = Boltzmann's constant

h = Planck's constant

T = temperature in K

a plot of ln(k/T) vs 1/T gives a straight line with a slope equal to $-\Delta H^{\ddagger}/R$ and an intercept equal to $\Delta S^{\ddagger}/R + \ln(k_B/h)$

Calculated Parameters: $\Delta H^{\ddagger}$ = 11.47 kcal/mol

$\Delta S^{\ddagger}$ = 5.7 kcal/mol K

Results

As described in the previous chapter, the precursor compound used for the generation of methylene-containing species involving the Rh/Os combination of metals was the cationic, tetracarbonyl [RhOs(CO)$_4$(dppm)$_2$][BF$_4$].[13] The analogous IrRu complex has now been synthesized in a similar sequence of reactions, as outlined in Scheme 3.1. In the first step the heterobinuclear framework is constructed via chloride displacement from [IrCl(dppm)$_2$] by the [HRu(CO)$_4$]⁻ anion accompanied by unwinding of the chelating, Ir-bound dppm ligands into positions bridging both metals. The ^{31}P{^{1}H} NMR spectrum of the product, [IrRu(CO)$_3$(μ-H)(dppm)$_2$] (1) is characteristic of an AA'BB' spin system in these dppm-bridged heterobinuclear systems.[16,21] The Ir-bound phosphine signal (15.0 ppm) appears upfield from that of the Ru end (48.4 ppm), as is typically observed for dppm complexes of these metals.[21-23] At -80 °C the NMR spectral data are consistent with the structure shown in Scheme 3.1. In the ^{1}H NMR spectrum the hydride resonance appears as an apparent quintet at -9.06 ppm, with essentially equal coupling (*ca.* 12 Hz) to both sets of inequivalent phosphorus nuclei, and the dppm methylene protons appear as two multiplets showing inequivalent environments on each side of the IrRuP$_4$ plane. The ^{13}C{^{1}H} NMR spectrum shows the expected three carbonyl resonances at 187.4, 212.0 and 223.5 ppm, with the high-field resonance corresponding to that bound to Ir, while the other two are due to Ru-bound carbonyls. The proposed structure for 1 is similar to those suggested previously for the RhRu[23,24] and RhFe[21] analogues, but differs from that proposed for the RhOs compound, in which the hydride is terminally bound to Os.[16] Apparently, in the RhOs compound the strong metal-hydride bond involving the late, third-row metal[25] favors a terminal Os-H bond instead of a bridging interaction. As the temperature is raised the spectral data for 1 indicate

that a fluxional process is occurring that interchanges the two Ru-bound carbonyls. As a result, the $^{13}C\{^1H\}$ NMR spectrum at ambient temperature shows only two carbonyl resonances in a 1:2 ratio at 185.6 and 215.8 ppm, respectively, with the second resonance corresponding to the two Ru-bound carbonyls. The

Scheme 3.1
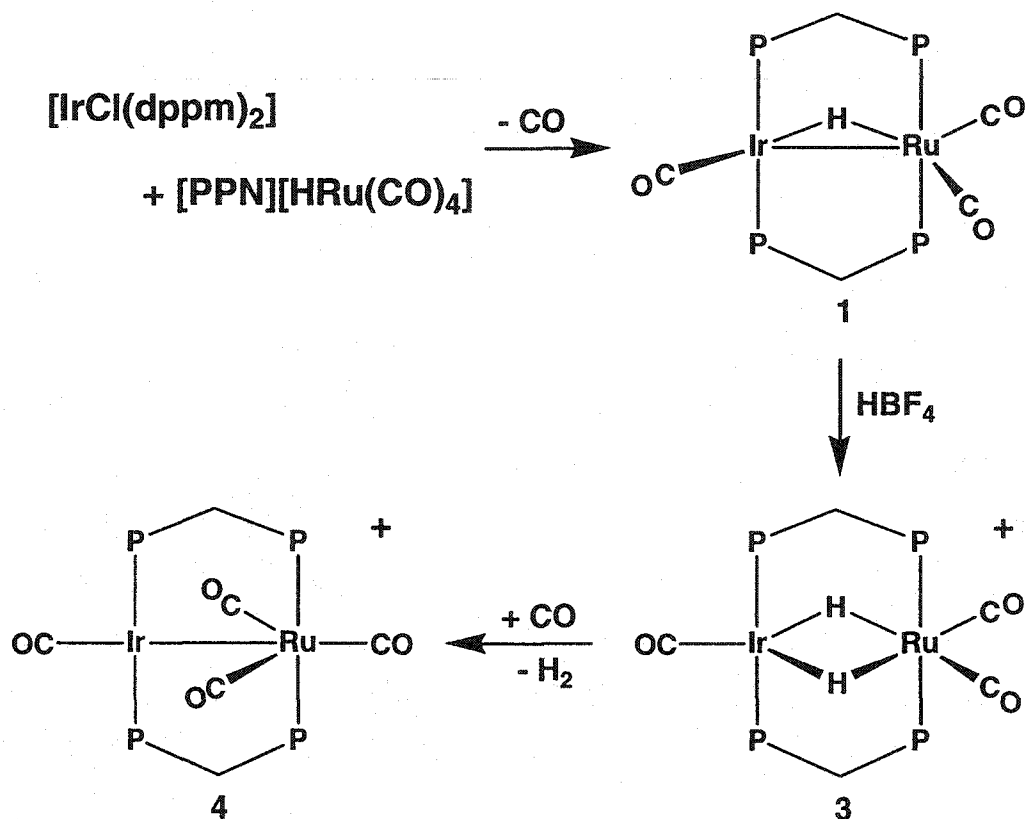
process that equilibrates both Ru-bound carbonyls probably occurs by an inversion of the "(OC)Ir(μ-H)Ru(CO)₂" core as shown in Chart 3.1 (dppm groups above and below the plane of the drawing omitted), in which the hydride ligand moves between the two metals with an accompanying twist of the metal coordination spheres. Also, as a result of this process, the environments on each side of the IrRuP₄ plane become averaged resulting in a single resonance in the ^1H NMR

spectrum for the four dppm methylene hydrogens. Such fluxionality is common for hydride- and dppm- bridged complexes.[21,26]

Chart 3.1
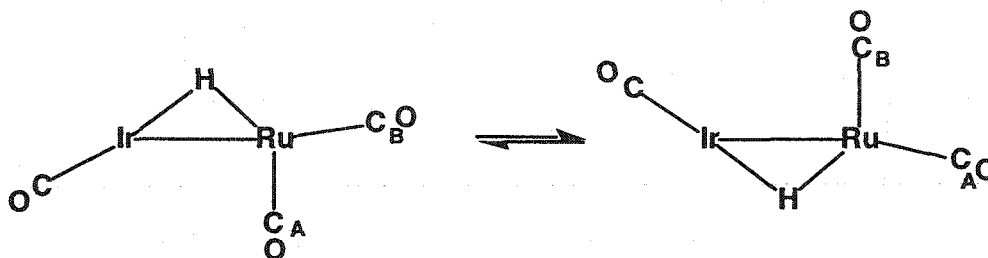
Conversion of **1** into [IrRu(CO)$_3$(μ-H)$_2$(dppm)$_2$][BF$_4$] (**3**) is readily accomplished by protonation with HBF$_4$, and this product appears to be exactly analogous to the known IrOs,[16] RhRu[23,24] and RhOs[10] complexes. In **3** both bridging hydrides are chemically equivalent and appear as a triplet of triplets in the ^{1}H NMR spectrum at -8.87 ppm. The coupling of these hydrides to the Ir-bound phosphines ($^2J_{PH}$ = 13 Hz) is greater than that involving the Ru-bound phosphines ($^2J_{PH}$ = 7 Hz), presumably reflecting stronger interactions with the heavier metal. In the ^{13}C{^{1}H} NMR spectrum the Ir-bound carbonyl is at characteristically higher field than those on Ru (175.5 (1C) *vs.* 198.3 (2C) ppm).

Reaction of **3** with CO results in H$_2$ displacement yielding the targeted tetracarbonyl precursor [IrRu(CO)$_4$(dppm)$_2$][BF$_4$] (**4**), the structure of which is supported by all spectroscopic parameters; in particular, the highest field carbonyl resonance in the ^{13}C{^{1}H} NMR spectrum corresponds to that bound to Ir, while the low-field resonance corresponds to the two carbonyls on Ru that are bent towards Ir. A low-field shift of such carbonyls has previously been noted[27] and presumably reflects a weak interaction with the second metal. This interaction is clearly not strong enough to constitute a conventional bridging arrangement since

the IR spectrum shows only terminal carbonyl stretches (ν(CO): 1983, 1962 cm^{-1}).
Compound **4** is analogous to the previously reported RhOs,[10] IrOs[16] and
RhRu[23,24] compounds.

The extreme air sensitivity of **1** and the resulting difficulties in handling this
compound meant that the preparation of **4** by the route shown in Scheme 3.1 was
unpredictable, often resulting in a number of unidentified decomposition products.
Certainly the preparation of **4** by this route was much less convenient than the
preparations of the analogous RhOs,[10] RhRu[23,24] and RhFe[28] compounds. We
therefore sought an alternate precursor to compound **4**. If instead of using
[IrCl(dppm)$_2$] in the preparation of **1**, the carbonyl adduct [Ir(CO)(dppm)$_2$][Cl] is
used, the *tetracarbonyl* compound [IrRu(H)(CO)$_3$(μ-CO)(dppm)$_2$] (**2**) is obtained,
as shown in Scheme 3.2.

Scheme 3.2
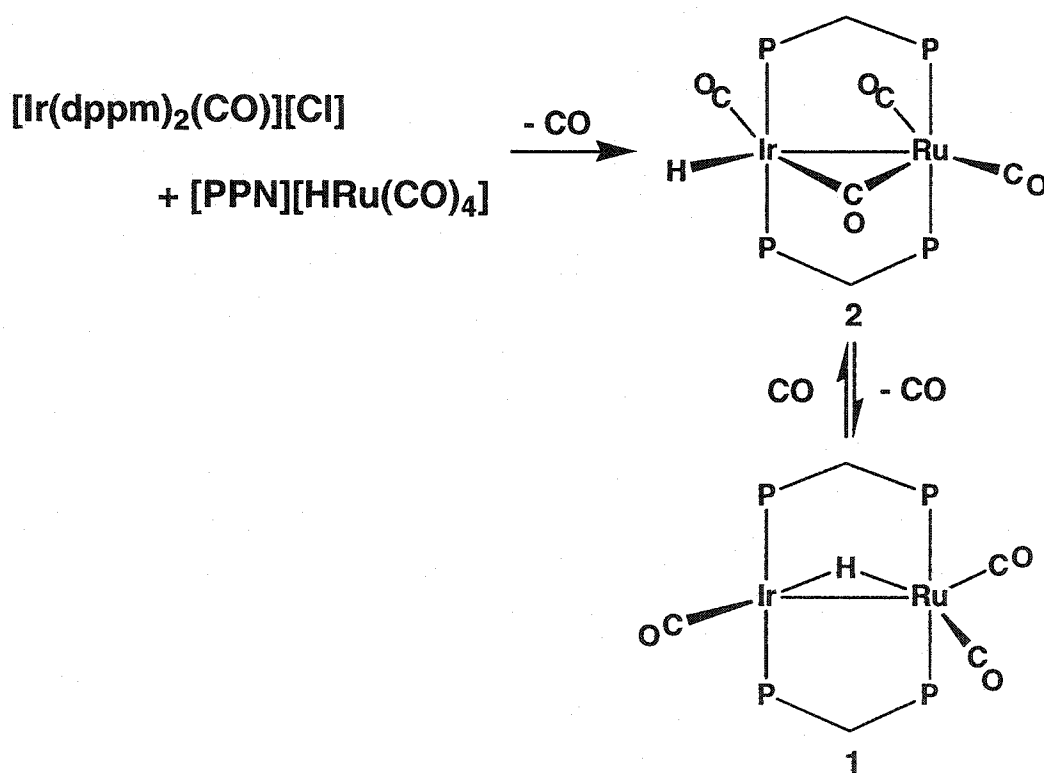
Compound **2** can be converted to **1** by reaction with Me$_3$NO, and reaction of **1** with CO generates **2**. Compounds **1** and **2** have surprisingly different structures. At temperatures below -60 °C the ^{13}C{^{1}H} NMR spectrum of a ^{13}CO-enriched sample of **2** displays four signals consistent with the structure shown in Scheme 3.2. At -105 °C, at which temperature all resonances are well resolved, two carbonyls (218.3, 207.8 ppm) are shown by selective ^{31}P-decoupling experiments to be bound terminally to Ru, while one (189.1 ppm) is terminally bound to Ir, and the fourth (262.7 ppm) is shown to bridge both metals, consistent with the low-frequency carbonyl stretch (1685 cm^{-1}) in the IR spectrum. The hydride resonance in the ^{1}H NMR spectrum appears as a triplet at -9.95 ppm with coupling to only the Ir-bound phosphines, indicating that the hydride is bound terminally to this metal.

This proposed structure has been confirmed by an X-ray determination, as shown in Figure 3.1. Bond lengths and angles are summarized in Table 3.4. Although the hydride ligand was not experimentally located, its approximate position is indicated by the vacant coordination site on Ir, falling between the carbonyl groups C(1)O(1) and C(2)O(2). Clearly, the carbonyl group C(1)O(1) is considerably removed from the site it would be expected to occupy opposite C(2), were the hydride ligand not present, and in fact C(1)O(1) on Ir occupies a position much like that of C(4)O(4) on Ru (compare: Ru-Ir-C(1) = 99.4(1)°, Ir-Ru-C(4) = 96.5(1)°). Each metal has a rather similar distorted octahedral geometry, in which the two octahedra are sharing an edge (Ir-Ru bond and bridging carbonyl), and the diphosphine ligands are mutually trans at each metal. The Ir-Ru distance (2.8091(3)Å) is normal for a single bond and the carbonyl (C(2)O(2)) is essentially symmetrically bridged. The smaller steric requirement of the hydride ligand on Ir compared to the carbonyl in the related position on Ru gives rise to subtle geometrical differences at the two metals; therefore, the phosphines on Ir are bent
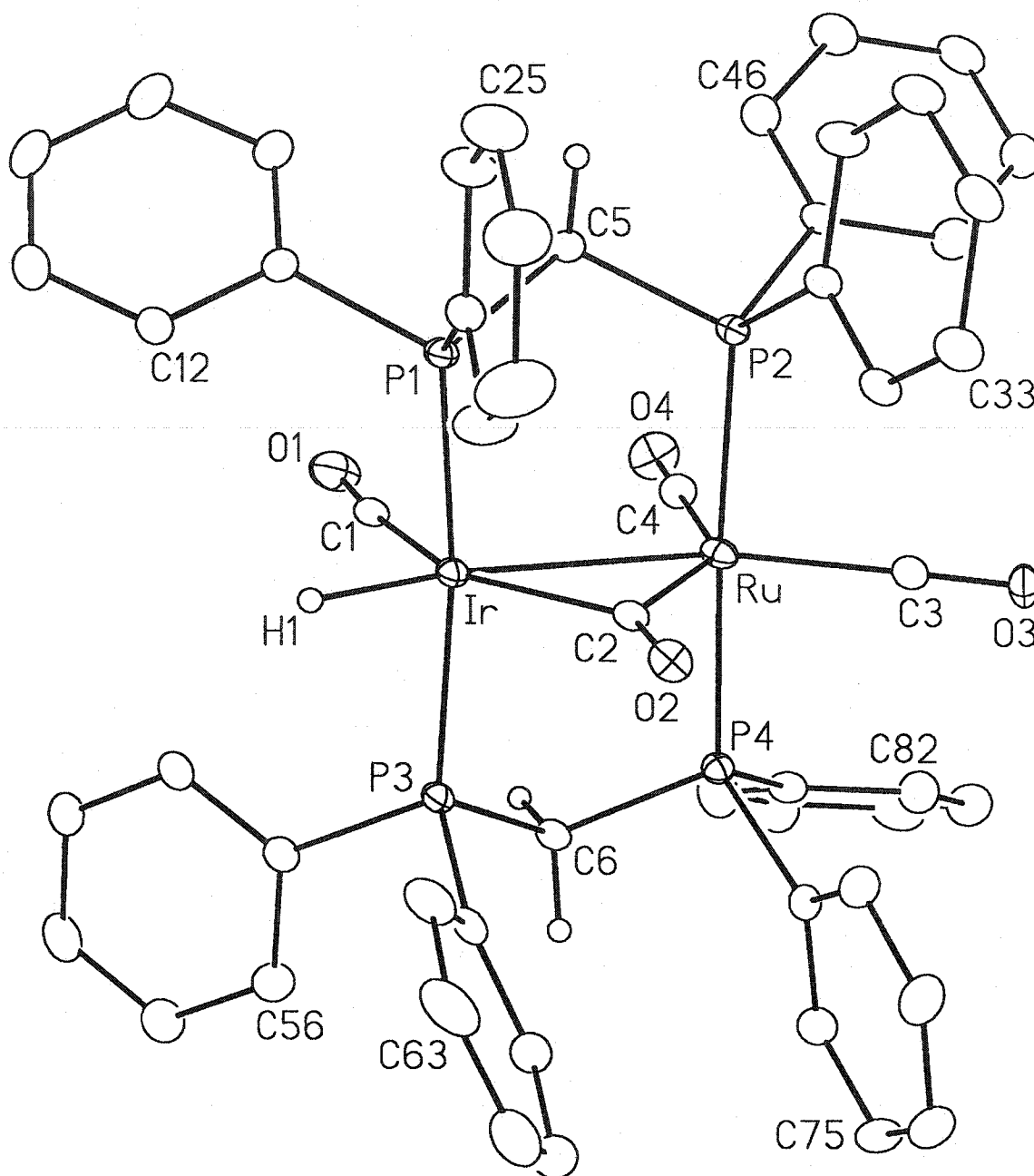
Figure 3.1. Perspective view of [IrRuH(CO)$_3$(μ-CO)(dppm)$_2$] (**2**) showing the atom-labeling scheme. Non-hydrogen atoms are represented by Gaussian ellipsoids at the 20% probability level. Hydrogen atoms are shown with arbitrarily small thermal parameters. Atom H(1) was not located but was placed in an idealized position, as described in the text.

Table 3.4 Selected Bond Distances and Angles of Compound 2

	(a) Distances			(b) Angles		
Atom 1	Atom 2	Distance (Å)	Atom 1	Atom 2	Atom 3	Angle (°)
Ir	Ru	2.8091(3)	P(1)	Ir	P(3)	167.34(4)
Ir	P(1)	2.3029(10)	C(1)	Ir	C(2)	147.96(16)
Ir	P(3)	2.3117(10)	C(1)	Ir	H(1)[a]	104
Ir	C(1)	1.935(4)	C(1)	Ir	H(1)[a]	108
Ir	C(2)	2.063(4)	Ir	Ru	C(2)	46.97(10)
Ru	P(2)	2.3361(10)	Ir	Ru	C(3)	151.65(15)
Ru	P(4)	2.3360(10)	Ir	Ru	C(4)	96.50(12)
Ru	C(2)	2.117(4)	P(2)	Ru	P(4)	176.95(4)
Ru	C(3)	1.925(5)	C(2)	Ru	C(3)	104.68(18)
Ru	C(4)	1.954(4)	C(2)	Ru	C(4)	143.47(16)
O(1)	C(1)	1.115(5)	C(3)	Ru	C(4)	111.8(2)
O(2)	C(2)	1.188(5)	Ir'	Ru'	C(3')[b]	144.8(7)
O(3)	C(3)	1.148(6)	C(1)	Ru'	C(3')	115.9(7)
O(4)	C(4)	1.112(5)	C(2)	Ru'	C(3')	96.2(7)
			Ir	C(2)	Ru	84.43(14)
			Ir	C(2)	O(2)	138.8(3)
			Ru	C(2)	O(2)	136.7(3)

[a]Atom H(1) was refined with the constraints described in the Experimental Section. [b]Primed atoms refer to the minor occupant (15%) in the disordered structure; refined with the distance restraints in the Experimental Section.

towards the small hydride ligand (P(1)-Ir-P(3) = 167.34(4)°), whereas those on Ru are almost exactly trans (P(2)-Ru-P(4) = 176.95(4)°). The slightly shorter Ir-P distances compared to Ru-P probably also reflect the less crowded environment at the heavier metal. All other parameters within the complex appear normal.

Compound **2** is shown to undergo two fluxional processes in solution. A spin-saturation-transfer experiment at -60 °C shows that the terminal, Ir-bound carbonyl and the bridging carbonyl are exchanging, as are the two on Ru. We propose the process shown in Chart 3.2 for this exchange (phosphines above and below the plane of the paper are not shown), in which CO_A and CO_B interchange, as do CO_C and CO_D. At 10 °C the four ^{13}CO signals have coalesced into two broad, unresolved signals at 225.7 and 212.2 ppm corresponding to the averaging

Chart 3.2
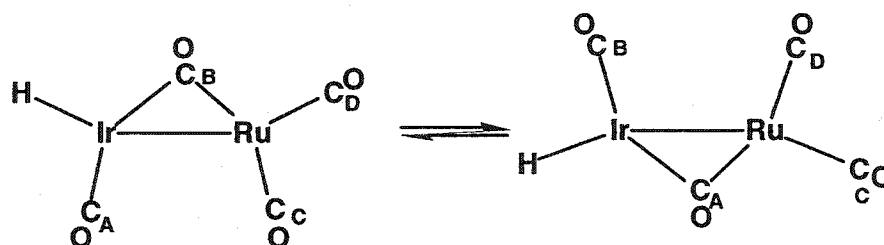
of the respective pairs of carbonyls as described above. At this temperature spin-saturation-transfer experiments show an additional process in which all carbonyls are exchanging, and warming the sample to 50 °C results in coalescence of these signals into one at 217.4 ppm. At all temperatures above -60 °C the hydride resonance appears as an unresolved signal. The second process that equilibrates all four carbonyls presumably involves a merry-go-round motion of all carbonyls and the hydride, in which these ligands move around the Ir-Ru core in the plane perpendicular to the phosphines, passing from metal to metal.

Compound **2** can also be used in the preparation of **3** except that protonation in this case is accompanied by loss of a carbonyl. As a result, this route always generates a mixture of **3** and **4**, with the CO generated in the protonation of **2** converting some of **3** into **4**. Under a CO atmosphere this mixture of **3** and **4** is converted cleanly to **4**. Owing to its much greater ease of handling compared to compound **1**, the tetracarbonyl hydride (**2**) is the precursor of choice for the preparation of **4**.

As in the RhOs chemistry,[13] the tetracarbonyl complex **4** serves as a convenient precursor for methylene-containing species. Therefore the reaction of **4** with diazomethane generates the methylene-bridged $[IrRu(CO)_4(\mu\text{-}CH_2)\text{-}(dppm)_2][BF_4]$ (**5**) as diagrammed in Scheme 3.3. In the ^1H NMR spectrum the $\mu\text{-}CH_2$ group appears as a triplet of triplets at 3.57 ppm, with the coupling to the Ir-bound phosphines ($^3J_{PH} = 23$ Hz) being greater than that involving the Ru-bound phosphines ($^3J_{PH} = 11$ Hz). The dppm methylene protons appear at 3.08 and 3.87 ppm and are readily differentiated from the metal-bound CH_2 group by their characteristic appearance (AB quartet with superimposed phosphorus coupling) and by the broad-band ^{31}P-decoupled ^1H NMR spectrum in which the dppm methylenes collapse to the expected AB quartet while the metal-bridged CH_2 group appears as a singlet. In the $^{13}C\{^1H\}$ NMR spectrum the carbonyls appear as four separate resonances. The low-field signal (211.3 ppm) for the bridging carbonyl appears as a doublet of multiplets with coupling to all ^{31}P nuclei, and 23 Hz coupling to the Ru-bound carbonyl at 191.7 ppm, indicating that these carbonyls are mutually trans. The chemical shifts of the remaining carbonyls are somewhat anomalous, with the low-field shift corresponding to the Ir-bound CO (in all other compounds the Ir-bound carbonyls appear at higher field than those on Ru). All ^{13}C NMR assignments have been confirmed by selective ^{31}P-decoupling experiments.

Scheme 3.3

*CH₂N₂
20°C

L
- CO

4

5

L = PMe₃ (7)

Me₃NO
CH₂N₂(xs)
or C₂H₄

L
- C₂H₄

6

OR

L = NCCH₃ (8)

= NC(H)C=CH₂ (9)
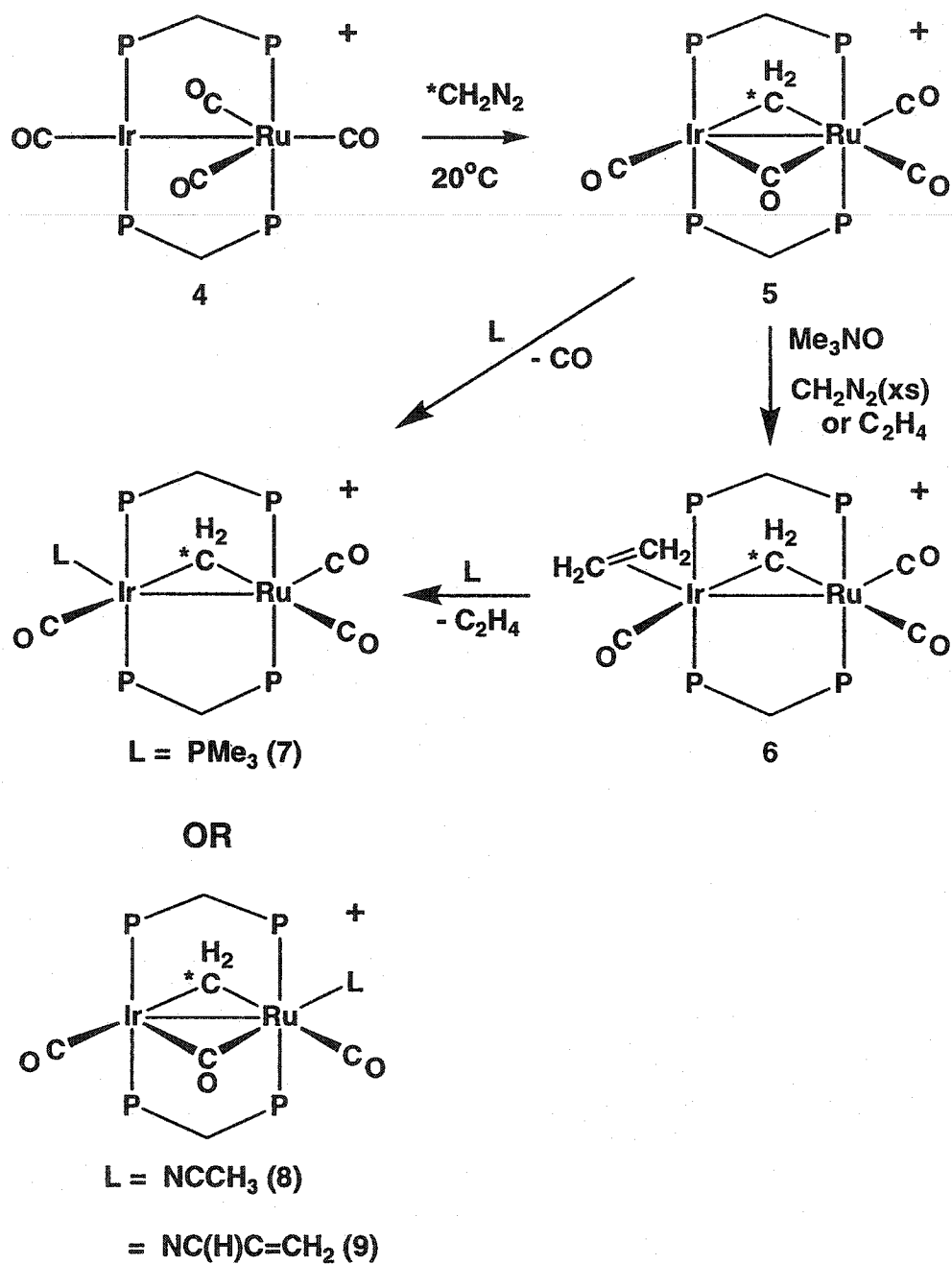
The structure of **5** has been determined by X-ray techniques in order to establish whether the bridging carbonyl has a conventional geometry or is semibridging, since the carbonyl stretch (1783 cm^{-1}) is consistent with either interpretation. In addition, it was deemed necessary to fully characterize this methylene-bridged species since subtle differences between it and the RhOs analogue may offer clues to their reactivity differences (*vide infra*). The structure shown in Figure 3.2 together with the parameters given in Table 3.5 clearly show a conventional bridging carbonyl with a normal accompanying metal-metal bond (2.8650(7)Å). This bridging carbonyl (C(2)O(2)) is slightly asymmetrically bonded to the metals as seen by the somewhat shorter Ir-carbon distance (Ir-C(2) = 2.033(8)Å, Ru-C(2) = 2.072(8)Å), but is shown to be conventionally bridged rather than semi-bridging by the close-to-symmetric angles at the carbonyl (Ir-C(2)-O(2) = 134.4(7)°, Ru-C(2)-O(2) = 137.1(7)°). The methylene group, on the other hand, shows significant asymmetry in its bonding to both metals, being more strongly bound to Ir (Ir-C(5) = 2.045(11)Å) than to Ru (Ru-C(5) = 2.305(12)Å). This observed asymmetry is consistent with the larger coupling of the methylene group to the Ir-bound phosphines in the ^{1}H NMR spectrum (*vide supra*). The differences in geometries at both metals result primarily from the additional carbonyl bound to Ru and the resulting greater crowding at this metal.

Although **5** does not react further with diazomethane at ambient temperature, removal of a carbonyl with trimethylamine oxide followed by addition of CH_2N_2 does lead to further "CH$_2$" incorporation to yield the methylene-bridged, ethylene complex [IrRu(C$_2$H$_4$)(CO)$_3$(μ-CH$_2$)(dppm)$_2$][BF$_4$] (**6**). At ambient temperature the ^{1}H NMR signal for the methylene group of **6** appears as a triplet of triplets at 6.20 ppm, displaying comparable coupling to the Ir- and Ru-bound phosphines ($^3J_{PH}$ = 8, 10 Hz, respectively); the signals due to the ethylene group are not observed at this temperature. At -80 °C the ethylene signals appear as broad singlets in the ^{1}H NMR spectrum at 1.73 and 0.54 ppm, which
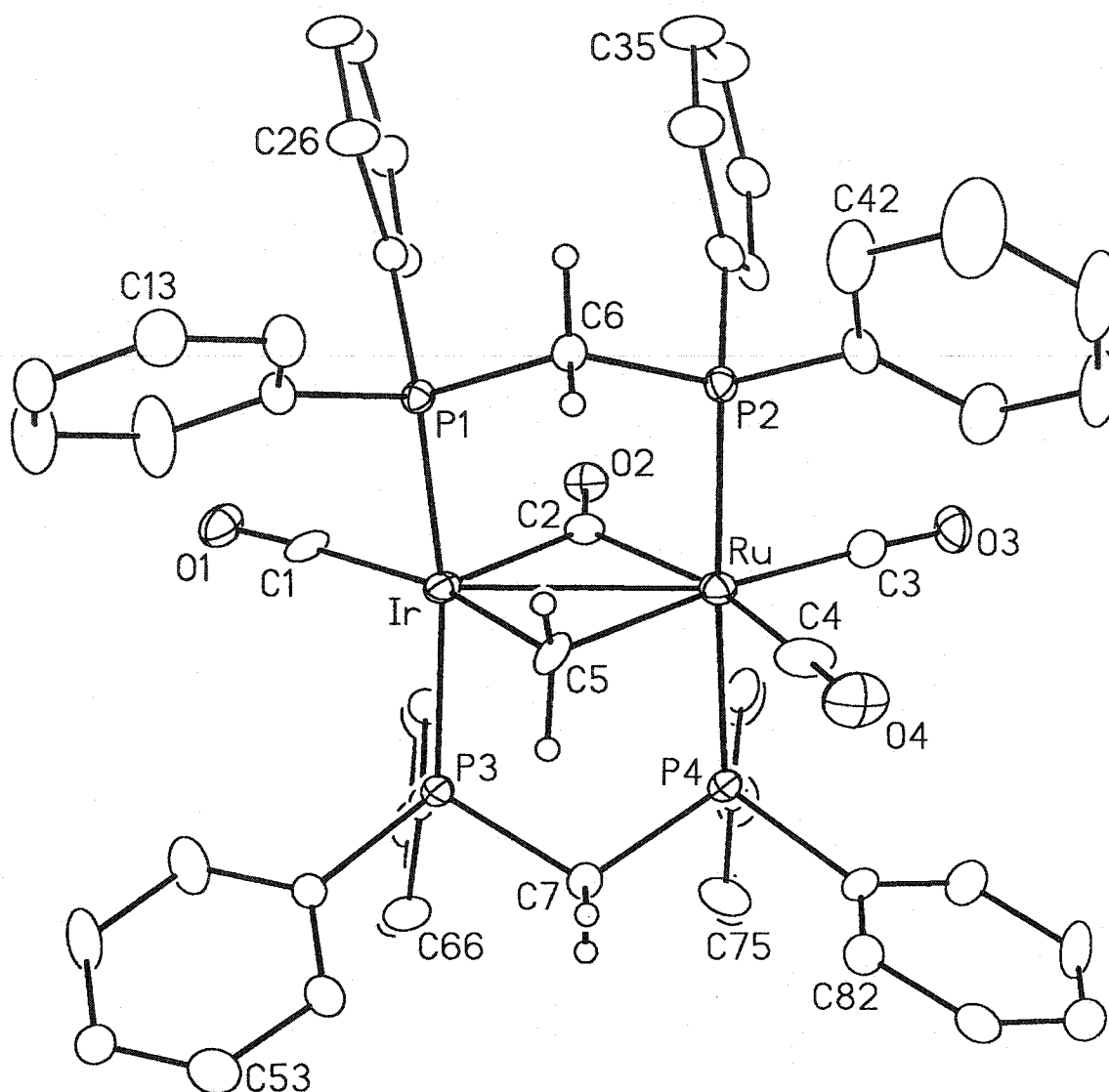
Figure 3.2. Perspective view of the [IrRu(CO)$_3$(μ-CH$_2$)(μ-CO)(dppm)$_2$]$^+$ cation of complex **5** showing the atom-labeling scheme. Non-hydrogen atoms are represented by Gaussian ellipsoids at the 20% probability level. Hydrogen atoms are shown with arbitrarily small thermal parameters.

Table 3.5 Selected Bond Distances and Angles of Compound **5**

(a) Distances

(b) Angles

Atom 1	Atom 2	Distance (Å)	Atom 1	Atom 2	Atom 3	Angle (°)
Ir	Ru	2.8650(7)	P(1)	Ir	P(3)	165.59(7)
Ir	P(1)	2.3516(19)	C(1)	Ir	C(2)	99.2(4)
Ir	P(3)	2.3503(19)	C(1)	Ir	C(5)	161.7(5)
Ir	C(1)	1.868(9)	C(2)	Ir	C(5)	99.1(4)
Ir	C(2)	2.033(8)	C(2)	Ir'	C(5)	98.1(3)
Ir	C(5)	2.045(11)	C(3)	Ir'	C(5')	162.3(4)
Ir'	C(5')[a]	2.05[b]	P(2)	Ru	P(4)	176.76(8)
Ru	P(2)	2.3726(19)	C(2)	Ru	C(3)	99.3(3)
Ru	P(4)	2.361(2)	C(2)	Ru	C(4)	162.1(5)
Ru	C(2)	2.072(8)	C(2)	Ru	C(5)	90.2(3)
Ru	C(3)	1.916(10)	C(3)	Ru	C(4)	98.5(5)
Ru	C(4)	1.981(12)	C(3)	Ru	C(5)	170.5(4)
Ru	C(5)	2.305(12)	C(4)	Ru	C(5)	72.1(5)
Ru'	C(4')	2.17(5)	C(1)	Ru'	C(4')	94(2)
Ru'	C(5')	2.31(3)	C(1)	Ru'	C(5')	169.3(4)
O(1)	C(1)	1.141(10)	C(2)	Ru'	C(4')	167(2)
O(2)	C(2)	1.194(9)	C(2)	Ru'	C(5')	91.4(3)
O(3)	C(3)	1.119(10)	C(4)'	Ru'	C(5')	76(2)
O(4)	C(4)	1.155(13)	Ir	C(2)	O(2)	134.4(7)
O(4')	C(4')	1.17(5)	Ru	C(2)	O(2)	137.1(7)

sharpen slightly upon decoupling of the Ir-bound ^{31}P signal, suggesting the structure shown in Scheme 3.3 in which the ethylene is bound to Ir. In addition, selective ^{31}P decoupling of the three [13]CO resonances indicates that two carbonyls are bound to Ru and one to Ir. The presence of two carbonyls on Ru, together with the methylene group and the pair of phosphines argues against the olefin also being on this metal owing to the steric crowding that would result. The breadth of the

ethylene ^{1}H resonances can be attributed to two fluxional processes, both of which have been investigated using spin-saturation-transfer experiments. Irradiating either ethylene resonance at temperatures between -60 ° and -90 °C results in a decrease in intensity of the other, indicating an exchange between the two environments, characteristic of ethylene rotation. The rates of rotation have been determined at five temperatures between -63 ° and -87 °C by selective inversion recovery ^{1}H NMR experiments[29] yielding $\Delta H^{\ddagger} = 11.47$ kcal/mol and $\Delta S^{\ddagger} = 5.7$ cal/mol K for this process. Above -63 °C the second process becomes significant involving the exchange of coordinated ethylene with free ethylene in solution. This exchange process has also been confirmed by a spin-saturation-transfer experiment in the presence of excess ethylene.

In order to determine the fate of the methylene group in the transformation of **5** to **6**, the labeled compound [IrRu(CO)$_4$([13]CH$_2$)(dppm)$_2$][BF$_4$] (**5-[13]C**) was reacted with unlabelled CH$_2$N$_2$ after brief reaction with Me$_3$NO. Based on the ^{1}H NMR spectrum, which shows the μ-CH$_2$ resonance primarily as a doublet of multiplets ([1]J$_{CH}$ = 140 Hz) with approximately 10% of a superimposed resonance resulting from [12]CH$_2$, the majority of the label (≈90%) is seen to remain in the bridging methylene group. This means that approximately 10% of the [13]CH$_2$ label has been incorporated into the ethylene produced, either coordinated to Ir or as a free ethylene. Integration of the ^{1}H NMR signals of the reaction mixture shows that approximately 1.2 equiv of free ethylene is present in solution.

The $^{13}C\{^1H\}$ NMR resonances for the bridging methylene and the ethylene carbons of compound **6** appear as singlets at 64.3, 26.4 and 22.6 ppm, respectively, and show no coupling to the ^{31}P nuclei. Both ethylene resonances are extremely weak owing to the small amount of ^{13}C incorporation into this group. Compound **6** can also be independently synthesized by the reaction of **5** with ethylene in the presence of trimethylamine oxide.

In order to establish whether the ethylene produced in the above reaction with diazomethane was generated by the presumed tricarbonyl species $[IrRu(CO)_3(\mu-CH_2)(dppm)_2][BF_4]$ or was independently produced in solution and subsequently bound to this unsaturated product, a blank experiment was carried out under identical conditions except in the absence of complex **5**. The absence of ethylene in this experiment confirms that an IrRu species is responsible for ethylene formation.

In the absence of excess ethylene the labile ethylene ligand in **6** is readily lost yielding several unidentified decomposition products. Not surprisingly, this ligand can also be displaced by ligands such as acetonitrile, trimethylphosphine and acrylonitrile. However, two structural types are obtained. In the case of the PMe$_3$ adduct, $[IrRu(PMe_3)(CO)_3(\mu-CH_2)(dppm)_3][BF_4]$ (**7**), the spectral parameters are in good agreement with those of the ethylene adduct (**6**), and it is assumed to have a similar structure in which the ethylene ligand has been displaced by PMe$_3$. In particular, the $^{31}P\{^1H\}$ resonances for the dppm groups are very similar in the two compounds, with those corresponding to the Ru-bound nuclei being almost superimposable while that of the Ir-bound nuclei of **7** is *ca.* 7 ppm upfield of the comparable resonance in **6**, consistent with the substitution of the ethylene ligand on Ir by the more basic PMe$_3$ group. The ^1H resonance for the bridging methylene group (4.17 ppm) shows the expected coupling to the three chemically inequivalent sets of phosphorus nuclei (two dppm ^{31}P nuclei on Ir, two on Ru and the PMe$_3$ group) and the upfield shift compared to that of the ethylene

adduct (6) is again consistent with replacement of ethylene by PMe3. The coupling patterns involving the ^{31}P and ^{13}CO nuclei in 7 are somewhat unusual. Although the PMe3 group is bound to Ir, it couples equally strongly to all four dppm ^{31}P nuclei; this means that the $^{3}J_{PP}$ value, that is a measure of the coupling between the PMe3 on Ir and the dppm ^{31}P nuclei on Ru, is essentially the same as $^{2}J_{PP}$ between the PMe3 and the dppm phosphorus nuclei bound to Ir. In a related complex, [IrRh(CH3)(CO)2(PMe3)(dppm)2][CF3SO3],[30] the Ir-bound PMe3 group displayed no P-P coupling to the adjacent Ir-bound dppm nuclei, but displayed 15 Hz coupling to the remote dppm groups on Rh. In addition, the $^{13}C\{^{1}H\}$ NMR spectrum of 7 shows that the Ir-bound carbonyl has the expected coupling to PMe3 and to the adjacent ends of the dppm ligands, whereas one Ru-bound carbonyl displays coupling to only the adjacent dppm ^{31}P nuclei. However, the second Ru-bound carbonyl shows coupling to the adjacent ^{31}P nuclei of dppm *and* 20 Hz coupling to the remote PMe3 group; the large magnitude of this latter P-C coupling presumably results from their arrangements essentially opposite the Ir-Ru bond (*vide infra*). Strong magnetic coupling through a metal-metal bond has previously been observed.[30,31] In spite of these NMR spectral anomalies, much of the connectivity can still be established from the P-C coupling between the dppm groups and the carbonyls. Any uncertainty in the position of the PMe3 group is overcome by the X-ray structure determination, which is shown in Figure 3.3, and which clearly shows the PMe3 group bound to Ir. Selected bond lengths and angles are given in Table 3.6. This structure is not unlike that shown previously for compound 2 (Figure 3.1), having two edge-shared octahedra shared along the metal-metal bond and the bridging methylene group. The steric demands of the PMe3 group are manifest in a bending of the dppm ligands on both metals away from the PMe3 group (P(1)-Ir-P(3) = 165.86(9)°, P(2)-Ru-P(4) = 160.9(1)°). The Ir-Ru distance (2.8892(9)Å) is consistent with a single bond and the geometry of the bridging methylene group is essentially symmetric and unexceptional. The

short Ir-C(1)O(1) distance (1.859(12)Å) is consistent with more π back-donation to this carbonyl as a result of the strong donor ability of the adjacent PMe$_3$ group. Surprisingly perhaps, the Ru-C(2)O(2) distance (1.859(13)Å) is also short (compare Ru-C(3)O(3) = 1.931(11)Å), and this may result from a transmission of electronic effects from the PMe$_3$ group through the Ir-Ru bond to which both groups are mutually trans. All other parameters within the complex cation appear normal.

The acetonitrile adduct [IrRu(NCCH$_3$)(CO)$_2$(μ-CO)(μ-CH$_2$)(dppm)$_2$][BF$_4$] (8) is stoichiometrically analogous to compounds 6 and 7, having an acetonitrile group instead of the ethylene and PMe$_3$ ligands, respectively. However, the structure of 8 appears to differ substantially from those of 6 and 7, instead resembling the structure observed for 5. This is most clearly seen in the IR and ^{31}P{^{1}H} NMR spectra. Unlike compounds 6 and 7, which show only terminal carbonyl bands in the IR spectra, 8 displays a band at 1745 cm^{-1}, corresponding to a bridging carbonyl stretch. This compares well to the analogous stretch for 5, observed at 1783 cm^{-1}. In addition, the ^{31}P{^{1}H} NMR spectrum of 8 has both sets of resonances (Ru- and Ir-bound ^{31}P nuclei) substantially downfield from those in 6 and 7, but in closer proximity to the resonances for 5. If 8 had a geometry analogous to those of 6 and 7, with the NCMe group bound to Ir, we would have expected a change in the resonances for the Ir-bound ^{31}P nuclei, owing to the different ligands on Ir, but would have expected the resonances for the Ru-bound ^{31}P nuclei to be closely comparable, having an identical ligand set at this metal. Instead, the Ru-bound ^{31}P resonances for 6 and 7 are approximately 14 ppm upfield from those of 8. In addition, the ^{13}C{^{1}H} resonances for the carbonyls in 8 are comparable to those in 5 apart from the absence of the fourth resonance of 5 at 191.7 ppm. In 5 this carbonyl resonance displays 23 Hz coupling to the bridging carbonyl, since they are mutually trans; the absence of similar coupling in 8
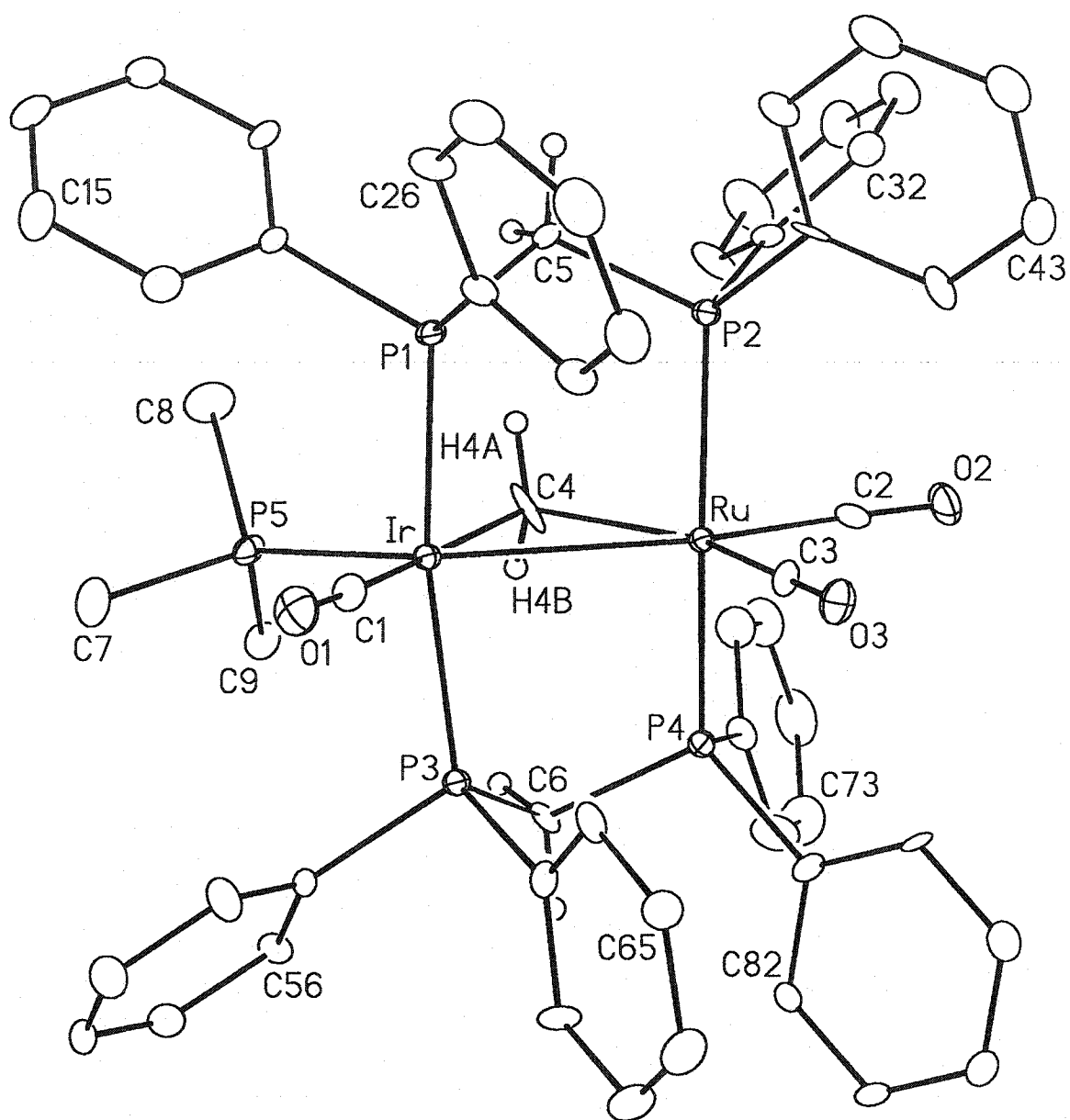
Figure 3.3 Perspective view of the [IrRu(PMe₃)(CO)₃(µ-CH₂)(dppm)₂]⁺ cation of complex **7** showing the atom-labeling scheme. Non-hydrogen atoms are represented by Gaussian ellipsoids at the 20% probability level. Hydrogen atoms are shown with arbitrarily small thermal parameters.

Table 3.6 Selected Bond Lengths and Angles for Compound 7

(a) Distances

(b) Angles

Atom 1	Atom 2	Distance (Å)	Atom 1	Atom 2	Atom 3	Angle (°)
Ir	Ru	2.8892(9)	Ru	Ir	P(5)	130.69(7)
Ir	P(1)	2.347(3)	Ru	Ir	C(1)	125.3(3)
Ir	P(3)	2.329(3)	Ru	Ir	C(4)	48.5(3)
Ir	C(1)	1.859(12)	P(1)	Ir	P(3)	165.86(9)
Ir	C(4)	2.152(11)	P(5)	Ir	C(1)	103.9(3)
Ru	P(2)	2.352(3)	P(5)	Ir	C(4)	82.8(3)
Ru	P(4)	2.373(3)	C(1)	Ir	C(4)	172.6(4)
Ru	C(2)	1.859(13)	Ir	Ru	C(2)	164.5(4)
Ru	C(3)	1.931(11)	Ir	Ru	C(3)	99.8(3)
Ru	C(4)	2.175(13)	Ir	Ru	C(4)	47.8(3)
O(1)	C(1)	1.168(13)	P(2)	Ru	P(4)	160.86(10)
O(2)	C(2)	1.159(14)	C(2)	Ru	C(3)	95.6(5)
O(3)	C(3)	1.133(12)	C(2)	Ru	C(4)	116.8(5)
			C(3)	Ru	C(4)	147.5(4)

identifies the site of the acetonitrile ligand as opposite the bridging carbonyl, as shown in Scheme 3.3.

In spite of the lability of the ethylene ligand in **6**, attempts to displace this group by other olefins (acrylonitrile, dimethyl maleate, methyl acrylate) succeeded only with acrylonitrile, yielding $[IrRu(\eta^1\text{-}NC(H)C=CH_2)(CO)_2(\mu\text{-}CH_2)(\mu\text{-}CO)\text{-}(dppm)_2][BF_4]$ (**9**), diagrammed below. However, it appears that the acrylonitrile is not bound through the olefinic moiety as in most low-valent, late-metal complexes,[32] but is N-bound through the nitrile functionality to give a product that spectroscopically is very similar to the acetonitrile adduct (**8**). Apart from the close similarity in the spectral parameters of **8** and **9** additional support for the N-bound formulation is obtained from the ^1H NMR spectrum in which the olefin protons

9
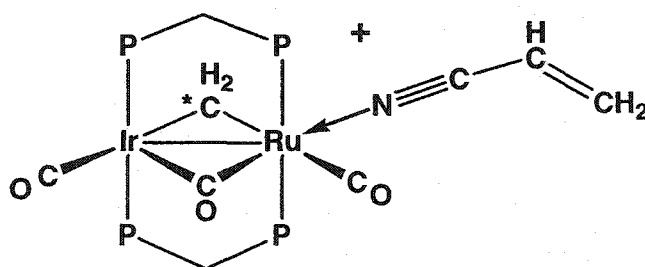
are essentially unperturbed from those of the uncomplexed olefin, in contrast to those of the ethylene ligand in **6** which are shifted substantially upfield from free ethylene. No band is observed in the IR spectrum for the olefin functionality; this is not surprising since the C=C stretch is also very weak in the free olefin. The C≡N stretch for **9** was observed as a very weak band at 2150 cm^{-1}; by comparison no peak attributable to $\nu(CN)$ was observed for the acetonitrile adduct **8**. Although this bonding mode for cyano olefins is uncommon for the heavier, late-transition metals, it has been observed[33] in complexes of Os(II) and Ir(I); in the latter case

the bridging TCNE ligand is a dianionic group. This bonding mode is relatively common with lighter metals having a preference for hard ligands.[34]

Two structural types have been observed for compounds **5-9** having formulations [IrRuL(CO)$_3$(μ-CH$_2$)(dppm)$_2$][BF$_4$], as diagrammed in Scheme 3.3. Compounds **5**, **8** and **9** have less symmetrical structures in which there is only a single terminal ligand on Ir (all others being bridging) whereas compounds **6** and **7** have more symmetrical structures having two terminal ligands on each of Ir and Ru. We suggest that the preference for the latter structural type is strongly favored by steric effects, with the two bulkier ligands (η^2-ethylene and PMe$_3$) favoring Ir rather than the more crowded environment at Ru in the alternate structure, shown for compounds **8** and **9**. The failure of substituted olefins to form π-adducts analogous to **6** probably results from steric repulsions between these substituents and the phenyl groups of dppm. The η^1-nitrile ligands are sterically comparable to a carbonyl, so similar structures are obtained with these ligands in compound **5**, **8** and **9**. Furthermore, assuming that the positive charge in these compounds is localized on Ru (giving a Ru(II) center), the σ-donor nitriles will be favored at this metal. The observation of the unusual nitrile-bound acrylonitrile ligand in these late-metal complexes presumably results from the need of the higher oxidation-state metal for electron density and steric repulsions that inhibit π coordination of this olefin. The synthesis of the acetonitrile adduct (**7**) was prompted by the instability of the putative tricarbonyl complex **B**, and the difficulties in carrying out the transformation of **5** to **6**. It seemed that an acetonitrile ligand in such a system would be labile and that **7** might serve as a convenient source of **B** through acetonitrile loss. However, this acetonitrile ligand is not displaced in the presence of diazomethane and **7** fails to react with this substrate. The inertness of **7** supports our earlier proposal of a Ru(II) oxidation state favoring strong binding of the σ-donor ligand.

Discussion

The bridging methylene unit has been shown to be a pivotal fragment in FT chemistry, and has been implicated in carbon-carbon bond formation through a number of proposed pathways.[1a,35-37] Following our success with coupling of up to four methylene fragments promoted by a Rh/Os compound,[21] we turned to the Ir/Ru and combinations of metals in order to determine the effect of substituting Rh by the less labile Ir, and Os by the more labile Ru.[38] The incorporation of a methylene group into $[IrRu(CO)_4(dppm)_2][BF_4]$ (**4**) is readily accomplished by reaction with diazomethane at ambient temperature, yielding the methylene-bridged $[IrRu(CO)_4(\mu-CH_2)(dppm)_2][BF_4]$ (**5**) as the sole product. The direct synthesis of methylene-bridged complexes via reactions of the appropriate complexes with diazomethane is well established.[13,35] The failure of **4** to incorporate more than a single methylene unit is in contrast to the ambient-temperature reaction involving the RhOs analogue in which *four* methylene groups are incorporated giving the C_3- and C_1-containing product, $[RhOs(\eta^1-C_3H_5)-(CH_3)(CO)_3(dppm)_2][BF_4]$,[13] as described in Chapter 2. Even at -60 °C the RhOs precursor yields the butanediyl adduct, $[RhOs(C_4H_8)(CO)_3(dppm)_2][BF_4]$, through coupling of four methylene groups. The RhOs and IrRu compounds also differ in their tendency to lose a carbonyl ligand. Therefore, the C-C bond-formation sequences that occur in the RhOs system are accompanied by carbonyl loss, whereas the IrRu compound **4** does not lose a carbonyl upon reaction with diazomethane. The RhOs analogue of **5** (namely $[RhOs(CO)_4(\mu-CH_2)(dppm)_2]-[BF_4]$) can be obtained at -80 °C, however this product readily loses a carbonyl in the presence of excess CH_2N_2 at higher temperatures, yielding the above C_3 and C_4 products under the appropriate conditions.[13] These observations suggest that carbonyl loss is an important component in the incorporation of additional methylene groups. The importance of carbonyl loss in the methylene coupling reactions can be confirmed by removal of a carbonyl from **5** using trimethylamine

oxide. Although the product of carbonyl loss, the putative tricarbonyl [IrRu(CO)$_3$(μ-CH$_2$)(dppm)$_2$][BF$_4$], is unstable and rapidly decomposes, it can be intercepted in the presence of excess diazomethane to give the methylene-bridged, ethylene adduct [IrRu(C$_2$H$_4$)(CO)$_3$(μ-CH$_2$)(dppm)$_2$][BF$_4$] (6), in which two additional methylene fragments have combined to yield ethylene.

The generation of the ethylene adduct 6 from the methylene-bridged precursor 5 upon reaction with diazomethane suggests the combination of the existing bridging methylene group with the newly generated methylene group, however, the labeling study clearly shows that this is not the case, at least for the dominant pathway. Retention of 90% of the ^{13}CH$_2$ label in the bridging site indicates that the dominant pathway for methylene dimerization is occurring between unlabelled, diazomethane-generated methylene groups. In the analogous RhOs system the labeled μ-^{13}CH$_2$ group was incorporated into the C$_3$ or C$_4$ fragment, and in Chapter 2 we proposed that this was facilitated by stepwise "CH$_2$" insertion into the Rh-CH$_2$ bond of the bridging methylene group. The failure of the Ir/Ru analogue to undergo methylene insertion into the Ir-(μ-CH$_2$) bond is consistent with a stronger Ir-C bond. The small amount of ^{13}C label incorporated into the ethylene ligand suggests that CH$_2$ insertion into either the Ir-CH$_2$ or the Ru-CH$_2$ bond of the bridging methylene group is also occurring as a secondary process. Although we are unable to establish whether ethylene formation occurs at Ir or Ru, analogies with the RhOs chemistry suggests that activation of diazomethane and subsequent ethylene formation occurs at Ir. Clearly, the failure of ^{13}C-labeled 5 to incorporate significant amounts of its label into the ethylene produced shows that ethylene formation occurs differently from the Rh/Os system, although how this occurs remains unclear. The blank experiment in which no ethylene is generated in the absence of compound 5 establishes the involvement of an Ir/Ru complex in ethylene formation.

In hopes of understanding the substantially different tendencies for CO loss in these methylene-bridged complexes of Rh/Os and Ir/Ru, we have compared their solid-state structures. A superficial comparison of these structures (compare Figures 2.1 and 3.2) indicates that both are very similar; having a bridging carbonyl and methylene groups on opposite faces of the complex, and similar geometries at both the Group 8 and 9 metals. However, it is useful to compare these structures to two valence bond extremes, as diagrammed as **D** and **E** in Chart 3.3 (dppm groups above and below the plane of the drawing are omitted). In structure **E**, Rh is coordinatively unsaturated, whereas in the metal-metal bonded **D**, both metals have 18e configurations. Structure **E** should therefore be more susceptible to substrate addition, which might induce CO loss as diagrammed

Chart 3.3

| D | E | F |
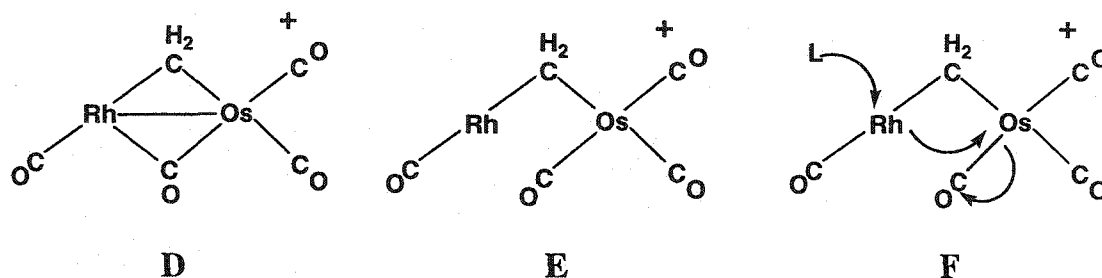
in **F**. Ligand (L) addition at Rh can lead to dative-bond formation to M (Ru or Os) assisting in the labilization of a carbonyl from this metal. With these ideas in mind, we looked back at the structures of $[IrRu(CO)_4(\mu\text{-}CH_2)(dppm)_2][BF_4]$ (5) and the Rh/Os analogue to determine their relationship to the extreme structures shown in **D** and **E**. The transition from **E** to **D** is accompanied by a number of structural changes, the most obvious of which include a shortening of the metal-metal bond, a change in the M-C-O angle from $180°$ to near $140°$ as this carbonyl assumes a bridging position, and a shortening of the separation between the Group 9 metal and the carbonyl as the latter approaches a bridging position. In addition,

as one carbonyl approaches the bridging position, the one on the Group 9 metal opposite the bridging methylene group should bend back, decreasing the H_2C-M-CO angle from the idealized 180°.

A comparison of these structural parameters for the two methylene-bridged compounds under discussion is given in Table 3.7 (numbering scheme is that of Figure 3.2). Although the Rh-C(2) and Ir-C(2) distances involving the bridging carbonyls are not diagnostic, all other parameters indicate that the Ir/Ru compound is significantly closer to the symmetrically bridged extreme **D**. For example, the Ir-Ru distance (2.8650(7)Å) is substantially shorter than Rh-Os (2.9413(4)Å), and the bridging carbonyl is almost symmetrical in the Ir-Ru case (Ru-C(2)-O(2) = 137.1(7)°; Ir-C(2)-O(2) = 134.4(7)°) while for RhOs this carbonyl is semibridging (Os-C(2)-O(2) = 141.7(3)°; Rh-C(2)-O(2) = 128.9(3)°).

Table 3.7. A Comparison of Selected Structural Parameters for the Compounds $[MM'(CO)_4(\mu\text{-}CH_2)(dppm)_2][BF_4]$ (MM' = RhOs, IrRu).

(a) Bond-lengths (Å)	RhOs	IrRu
M-M'	2.9413(4)	2.8650(7)
M'-C(2)	2.157(4)	2.072(8)
M-C(2)	2.027(4)	2.033(8)
M'-C(5)	2.210(4)	2.305(12)
M-C(5)	2.088(4)	2.045(11)
(b) Angles (deg)		
M'-C(2)-O(2)	141.7(3)	137.1(7)
M-C(2)-O(2)	128.9(3)	134.4(7)
C(5)-M-C(1)	169.1(2)	161.7(5)

Both structures lie close to extreme **D**, however, the slight tendency of the Rh/Os compound away from this extreme and towards extreme **E** is consistent with a weakening of the Rh-C(2) interaction suggesting that nucleophilic displacement of this carbonyl by the weak nucleophile, diazomethane, should more readily give intermediate **F**, which subsequently loses a carbonyl.

Conclusions

This study on the reaction of $[IrRu(CO)_4(dppm)_2][BF_4]$ with diazomethane was undertaken as a comparison with the analogous RhOs system, which was observed at temperatures above -60 °C to give rise to facile coupling of methylene units yielding C_3 or C_4 fragments at the metals. Under similar conditions the IrRu compound yields only the methylene-bridged compound $[IrRu(CO)_3(\mu\text{-}CH_2)\text{-}(\mu\text{-}CO)(dppm)_2][BF_4]$ (**5**). Although in this comparison both metals were exchanged (Ir for Rh and Ru for Os), it appears that the major difference between these two systems results from the replacement of Rh by Ir. This exchange results in two important differences that inhibit subsequent C-C bond formation. First, it inhibits CO loss, which is apparently needed before subsequent coupling of methylene groups can occur, and second the stronger Ir-C bond involving the bridging methylene group compared to Rh-C inhibits subsequent coupling involving the bridging methylene group in the IrRu system. Coupling of methylene groups can be induced upon removal of a carbonyl from **5** in the presence of diazomethane. However, labeling studies show that the dominant pathway for ethylene formation does not involve the bridging methylene group of **5**; the ethylene ligand instead results primarily from coupling of diazomethane-generated methylene groups. The formation of ethylene from diazomethane over Fischer-Tropsch catalysts in the absence of hydrogen is well known.[37]

References and Notes

1. (a) Biloen, P.; Sachtler, W.M.H. *Adv. Catal.* **1981**, *30*, 165.

   (b) Van der Laan, G.P.; Beenackers, A.A.C.M. *Catal. Rev.-Sci. Eng.* **1999**, *41*, 255.

   (c) Schulz, H. *Appl. Catal. A* **1999**, *186*, 3.

2. Vannice, M.A. *J. Catal.* **1975**, *37*, 462.

3. Vannice, M.A. *J. Catal.* **1975**, *37*, 449.

4. (a) Bhasin, M.; Hartley, W.J.; Ellgen, P.C.; Wilson, T.P. *J. Catal.* **1978**, *54*, 120.

   (b) Ichikawa, M.; *Bull. Chem. Soc. Jpn.* **1978**. *51*, 2273.

   (c) Ichikawa, M.;*J. Catal.* **1979**, *56*, 127.

   (d) Watson, P.R.; Somorjai, G.A. *J. Catal.* **1981**, *72*, 347.

   (e) Watson, P.R.; Somorjai, G.A. *J. Catal* **1982**, *74*, 282.

   (f) Kip, B.J.; Hermans, E.G.F.; van Wolput, J.H.M.C.; Haermans, N.M.A.; van Grondelle, J.; Prins, R. *Appl. Catal.* **1987**, *35*, 109.

   (g) Lavalley, J.C.; Saussey, J.; Lamotte, J.; Breault, R.; Hindermann, J.P.; Kiennemann, A. *J. Phys. Chem.* **1990**, *94*, 5941.

   (h) Bowker, M. *Catal. Today* **1992**, *15*, 77.

5. Sinfelt, J.H. *Bimetallic Catalysts: Discoveries, Concepts, and Applications*, John Wiley & Sons, New York, NY, 1983, Chapter 2.

6. Iglesia, E.; Soled, S.L.; Fiato, R.A.; Via, G.H. *J. Catal.* **1993**, *143*, 345.

7. (a) Beuther, H.; Kobylinski, T.P.; Kibby, C.L.; Pannell, R.B. US Patent
    4,585,798; **1986**, assigned to Gulf Research and Development Co.
    (b) Beuther, H.; Kibby, C.L.; Kobylinski, T.P.; Pannell, R.B. US Patent
    4,413,064; **1983**, assigned to Gulf Research and Development Co.
    (c) Beuther, R.B.; Kibby, C.L.; Kobylinski, T.P.; Pannell, R.B. US Patent
    4,493,905; **1985**, assigned to Gulf Research and Development Co.
    (d) Kobylinski, T.P.; Kibby, C.L.; Pannell, R.B.; Eddy, E.L. US Patent
    4,605,676; **1986**, assigned to Chevron Research Co.

8. See for example: (a) Fukushima, T.; Arakawa, H.; Ichikawa, M. *J. Phys.
    Chem.* **1985**, *89*, 4440. (b) Ichikawa, M. *Polyhedron* **1988**, *7*, 2351. (c) Xiao,
    F.-S.; Fukuoka, A.; Ichikawa, M. *J. Catal.* **1992**, *138*, 206.

9. Xiao, F.-S.; Ichikawa, M. *J. Catal.* **1994**, *147*, 578.

10. Hilts, R.W.; Franchuk, R.A.; Cowie, M. *Organometallics* **1991**, *10*, 304.

11. Sterenberg, B.T.; Hilts, R.W.; Moro, G.; McDonald, R.; Cowie, M. *J. Am.
    Chem. Soc.* **1995**, *117*, 245.

12. Sterenberg, B.T.; McDonald, R.; Cowie, M. *Organometallics* **1997**, *16*, 2297.

13. Trepanier, S.J.; Sterenberg, B.T.; McDonald, R.; Cowie, M. *J. Am. Chem. Soc.*
    1999, *121*, 2613.

14. Bruce, M.I.; Matisons, J.G.; Wallis, R.C.; Patrick, J.M.; Skelton, B.W.; White,
    A.H. *J. Chem. Soc. Dalton* **1983**, 2365.

15. Walker, H.W.; Ford, P.C. *J. Organomet. Chem.* **1981**, *214*, C43.

16. Hilts, R.W.; Franchuk, R.A.; Cowie, M. *Organometallics* **1991**, *10*, 1297.

17. Miller, J.S.; Caulton, K.G. *J. Am. Chem. Soc.* **1975**, *97*, 1067.

18. Programs for diffractometer operation, data reduction and absorption correction were those supplied by Bruker.

19. (a) Sheldrick, G.M. *Acta Crystallogr.*, **1990**, *A46*, 467. (b) Sheldrick, G.M. *SHELXL-93*. Program for crystal structure determination. University of Göttingen, Germany, 1993. Refinement on F_o^2 for all reflections (having $F_o^2 \geq 3\sigma(F_o^2)$). Weighted R-factor wR_2 and goodness of fit S are based on F_o^2; conventional R-factor R_1 is based on F_o, with F_o set to zero for negative F_o^2. The observed criterion of $F_o^2 > 2\sigma(F_o^2)$ is used only for calculating R_1, and is not relevant to the choice of reflections for refinement. R-factors based on F_o^2 are statistically about twice as large as those based on F_o, and R-factors based on all data will be even larger.

20. Muhandiram, D. R.; McClung, R. E. D. *J. Magn. Reson.* **1987**, *71*, 187.

21. Antonelli, D.M.; Cowie, M. *Organometallics* **1990**, *9*, 1818.

22. See for example: (a) Xiao, J.; Cowie, M. *Organometallics* **1993**, *12*, 463. (b) Xiao, J.; Santarsiero, B.D.; Vaartstra, B.A.; Cowie, M. *J. Am. Chem. Soc.* **1993**, *115*, 3212.

23. Sterenberg, B.T.; Ph.D. Thesis, University of Alberta, Edmonton, AB, Canada, Chapter 5, 1997.

24. Rowsell, B.D.; Sterenberg, B.T.; McDonald, R.; Cowie. M. to be published.

25. (a) Ziegler, T.; Tschinke, V. *Bonding Energetics in Organometallic Compounds*, Amer. Chem. Soc., Washington DC, 1990, Chapter 19.

(b) Ziegler, T. *Can. J. Chem.* **1995**, *73*, 743.

26. (a) Antonelli, D.M.; Cowie, M. *Inorg. Chem.* **1990**, *17*, 2553.

(b) McDonald, R.; Cowie, M. *Inorg. Chem.* **1990**, *29*, 1564.

(c) Elliot, D.J.; Ferguson, G.; Holah, D.G.; Hughes, A.N.; Jennings, M.; Magnuson, V.R.; Potter, D.; Puddephatt, R.J. *Organometallics* **1990**, *9*, 1336.

27. George, D.S.A.; McDonald, R.; Cowie, M. *Organometallics* **1998**, *17*, 2553.

28. Lo, J.; Cowie, M. unpublished results.

29. Data analysis was carried out according to the method of McClung and coworkers: Muhandiram, D.R.; McClung, R.E.D. *J. Magn. Reson.* **1987**, *71*, 187.

30. Oke, O.; McDonald, R.; Cowie, M. *Organometallics* **1999**, *18*, 1629.

31. (a) Vaartstra, B.A.; Xiao, J.; Jenkins, J.A.; Verhagen, R.; Cowie, M. *Organometallics*, **1991**, *10*, 2708.

(b) Antwi-Nsiah, F.H.; Torkelson, J.R.; Cowie, M. *Inorg. Chim. Acta* **1997**, *259*, 213.

(c) Mague, J.T. *Organometallics* **1986**, *5*, 918.

(d) Brown, M.P.; Fisher, J.R.; Hill, R.H.; Puddephatt, R.J.; Seddon, R.R. *Inorg. Chem.* **1981**, *20*, 2516.

32. See for example: (a) Grant, S.M.; Manning, A.R. *J. Chem. Soc., Dalton Trans.* **1979**, 1789.

(b) Connelly, N.G.; Kelly, R.L.; Whiteley, M.W. *J. Chem. Soc., Dalton Trans.* **1981**, 34.

(c) Werner, H.; Juthani, B. *J. Organomet. Chem. 1981*, 209, *211*.

(d) Albers, M.O.; Colville, N.J.; Singleton, E. *J. Chem. Soc., Dalton Trans.* **1982**, 1069.

(e) Ashton, H.C.; Manning, A.R. *Inorg. Chem.* **1983**, *22*, 1440.

(f) Morrow, J.R.; Tonker, T.L.; Templeton, J.L. *J. Am. Chem. Soc.* **1985**, *107*, 6957; and references therein.

33. (a) McQueen, A.E.D.; Blake, A.J.; Stephenson, T.A.; Schröder, M.; Yellowlees, L.J. *J. Chem. Soc., Chem. Commun.* **1988**, 1533.

(b) Yee, G.T.; Calabrese, J.C.; Vazques, C.; Miller, J.S. *Inorg. Chem.* **1993**, *32*, 377.

34. (a) Rettig, M.F.; Wing, R.M. *Inorg. Chem.* **1969**, *8*, 2685.

(b) Zavalii, P.Y.; Mys'kiv, M.G.; Fundomenskii, V.S. *Kristallograf.* **1984**, *29*, 60.

(c) Braunswarth, H.; Huttner, G.; Zsolnai, L. *J. Organomet. Chem.* **1989**, *372*, C23.

(d) Bunn, A.G.; Carroll, P.J.; Wayland, B.B. *Inorg. Chem.* **1992**, *31*, 1297.

(e) Miller, J.S.; Calabrese, J.C.; McLean, R.S.; Epstein, A.J. *Adv. Mater.* **1992**, *4*, 498.

(f) Cotton, F.A.; Kim, Y. *J. Am. Chem. Soc.* **1993**, *115*, 8511.

(g) Cotton, F.A.; Kim, Y.; La, J. *Inorg. Chim. Acta* **1994**, *221*, 1.

(h) Olmstead, M.M.; Speier, G.; Szabo, L. *Chem. Commun.* **1994**, 541.

(i) Miller, J.S.; Vazquez, C.; Jones, N.L.; McLean, R.S.; Epstein, A.J. *J. Mater. Chem.* **1995**, *5*, 707.

(j) Bohm, A.; Vazquez, C.; McLean, R.A.; Calabrese, J.C.; Kalm, S.E.; Manson, J.L.; Epstein, A.J.; Miller, J.S. *Inorg. Chem.* **1996**, *35*, 3083.

(k) Vernik, I.; Stynes, D.V. *Inorg. Chem.* **1996**, *35*, 6210.

(l) Sugiura, K.-I.; Mikami, S.; Tanaka, T.; Sawada, M.; Manson, J.L.; Miller, J.S.; Sakata, Y. *Chem. Lett.* **1997**, 1071.

(m) Dreos, R.; Geremia, S.; Nardin, G.; Randaccio, L.; Tauzher, G.; Vuano, S.

Inorg. Chim. Acta **1988**, *272*, 74.

(n) Brandon, E.J.; Rittenberg, D.K.; Arif, A.M.; Miller, J.S. *Inorg. Chem.* **1998**, *37*, 3376.

35. See for example: (a) Herrmann, W.A. *Adv. Organometal. Chem.* **1982**, *20*, 159, and references therein. (b) McKeer, I.R.; Cowie, M. *Inorg. Chim. Acta* **1982**, *65*, L107. (c) Azam, K.A.; Frew, A.A.; Lloyd, B.R.; Manojlović -Muir, L.; Muir, K.W.; Puddephatt, R.J. *Chem. Commun.* **1982**, 614. (d) Laws, W.J.; Puddephatt, R.J. *Chem. Commun.* **1983**, 1020.

36. Shen, J.-K.; Tucker, D.S.; Basolo, F.; Hughes, R.P. *J. Am. Chem. Soc.* **1993**, *115*, 11312.

37. Brady, R.C.; Pettit, R. *J. Am. Chem.Soc.* **1980**, *102*, 6181.

Chapter 4

Methylene-to-Acetyl Conversion in Complexes of Rh/Os

Introduction

As part of our continued interest in bimetallic compounds containing hydrocarbyl fragments having relevance to Fischer-Tropsch (FT) chemistry,[1] we have been pursuing chemistry resulting from the reactivity of methylene-bridged units in heterobinuclear Rh/Os,[2] Ir/Ru,[3] and Rh/Ru[4] complexes. Our primary interest has been in the involvement of methylene groups in carbon-carbon bond formation, seeking information on the steps in hydrocarbon formation. We are also interested in the mechanisms of oxygen incorporation into the hydrocarbons. Although the major products in the FT reaction are olefins and alkanes, oxygen-containing products such as alcohols, aldehydes, acids, and ketones are also obtained.[5] Historically, the formation of hydrocarbons for use as liquid fuels was the primary objective; however, emphasis has changed such that the generation of feedstocks for the chemical industry is now the primary objective.[1c,6] Among these feedstocks, oxygenates are of current interest and attempts are underway to optimize their production.[5,7] Some bimetallic catalysts involving late-metal combinations have been investigated for oxygenate formation; a rhodium-ruthenium-based catalyst has been developed which has a high selectivity for the production of ethylene glycol from syngas[8] and several cobalt-ruthenium catalysts have been discovered which have a propensity for ethylene hydroformylation.[9] There is also considerable interest in the formation of alcohols such as methanol and ethanol, and catalysts involving Rh/Fe and Pd/Fe metal combinations have demonstrated higher activities and improved selectivities for methanol and ethanol production from syngas compared to their respective monometallic analogues.[10]

Although oxygenates are commonly produced in the FT reaction, little is known about the mechanisms involved in their formation. Based on analogies

with the ubiquitous, and well-studied migratory insertion of alkyl and carbonyl groups in transition-metal complexes,[11] proposals have been put forward implicating this process in oxygenate formation in the FT reaction.[12] The so-formed acyl moiety could then react with other surface fragments to produce the appropriate oxygenated compounds. Using bimetallic model complexes, it is possible to monitor potentially relevant reaction steps in the transformations and to study the mobilities of ligands and their migratory insertion tendencies on the bimetallic core. The carbonylation of methyl groups and subsequent reactivity has been studied to some extent in several dppm-bridged bimetallic systems (Rh/Rh,[13] Ru/Ru[14]), and an analogous dmpm-bridged diruthenium system (dmpm = $Me_2PCH_2PMe_2$).[15] We are interested in extending the investigation of migratory insertions to include combinations of different group 8/9 metals (Rh/Os, Ir/Ru), focusing on the roles of the different metals in the product formation. In this study we investigate the conversion of a bridging methylene group on a Rh/Os core into an acetyl group.

Experimental

General Comments

All solvents were dried (using appropriate drying agents), distilled before use, and stored under nitrogen. Reactions were performed under an argon atmosphere using standard Schlenk techniques. Rhodium(III)chloride trihydrate was purchased from Johnson Matthey Ltd., $Os_3(CO)_{12}$ was purchased from Strem and PMe_3 (in THF), $HBF_4 \cdot Me_2O$ and CF_3SO_3H were purchased from Aldrich. Carbon-13-enriched CO (99.4% enrichment) was purchased from Isotec Inc. The compound $[RhOs(CO)_4(\mu-CH_2)dppm)_2][BF_4]$ was prepared by the published procedure.[2]

NMR spectra were recorded on a Bruker AM-400 or Varian spectrometer operating at 400.1 MHz for ^{1}H, 161.9 MHz for ^{31}P, and 100.6 MHz for [13]C

nuclei. The $^{13}C\{^1H\}\{^{31}P\}$ NMR spectra were obtained on a Bruker WH-200 spectrometer operating at 50.3 MHz. Infrared spectra were obtained on a Nicolet Magna 750 FTIR Spectrometer with a NIC-Plan IR Microscope. The elemental analyses were performed by the microanalytical service within the department. Electron ionization mass spectra were run on a Micromass ZabSpec spectrometer. In all cases the distribution of isotope peaks for the appropriate parent ion matched very closely that calculated for the formulation given.

Spectroscopic data for all compounds are given in Table 4.1.

Preparation of Compounds

(a) **[RhOs(CO)$_4$(μ-CH$_3$)(dppm)$_2$][CF$_3$SO$_3$]$_2$ (1).** Triflic acid (CF$_3$SO$_3$H) (0.7 μL, 0.0075 mmol) was added to a CD$_2$Cl$_2$ solution (0.5 mL) of [RhOs(CO)$_4$(μ-CH$_2$)(dppm)$_2$][CF$_3$SO$_3$] (10 mg, 0.0075 mmol) in an NMR tube at -78°C. The solution changed from yellow to pale yellow. Compound **1** was only characterized spectroscopically since warming the solution to -20°C resulted in conversion of **1** to compound **2**, and subsequent warming to ambient temperature resulted in further conversion to **3** as described below.

(b) **[RhOs(CH$_2$D)(CO)$_4$(dppm)$_2$][CF$_3$SO$_3$]$_2$ (1-CH$_2$D).** Deuterated triflic acid (CF$_3$SO$_3$D) (0.7 μL, 0.0075 mmol) was added to a CD$_2$Cl$_2$ solution (0.5 mL) of [RhOs(CO)$_4$(μ-CH$_2$)(dppm)$_2$][CF$_3$SO$_3$] (10 mg, 0.0075 mmol) in an NMR tube at -78°C. NMR spectroscopy indicated a mixture of both **1** and **1-CH$_2$D**.

(c) **[RhOs(CHD$_2$)(CO)$_4$(dppm)$_2$][CF$_3$SO$_3$]$_2$ (1-CHD$_2$).** Triflic acid (CF$_3$SO$_3$H) (0.7 μL, 0.0075 mmol) was added to a CD$_2$Cl$_2$ solution (0.5 mL) of [RhOs(CO)$_4$(μ-CD$_2$)(dppm)$_2$][CF$_3$SO$_3$] (10 mg, 0.0075 mmol) in an NMR tube at -78°C. NMR spectroscopy indicated a mixture of the three isotopomers **1**, **1-CH$_2$D**, and **1-CHD$_2$**.

Table 4.1. Spectroscopic Data for the Compounds

Compound	IR $(cm^{-1})^f$	NMR[a,b] $^{31}P\{^1H\}$ (ppm)^c	^1H (ppm)^{d,e}	$^{13}C\{^1H\}$ (ppm)^d
$[RhOs(CH_3)(CO)_4$-$(dppm)_2][CF_3SO_3]_2$ (1)		P(Rh): 21.0 (m) P(Os): -15.1 (m)	CH_3: 0.21(s, br, 3H) dppm: 3.72 (m, 2H); 3.98 (m,2H)	CH_3: -32.2 (s, br) dppm: 20.2 (m, 2C) CO(Os):170.3 (br); 171.2 (br); 201.9 (dt, $^2J_{PC} = 8$ Hz, $^1J_{RhC} = $ 23 Hz) CO(Rh): 185.6 (dt, $^2J_{PC} = 14$ Hz, $^1J_{RhC} = 82$ Hz)
$[RhOs(CH_3)(CO)_4$-$(dppm)_2][CF_3SO_3]_2$ (2)		P(Rh): 28.9 (m) P(Os): -10.7 (m)	CH_3: 1.65 (dt, 3H, $^3J_{PH}$ 8.0 = Hz, $^2J_{RhH} = 2.1$ Hz) dppm: 3.61 (m, 4H)	CH_3: 43.1 (d, $^1J_{Rh-C}= 25$ Hz) CO(Os): 167.2 (m, 2C, $^2J_{PC} = 7$ Hz); 210.9 (dm, 2C, $^1J_{RhC} = 25$ Hz)
$[RhOs(\mu-CH_3CO)(CO)_3$-$(CF_3SO_3)(dppm)_2]$-$[CF_3SO_3]$ (3)	2070 (s),1989 (s), 1715 (s),1437 (m)	P(Rh): 5.5 (dm, $^1J_{RhP} = 150$ Hz) P(Os): -5.0 (m)	CH_3CO: 2.08 (s, 3H) dppm: 3.22 (m, 4H)	dppm: 22.5 (m, 2C) CH_3: 46.6 (s, br) CH_3CO: 313.3 (dm, $^1J_{RhC} = 42$ Hz) μ-CO: 239.9 (m) CO(Os): 174.7 (t, $^2J_{PC} = 6$ Hz); 174.2 (m, br)

[RhOs(μ-CH$_3$CO)(CO)$_4$ (dppm)$_2$][CF$_3$SO$_3$]$_2$ (4)		P(Rh): 13.3 (dm, $^1J_{RhP}$ = 128 Hz) P(Os): -4.5 (m)	CH$_3$CO: 1.81 (s, 3H) dppm: 3.44 (m, 2H); 3.86 (m, 2H)	CH$_3$CO: 321.8 (dm, $^1J_{RhC}$ = 30 Hz) μ-CO: 223.9 (m) CO(Rh): 187.6 (dm, $^1J_{RhC}$ = 47 Hz) CO(Os): 172.3 (s, br); 171.4 (s,br)
[RhOs(μ-CH$_3$CO)(CO)$_3$ (PMe$_3$)(dppm)$_2$]- [CF$_3$SO$_3$]$_2$ (5a)		P(Rh): 14.5 (dm, $^1J_{RhP}$ = 137 Hz) P(Os): -3.9 (m) PMe$_3$: -38.3(ddt, $^1J_{RhP}$ = 101 Hz)	CH$_3$: 0.91 (d, 9H; $^2J_{PH}$ = 8 Hz) dppm: 3.07 (m, 2H); 3.48 (m, 2H)	CH$_3$CO: 325.8 (ddt, $^1J_{RhC}$ = 30 Hz; $^2J_{P(Me3)C}$ = 82 Hz; $^2J_{PC}$ = 9 Hz) μ-CO: 237.0 (m) CO(Os): 174.8 (s, br); 171.2 (m)
[RhOs(μ-CH$_3$CO)(CO)$_3$ (PMe$_3$)(dppm)$_2$][CF$_3$SO$_3$] [BF$_4$] (5b)		P(Rh): 22.8 (dm, $^1J_{RhP}$ = 125 Hz) P(Os): -8.8 (m) PMe$_3$: -9.5(dt, $^1J_{RhP}$ = 100 Hz; $^2J_{PP}$ = 32 Hz)	CH$_3$: 0.98 (d, 9H; $^2J_{PH}$ = 8 Hz) dppm: 3.99 (m, 2H); 3.74 (m, 2H)	CH$_3$CO: 293.4 (m) μ-CO: 218.1 (m) CO(Os): 183.0 (m); 172.5 (m)
[RhOs(μ-CH$_3$CO)(CO)$_2$ (CF$_3$SO$_3$)(dppm)$_2$]- [CF$_3$SO$_3$] (6)	2033 (s), 1974 (s), 1436 (m)	P(Rh): 16.6 (m) P(Os): -4.7 (m)	CH$_3$CO: 2.03 (s, 3H) dppm: 2.60 (m, 2H); 3.92 (m, 2H)	CH$_3$CO: 274.2 (dt, $^1J_{RhC}$ = 31 Hz, $^2J_{PC}$ = 8 Hz) CO(Os): 181.6 (t, $^2J_{PC}$ = 6 Hz); 163.2 (dt, $^2J_{PC}$ = 7 Hz, $^2J_{RhC}$ = 7 Hz)

[RhOs(CF$_3$SO$_3$)(μ-H)(CO)$_4$dppm)$_2$] [CF$_3$SO$_3$] (7a)	P(Rh): 27.2 (m) P(Os): -7.3 (m)	μ-H: -10.46 (dtt, 1H; $^1J_{RhH}$ = 21 Hz, $^2J_{P(Rh)H}$ = 9 Hz, $^2J_{P(Os)H}$ = 8 Hz dppm: 4.92 (m, 4H); 4.31(m, 2H)	CO(Os): 200.0 (br); 171.8 (br); 169.4 (s) CO(Rh): 181.8 (dt, $^1J_{Rh-C}$ = 79 Hz; $^2J_{P-C}$ = 15 Hz)
[RhOs(BF$_4$)(μ-H)(CO)$_4$dppm)$_2$][BF$_4$] (7b)	P(Rh): 27.5 (m) P(Os): -6.7 (m)		CO(Os): 200.7 (br); 171.9 (br); 170.6 (s) CO(Rh): 182.7 (dt, $^1J_{Rh-C}$ = 79 Hz; $^2J_{P-C}$ = 15 Hz)

[a]NMR abbreviations: s = singlet, d = doublet, t = triplet, m = multiplet, dt = doublet of triplets, dm = doublet of multiplets, ddt = doublet of doublets of triplets, br = broad. [b]NMR data at 298K in CD$_2$Cl$_2$ unless otherwise state. [c] ^{31}P{^{1}H} NMR chemical shifts are referenced *versus* external 95% H$_3$PO$_4$. [d] ^{1}H and ^{13}C chemical shifts are referenced *versus* external TMS. [e]Chemical shifts for the phenyl hydrogens are not given. [f]IR abbreviations (ν(CO) unless otherwise stated): s = strong, m = medium. [g] ^{13}C resonances for methylene carbons of the dppm ligands.

(d) [RhOs(CH₃)(CO)₄(dppm)₂][CF₃SO₃]₂ (2). An NMR sample of **1** was prepared as outlined in part (a). The sample was then warmed to -20°C. Quantitative conversion of **1** to **2** occurred in approximately 1 h at this temperature. As was the case for **1** in part (a), characterization of **2** was carried out spectroscopically since above -20°C conversion to **3** occurred.

(e) [RhOs(CF₃SO₃)(CO)₂(μ-CO)(μ-C(CH₃)O)(dppm)₂][CF₃SO₃] (3). The compound [RhOs(CO)₄(μ-CH₂)(dppm)₂][CF₃SO₃] (50 mg, 0.037 mmol) was dissolved in 5 mL of CH₂Cl₂, and CF₃SO₃H (3.3 μL, 0.037 mmol) was added, causing the solution to immediately change to pale yellow. The solution was stirred for 30 min. during which time the solution became yellow-orange. Ether (40 mL) was then added to precipitate an orange solid. This precipitate was washed with three 10 mL portions of diethyl ether and dried *in vacuo* (yield 82 %). The solid also contained approximately 10% of an impurity identified as compound **6** (see below), which we failed to separate. Elemental analysis was not performed on this mixture of products, however the mass spectrum showed the expected parent ion without the triflate anion. MS m/z 1339 (M^+ - CF₃SO₃). Compound **3**, with **6** as an accompanying impurity, was also obtained on warming a sample of **2** to ambient temperature.

(f) [RhOs(CO)₄(μ-C(CH₃)O)(dppm)₂][CF₃SO₃]₂ (4). CO was passed through a solution of **3** in an NMR tube at -60°C. The solution changed from yellow to pale yellow. Upon warming to room temperature, **4** converted to **3**. Characterization of **4** was by multinuclear NMR techniques at -60°C.

(g) [RhOs(CO)₄(PMe₃)(μ-C(CH₃)O)(dppm)₂][CF₃SO₃]₂ (5). A 1.0 M THF solution of PMe₃ (14 μL) was added to a CD₂Cl₂ solution (0.7 mL) of **3** (10 mg) in an NMR tube at -80°C. Characterization of the first product **5a** was by

multinuclear NMR techniques at -80°C, since warming to ambient temperature resulted in quantitative transformation of this product into an isomer (**5b**). Spectroscopic data for the two species indicate that these isomers differ only in the coordination of the bridging acetyl group, which is C-bound to Rh in **5a** and to Os in **5b** (see Table 4.1 for spectroscopic data). Attempts to isolate **5b** as a solid led to decomposition to unidentified species.

(h) **[RhOs(CF$_3$SO$_3$)(CO)$_2$(μ-C(CH$_3$)O)(dppm)$_2$][CF$_3$SO$_3$] (6)**. Compound 3 (30 mg, 0.02 mmol) was dissolved in 10 mL of CH$_2$Cl$_2$ and the solution was refluxed for 1 h under a slow argon purge. Ether (40 mL) was then added to precipitate an orange solid, which was recrystallized from CH$_2$Cl$_2$/ether and dried *in vacuo* (yield 90%). Anal. Calcd for C$_{56}$H$_{47}$F$_6$O$_9$P$_4$S$_2$RhOs: C, 46.06; H, 3.24. Found: C, 45.67; H, 3.27. MS m/z 1311 (M$^+$ - CF$_3$SO$_3$).

(i) **[RhOs(CF$_3$SO$_3$)(CO)$_4$(μ-H)(μ-CO)(dppm)$_2$][CF$_3$SO$_3$] (7a)**. Triflic acid (7 μL, 0.076 mmol) was added to a CD$_2$Cl$_2$ solution (5 mL) of [RhOs(CO)$_4$(dppm)$_2$][CF$_3$SO$_3$] (100 mg, 0.0076 mmol). The solution was stirred for 30 min and remained yellow. Ether (20 mL) was then added to precipitate a yellow solid, which was recrystallized from CH$_2$Cl$_2$/ether and dried *in vacuo* (yield 91%).

(j) **[RhOs(BF$_4$)(CO)$_4$(μ-H)(μ-CO)(dppm)$_2$][BF$_4$] (7b)**. A solution of HBF$_4$ in ether (11 μL, 0.079 mmol) was added to a CD$_2$Cl$_2$ solution (5 mL) of [RhOs(CO)$_4$(dppm)$_2$][CF$_4$] (100 mg, 0.079 mmol). The solution was stirred for 30 min and remained yellow. Ether (20 mL) was then added to precipitate a yellow solid, which was recrystallized from CH$_2$Cl$_2$/ether and dried *in vacuo* (yield 86%). Anal. Calcd for C$_{54}$H$_{45}$B$_2$F$_8$O$_4$P$_4$RhOs: C, 48.09; H, 3.36. Found: C, 47.70; H, 3.26.

X-ray Data Collection

X-ray data collection and structure solutions were carried out by Dr. R. McDonald in the departmental X-ray Structure Determination Laboratory. Pale yellow crystals of $[RhOs(CO)_2(O_3SCF_3)(\mu\text{-}CO)(\mu\text{-}C(CH_3)O)(dppm)_2]$-$[BF_4]\cdot2.5CH_2Cl_2$ (**3**) were obtained *via* slow evaporation of a dichloromethane solution of the complex. Data were collected on a Bruker PLATFORM/SMART 1000 CCD diffractometer[16] using Mo Kα radiation at -80°C. Unit cell parameters were obtained from a least-squares refinement of the setting angles of 7281 reflections from the data collection. The space group was determined to be $P2_1/n$ (an alternate setting of $P2_1/c$ [No.14]). The data were corrected for absorption through use of the *SADABS* procedure. See Table 4.2 for a summary of crystal data and X-ray data collection information.

Orange crystals of $[RhOs(CO)_2(O_3SCF_3)(\mu\text{-}C(CH_3)O)(dppm)_2][CF_3SO_3]$ $\cdot2CH_2Cl_2$ (**6**) were obtained *via* slow diffusion of diethyl ether into a dichloromethane solution of the compound. Data were collected and corrected for absorption as for **3** above (see Table 4.2). Unit cell parameters were obtained from a least-squares refinement of the setting angles of 6151 reflections from the data collection, and the space group was determined to be $P2_12_12_1$ (No. 19). Yellow crystals of $[RhOs(O_3SCF_3)(CO)_3(\mu\text{-}H)(\mu\text{-}CO)(dppm)_2][CF_3SO_3]\cdot2H_2O$ (**7a**) were obtained as for **6**. Data were collected and corrected as outlined in Table 4.2. Unit cell parameters were obtained from a least-squares refinement of the setting angles of 4220 reflections from the data collection, and the space group was determined to be $Pca2_1$ (No. 29).

Structure Solution and Refinement

The structure of **3** was solved using automated Patterson location of the heavy metal atoms and structure expansion *via* the *DIRDIF-96* program system.[17] Refinement was completed using the program *SHELXL-93*.[18] Hydrogen atoms

were assigned positions based on the geometries of their attached carbon atoms, and were given thermal parameters 20% greater than those of the attached carbons. The coordinated triflate group was disordered over two orientations in a 70:30 ratio, having a common site for the oxygen coordinated to Rh. An idealized geometry was imposed upon the minority ($^1/_3$) conformer for the coordinated triflate group by assigning fixed idealized values to the S-C (1.80 Å) and F-C (1.35 Å) distances; interatomic distances within the half-occupancy solvent dichloromethane molecule were also assigned idealized values (d(Cl(5S)-d(C(3S)) = d(Cl(6S)-d(C(3S)) = 1.80 Å; d(Cl(5S)...d(Cl(6S)) = 2.95 Å). The final model for **3** refined to values of $R_1(F)$ = 0.0544 (for 10092 data with $F_o^2 \geq 2\sigma(F_o^2)$) and $wR_2(F^2)$ = 0.1475 (for all 13179 independent data).

The structures of **6** and **7a** were also solved using the *DIRDIF-96* program system in the same manner as for **3** above. Refinement was completed using the program *SHELXL-93*, during which the hydrogen atoms were treated as for **3**. The final model for **6** refined to values of $R_1(F)$ = 0.0339 (for 11389 data with $F_o^2 \geq 2\sigma(F_o^2)$) and $wR_2(F^2)$ = 0.0766 (for all 12533 independent data).

For compound **7a** two water molecules were located in the unit cell. The final model converged to R_1 = 0.0503 for 10069 reflections with $F_o^2 \geq 2\sigma(F_o^2)$, and $wR_2(F^2)$ = 0.1520 for all 13495 independent data.

Table 4.2 Crystallographic Experimental Details for Compounds **3, 6** and **7a**.

compound	3	6	7a
formula	$C_{58.5}H_{52}BCl_5F_7O_7OsP_4RhS$	$C_{58}H_{51}Cl_4F_6O_9OsP_4RhS_2$	$C_{56}H_{49}F_6O_{12}OsP_4RhS_2$
formula weight	1637.11	1628.90	1509.06
crystal dimensions (mm)	0.72 x 0.17 x 0.03	0.30 x 0.19 x 0.07	0.41 x 0.08 x 0.06
crystal system	monoclinic	orthorhombic	orthorhombic
space group	$P2_1/n$ (an alternate setting of $P2_1/c$ [No. 14])	$P2_12_12_1$ (No. 19)	$Pca2_1$ (No. 29)
unit cell parameters			
a (Å)	10.2572 (10)[a]	14.5915 (7)[b]	24.229(2)[c]
b (Å)	24.675 (2)	17.0016 (8)	22.8565(10)
c (Å)	25.890 (2)	24.6970 (12)	23.376(2)
b (deg)	95.4565 (19)	90	90
V (Å^3)	6522.9 (11)	6126.8 (5)	6715.3(10)
Z	4	4	4
r_{calcd} (g cm^{-3})	1.667	1.766	1.493
μ (mm^{-1})	2.603	2.762	2.363

B. Data Collection and Refinement Conditions

diffractometer	Bruker PLATFORM/SMART 1000 CCD	Bruker PLATFORM/SMART 1000 CCD	Bruker PLATFORM/SMART 1000 CCD
radiation (λ [Å])	graphite-monochromated Mo Kα (0.71073)	graphite-monochromated Mo Kα (0.71073)	graphite-monochromated Mo Kα (0.71073)
temperature (°C)	–80	–80	-80
scan type	w scans (0.2°) (20 s exposures)	w scans (0.2°) (20 s exposures)	w scans (0.2°) (30 s exposures)
data collection $2h$ limit (deg)	52.84	52.82	52.82
total data collected	34036 (-12 ≤ h ≤ 11, -30 ≤ k ≤ 30, -32 ≤ l ≤ 28)	28744 (-18 ≤ h ≤ 11, -20 ≤ k ≤ 21, -30 ≤ l ≤ 30)	30173 (-29 ≤ h ≤ 30, -14 ≤ k ≤12, -29 ≤ l ≤ 29)
independent reflections	13179 (R_{int} = 0.0588)	12533 (R_{int} = 0.0378)	13495 (R_{int} = 0.0500)

number of observed reflections (NO)	10092 $[F_o{}^2 \geq 2\sigma(F_o{}^2)]$	11389 $[F_o{}^2 \geq 2\sigma(F_o{}^2)]$	10069 $[F_o{}^2 \geq 2\sigma(F_o{}^2)]$
structure solution method	Patterson search/structure expansion ($DIRDIF$–96)	Patterson search/structure expansion ($DIRDIF$–96)	Patterson search/structure expansion ($DIRDIF$-96)
refinement method	full-matrix least-squares on F^2 ($SHELXL$–93^d)	full-matrix least-squares on F^2 ($SHELXL$–93^d)	full-matrix least-squares on F^2 ($SHELXL$-93^d)
absorption correction method	empirical ($SADABS$)	empirical ($SADABS$)	empirical ($SADABS$)
range of transmission factors	0.9260–0.2558	0.8302–0.4912	0.8712-0.4442
data/restraints/parameters	13179 $[F_o{}^2 \geq -3\sigma(F_o{}^2)]/7^e/763$	12533 $[F_o{}^2 \geq -3\sigma(F_o{}^2)]/0/768$	13495 $[F_o{}^2 \geq -3\sigma(F_o{}^2)]/3^f/658$
Flack absolute structure parameter^g	-	0.485 (4)	0.016(8)
goodness-of-fit (S)^h	1.049 $[F_o{}^2 \geq -3\sigma(F_o{}^2)]$	1.041 $[F_o{}^2 \geq -3\sigma(F_o{}^2)]$	1.068 $[F_o{}^2 \geq -3\sigma(F_o{}^2)]$
final R indices^i			
R_1 $[F_o{}^2 \geq 2\sigma(F_o{}^2)]$	0.0544	0.0339	0.0563
wR_2 $[F_o{}^2 \geq -3\sigma(F_o{}^2)]$	0.1475	0.0766	0.1520
largest difference peak and hole	1.867 and –1.659 e Å^{-3}	1.257 and –0.593 e Å^{-3}	1.713 and -0.942 e Å^{-3}

^{a}Obtained from least-squares refinement of 7281 centered reflections.

^{b}Obtained from least-squares refinement of 6151 centered reflections.

^{c}Obtained from least-squares refinement of 4220 centered reflections.

^{d}Refinement on $F_o{}^2$ for all reflections (all of these having $F_o{}^2 \geq -3\sigma(F_o{}^2)$). Weighted R-factors wR_2 and all goodnesses of fit S are based on $F_o{}^2$; conventional R-factors R_1 are based on F_o, with F_o set to zero for negative $F_o{}^2$. The observed criterion of $F_o{}^2 \geq 2\sigma(F_o{}^2)$ is used only for calculating R_1, and is not relevant to the choice of reflections for refinement. R-factors based on $F_o{}^2$ are statistically about twice as large as those based on F_o, and R-factors based on ALL data will be even larger.

^{e}The S–C (1.80 Å) and F–C (1.35 Å) distances within the minority ($^1/3$) conformer for the coordinated triflate group were assigned fixed idealized values, as were interatomic distances within the half-occupancy solvent dichloromethane molecule (d(Cl(5S)–d(C(3S)) = d(Cl(6S)–d(C(3S)) = 1.80 Å; d(Cl(5S)···d(Cl(6S)) = 2.95 Å).

fThe bridging hydrido ligand (H(1)) was refined with an idealized geometry by fixing the Os-H and Rh-H distances at 1.85Å, and by constraining the Os, Rh, C(3) and H(1) atoms to planarity.

gFlack, H.D. *Acta Crystallogr.* **1983**, *A39*, 876. The Flack parameter will refine to a value near zero if the structure has the correct configuration and near one for the inverted configuration. The value observed for compound **6** is indicative of racemic twinning and was accommodated during refinement using the *SHELXL-93* TWIN instruction (see ref. 18).

$hS = [\Sigma w(F_o{}^2 - F_c{}^2)^2/(n - p)]^{1/2}$ (n = number of data; p = number of parameters varied; $w = [\sigma^2(F_o{}^2) + (a_0 P)^2 + a_1 P]^{-1}$ where $P = [\text{Max}(F_o{}^2, 0) + 2F_c{}^2]/3)$ and the values of a_0 and a_1 are adjusted by the refinement program; for **3**, $a_0 = 0.0738$, $a_1 = 21.7034$; for **6**, $a_0 = 0.0402$, $a_1 = 0$; for **7a**, $a_0 = 0.0775$, $a_1 = 0$).

$iR_1 = \Sigma||F_o| - |F_c||/\Sigma|F_o|$; $wR_2 = [\Sigma w(F_o{}^2 - F_c{}^2)^2/\Sigma w(F_o{}^4)]^{1/2}$.

Results

Protonation of the methylene-bridged compound $[RhOs(CO)_3(\mu\text{-}CO)(\mu\text{-}CH_2)(dppm)_2][CF_3SO_3]$, using triflic acid (CF_3SO_3H), at -80°C yields a dicationic methyl compound $[RhOs(CO)_4(CH_3)(dppm)_2][CF_3SO_3]_2$ (**1**) (Scheme 4.1). No evidence of a methylene-bridged hydride species resulting from protonation at either metal was observed. $^1H/^{31}P$ NMR correlation spectroscopy shows strong coupling between the osmium-bound phosphines and the methyl protons and a much weaker coupling between the rhodium-bound phosphines and the methyl group. This suggests that the methyl group is primarily bound to osmium but that there is also a weak interaction between the methyl protons and rhodium. The observed ^1H resonance is broad at -80°C, sharpening somewhat, but not resolving, at -40°C. The spectra of **1** could not be obtained at higher temperatures since it transforms to a new compound (**2**). At lower temperatures (-100°C) the signal breadth increases.

The coupling of the methyl protons to the phosphines on both metals suggests that this group may be bridging. To investigate this further, the isotopomers of **1** incorporating CH_3, CH_2D and CHD_2 groups were prepared. The CH_2D isotopomer (**1-CH2D**) was obtained by reaction of $[RhOs(CO)_2(\mu\text{-}CO)(\mu\text{-}CH_2)(dppm)_2][CF_3SO_3]$ with CF_3SO_3D, whereas **1-CHD2**, (as well as amounts of the other isotopomers) was obtained by protonation of $[RhOs(CO)_2(\mu\text{-}CO)(\mu\text{-}CD_2)(dppm)_2][CF_3SO_3]$. At -40°C the CH_3 methyl resonance of **1** is observed at 0.25 ppm in the ^1H NMR spectrum, whereas the signal for **1-CH2D** appears at 0.07 ppm and that for **1-CHD2** is further upfield shifted to -0.15 ppm (see Figure 4.1).

The shift of the ^1H NMR resonance of a methyl group to higher fields as the deuteration is increased is characteristic of an agostic interaction. Due to the lower zero-point energy of a C-D bond relative to C-H, an agostic interaction

Scheme 4.1

$$X = CF_3SO_3{}^-$$
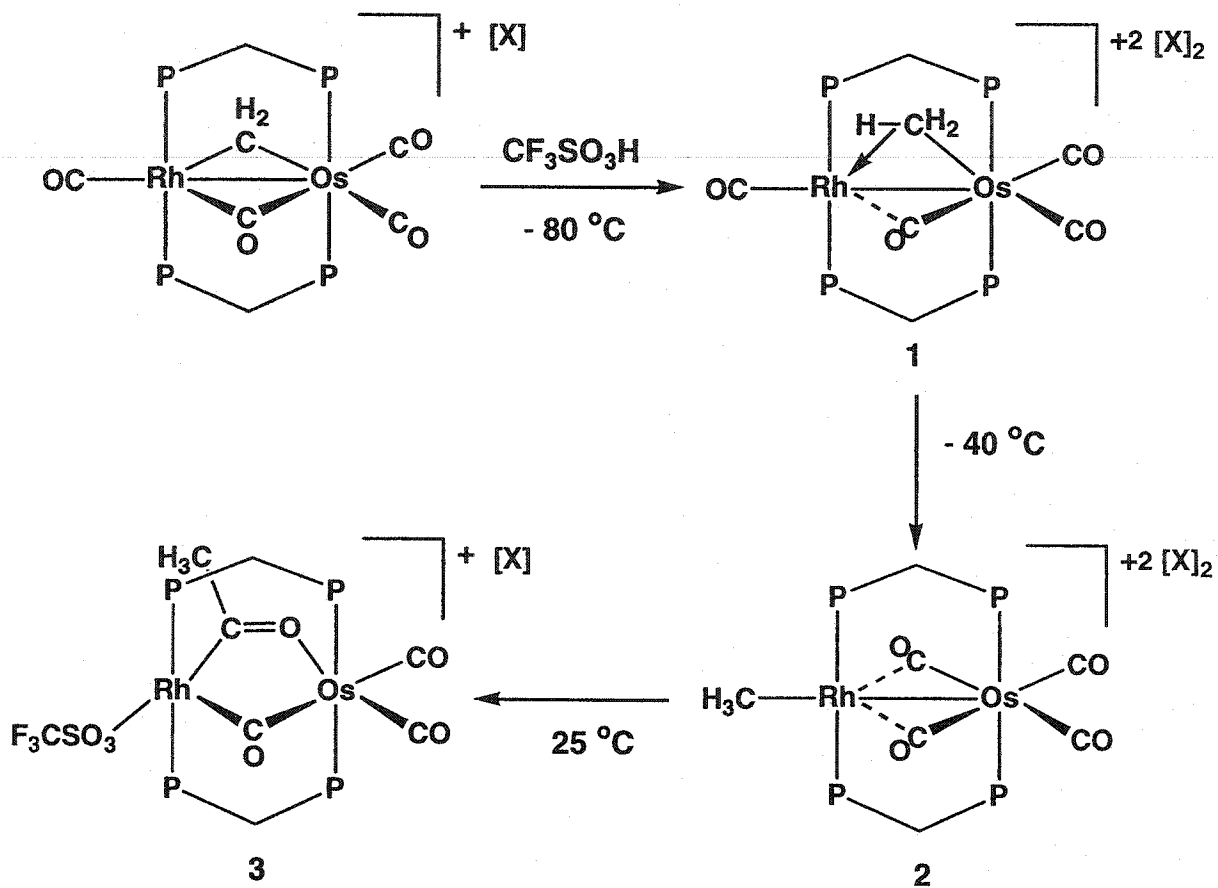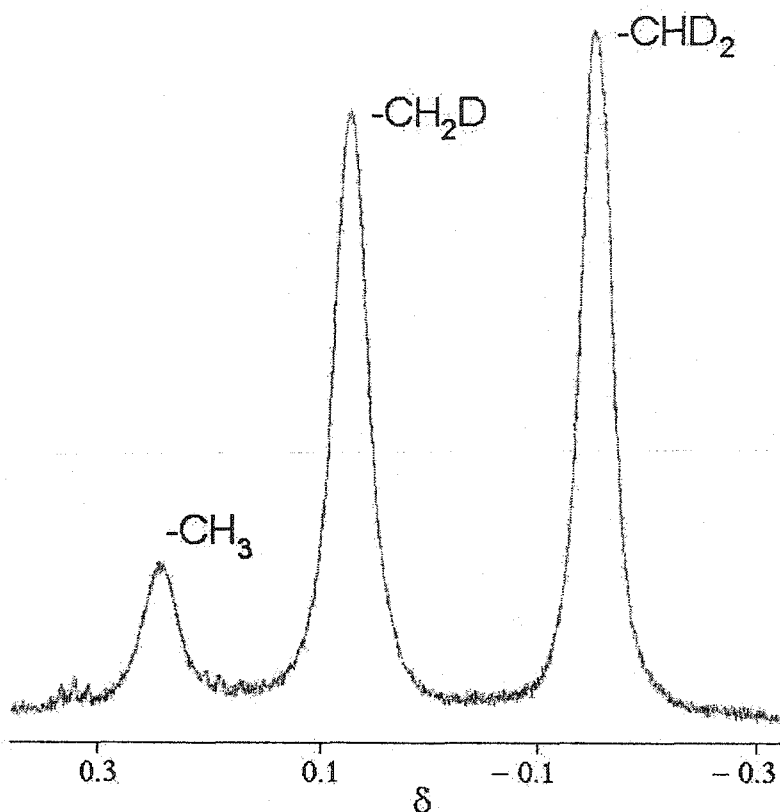
Figure 4.1 ^{1}H NMR spectrum of the methyl isotopomers of **2**.

involving a C-H bond (**A** in Chart 4.1) is favored over that involving a C-D bond (**B**). Thus, as the deuteration is increased, the remaining proton(s) in the isotopomers of the methyl group will spend an increased amount of time bound to the rhodium center (**A**) leading to upfield chemical shifts for the protons in the

Chart 4.1
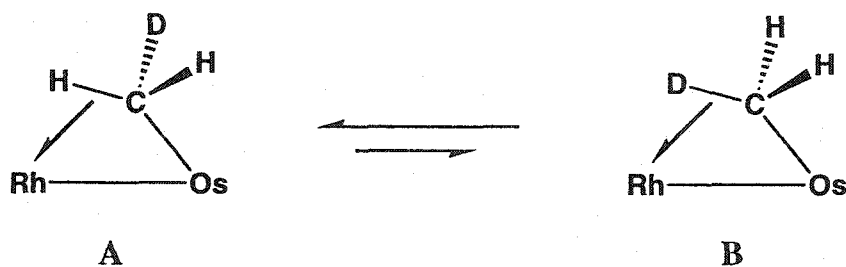
^{1}H NMR spectrum. A similar agostic interaction of a methyl group has recently been reported in a dppm-bridged diruthenium complex.[14] This NMR technique, called isotopic perturbation of resonance (IPR), was first described by Saunders[19] in studies of carbocations, but was later developed by Shapley[20] and others[21,22] to investigate the agostic bonding of bridging methyl groups in transition metal complexes.

The IPR effect observed here could also be a consequence of a rapidly exchanging bridging-methylene/hydride complex (Chart 4.2) as recently reported in a dppm-bridged diiridium compound.[23] In a methylene-bridged hydride structure such as **C** or **D** zero-point energy effects favor retention of a C-D bond (**D**) over a C-H bond (**C**), resulting in a similar upfield ^{1}H NMR signal as deuteration

Chart 4.2

C   D
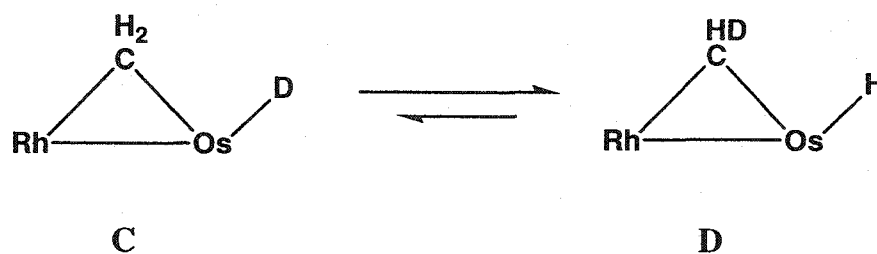
increases.[24] In the aforementioned diiridium complex, the sharp ^{1}H resonance observed at ambient temperature collapsed into the baseline at ca. -60°C, and by -100°C two broad resonances (at 4.2 and -14.6 ppm) for the methylene and hydride signals, respectively, had started to emerge.[23] For compound **1** the low-temperature limiting structure has not been observed at -100°C as the signal remains broad at this temperature, indicating a lower activation energy than observed for the C-H activation step in the "Ir$_2$" complex, suggesting to us that

equilibration of an agostic structure by methyl rotation about the Os-CH$_3$ bond is occurring, as shown by the process in Chart 4.1.

In principle, further evidence for agostic bonding involving a bridging methyl group is the reduced $^1J_{CH}$ value for this group. However, the observed average $^1J_{CH}$ value of 125 Hz in a $^{13}CH_3$-enriched sample of compound **1** lies in the normal range for terminally bound methyl groups, which can lie between 120 and 145 Hz for late-metal complexes.[25] Nevertheless, the observed value is close to the 121 Hz observed in [Os$_3$(CO)$_{10}$(μ-H)(μ-CH$_3$)][20] and [Cp$_2$Fe$_2$(CO)$_2$-(μ-CH$_3$)(μ-CO)],[22a] which have been shown to have bridged agostic methyl groups and is significantly less than the observed 139 Hz in compound **2** (vide infra) in which the methyl group adopts a conventional η^1 bonding mode. In a methylene-bridged hydride complex, coupling between the methylene carbon and the hydride ligand should be close to 0 Hz, giving rise to an average coupling of *ca.* 93 Hz (assuming $^1J_{C-H}$ = 140 Hz for a methylene group),[22,23,24a] as observed in the Ir$_2$ compound. Clearly, the observed $^1J_{CH}$ value for **1** is inconsistent with a methylene-hydride exchange process, and is instead consistent with an asymmetrically bridged methyl group.

In the $^{13}C\{^1H\}$ NMR spectrum at -60°C, the methyl resonance appears as a broad singlet at -32.2 ppm; no coupling to the ^{31}P or ^{103}Rh nuclei is evident. The high-field chemical shift of this carbon is also supportive of an agostic methyl group rather than a methylene-hydride complex, and can be contrasted to the ^{13}C resonance at +36.1 ppm observed for the methylene carbon in the diiridium species.[23] Furthermore, the lack of coupling between this carbon and rhodium is clearly inconsistent with a bridging methylene group and again suggests a weak agostic interaction between a methyl group and rhodium. In the carbonyl region, two broad signals at 170.3 and 171.2 ppm are assigned to osmium-bound carbonyls since they show no rhodium coupling, whereas a doublet of triplets at 185.6 ppm corresponds to a rhodium-bound carbonyl ($^1J_{Rh-C}$ = 82 Hz, $^2J_{P(Rh)-C}$ = 14 Hz). A

fourth signal, a doublet of triplets at 201.9 ppm, is assigned to a semi-bridging carbonyl on the basis of the rhodium coupling ($^1J_{Rh-C}$) of 23 Hz as well as a lower coupling constant with the osmium-bound phosphorus nuclei ($^2J_{P(Os)-C} = 8$ Hz) compared to the terminally-bound carbonyls. The down-field chemical shift of this carbonyl is also characteristic of a semi-bridging carbonyl.

Upon warming a solution of **1** to -20°C a new compound, [RhOs(CH$_3$)-(CO)$_4$(dppm)$_2$][CF$_3$SO$_3$]$_2$ (**2**) forms, which is an isomer of **1**, containing a rhodium-bound methyl group (see Scheme 4.1). In the ^{1}H NMR spectrum this methyl group appears at 1.65 ppm as a doublet of triplets due to coupling to rhodium ($^2J_{Rh-H} = 9$ Hz) and the rhodium-bound phosphines ($^3J_{P-H} = 7$ Hz). As noted earlier, the C-H coupling constant of 139 Hz observed when the methyl group is ^{13}C enriched, is consistent with a terminally bound methyl ligand. The dppm methylene protons appear as a single multiplet indicating front/back symmetry in the molecule, in contrast to the two dppm resonances observed in **1** where the environment on one side of the RhOsP$_4$ plane differs from that on the other. The ^{13}C{^{1}H} NMR spectrum of **2** contains two resonances in the carbonyl region; the resonance at 167.2 ppm represents two equivalent osmium-bound carbonyls, and the signal at 210.9 ppm is assigned to two equivalent osmium-bound carbonyls having a semi-bridging interaction with the rhodium center ($^1J_{Rh-C} = 25$ Hz). The chemical shift of the methyl carbon appears at 43.1 ppm, considerably downfield with respect to its precursor **1**, in which the methyl group was bound to osmium, and the coupling of this methyl carbon to Rh ($^1J_{Rh-C} = 25$ Hz) unambiguously establishes the connectivity for **2**. A downfield shift for the rhodium-bound methyl group compared to that bound to Os was also seen in the dimethyl compound [RhOs(CH$_3$)$_2$(CO)$_3$(dppm)$_2$][CF$_3$SO$_3$] in which the osmium-bound methyl group appears at -18.1 ppm while that bound to rhodium appears at 22.8 ppm.[26]

Upon warming to ambient temperature, compound **2** transforms into yet another compound, [RhOs(CF$_3$SO$_3$)(CO)$_2$(μ-CO)(μ-C(CH$_3$)O)(dppm)$_2$][CF$_3$SO$_3$] (**3**), as can be seen in the ^{31}P NMR spectrum, where new resonances at 5.5 ppm and -5.0 ppm appear; the low-field signal represents the rhodium-bound phosphorus nuclei ($^1J_{Rh-P}$ = 150 Hz). The pattern of this signal is characteristic of a "RhOs(dppm)$_2$" complex in which there is no metal-metal bond. In similar, bis dppm-bridged compounds containing metal-metal bonds, the intraligand P-P coupling is comparable to the Rh-P coupling resulting in an observed ^{31}P{^{1}H} signal for the rhodium-bound phosphines that is best described as a multiplet.[26,27] In non-metal-metal bonded species the absence of a metal-metal bond results in a decrease in the P-P couplings resulting in a signal that can be described as a doublet of pseudo-triplets. In the ^{1}H NMR spectrum the methyl group appears as a sharp singlet at 2.08 ppm indicating no coupling to either ^{31}P or ^{103}Rh nuclei. When a ^{13}CO enriched sample was examined, the methyl protons appear as a doublet signal with coupling to a carbonyl carbon ($^2J_{C-H}$ = 4 Hz). This suggests the assignment [RhOs(CF$_3$SO$_3$)(CO)$_2$(μ-CO)(μ-C(CH$_3$)O)(dppm)$_2$][CF$_3$SO$_3$] for **3** shown in Scheme 4.1, in which an acetyl group has formed by migratory insertion. Although the dppm-methylene protons appear as a single multiplet suggesting a front/back symmetry to the molecule, the subsequent structural determination (*vide infra*) clearly indicates that the proposed structure is correct, in which the acyl group bridges the metals, indicating an accidental equivalence of the two inequivalent dppm-methylene protons.

Support for the acyl formulation comes from the ^{13}C NMR spectrum in which the acyl carbon resonates at 313.3 ppm showing a strong coupling to Rh ($^1J_{Rh-C}$ = 42 Hz). The significant downfield shift of this carbon is characteristic of a bridging acyl group and suggests some degree of carbene character,[15,28] and can be contrasted to terminally-bound acyl groups that typically appear in the 230-260 ppm range in the ^{13}C NMR spectrum.[13-15,28] Similar downfield shifts have been

observed in other binuclear dppm- or dmpm-bridged systems (Rh-Rh,[13] Ru-Ru[14,15]) containing bridging acetyl groups, and these complexes have also been assigned carbene character. This bridging mode allows for two resonance structures as depicted in Chart 4.3, the latter of which (F) contributes to the observed low-field ^{13}C shift.

Chart 4.3

E   F
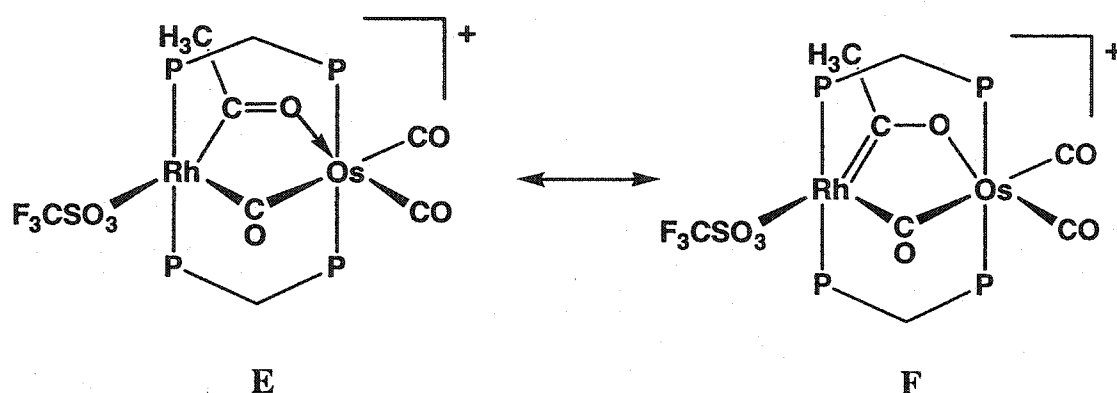
Also, in the $^{13}C\{^{1}H\}$ NMR spectrum the bridging carbonyl resonance appears as a low-field multiplet at 239.9 ppm; the coupling to Rh could not be resolved owing to coupling to the phosphines and to the other carbonyls. The terminal carbonyls appear at 174.7 and 174.2 ppm and are established as being bound to osmium on the basis of the absence of Rh coupling. The methyl carbon of the acyl group, at 46.6 ppm, is slightly broad possibly indicating a small unresolved coupling to rhodium. The IR spectrum is also consistent with this formulation, showing a bridging carbonyl stretch at a characteristic low frequency (1716 cm^{-1}). Unfortunately, no stretch corresponding to the acyl carbonyl was observed, even using comparisons with the spectrum for the ^{13}CO-labeled sample.

The above structural assignment for **3** has been confirmed by an X-ray structure determination which clearly shows the bridging acyl/bridging carbonyl arrangement, in which the acyl group is carbon-bound to rhodium, and oxygen-bound to osmium (see Figure 4.2). Bond lengths and angles are summarized in Table 4.3. Both dppm ligands have the normal "trans-bridging" arrangement typical of "A-frame" complexes. About Os, the geometry is octahedral, having mutually trans phosphine ligands and the mutually-cis bridging acyl and carbonyl groups opposite the two terminal carbonyls. At rhodium, the geometry is a distorted tetragonal pyramid in which two sites are occupied by the trans phosphines (P(2)-Rh-P(4) = 171.16(7)°), and the other three by the acyl carbon, the bridging carbonyl, and a triflate anion (opposite the acyl group). The coordination site opposite the apical bridging carbonyl is vacant. The geometry at the bridging acyl group is consistent with sp^2 hybridization of the acyl carbon with angles at C(4) of approximately 120°. Both the short Rh-C(4) (1.907(7) Å) and the long C(4)-O(4) (1.258(8) Å) distances are consistent with a high degree of carbene character;[29] the Rh-C(4) distance is substantially shorter than typical acetyl groups and is even shorter than that reported for a carbene-like acyl group in $[Rh_2(CO)_2(\mu\text{-}C(CH_3)O)(dppm)_2][CF_3SO_3]$ (2.05(2) Å).[13] Certainly the Rh-acyl distance in **3** is comparable to the Os-CO distances for which significant π back-bonding is assumed (*cf.* Os-C(1), Os-C(2) = 1.958(7), 1.874(7) Å). Similarly, the C(4)-O(4) distance is substantially longer than observed in normal η^1-acetyl groups and is comparable to that reported by Eisenberg (1.28(2) Å).[13] The structural parameters for the bridging acyl group are in support of the oxycarbene formulation as suggested by the ^{13}C NMR data (*vide infra*).

The long Rh-Os separation (3.4417(6) Å) is much longer than the average intraligand P-P separation (3.165(2) Å) and is consistent with the absence of a metal-metal bond, resulting in a large Rh-C(3)-Os angle of 113.2(3)°. Although
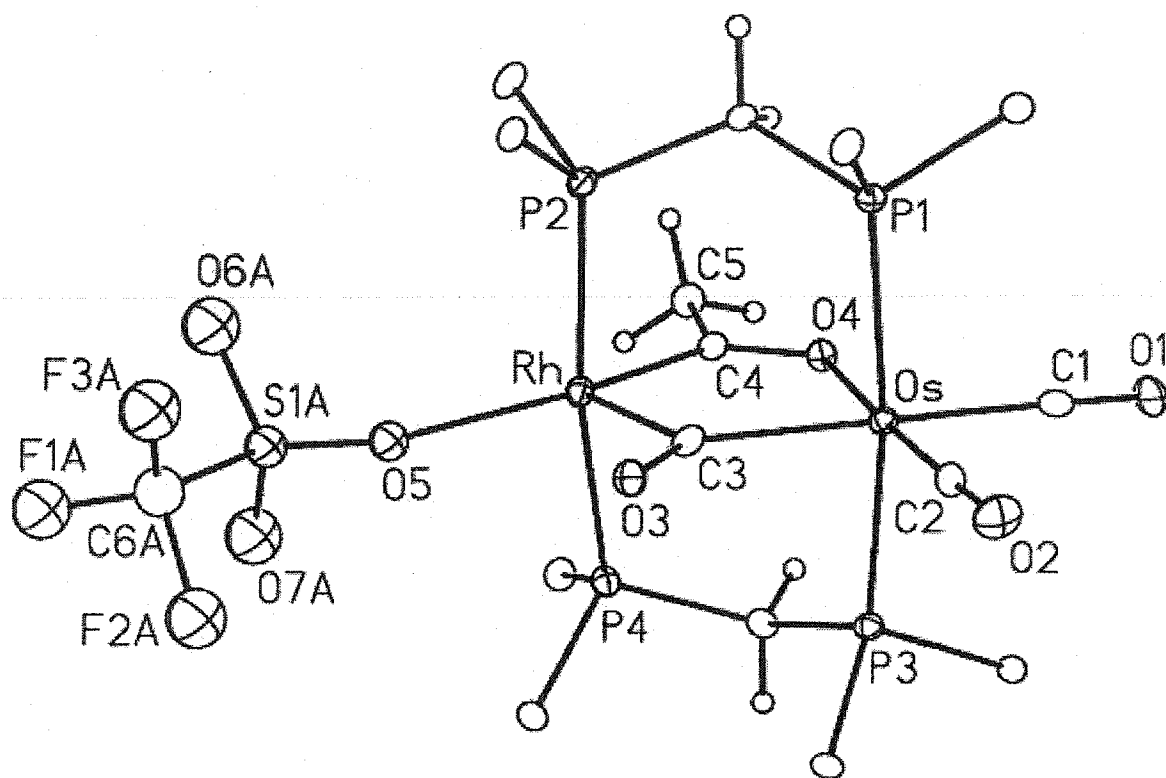
Figure 4.2. Perspective view of [RhOs(CF$_3$SO$_3$)(CO)$_2$(μ-CO)(μ-C(O)CH$_3$)-(dppm)$_2$][CF$_3$SO$_3$] (**3**) showing the atom-labeling scheme. Non-hydrogen atoms are represented by Gaussian ellipsoids at the 20% probability level. Hydrogen atoms are shown with arbitrarily small thermal parameters. Only the ipso carbons of the dppm phenyl groups are shown for clarity. Only the major occupant for the disordered coordinated triflate group is shown.

Table 4.3 Selected Bond Distances and Angles for compound **3**.

Atom 1	Atom 2	Distance (Å)	Atom 1	Atom 2	Atom 3	Angle (°)
Os	Rh	3.4417(6)	P(1)	Os	P(3)	171.40(6)
Os	P(1)	2.3924(19)	O(4)	Os	C(1)	87.7(2)
Os	P(3)	2.3969(19)	O(4)	Os	C(2)	177.8(3)
Os	O(4)	2.128(4)	O(4)	Os	C(3)	87.8(2)
Os	C(1)	1.958(7)	C(1)	Os	C(2)	90.6(3)
Os	C(2)	1.874(7)	C(1)	Os	C(3)	175.2(3)
Os	C(3)	2.097(7)	C(2)	Os	C(3)	93.9(3)
Rh	P(2)	2.374(2)	P(2)	Rh	P(4)	171.16(7)
Rh	P(4)	2.367(2)	O(5)	Rh	C(3)	99.4(2)
Rh	O(5)	2.240(5)	O(5)	Rh	C(4)	167.1(2)
Rh	C(3)	2.025(7)	C(3)	Rh	C(4)	93.4(3)
Rh	C(4)	1.907(7)	Os	O(4)	C(4)	120.2(4)
S(1)	O(5)	1.419(6)	Rh	O(5)	S(1)	136.3(4)
P(1)	P(2)	3.168(2)	Os	C(3)	Rh	113.2(3)
P(3)	P(4)	3.161(2)	Os	C(3)	O(3)	132.7(5)
O(1)	C(1)	1.123(8)	Rh	C(3)	O(3)	114.1(5)
O(2)	C(2)	1.140(8)	Rh	C(4)	O(4)	125.3(5)
O(3)	C(3)	1.182(8)	Rh	C(4)	C(5)	118.8(5)
O(4)	C(4)	1.258(8)	P(1)	C(7)	P(2)	118.8(4)
			P(3)	C(8)	P(4)	118.2(4)

the Rh-C(3) and Os-C(3) distances (2.025(7), 2.097(7) Å) suggest a close-to-symmetric binding of the bridging carbonyl, the angles at C(3) (Os-C(3)-O(3) = 132.7(5)°, Rh-C(3)-O(3) = 114.1(5)°) indicate asymmetric binding of this carbonyl group. We suggest that this results from close interactions with the ortho hydrogens of the dppm phenyl rings which have four short O(3)-H non-bonded contacts of between 2.41 and 2.68 Å, involving phenyl rings 2, 3, 6 and 7, which are aimed in the direction of C(3)O(3), and therefore appear to be influencing its orientation (see Figure 4.2).

The X-ray structure determination of **3** also reveals that one of the triflate anions is bound to Rh opposite the acyl group, with a normal Rh-O(5) distance of 2.240(5) Å. We assume that the solution structure matches that observed in the solid state, having the triflate ion coordinated to Rh. Not only is this necessary in order to achieve a sixteen-electron configuration, but the ^{13}C NMR spectral data in solution clearly show the carbonyl and acyl ligands in the arrangement shown in the solid state structure, leaving no other ligand except triflate to coordinate to a terminal site on Rh. However, the spectral data regarding triflate ion coordination are equivocal. The IR spectra of **3**, in the solid state and in solution, contain peaks in the 1200-1300 cm^{-1} region but no significant signals in the 1300-1400 cm^{-1} area, which are typically observed for covalently-bound triflate groups.[30] The ^{19}F NMR spectrum has also been examined in order to determine the nature of the triflate group in solution. However there appears to be no perceptible difference in the ^{19}F chemical shifts between free and coordinated triflate in this case. Further confirmation of triflate ion coordination is obtained from the electrospray mass spectrum which shows a parent peak at 1339 amu which indicates a monocationic parent ion containing a coordinated triflate group.

Although the triflate anion is coordinated in CH_2Cl_2 and THF solutions of **3**, the bonding is relatively weak and this anion can be readily displaced by more strongly coordinating ligands such as CO and PMe_3. Addition of CO to a solution of the tricarbonyl species $[RhOs(CF_3SO_3)(CO)_2(\mu\text{-}CO)(\mu\text{-}C(CH_3)O)(dppm)_2]$-

[CF$_3$SO$_3$] (3) at -80°C results in the formation of the tetracarbonyl species

[RhOs(CO)$_3$(μ-CO)(μ-C(CH$_3$)O)(dppm)$_2$][CF$_3$SO$_3$]$_2$ (4) (Scheme 4.2). In the ^{1}H

NMR spectrum the protons of the acetyl group appear as a singlet at 1.81 ppm,

while the dppm-methylene protons are observed as multiplets at 3.44 and 3.86

ppm. The ^{13}C NMR spectrum of a ^{13}CO-enriched sample displays five signals: a

doublet of multiplets at 321.8 ppm (^{1}J$_{Rh-C}$ = 30 Hz) represents the rhodium-bound,

acyl carbon; a multiplet at 223.9 ppm is consistent with a bridging carbonyl; a

Scheme 4.2
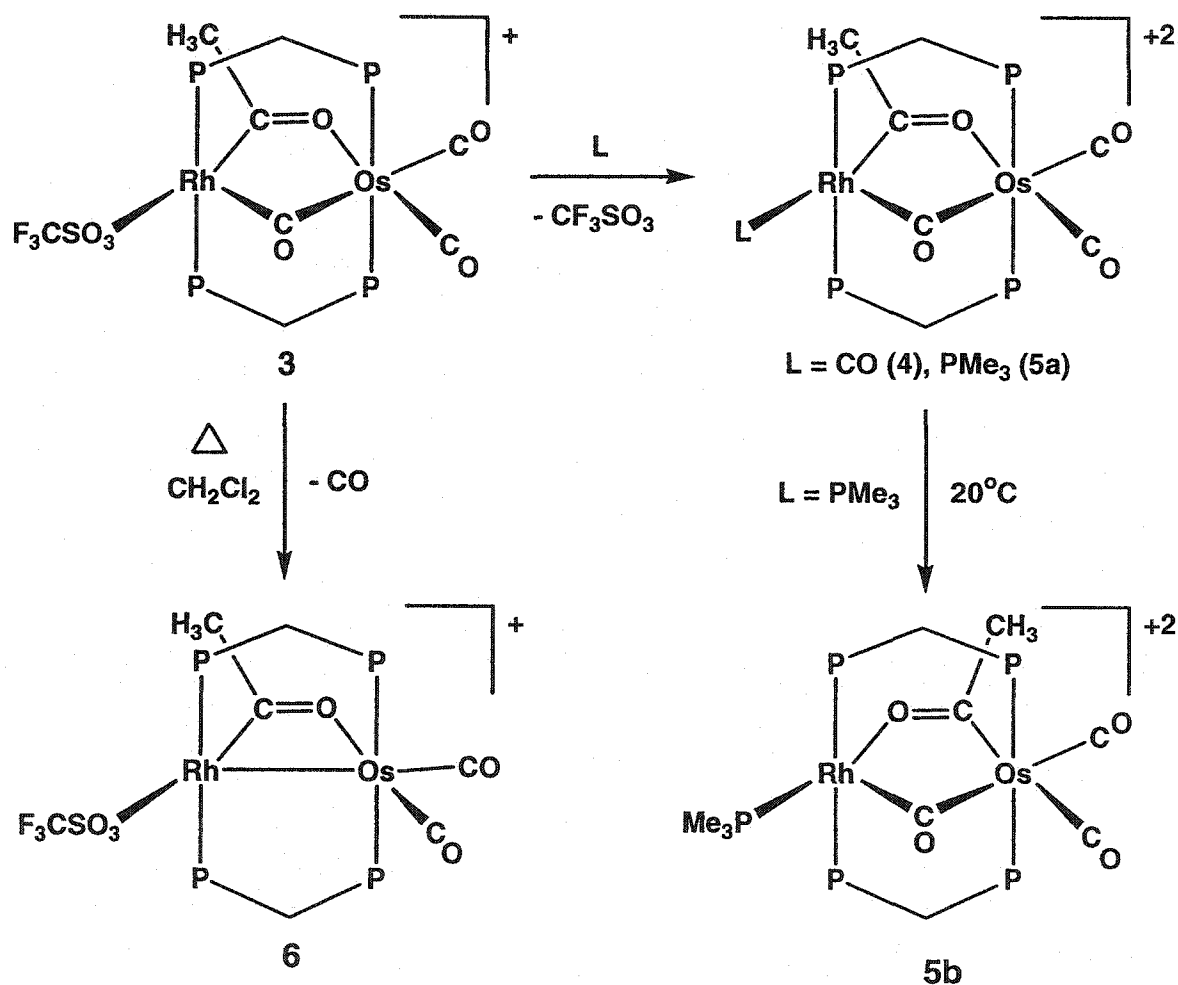
doublet of multiplets at 187.6 ppm is due to the carbonyl group bound to Rh ($^1J_{Rh-C}$ = 47 Hz), which we suggest has taken the coordination site previously occupied by the triflate anion; and two broad singlets at 171.4 and 172.3 ppm are due to the osmium-bound carbonyls. The Rh-bound carbonyl, however, is relatively weakly coordinated and is readily replaced by the triflate group, reforming compound **3**, at temperatures greater than -60°C. It is interesting that the coupling to Rh of this labile carbonyl (47 Hz) is substantially less than normally observed for terminal carbonyls (ca. 60-80 Hz).

Addition of PMe$_3$ to **3** at -40°C results in replacement of the coordinated triflate by PMe$_3$ (Scheme 4.2) to yield [RhOs(PMe$_3$)(CO)$_2$(μ-CO)(μ-C(CH$_3$)O)-(dppm)$_2$][CF$_3$SO$_3$]$_2$ (**5a**). In the ^{31}P NMR spectrum the rhodium- and osmium-bound dppm-phosphorus nuclei appear as a doublet of multiplets at 14.5 ppm ($^1J_{Rh-P}$ = 137 Hz) and a multiplet at -3.9 ppm, respectively, while the PMe$_3$ signal appears as a doublet of multiplets at -39.3 ppm ($^1J_{Rh-P}$ = 101 Hz). The ^{13}C NMR spectrum of **5a** again shows the characteristic downfield signal for the acyl carbonyl 325.8 ppm ($^1J_{Rh-C}$ = 30 Hz) with a large doublet coupling ($^2J_{P-C}$ = 82 Hz) to the PMe$_3$ group, suggesting that the phosphine is located trans to the acyl carbon in the site of the displaced triflate anion. This has been confirmed by an X-ray structure determination.[31] A multiplet at 237.0 ppm is indicative of a bridging carbonyl, and two multiplets at 174.8 and 171.2 ppm are due to the osmium-bound carbonyls.

Upon warming **5a** to ambient temperature a new species (**5b**), having the same formulation as **5a**, appears. The only difference appears to be in the coordination mode of the acetyl group which is reversed in **5b**, having the acyl carbon bound to Os. This acyl carbon appears as a narrow multiplet at 293.4 ppm, and displays no obvious coupling to Rh or to the PMe$_3$ group, which remains bound to Rh as shown by the coupling to this nucleus of 100 Hz. The bridging carbonyl in **5b** resonates at 218.1 ppm in the ^{13}C NMR spectrum, and those of the

Os-bound carbonyls appear at 183.0 and 172.5 ppm. The lower-field terminal carbonyl appears to be opposite the acyl carbonyl as shown by selective ^{13}C-^{13}C decoupling experiments of a ^{13}CO-labeled sample.

Replacement of the triflate anions by tetrafluoroborate by protonation of [RhOs(CO)$_4$(μ-CH$_2$)(dppm)$_2$][BF$_4$] using HBF$_4$ (instead of CF$_3$SO$_3$H) yields both low-temperature compounds **1** and **2** as the BF$_4^-$ salts. However, upon warming to room temperature, conversion to the BF$_4^-$ salt of **3** is not observed; instead decomposition to a mixture of several products occurs. Thus, it appears that coordination of the triflate group is necessary to stabilize the acyl compound **3**, and apparently the poorer coordinating ability of BF$_4^-$ [32] is insufficient to stabilize the acetyl-bridged species as the BF$_4^-$ adduct. Since the low temperature NMR spectra (^{31}P, ^{13}C, ^{1}H) of either **1** or **2**, having either triflate or tetrafluoroborate anions are identical, it seems clear that these compounds do not have coordinated anions.

In the synthesis of **3** by the above route another species was observed as a minor (~10%) impurity; this product can be quantitatively obtained upon refluxing **3** in CH$_2$Cl$_2$ for one hour under an argon purge. The ^{1}H NMR spectrum of this new compound contains a singlet at 2.02 ppm representative of an acyl methyl group, and the electrospray mass spectrum of this new compound shows a parent peak at 1311 amu consistent with the dicarbonyl formulation, [RhOs(CF$_3$SO$_3$)-(CO)$_2$(μ-C(CH$_3$)O)(dppm)$_2$][CF$_3$SO$_3$] (**6**). This formulation is supported by the IR spectrum which displays bands at 2033 and 1974 cm^{-1} for the terminal carbonyls; again no stretch is obvious for the acyl group. In addition, the ^{13}C{^{1}H} NMR spectrum of a ^{13}CO-enriched sample shows only three resonances at 274.2, 181.6 and 163.2 ppm corresponding to the acyl and two terminal carbonyl groups, respectively. Although the high-field carbonyl resonance displays a 6 Hz coupling to rhodium, suggesting a possible weak interaction with this metal (possibly through a weak semi-bridging interaction) the chemical shift is inconsistent with

any bridging interaction. We therefore propose that this carbonyl occupies the site on osmium opposite the Rh-Os bond. Two-bond [103]Rh-^{13}C coupling via the metal-metal bond has previously been observed with carbonyls in the site trans to the Rh-M bond.[33]

Again this structural formulation of **6** is confirmed by the X-ray structure determination, as shown in Figure 4.3. Relevant bond lengths and angles are summarized in Table 4.4. The most obvious structural differences between **3** and **6** are the absence of the bridging carbonyl in the latter and the substantial compression of the Rh-Os separation from 3.4417(6) Å in **3** to 2.7061(4) Å in **6**. This compression has little influence on the bond lengths within the bridging acetyl group. As a result, the Rh-acyl distance (Rh-C(3) = 1.913(5) Å) and the acyl carbonyl distance (C(3)-O(3) = 1.271(6) Å) again suggest involvement of the carbene structure **F**, shown earlier. In addition, compression along the metal-metal axis also has had little effect on the angles at the acyl carbon, with all remaining near the idealized value of 120°. The major change in the acyl binding shows up in the C(3)-O(3)-Os angle which has been compressed from 120.7(4)° in **3** to 100.8(3)° in **6**.

The geometry at Os can be described as a distorted octahedral coordination whereas that of Rh can be regarded as a tetragonal pyramid having the surrounding ligands in the square plane and Os in the fifth site. The diphosphine ligands have the typical trans arrangement at Rh (P(2)-Rh-P(4) = 167.76(5)°) while the acetyl carbon is trans (O(4)-Rh-C(3) = 178.78(19)°) to the oxygen atom of a coordinated triflate group. The triflate oxygen-Rh bond distance (Rh-O(4)) is 2.218(3) Å, similar to that in compound **3**. Again the ^{13}C NMR data and X-ray-derived structural data are in agreement and support an oxy-carbene character of the bridging acetyl group.

At osmium, the major distortion from idealized octahedral geometry results from the bridging nature of the acetyl group which results in an acute Rh-Os-O(3)
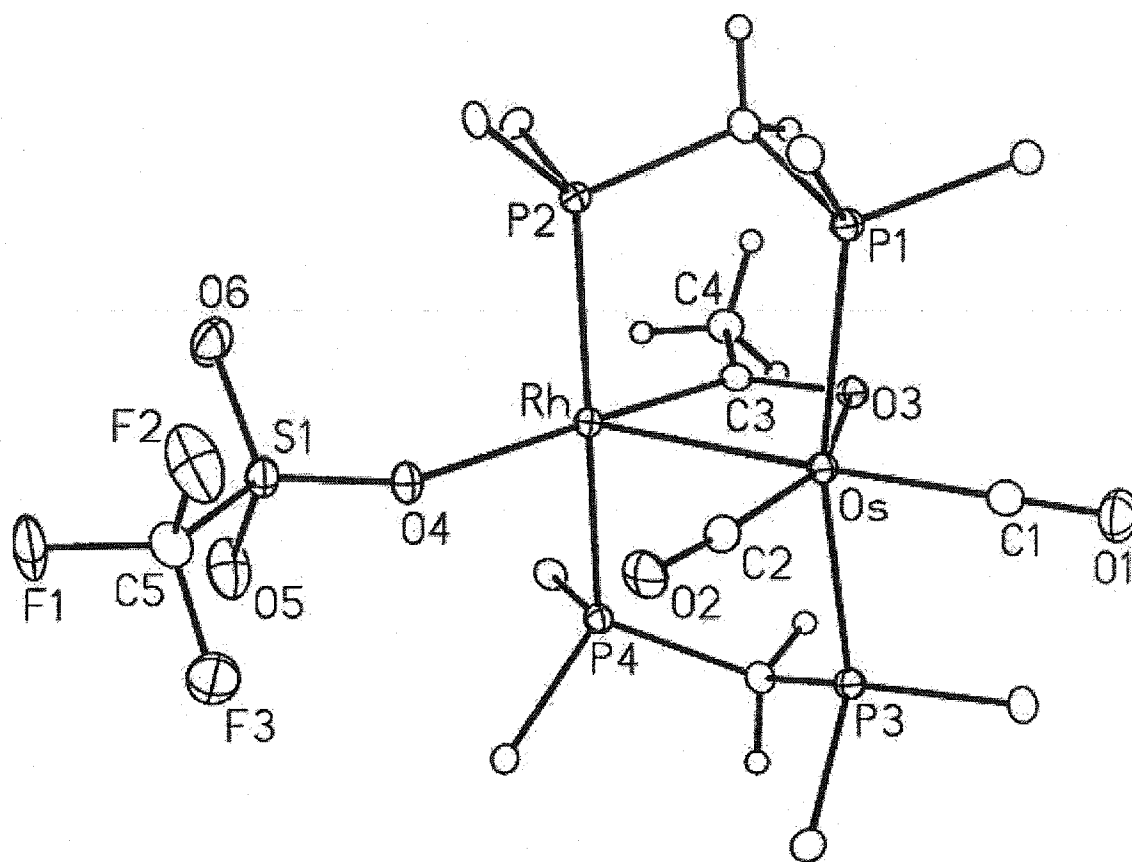
Figure 4.3. Perspective view of [RhOs(CF₃SO₃)(CO)₂(μ-C(O)CH₃)(dppm)₂]-[CF₃SO₃] (6) showing the atom-labeling scheme. Non-hydrogen atoms are represented by Gaussian ellipsoids at the 20% probability level. Hydrogen atoms are shown with arbitrarily small thermal parameters. Only the ipso carbons of the dppm phenyl groups are shown for clarity.

Table 4.4 Selected Bond Distances and Angles of compound **6**.

Atom 1	Atom 2	Distance (Å)	Atom 1	Atom 2	Atom 3	Angle (°)
Os	Rh	2.7061(4)	Rh	Os	P(1)	92.82(4)
Os	P(1)	2.4095(13)	Rh	Os	P(3)	93.01(3)
Os	P(3)	2.4145(12)	Rh	Os	O(3)	69.06(9)
Os	O(3)	2.150(3)	Rh	Os	C(1)	176.54(15)
Os	C(1)	1.883(5)	Rh	Os	C(2)	90.07(15)
Os	C(2)	1.882(5)	P(1)	Os	P(3)	164.73(5)
Rh	P(2)	2.3286(14)	O(3)	Os	C(1)	107.49(18)
Rh	P(4)	2.3254(14)	C(1)	Os	C(2)	93.4(2)
Rh	O(4)	2.218(3)	Os	Rh	O(4)	110.19(9)
Rh	C(3)	1.913(5)	Os	Rh	C(3)	68.96(14)
S(1)	O(4)	1.456(4)	P(2)	Rh	P(4)	167.76(5)
P(1)	C(6)	1.826(5)	Os	O(3)	C(3)	100.8(3)
P(2)	C(6)	1.825(5)	Rh	O(4)	S(1)	133.8(2)
O(1)	C(1)	1.138(6)	Rh	C(3)	O(3)	121.1(3)
O(2)	C(2)	1.138(6)	Rh	C(3)	C(4)	123.9(3)
O(3)	C(3)	1.271(6)	O(3)	C(3)	C(4)	115.0(4)
C(3)	C(4)	1.516(6)				

angle (69.06(9)°) and an obtuse C(1)-Os-O(3) angle (107.49(18)°). In addition, the P(1)-Os-P(3) angle (164.73(5)°) is substantially distorted from 180° reflecting the attraction of both metals as a result of metal-metal bonding. The Rh-Os separation (2.7061(4) Å) is typical of a Rh-Os single bond.

We have also attempted to generate the cationic acetyl-bridged species (3) by reaction of an appropriate hydride species with diazomethane. These hydride complexes, [RhOsX(CO)$_3$(μ-H)(μ-CO)(dppm)$_2$][X] (X = CF$_3$SO$_3$ (7a), BF$_4$ (7b)), were obtained by protonation of the appropriate precursor [RhOs(CO)$_4$(dppm)$_2$]-[X] with the acid having the corresponding anion. For 7a the hydride resonance appears as a doublet of multiplets at -10.5 ppm in the ^{1}H NMR spectrum ($^1J_{Rh-H}$ = 21 Hz, $^2J_{P(Os)-H}$ = 8 Hz, $^2J_{P(Rh)-H}$ = 9 Hz). The comparable coupling of the hydride ligand to both sets of ^{31}P nuclei (Rh- and Os-bound) suggests that this hydride is symmetrically bridging. The ^{13}C{^{1}H} NMR spectrum at ambient temperature shows four carbonyl resonances; a doublet of triplets at 181.8 ppm ($^1J_{Rh-C}$ = 79 Hz; $^2J_{P-H}$ = 15 Hz) is due to a Rh-bound carbonyl, a slightly broadened singlet at 169.4 ppm is due to an Os-bound carbonyl, and two very broad signals at 200.0 and 171.8 ppm are also due to Os-bound carbonyls. At -90°C all signals sharpen somewhat, although coupling of the Os-bound carbonyls to the adjacent ^{31}P nuclei is never resolved. Nevertheless, the absence of Rh coupling in these signals establishes that they are on Os. The low-field signal suggests a weakly semibridging bonding mode for which Rh coupling is not resolved. A spin-saturation-transfer experiment, in which irradiation of the carbonyl signal at 171.8 ppm leads to the disappearance of the signal at 200.0 ppm, indicates that the carbonyls giving rise to these signals are exchanging. This most probably occurs by tunneling of the hydride between the metals accompanied by rotation of the metal-carbonyl framework as shown in Chart 4.4 (dppm ligands above and below the plane of the drawing are omitted). Dissociation of the triflate anion and recoordination is also presumed to occur in this exchange mechanism.

Chart 4.4
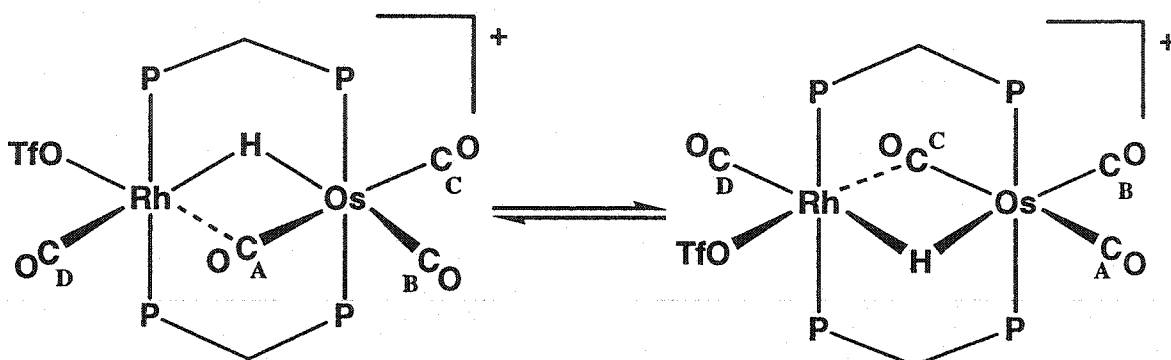
The BF_4^- analogue of **7a**, namely [RhOs(FBF$_3$)(CO)$_3$(μ-H)(μ-CO)-(dppm)$_2$][BF$_4$] (**7b**), was prepared using HBF$_4$. This species has spectral parameters almost identical to that of **7a**. At ambient temperature only one broad signal, at -151.3 ppm, was observed in the ^{19}F NMR spectrum for the BF_4^- anions. However, at -90°C two signals are observed at -153.9 ppm, corresponding to free BF_4^-, and at -149.7 for the coordinated BF_4^-; the latter signal appears somewhat broader than the other. Both signals appear as two peaks in an approximate 1:4 ratio corresponding to the relative abundance of ^{10}B and ^{11}B isotopes. We propose that **7b** has the BF_4^- anion coordinated to Rh, analogous to the triflate anion in **7a**. The absence of Rh coupling to the coordinated BF_4^- group presumably results from a combination of weak BF_4^- coordination and exchange of all four fluorines on this group between Rh-bound and unbound sites. This proposal has been supported by a poor quality X-ray structure determination of **7b**, which showed a disordered BF_4^- group bound to Rh.[31]

In any case, the spectral similarities of **7a** and **7b** suggest comparable structures and the structure of **7a** has been unambiguously established by X-ray
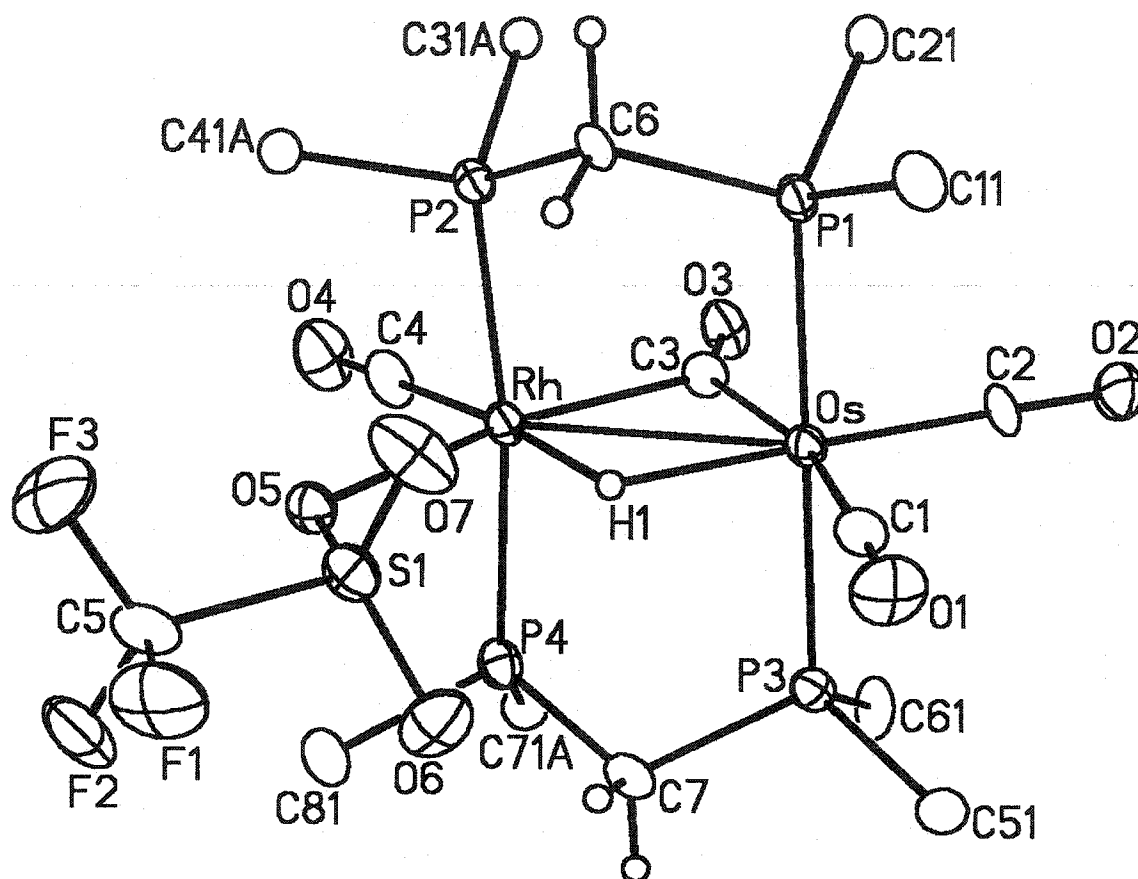
Figure 4.4. Perspective view of [RhOs(CF$_3$SO$_3$)(CO)$_3$(μ-H)(μ-CO)(dppm)$_2$]-
[CF$_3$SO$_3$] (**7a**) showing the atom-labeling scheme. Non-hydrogen atoms are
represented by Gaussian ellipsoids at the 20% probability level. Hydrogen atoms
are shown with arbitrarily small thermal parameters. Only the ipso carbons of the
dppm phenyl groups are shown for clarity.

Table 4.5. Selected Bond Distances and Angles of compound **7a**.

Atom 1	Atom 2	Distance (Å)	Atom 1	Atom 2	Atom 3	Angle (°)
Os	Rh	2.8742(9)	Rh	Os	C(1)	119.9(4)
Os	P(1)	2.383(3)	Rh	Os	C(2)	144.0(3)
Os	P(3)	2.382(3)	Rh	Os	C(3)	46.4(3)
Os	C(1)	1.956(14)	P(1)	Os	P(3)	174.02(11)
Os	C(2)	1.879(9)	C(1)	Os	C(2)	96.2(5)
Os	C(3)	2.047(11)	C(1)	Os	C(3)	166.2(5)
Os	H(1)	1.85$^+$	C(2)	Os	C(3)	97.6(4)
Rh	P(2)	2.360(3)	Os	Rh	O(5)	113.00(17)
Rh	P(4)	2.371(3)	Os	Rh	O(3)	45.4(3)
Rh	O(5)	2.424(7)	Os	Rh	C(4)	147.9(4)
Rh	C(3)	2.081(11)	P(2)	Rh	P(4)	170.63(11)
Rh	C(4)	1.842(13)	O(5)	Rh	C(3)	158.4(3)
Rh	H(1)	1.85$^+$	O(5)	Rh	C(4)	99.1(4)
S(1)	O(5)	1.451(8)	C(3)	Rh	C(4)	102.5(5)
O(1)	C(1)	1.131(15)	Os	C(3)	Rh	88.3(4)
O(2)	C(2)	1.165(11)	Os	C(3)	O(3)	145.0(9)
O(3)	C(3)	1.196(13)	Rh	C(3)	O(3)	126.8(9)
O(4)	C(4)	1.158(14)				

crystallography, as shown in Figure 4.4, which clearly shows that the triflate anion is coordinated to Rh opposite the bridging carbonyl. Both metals have distorted octahedral geometries if the metal-metal bond is ignored. As is typical for hydride complexes, the angles involving the other ligands are greater than the idealized values owing to smaller steric demands of the hydride ligand; these angles range from 96.2(5)° to 102.5(5)° as given in Table 4.5. Carbonyl C(1)O(1), opposite the bridging carbonyl, has the longest metal-carbonyl distance, and the Rh-O(5) distance (2.424(7)Å), involving the coordinated triflate ion, also opposite the bridging carbonyl, is also significantly longer than the analogous distances in compounds 3 and 6 (2.237(6) and 2.218(3)Å, respectively).

Attempts to generate compound 3 by reaction of 7a with diazomethane failed; no reaction occurred even after extended reaction times in the presence of excess CH_2N_2. Similarly the BF_4^- salt (7b) also failed to react with diazomethane.

Discussion

Protonation of the methylene-bridged compound $[RhOs(CO)_4(\mu\text{-}CH_2)\text{-}(dppm)_2][BF_4]$ with either HBF_4 or CF_3SO_3H at -80°C results in the formation of an osmium-bound methyl complex (1) in which the methyl group is asymmetrically bridging and involved in an agostic interaction with rhodium. The donation of the pair of C-H electrons of the agostic bridging methyl group to Rh is presumably necessary to alleviate the electron deficiency brought about by the dicationic charge of the complex. This agostic interaction appears to facilitate the migration of the methyl group from one metal to the other by bringing this osmium-bound methyl group into a simultaneous bonding interaction with rhodium. From this bridging position in 1 methyl transfer to Rh occurs at -40°C to give 2. Why this migration occurs is not clear, although we assume that the stabilization gained from the stronger Os-CO vs. Rh-CO bond[34] is greater than that lost by conversion of a stronger Os-CH_3 bond to a weaker Rh-CH_3 bond.[34] It

should also be pointed out however, that the exchange of an agostic interaction in 1 for a semi-bridging carbonyl in 2 may also favor the observed transformation.

Warming a solution of the triflate complex **2-OTf** to ambient temperature results in migratory insertion of the methyl and a carbonyl group, yielding a bridging acetyl complex. The formation of the acetyl group from **2** rather than **1** can be understood based on the migratory insertion tendencies of a 2nd-row *versus* a 3rd-row metal.[11] It seems likely that migratory insertion is favored when the methyl group is on Rh, due to the weaker Rh-CH$_3$ bond compared to the Os–CH$_3$. In addition, methyl migratory insertion in **2** appears to be facilitated by the semi-bridging carbonyls which are positioned suitably for migratory insertion of a rhodium-bound methyl group.

Coordination of a triflate anion to rhodium appears to be necessary to stabilize this acetyl-bridged complex, allowing Rh to have a 16-electron configuration. In contrast, the BF$_4^-$ analogue (**2-BF$_4$**) does not transform to an acyl complex upon warming to 25°C, and instead decomposes to a mixture of products. The weaker coordinating ability of BF$_4^-$ relative to CF$_3$SO$_3^-$ appears to prevent formation of a stable BF$_4$-coordinated acyl complex analogous to **3**. The coordination of CF$_3$SO$_3^-$, which is generally considered a weak donor group, is facilitated by the high electrophilicity of what would be a dicationic species without coordination of this anion. A similar example was observed by Puddephatt,[14] who recently reported that protonation of the complex [Ru$_2$(CO)$_4$(μ-CH$_2$)(dppm)$_2$] with various acids (HBF$_4$, CF$_3$SO$_3$H, HCO$_2$H, CH$_3$CO$_2$H) resulted in the formation of the cationic methyl complex [Ru$_2$(CO)$_4$(μ-CH$_3$)(dppm)$_2$]$^+$, which was stable at low temperature. However, in this system only the formate and acetate complexes resulted in the formation of stable acetyl compounds at higher temperature; the BF$_4^-$ and CF$_3$SO$_3^-$ anions had insufficient coordinating abilities to stabilize the acetyl species, resulting in decay of these compounds into a mixture of products.

The lability of the coordinated triflate anion in **3** is demonstrated by its facile displacement by CO and PMe₃. In both cases the initial products **4** and **5a**, observed at low temperature, appear to result from replacement of the triflate anion and substrate coordination at Rh. In the case of the PMe₃ adduct **5a**, an interesting transformation of the acetyl group occurs upon warming in which it reverses its coordination mode becoming C-bound to Os rather than to Rh. This transformation may be initiated by the high trans effect of PMe₃ which labilizes the Rh-C(O)CH₃ linkage in the initial adduct **5a**. It is not known how this acetyl rearrangement occurs.

One of the carbonyls in [RhOs(CF₃SO₃)(CO)₂(μ-CO)(μ-C(O)CH₃)-(dppm)₂][CF₃SO₃] (**3**) is labile and is lost slowly at ambient temperature or rapidly in refluxing CH₂Cl₂ to give the dicarbonyl complex **6**. Loss of a carbonyl is accompanied by the formation of a metal-metal bond in order to maintain 16- and 18-electron configurations of Rh and Os, respectively. The nature of this metal-metal interaction is clearly dependent on the bonding formulation for the acetyl group. If an oxycarbene formulation is considered, the oxidation states are best thought of as Rh^{+1}/Os^{+2}, in which the square-planar Rh^{+1} center forms a dative bond *via* its dz² orbital to Os^{+2}, giving the latter the expected 18-electron configuration. We favor this description over an acetyl formulation which would yield the Rh^{+3}/Os^0 combination of oxidation states, in which the Rh^{+3} center achieves a 16-electron configuration *via* an Os→Rh dative bond. Although structures **3-6** are all drawn in the Schemes with bridging acetyl formulations, we consider their bonding more consistent with oxycarbenes. Surprisingly perhaps, carbonyl loss from **3** is not accompanied by "deinsertion" of the acyl carbonyl to give methyl and carbonyl groups. This may be a consequence of the carbene-like bonding of this group, although bridging acyls are already 3-electron donors so nothing is gained in terms of electron count by converting to a methyl and a carbonyl ligand.

We find it surprising that the hydride-bridged species **7a** and **7b** do not react with diazomethane; in the case of **7a** we had anticipated obtaining the acetyl-bridged **3**. Although we have observed failures of neutral bimetallic complexes such as [RhIr(CO)$_3$)(dppm)$_2$] and [Ir$_2$(CO)$_3$(dppm)$_2$] to react with diazomethane,[35] cationic complexes such as [MM'(CO)$_4$(dppm)$_2$]$^+$ (M = Rh, Ir; M' = Fe, Ru, Os) have reacted readily giving the methylene-bridged species [MM'(CO)$_3$(μ-CH$_2$)(μ-CO)(dppm)$_2$]$^+$.[2-4,36] We assume that the failure of the cationic species **7a** and **7b** to react with diazomethane results from the coordinative saturation brought about by anion coordination in each case. Even these weakly associated anions appear to compete more effectively for a coordination site on Rh than diazomethane.

A rationale for studying acetyl complexes was the possibility of converting these groups into oxygen-containing substrates *via* reaction with H$_2$. Such a transformation would mimic another step in the **FT** production of oxygenates. In this regard, the formulation of the bridging acetyl groups as oxycarbenes has potential implications for the involvement of such groups in ethanol formation. Whereas reaction of an η^1-acetyl group with H$_2$ is expected to yield acetaldehyde, a bridging oxycarbene could instead yield ethanol by initial hydrogen transfer to oxygen, giving a hydroxycarbene, followed by hydrogenation of the metal-carbene linkage, to give a hydroxyethyl group, followed by reductive elimination of ethanol. Another aspect of relevance to ethanol formation in the isomerization of **5a** to **5b** (Scheme 4.2) in which the acetyl group rearranges from one that is carbon-bound to Rh to one that is carbon-bound to Os. Whether the different coordination modes show differing reactivities with H$_2$ is of obvious interest since in **5b** the acetyl oxygen is adjacent to the vacant site on Rh, suggesting that H$_2$ oxidative addition at this site could lead to H-transfer to oxygen, yielding a hydroxycarbene. Unfortunately compounds **3** and **6**, containing the bridging acetyl groups that are carbon-bound to Rh do not yield detectable amounts of oxygenates

on reaction with H_2. Compound **3** is unreactive with H_2, while reaction of **6** with H_2 does occur slowly at ambient temperature, but yields a complex mixture of unidentified organic and metal-containing products. ^{1}H NMR spectra of the product mixture does establish the presence of a number of hydride species (as indicated by the high-field ^{1}H signals), but no oxygenates such as acetaldehyde or ethanol were detected. Initial studies with the PMe_3 adducts **5a** and **5b** are much more promising. H_2 addition to either of these compounds at room temperature and pressure yields the previously known dihydride complex $[RhOs(CO)_3(\mu-H)_2(dppm)_2][CF_3SO_3]$ cleanly, and uncharacterized organic products. It appears that neither acetaldehyde nor ethanol are yielded. We are currently working on identifying these products.

It is now of interest to isolate and characterize intermediates in the hydrogenation of these bridging acetyl groups. In the Appendix we report our initial studies on the synthesis of analogous complexes involving the Ir/Ru combination of metals, which will be used as model systems in reaction with H_2 and related substrates.

References

(1) (a) Biloen, P.; Sachtler, W.M.H. *Adv. Catal.* **1981**, *30*, 165. (b) Van der Laan, G.P.; Beenachers, A.A.C.M. *Catal. Rev.-Sci. Eng.* **1999**, *41*, 255. (c) Schulz, H. *Appl. Catal. A.* **1999**, *186*, 3. (d) Maitlis, P.M.; Quyoum, R.; Long, H.C.; Turner, M.L. *Appl. Catal. A.* **1999**, *186*, 363.

(2) Trepanier, S.J.; Sterenberg, B.T.; McDonald, R.; Cowie, M. *J. Am. Chem. Soc.* **1999**, *121*, 2613.

(3) Dell'Anna, M.M.; Trepanier, S.J.; McDonald, R.; Cowie, M. *Organometallics* **2001**, *20*, 88.

(4) Rowsell, B.D.; Trepanier, S.J.; Lam, R.; McDonald, R.; Cowie, M. *Organometallics*, **2002**, *21*, 3228.

(5)   (a) Vannice, M.A. *J. Catal.* **1975**, *37*, 449. (b) Verkerk, K.A.N.; Jaeger, B.;
      Finkeldai, C.-H.; Keim, W. *Appl. Catal. A*: **1999**, *186*, 407. (c) Watson, P.R.;
      Samorjai, G.A. *J. Catal.* **1981**, *72*, 347.

(6)   Overett, M.J.; Hill, R.O.; Moss, J.R. *Coord. Chem. Rev.* **2000**, *206-207*, 581.

(7)   Ichikawa, M.; Fukuoka, A.; Xiao, F. *J. Catal.* **1992**, *138*, 206.

(8)   Dombek, B.D. *Organometallics,* **1985**, *4*, 1707.

(9)   Ichikawa, M.; Xiao, F. *J. Catal.* **1994**, *147*, 578.

(10) (a) Ichikawa, M.; Fukouka, A.; Hriljac, J.A.; Shriver, D.F. *Inorg. Chem.* **1987**,
      26, 3643. (b) Fukuoka, A.; Rao, L.-F.; Ichikawa, M. *Catal. Today* **1989**, *6*, 55.
      (c) Ichikawa, M.; Fukuoka, A.; Kimura, T. *Proc. 9th Int. Congress on
      Catalysis*, Calgary 1988. Vol. 2, p258. Chemical Institute of Canada, Ottawa,
      1988.

(11) Collman, J.P.; Hegedus, L.S.; Norton, J.R.; Finke, R.G.; "*Principles and
      Applications of Organotransition Metal Chemistry*", University Science Books,
      Mill Valley, CA, 1987, Chapter 6.

(12) (a) Pichler, H.; Schultz, H. *Chem. Ing. Tech.* **1970**, *12*, 1160. (b) Masters, C.
      Adv. Organometal. Chem. **1979**, *17*, 61. (c) Henrici-Olive, G.; Olive, S.
      Angew. Chem. Int. Ed. Engl. **1976**, *15*, 136.

(13) Shafiq, F.; Kramarz, K.W.; Eisenberg, R. *Inorg. Chim. Acta* **1993**, *213*, 111.

(14) Gao, Y.; Jennings, M.C.; Puddephatt, R.J. *Organometallics* **2001**, *20*, 1882.

(15) Johnson, K.A.; Gladfelter, W.L. *Organometallics* **1990**, *9*, 2101.

(16) Programs for diffractometer operation, data collection, data reduction and
      absorption correction were those supplied by Bruker.

(17) Beurskens, P.T.; Beurskens, G.; Bosman, W.P.; deGelder, R.; Garcia Granda,
      S.; Gould, R.O.; Israel, R.; Smits, J.M.M. (1996). The *DIRDIF-96* program
      system. Crystallography Laboratory, University of Nijmegen, The Netherlands.

(18) Sheldrick, G.M. *SHELXL-93*. Program for crystal structure determination.
      University of Göttingen, Germany, 1993.

(19) Saunders, M.; Jaffe, M.H.; Vogel, P. *J. Am. Chem. Soc.* **1971**, *93*, 2558.

(20) Calvert, R.B.; Shapley, J.R. *J. Am. Chem. Soc.* **1978**, *100*, 7726.

(21) Dawkins, G.M.; Green, M.; Orpen, A.G.; Stone, F.G.A. *J. Chem. Soc., Chem. Commun.* **1982**, 41.

(22) (a) Casey, C.P.; Fagan, P.J.; Miles, W.H. *J. Am. Chem. Soc.* **1982**, *104*, 1134. (b) Green, M.L.H.; Hughes, A.K.; Popham, N.A.; Stephens, A.H.H.; Wong, L.-L. *J. Chem. Soc., Dalton Trans.* **1992**, 3077.

(23) Torkelson, J.R.; Antwi-Nsiah, F.H.; McDonald, R.; Cowie, M.; Pruis, J.G.; Talkanen, K.J.; DeKock, R.L. *J. Am. Chem. Soc.* **1999**, *121*, 3666.

(24) (a) Brookhart, M; Green, M.L.H.; Wong, L.-L. *Prog. Inorg. Chem.* **1988**, *36*, 1. (b) Tolman, C.A.; Faller, J.W. In *Homogeneous Catalysis with Metal Phosphine Complexes*; Pignolet, L.H., Ed.; Plenum Press: New York, 1983; pp 30-34.

(25) See for example: (a) Kulzick, M.A.; Price, R.T.; Andersen, R.A.; Muetterties, E.L. *J. Organometal. Chem.* **1987**, *333*, 105. (b) Siedle, A.R.; Newmark, R.A.; Pignolet, L.H. *Organometallics* **1984**, *3*, 855. (c) Haynes, A.; Mann, B.E.; Morris, G.E.; Maitlis, P.M. *J. Am. Chem. Soc.* **1993**, *115*, 4093.

(26) Sterenberg, B.T., Ph.D. Thesis, University of Alberta **1987**, Chapter 2.

(27) (a) Antonelli, D.M., Ph.D. Thesis, University of Alberta 1991. (b) Cowie, M., unpublished data.

(28) Jeffrey, J.C.; Orpen, A.G.; Stone, F.G.A.; Went, M.J. *J. Chem. Soc., Dalton Trans.* **1986**, 173.

(29) (a) Erker, G. *Angew. Chem., Int. Ed. Engl.* **1989**, *28*, 397. (b) Schubert, U. *Coord. Chem. Rev.* **1984**, *55*, 261.

(30) Lawrance, G.A. *Chem. Rev.* **1986**, *86*, 17.

(31) Ferguson, M.J.; Trepanier, S.J.; Cowie, M. unpublished data.

(32) Beck, W.; Sünkel, K. *Chem. Rev.* **1988**, *88*, 1405.

(33) (a) Jenkins, J.A.; Cowie, M. *Organometallics*, **1992**, *11*, 2767. (b) Sterenberg, B.T., Ph.D. Thesis, University of Alberta **1997**, p.45.

(34) (a) Ziegler, T.; Tschinke, V. *Bonding Energetics in Organometallic Compounds*; Marks, T.J., Ed.; American Chemical Society: Washington, DC, 1990; Chapter 19. (b) Ziegler, T.; Tschinke, V.; Urenbach, B. *J. Am. Chem. Soc.* **1987**, *1-0*, 4825. (c) Armentrout, P.B. *Bonding Energetics in Organometallic Compounds*; Marks, T.J., Ed.; American Chemical Society: Washington, DC, 1990; Chaper 2.

(35) Oke, O.; Torkelson, J.R.; Cowie, M., unpublished results.

(36) Lo, J., Cowie, M., unpublished results.

Chapter 5

Conclusions

The goal of this thesis was to synthesize bimetallic organometallic compounds, based on a dppm-bridged Rh/Os or Ir/Ru framework, which could be used to model potential transformations in the Fischer-Tropsch (FT) reaction, catalyzed by combinations of Group 8 and 9 metals. Since the methylene group is commonly believed to be of fundamental importance in this reaction,[1] we have synthesized methylene-bridged complexes involving the above combinations of metals to investigate how these compounds react with other organic fragments which may have relevance in the FT process. Of particular interest to us was the role that each of the metals would play in these reactions, and how different combinations of metals would alter the reactivity of the complexes.

We were able to successfully synthesize the methylene-bridged Rh/Os complex [RhOs(CO)$_4$(μ-CH$_2$)(dppm)$_2$][BF$_4$] (2) by the reaction of CH$_2$N$_2$ with the complex [RhOs(CO)$_4$(dppm)$_2$][BF$_4$] (1) at -78°C. At higher temperatures (-40°C), this methylene-bridged complex continues to react with CH$_2$N$_2$ to selectively form an osmacyclopentane compound [RhOs(CO)$_4$(C$_4$H$_8$)(dppm)$_2$][BF$_4$] (3) which results from the coupling of four methylene groups. Using our results from labeling studies, we have proposed a mechanism for the formation of this C$_4$ complex based on stepwise methylene-group insertions into the Rh-CH$_2$ bond of 2. We propose that insertions occur at Rh due to its incipient coordinative unsaturation, which allows diazomethane coordination and subsequent activation. Insertion at Rh is further aided by a weaker Rh-C versus Os-C bond.[2] Attempts to synthesize the proposed C$_2$H$_4$- and C$_3$H$_6$- bridged intermediates in this reaction have been unsuccessful. However, in related chemistry a bridging C$_3$ species has been observed from the reaction of the tricarbonyl complex [RhOs(CO)$_3$(μ-

CH$_2$)(dppm)$_2$][BF$_4$] (**8**) with dimethyl acetylenedicarboxylate;[3] again substrate insertion into the Rh-CH$_2$ bond has occurred. In another attempt to model a C$_3$-bridged intermediate, the reaction of **2** with dimethylallene was attempted. Although no ligated hydrocarbyl product was observed, the formation of 1,1-dimethyl,-1, 3-butadiene suggests that insertion into the Rh-CH$_2$ bond occurs, followed by β-hydride elimination and subsequent reductive elimination of the resulting hydride and substituted vinyl fragment to give the butadiene molecule.

Attempts to more clearly model a C$_3$H$_6$-bridged species by insertion of mono-olefins into the Rh-CH$_2$ bond of **2** or **8** may not be possible owing to steric interactions involving the substituted olefins, which prevent their coordination in these bulky dppm systems, and the possibility of β-hydride elimination for partially-substituted olefins. We propose that the failure of dimethylallene to form a stable insertion product results from such a β-hydride elimination step followed by reductive elimination.

At room temperature, [RhOs(CO)$_4$(μ-CH$_2$)(dppm)$_2$][BF$_4$] (**2**) reacts with excess diazomethane to selectively yield the allyl/methyl complex [RhOs(C$_3$H$_5$)(CH$_3$)(CO)$_3$(dppm)$_2$][BF$_4$] (**4**). Of particular interest was the complete absence of compound **3** in this reaction. We have suggested that this may be due to inhibited diazomethane coordination to our proposed C$_3$ intermediate at this temperature which results in the C$_3$ species undergoing solely β-hydride elimination leading to an allyl/hydride intemediate which presumably reacts with another equivalent of CH$_2$N$_2$ to yield the allyl/methyl complex (**4**). We are currently attempting to independently synthesize this allyl/hydride intermediate to determine whether it will indeed react with diazomethane to yield compound **4**.

We have also successfully modeled the elimination of organic fragments from a FT catalyst by reacting **3** and **4** with H$_2$. Both complexes undergo

hydrogenolysis at room temperature and pressure, yielding butane in the case of **3**, and propene and methane in the case of **4**.

In attempts to determine the roles of different metal combinations in C-C bond formation involving methylene-bridged units, we have synthesized [IrRu(CO)$_4$(μ-CH$_2$)(dppm)$_2$][BF$_4$] (**5**) by routes analogous to that of the Rh/Os system. This species results from reaction of the carbonyl precursor [IrRu(CO)$_4$(dppm)$_2$][BF$_4$] with diazomethane over the broad temperature range from -78°C to 25°C. In contrast to the behaviour of the analogous Rh/Os system, no further reaction with CH$_2$N$_2$ is observed, even at higher temperature.

The importance of CO loss in methylene-group coupling was established by the subsequent reaction of **5** with diazomethane in the presence of Me$_3$NO yielding the ethylene adduct [IrRu(C$_2$H$_4$)(CO)$_3$(μ-CH$_2$)(dppm)$_2$][BF$_4$]. A comparison of the structural details of [RhOs(CO)$_3$(μ-CH$_2$)(μ-CO)(dppm)$_2$][BF$_4$] and the Ir/Ru analogue gives a clue to the reason for CO lability in the former species. We propose that the weaker link between Rh and the bridging CO allows a weak nucleophile such as diazomethane[4] to displace it from Rh, leading to subsequent CH$_2$N$_2$ activation yielding an additional CH$_2$ fragment. Support for this proposal comes from an independent study of the related Rh/Ru system which, like Ir/Ru, is inert to diazomethane at ambient temperature but reactive upon subsequent CO loss. Structural comparisons of the methylene-bridged Rh/Ru species with the Rh/Os and Ir/Ru systems are again consistent with our arguments above showing stronger coordination of the bridging CO to Rh, presumably making it more difficult to displace by diazomethane.

Labeling studies on the ethylene adduct [IrRu(C$_2$H$_4$)(CO)$_3$(μ-CH$_2$)-(dppm)$_2$][BF$_4$], noted earlier, indicates that the dominant pathway for ethylene formation does not involve coupling of the metal-bound methylene group with diazomethane-generated CH$_2$; instead it results from coupling of two diazomethane-generated methylenes, leaving the metal-bound group intact. This

result presumably reflects the stronger Ir-CH$_2$ bond which doesn't allow methylene insertion to occur.

Conversion of a bridging methylene group to a bridging acetyl group was achieved through protonation of 2 followed by migratory insertion of the resulting methyl group with a carbonyl ligand. By lowering the temperature a series of intermediates was observed. Addition of protic acids HX (X= BF$_4$, CF$_3$SO$_3$) to [RhOs(CO)$_4$(μ-CH$_2$)(dppm)$_2$][X] at -80°C results in the formation of an osmium-bound methyl group, which has an agostic interaction with Rh. At -40°C migration of the methyl group from Os to Rh occurs, followed by migratory insertion at room temperature, generating a bridging acetyl group. Migratory insertion of the Rh-bound methyl complex instead of that in which the methyl group is Os-bound can be rationalized on the basis of the stronger Os-CH$_3$ versus Rh-CH$_3$ bond,[2] and is consistent with the greater tendency for migratory insertion in second row versus third row metals.[5] Based on NMR spectroscopic and X-ray structural data, we propose that the acetyl group has a high degree of oxycarbene character. We propose that these oxycarbene-like bridging acyl groups could effectively model ethanol formation in FT chemistry. Unlike an η^1-acetyl moiety, for which reaction with H$_2$ should yield acetaldehyde by hydrogenolysis of the metal-acetyl bond, an oxycarbene may result in hydrogenation of this group while initially retaining the metal-carbon bond. This sequence we envisage involves stepwise transformation of the oxycarbene to formation of a hydroxycarbene, then to a hydroxyethyl group, followed by reductive elimination of ethanol. Although reactions of the acetyl-bridged Rh/Os compounds with hydrogen have not yielded detectable amounts of ethanol, the PMe$_3$ adducts do react, and this is being pursued.

The triflate group is weakly coordinated in [RhOs(CF$_3$SO$_3$)(CO)$_2$(μ-C(CH$_3$)O)(dppm)$_2$][CF$_3$SO$_3$] and can be readily displaced by addition of PMe$_3$ yielding the compound [RhOs(PMe$_3$)(CO)$_2$(μ-C(CH$_3$)O)(dppm)$_2$][CF$_3$SO$_3$]$_2$. Although the PMe$_3$ group initially displaces the triflate anion with little additional

structural changes, it undergoes a surprising isomerization with time in which reversal of the μ-acetyl coordination occurs in which the acetyl carbon is now bound to osmium and the oxygen bound to Rh. This species is interesting as a model for acetyl hydrogenation for two reasons. First, the strong ability of PMe$_3$ as an electron donor should increase the tendency of Rh to undergo oxidative addition of H$_2$. Second, with the oxygen bound to Rh, hydrogen transfer from Rh to oxygen could occur giving a hydroxycarbene - the first step in the transformation of an acetyl group to ethanol. Treatment of these PMe$_3$ complexes with H$_2$ results in facile hydrogenolysis, going to completion after 24 hrs at room temperature and pressure. The organic products have not yet been characterized although it appears that neither acetaldehyde nor ethanol are produced.

An obvious extension of this study was to prepare the acyl-bridged analogues involving the Ir/Ru combination of metals in attempts to arrest the products of oxidative addition of H$_2$, which presumably will occur at Ir. In addition, we have plans to model the reactivity of such species (and that of the Rh/Os acyl species) with silanes on the assumption that the oxophilicity of silicon will promote migration of the silyl fragment to the acyl oxygen. Such products could model additional steps in the possible conversion of an acetyl group to ethanol. At the time this thesis was written only a few acyl complexes of Ir/Ru have been synthesized, as briefly noted below, and their reactivities have not been investigated. This preliminary chemistry appears in Appendix 1.

Addition of protic acids HX (X= BF$_4$, CF$_3$SO$_3$) to [IrRu(CO)$_4$(μ-CH$_2$)-(dppm)$_2$][X] at low temperature (-80°C) results in the formation of a terminal, iridium-bound methyl group. As the Ir/Ru methyl complex [IrRu(CH$_3$)(CO)$_4$-(dppm)$_2$][CF$_3$SO$_3$]$_2$ is warmed to room temperature it undergoes a disproportionation reaction, yielding a pentacarbonyl and tricarbonyl methyl complexes (in which the methyl remains on Ir) which are in equilibrium with the starting material. Whereas the tricarbonyl complex decomposes into several unknown products, the pentacarbonyl complex slowly yields (due to the strong M-

C bonds of row 3 metals which inhibits migratory insertion reactions) a tetracarbonyl acetyl complex $[IrRu(CO)_4(\mu-C(CH_3)O)(dppm)_2][CF_3SO_3]_2$ in which the acetyl carbon is bound to Ir. Two other acetyl complexes have been generated from this reaction, and interestingly have opposite η^2 acyl bonding modes, which would make an interesting study for H_2 addition. Unfortunately, the rational syntheses for these compounds is not yet known. Work is currently underway toward this goal.

A strategy that has been widely used in the Cowie group to instill reactivity to mixed-metal species has been to use a coordinatively unsaturated Rh or Ir centre as one of the metals. This has worked extremely well for the Rh/Os systems described in Chapters 2 and 4. Even at -80°C insertion of a diazomethane-generated methylene group into the Rh-Os bond of **1** occurs to give the methylene-bridged **2** and temperatures as low as -60°C result in the subsequent insertion of three additional methylene groups to give the butanediyl fragment. Although our arguments above, in which we compared the Rh/Os system to that of Ir/Ru, address the obvious reasons for their chemical differences as the replacement of Rh by the less labile Ir, resulting in stronger metal-ligand bonds involving the latter, this is not the only reason for differences, as demonstrated by other studies in our group on the analogous Rh/Ru system.[7] Although one might expect that this system, in which Os has been substituted by the more labile Ru, should be more reactive, the opposite is true. This appears to result from secondary effects relating to the effects of the adjacent metals. Loss of a carbonyl from the species $[MM'(CO)_4(\mu-CH_2)(dppm)_2][BF_4]$ (M = Rh, Ir; M' = Os, Ru) appears to depend on the strength of the bridging carbonyl interaction, which is more strongly bridging for the Rh/Ru combination than for Rh/Os. Subsequent work in the group will address such differences in chemistry resulting in changes in metal combinations.

References and Notes

1. (a) Biloen, P.; Sachtler, W.M.H. *Adv. Catal.* **1981**, *30*, 165. (b) Van der Laan, G.P.; Beenachers, A.A.C.M. *Catal. Rev.-Sci. Eng.* **1999**, *41*, 255. (c) Schulz, H. *Appl. Catal. A.* **1999**, *186*, 3. (d) Maitlis, P.M.; Quyoum, R.; Long, H.C.; Turner, M.L. *Appl. Catal. A.* **1999**, *186*, 363. (e) Overett, M.J.; Hill, R.O.; Moss, J.R. *Coord. Chem. Rev.* **2000**, *206-207*, 581.

2. (a) Ziegler, T.; Tschinke, V. *Bonding Energetics in Organometallic Compounds*; Marks, T.J., Ed.; American Chemical Society: Washington, DC, 1990; Chapter 19. (b) Ziegler, T.; Tschinke, V.; Urenbach, B. *J. Am. Chem. Soc.* **1987**, *1-0*, 4825. (c) Armentrout, P.B. *Bonding Energetics in Organometallic Compounds*; Marks, T.J., Ed.; American Chemical Society: Washington, DC, 1990; Chapter 2.

3. Rowsell, B. D.; Cowie, M. unpublished results.

4. Herrmann, W. A. *Angew. Chem. Int. Ed.* **1978**, *17*, 800.

5. Collman, J.P.; Hegedus, L.S.; Norton, J.R.; Finke, R.G.; "*Principles and Applications of Organotransition Metal Chemistry*", University Science Books, Mill Valley, CA, 1987, Chapter 6.

6. (a)Shafiq, F.; Kramarz, K.W.; Eisenberg, R. *Inorg. Chim. Acta* **1993**, *213*, 111. (b) Akita, M.; Hua, R.; Knox, S. A. R.; Moro-oka, Y.; Nakanishi, S.; Yates, M. I. *Chem. Commun.* **1997**, 51.

7. Rowsell, B. D.; Trepanier, S. J.; Lam, R.; McDonald, R.; Cowie, M. *Organometallics* 2002, *21*, 3228.

Appendix 1

Methylene to Acetyl Conversion in Ir/Ru Complexes

Introduction

In the previous chapter we observed conversion of a methylene group to a methyl group, and subsequently to an acetyl moiety in a dppm-bridged Rh/Os system. This reaction sequence has utility in modeling potential steps in the synthesis of oxygenates in the Fischer-Tropsch reaction.[1,2] The termination step in the FT reaction, in which the newly-formed organic products are released from the metal surface, is believed to involve coupling with a hydride group. In order to model this step in the previous chapter, we reacted our Rh/Os acetyl complexes with dihydrogen in an effort to liberate organic compounds such as ethanol or acetaldehyde. Some of these complexes, however, were not very reactive with H_2. In order to synthesize binuclear Group 8/9 metal complexes with a greater reactivity toward dihydrogen, we decided to investigate the analogous Ir/Ru acetyl complexes since iridium has a greater propensity for oxidative addition than rhodium and hydrogen addition is thought to occur on the unsaturated Group 9 metal.

Experimental Section

General Comments

All solvents were dried (using appropriate drying agents), distilled before use, and stored under nitrogen. Reactions were performed under an argon atmosphere using standard Schlenk techniques. $HBF_4 \cdot Me_2O$ and CF_3SO_3H were purchased from Aldrich. Carbon-13-enriched CO (99.4% enrichment) was purchased from Isotec Inc. $[IrRu(CO)_4(\mu-CH_2)(dppm)_2][CF_3SO_3]$ was prepared as reported in Chapter 3. NMR spectra were recorded on a Bruker AM-400 or

Varian spectrometer operating at 400.1 MHz for ^{1}H, 161.9 MHz for ^{31}P, and 100.6 MHz for ^{13}C nuclei. The ^{13}C{^{1}H}{^{31}P} NMR spectra were obtained on a Bruker WH-200 spectrometer operating at 50.3 MHz. Infrared spectra were obtained on a Nicolet Magna 750 FTIR Spectrometer with a NIC-Plan IR Microscope. The elemental analyses were performed by the micro-analytical service within the department. Spectroscopic data for the compounds prepared are presented in Table A.1. Electron ionization mass spectra were run on a Micromass ZabSpec spectrometer. In all cases the distribution of isotope peaks for the appropriate parent ion matched very closely that calculated for the formulation given.

Preparation of Compounds

(a) [IrRu(CO)$_4$(CH$_3$)(dppm)$_2$][CF$_3$SO$_3$]$_2$ (1). CF$_3$SO$_3$H (0.7 μL, 0.0075 mmol) was added to a CD$_2$Cl$_2$ solution (0.5 mL) of [IrRu(CO)$_4$(μ-CH$_2$)(dppm)$_2$][CF$_3$SO$_3$] (10 mg, 0.0075 mmol) in an NMR tube at -78°C. The solution remained yellow. Compound 1 is unstable at higher temperatures and was therefore characterized by multinuclear NMR techniques at -80 °C.

(b) [IrRu(CO)$_3$(CH$_3$)(CF$_3$SO$_3$)(dppm)$_2$][CF$_3$SO$_3$] (2) and [IrRu(CO)$_5$(CH$_3$)-(dppm)$_2$][CF$_3$SO$_3$]$_2$ (3). An NMR sample of 1 at -78°C was warmed to 25°C over a 30 min period. The ^{1}H and ^{31}P NMR spectra indicated that there was a 1:1 mixture of 2 and 3. Compound 2 did not persist in solution over a 24 h period, decomposing into several unidentified products. Both species were identified by ^{31}P, ^{1}H, and ^{13}C NMR spectroscopy.

(c) [IrRu(CO)$_5$(CH$_3$)(dppm)$_2$][CF$_3$SO$_3$]$_2$ (3). CO was passed through a solution of 1 (40 mg, 0.027 mmol) in CH$_2$Cl$_2$ (5mL) at -78°C for one min. The solution

Table A.1 Spectroscopic Data for Compounds

Compound	IR (cm⁻¹)[a,b]	NMR[c,d]		
		$^{31}P\{^1H\}^e$ (ppm)	^1H (ppm)[f,g]	$^{13}C\{^1H\}$ (ppm)[g]
[IrRu(CH₃)(CO)₄(dppm)₂]-[CF₃SO₃]₂ (1)		P(Ru): 21.2 (m) P(Ir): 16.5 (m)	CH₃: 2.10(t, 3H, $^3J_{P(Ir)H}$ = 9 Hz) dppm: 3.79 (m, 4H)	CH₃: -17.5 (s, 1C) μ-CO: 215.8 (m, 2C) CO(Ru): 187.0 (t, 2C, $^2J_{PC}$ = 9 Hz)
[IrRu(CH₃)(CF₃SO₃)(CO)₃-(dppm)₂][CF₃SO₃] (2)		P(Ru): 21.2 (m) P(Ir): -16.5 (m)	CH₃: 1.58(t, 3H, $^3J_{P(Ir)H}$ = 8 Hz) dppm: 3.08 (m, 2H); 3.42 (m, 2H)	CO(Ir): 222.6 (t, 1C, $^2J_{P(Ir)-C}$ =) CO(Ru): 212.4 (m, 1C); 188.4 (m, 1C)
[IrRu(CH₃)(CO)₅ (dppm)₂]-[CF₃SO₃]₂ (3)		P(Ru): 20.9 (m) P(Ir): -19.5 (m)	CH₃: 1.11(t, br, 3H, $^3J_{P(Ir)-H}$ = 5 Hz) dppm: 4.58 (m, 4H)	CO(Ru): 202.0 (t, 2C, $^2J_{P(Ru)-C}$ = 12 Hz); 185.7 (t, 1C, $^2J_{P(Ru)-C}$ = 9 Hz) CO(Ir): 181.6 (t, 2C, $^2J_{P(Ir)-C}$ = 11 Hz)
[IrRu(μ-CH₃CO)(CO)₄-(dppm)₂][CF₃SO₃]₂ (4)		P(Ru): 16.4 (m) P(Ir): -17.9 (m)	CH₃: 2.43(s, 3H) dppm: 4.37 (m, 2H); 4.51 (m, 2H)	CH₃CO: 251.2 (m, 1C) CO(Ru): 204.6 (m, 1C); 187.5 (m, 1C) CO(Ir):172.4 (m, 1C); 157.7 (m, 1C)

[a]NMR abbreviations: s = singlet, d = doublet, t = triplet, m = multiplet, dt = doublet of triplets, dm = doublet of multiplets, ddt = doublet of doublets of triplets, br = broad. [b]NMR data at 298K in CD_2Cl_2 unless otherwise state. [c] $^{31}P\{^1H\}$ NMR chemical shifts are referenced *versus* external 95% H_3PO_4. [d] ^1H and ^{13}C chemical shifts are referenced *versus* external TMS. [e]Chemical shifts for the phenyl hydrogens are not given. [f]IR abbreviations (ν(CO) unless otherwise stated): s = strong, m = medium. [g] ^{13}C resonances for methylene carbons of the dppm ligands.

immediately became a paler shade of yellow. The solution was stirred for 30 min as it warmed to room temperature. Ether (20 mL) was then added to precipitate a yellow solid. This precipitate was then washed with three 5 mL portions of ether and dried in vacuo (yield 86%). Elemental analysis has not yet been obtained.

(d) [IrRu(CO)$_4$(μ-C(O)CH$_3$)(dppm)$_2$][CF$_3$SO$_3$]$_2$ (4). A solution of **3** (40 mg, 0.026 mmol) in CH$_2$Cl$_2$ (10 mL) was stirred for two days. The solution was concentrated to 5 mL using an argon stream and ether (20 mL) was then added to precipitate a yellow solid. This precipitate was then washed with three 5 mL portions of ether and dried in vacuo (yield 91%). Elemental analysis has not yet been obtained.

(e) [IrRu(CO)$_3$(μ-C(O)CH$_3$)(dppm)$_2$][BF$_4$]$_2$ (5). An NMR tube containing a CD$_2$Cl$_2$ solution of [IrRu(CO)$_4$(μ-C(O)CH$_3$)(dppm)$_2$][BF$_4$]$_2$ was prepared. After several weeks, red-orange crystals of **5** appeared in the NMR tube. A rational synthesis for **5** has not yet been developed.

(f) [IrRu(CO)$_2$(μ-C(O)CH$_3$)(dppm)$_2$][CF$_3$SO$_3$]$_2$ (6). An NMR tube containing the reaction mixture of [IrRu(CO)$_4$(μ-CH$_2$)(dppm)$_2$][CF$_3$SO$_3$] and CF$_3$SO$_3$H in a CD$_2$Cl$_2$ solution was prepared. After several weeks, orange crystals of **6** appeared in the NMR tube. A rational synthesis for **6** has not yet been developed.

X-Ray Data Collection and Structure Solution

Colorless crystals of [IrRu(CO)$_4$(μ–C(O(CH$_3$)(dppm)$_2$][BF$_4$]•3CH$_2$Cl$_2$ (4) were obtained via slow evaporation of a dichloromethane solution of the compound. Data were collected on a Bruker PLATFORM/SMART 1000 CCD

diffractometer[a] using Mo Kα radiation at -80 °C. Unit cell parameters were obtained from a least-squares refinement of the setting angles of 5570 reflections from the data collection. The space group was determined to be $C2/c$ (No. 15). The data were corrected for absorption through use of the *SADABS* procedure. See Table A.2 for a summary of crystal data and X-ray data collection information.

The structure of **4** was solved using direct methods (*SHELXS–86[b]*). Refinement was completed using the program *SHELXL-93*.[c] Hydrogen atoms were assigned positions based on the geometries of their attached carbon atoms, and were given thermal parameters 20% greater than those of the attached carbons. One of the tetrafluoroborate ions was disordered over two crystallographically-distinct sites; refinement of this ion as two sets of one boron and four flourine atoms (each with an occupancy factor of 50%) yielded satisfactory results. The carbon atom of one of the solvent dichloromethane molecules was found to be disordered over two sites (in an abundance ratio of 55%:45%); all Cl–C distances within this molecule were fixed at 1.80 Å. The final model for **4** was refined to values of $R_1(F) = 0.0516$ (for 8788 data with $F_o{}^2 \geq 2\sigma(F_o{}^2)$) and $wR_2(F^2) = 0.1159$ (for all 13011 independent data).

[a]Programs for diffractometer operation, data collection, data reduction and absorption correction were those supplied by Bruker.

[b]Sheldrick, G. M. *Acta Crystallogr.* **1990**, *A46*, 467–473.

[c]Sheldrick, G. M. *SHELXL-93*. Program for crystal structure determination. University of Göttingen, Germany, 1993.

Red-orange crystals of [IrRu(CO)$_3$(μ–MeCO)(dppm)$_2$][BF$_4$]$_2$•3CH$_2$Cl$_2$ (**5**) were obtained via slow evaporation of a dichloromethane solution of the compound. Data were collected on a Bruker P4/RA/SMART 1000 CCD diffractometer[a] using Mo Kα radiation at –80 °C. Unit cell parameters were

obtained from a least-squares refinement of the setting angles of 5177 reflections from the data collection. The space group was determined to be $P2_1/n$ (No. 14). The data were corrected for absorption through use of the *SADABS* procedure. See Table A.2 for a summary of crystal data and X-ray data collection information.

The structure of **5** was solved using automated Patterson location of the heavy metal atoms and structure expansion via the *DIRDIF-96* program system. Refinement was completed using the program *SHELXL-93*.[c] Hydrogen atoms were assigned positions based on the geometries of their attached carbon atoms, and were given thermal parameters 20% greater than those of the attached carbons. The final model for **5** was refined to values of $R_1(F) = 0.0560$ (for 7896 data with $F_o^2 \geq 2\sigma(F_o^2)$) and $wR_2(F^2) = 0.1499$ (for all 13001 independent data).

[a]Programs for diffractometer operation, data collection, data reduction and absorption correction were those supplied by Bruker.

[b]Beurskens, P. T.; Beurskens, G.; Bosman, W. P.; de Gelder, R.; Garcia Granda, S.; Gould, R. O.; Israel, R.; Smits, J. M. M. (1996). The *DIRDIF-96* program system. Crystallography Laboratory, University of Nijmegen, The Netherlands.

[c]Sheldrick, G. M. *SHELXL-93*. Program for crystal structure determination. University of Göttingen, Germany, 1993.

Table A.2 Crystallographic Experimental Details

|	[IrRu(CO)$_4$(μ-C(O)CH$_3$)(dppm)$_2$]-[CF$_3$SO$_3$]$_2$ (4)	[IrRu(CO)$_3$(μ-C(O)CH$_3$)(dppm)$_2$]-[CF$_3$SO$_3$]$_2$ (5)
formula	C$_{59}$H$_{53}$B$_2$Cl$_6$F$_8$IrO$_5$P$_4$Ru	C$_{58}$H$_{53}$B$_2$Cl$_6$F$_8$IrO$_4$P$_4$Ru
formula weight	1645.48	1617.47
crystal dimensions (mm)	0.23 × 0.10 × 0.08	0.24 × 0.24 × 0.06
crystal system	monoclinic	monoclinic
space group	C2/c (No. 15)	P2$_1$/c (No. 14)
unit cell parameters		
a (Å)	37.384 (3)	18.899 (3)
b (Å)	14.5048 (11)	14.728 (3)
c (Å)	23.9474 (19)	24.634 (4)
β (deg)	99.1270 (18)	112.097 (3)
V (Å^3)	12820.9 (17)	6353.4 (18)
Z	8	4
ρ_{calcd} (g cm^{-3})	1.705	1.691
μ (mm^{-1})	2.730	2.752
Diffractometer	Bruker PLATFORM/SMART 1000 CCD	Bruker P4/RA/SMART 1000 CCD
radiation (λ [Å])	graphite-monochromated Mo Kα (0.71073)	graphite-monochromated Mo Kα (0.71073)
temperature (°C)	–80	–80
scan type	ω scans (0.2°) (25 s exposures)	ϕ rotations (0.3°) / ω scans (0.3°) (30 s exposures)
data collection 2θ limit (deg)	52.78	52.90
total data collected	30683 (-46 ≤ h ≤ 39, -17 ≤ k ≤ 18, -29 ≤ l ≤ 29)	30759 (-23 ≤ h ≤ 23, -16 ≤ k ≤ 18, -16 ≤ l ≤ 30)
independent reflections	13011	13001
number of observed reflections (NO)	8788 [$F_o^2 \geq 2\sigma(F_o^2)$]	7896 [$F_o^2 \geq 2\sigma(F_o^2)$]
structure solution method	direct methods (SHELXS–86)	direct methods/fragment search (DIRDIF–96)
refinement method	full-matrix least-squares on F^2 (SHELXL–93)	full-matrix least-squares on F^2 (SHELXL–93)
absorption correction method	empirical (SADABS)	SADABS
range of transmission factors	0.8112–0.5725	0.8310–0.5203
data/restraints/parameters	13011 [$F_o^2 \geq -3\sigma(F_o^2)$] / 4^e / 763	13001 [$F_o^2 \geq -3\sigma(F_o^2)$] / 0 / 758
goodness-of-fit (S)	1.003 [$F_o^2 \geq -3\sigma(F_o^2)$]	0.968 [$F_o^2 \geq -3\sigma(F_o^2)$]

final R indices

R_1 $[F_o^2 \geq 2\sigma(F_o^2)]$	0.0516	0.0560
wR_2 $[F_o^2 \geq -3\sigma(F_o^2)]$	0.1159	0.1499
largest difference peak and hole	2.191 and -0.858 e Å^{-3}	3.711 and -3.108 e Å^{-3}

Results

Protonation of the methylene-bridged compound [IrRu(CO)$_3$(μ-CO)(μ-CH$_2$)(dppm)$_2$][CF$_3$SO$_3$], using triflic acid (CF$_3$SO$_3$H), at low temperature (-80 °C) yields a dicationic methyl compound [IrRu(CO)$_4$(CH$_3$)(dppm)$_2$][CF$_3$SO$_3$]$_2$ (1), as shown in Scheme A.1. No evidence of a methylene-bridged hydride species resulting from protonation at a metal was observed, nor was a species analogous to the compound [RhOs(CO)$_4$(CH$_3$)(dppm)$_2$][CF$_3$SO$_3$]$_2$ in Chapter 4 observed, in which the methyl group was bound to the Group 8 metal while involved in an agostic interaction with the Group 9 metal. The ^{31}P NMR spectrum of 1 shows the dppm-phosphine resonances at 20.8 and 18.3 ppm. The proximity of these resonances leads to ambiguity in the structural characterization since the resonances corresponding to the Ir- or Ru-bound phosphorus nuclei cannot be distinguished. Typically the iridium-bound phosphines appear considerably upfield (ca. 30 ppm difference) from the ruthenium-bound phosphines in the ^{31}P NMR spectrum. This small chemical shift difference also results in difficulties in obtaining definitive selective ^{1}H{^{31}P} and ^{13}C{^{31}P, ^{1}H} NMR spectra, which are necessary for characterizing the compounds in these systems. In this case it was assumed that the upfield resonance at 18.3 ppm in the ^{31}P spectrum was due to the iridium-bound, dppm phosphines while the resonance at 20.8 ppm was due to the ruthenium-bound, dppm phosphines. The results obtained under this assumption lead to structural assignments that are more characteristically observed in these systems. Selective ^{1}H{^{31}P} NMR spectroscopy indicates that the methyl group is bound to the iridium centre ($^3J_{P(Ir)-H}$ = 9 Hz). In the ^{13}C{^{1}H} NMR spectrum there are two signals representing the carbonyl carbons. A triplet resonance at 187.0 ppm results from two carbonyls terminally bound to ruthenium. A multiplet at 215.8 ppm represents two bridging or semi-bridging carbonyls.

As a CD$_2$Cl$_2$ solution of 1 is warmed to -60 °C, two new species (2 and 3) begin to appear in a 1:1 ratio until at 25 °C an approximately equimolar ratio of

Scheme A.1
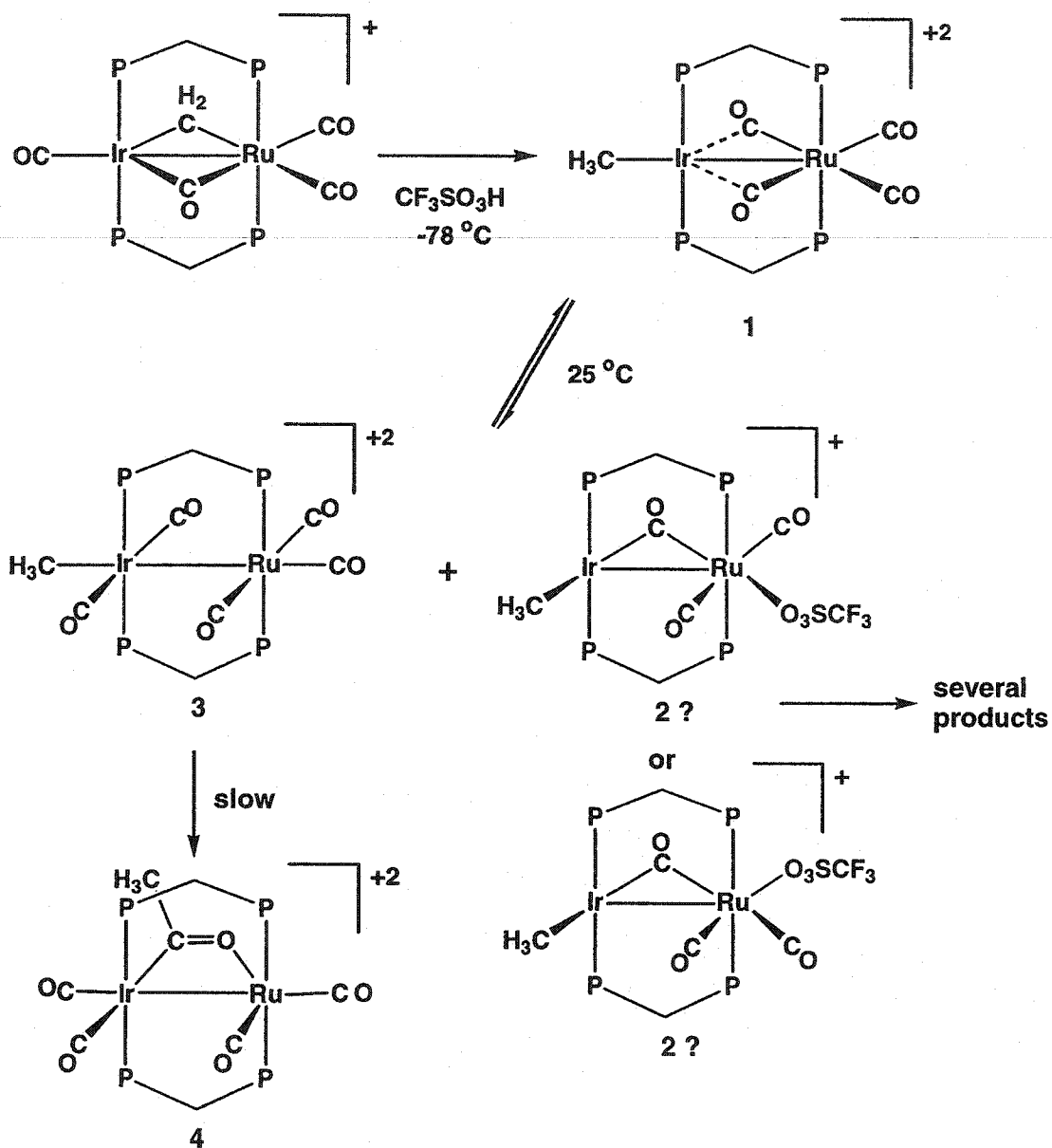
compounds **1**, **2**, and **3** is reached; this ratio is maintained over the temperature range -78 °C to 25 °C. The ^{31}P NMR spectrum of **3** contains two signals at 20.9 and -19.5 ppm assumed to correspond to the phosphorus atoms bound to ruthenium and iridium respectively, on the basis of the chemical shifts. In the ^{1}H NMR spectrum a triplet at 1.11 ppm is due to a methyl group bound to the iridium centre ($^3J_{P(Ir)-H} = 5$ Hz), on the basis of coupling of the methyl protons with the high-field phosphorus nuclei. The dppm-methylene protons appear as a single multiplet at 4.58 ppm indicating front/back symmetry in the molecule. In the ^{13}C{^{1}H} NMR spectrum three carbonyl signals are observed in a 2:2:1 ratio; a triplet at 181.6 ppm is due to two equivalent carbonyls bound to iridium ($^2J_{P(Ir)-C} = 11$ Hz), a triplet of equal intensity at 202.0 ppm represents two equivalent carbonyls bound to ruthenium ($^2J_{P(Ru)-C} = 12$ Hz), and a triplet at 185.7 ppm indicates the presence of a single unique carbonyl on ruthenium ($^2J_{P(Ru)-C} = 9$ Hz). On the basis of this NMR data the structure for **3**, shown in Scheme 5.1, is proposed.

The ^{31}P NMR spectrum of **2** contains two signals at 21.2 and 16.5 ppm; reminiscent of compound **1**, in which the small separation between the two ^{31}P signals makes their assignment equivocal. On the basis that the Ru-bound phosphines show little variation in chemical shift in this system, it is assumed that the more upfield signal represents the phosphorus nuclei bound to iridium while the low-field signal belongs to the ruthenium-bound phosphines. In the ^{1}H NMR spectrum a triplet at 1.58 ppm corresponds to a methyl group bound to iridium ($^3J_{P(Ir)-H} = 8$ Hz) since this resonance displays coupling to the ^{31}P nuclei at high field. The dppm-methylene protons appear as two multiplets at 3.08 and 3.42 ppm indicating front/back asymmetry in the molecule. In the ^{13}C{^{1}H} NMR spectrum three signals are observed in a 1:1:1 ratio. A triplet at 222.6 ppm is due to an iridium-bound carbonyl showing coupling to only the iridium-bound phosphines, however, the characteristic low-field position of this signal also indicates a bridging interaction with ruthenium. The lack of coupling of this bridging

carbonyl to the Ru-bound phosphines may suggest a weaker interaction between this carbonyl and the ruthenium; whether it is merely asymmetrically bound, by virtue of the two different metals, or whether it is semi-bridging, is not clear. The other signals appear as multiplets at 212.4 and 188.4 ppm and are due to ruthenium-bound carbonyls. The lower-field resonance presumably corresponds to that which is aimed between the two metals while the high-field signal corresponds to that which is remote from Ir. Such low-field shifts of terminal carbonyls in the vicinity of another metal have been observed in related Rh/Ir compounds. We also propose that a triflate group is bound to Ru yielding the structure(s) (two isomers are possible) shown in Scheme A.1. Although we have no spectroscopic evidence (^{19}F and ^{13}C NMR chemical shifts of the triflate group are inconclusive) supporting the coordination of a triflate ion, it would allow ruthenium to achieve an eighteen-electron configuration. Triflate coordination in these "dicationic" systems was previously observed in Chapter 4, describing related Rh/Os work, although the triflate was bound to the Group 9 metal (Rh) in that case. However, we have observed in this Ir/Ru system (via X-ray structure determination) triflate coordination to ruthenium (vide infra).

Examining the conversion of **1** to **2** and **3**, we propose that the tetracarbonyl complex (**1**) undergoes a disproportionation reaction resulting in the formation of a tricarbonyl complex (**2**) and a pentacarbonyl complex (**3**) which explains why **2** and **3** are always observed in a 1:1 ratio. We conclude that these compounds are in equilibrium with **1** since there is never complete conversion of **1** to **2** and **3** and the net conversion ceases coincidentally at a **1**:**2**:**3** ratio of 1:1:1 in the -78 °C to 25 °C temperature range observed. Under an atmosphere of CO, this equilibrium mixture is converted completely to the pentacarbonyl species **3**.

Further examination of this reaction after 12 hours (at room temperature) led to the discovery of another new compound (**4**), which becomes the exclusive species after two days. Unlike the previous three compounds, the methyl group of **4** is represented by a singlet resonance in the ^{1}H NMR spectrum at 2.43 ppm

indicating that the methyl group no longer has any ^{31}P coupling and is probably not directly bonded to a metal. There are also two multiplets due to the dppm-methylene protons indicating that the molecule possesses front/back asymmetry. Based on our experience with the analogous Rh/Os system (Chapter 4),[8] we concluded that this compound contains an acetyl group. The ^{13}C{^{1}H, ^{31}P} NMR spectrum also has a signal at 251.4 ppm representing the acyl carbon bound to the iridium centre. The high-field shift of this carbon indicates that the acetyl group may be terminally bound (typically 230-260 ppm), however this may also be due to a lower degree of carbene character. This spectrum also indicates the presence of four other carbonyls which all appear as multiplets in the spectrum of the ^{13}C-labeled compound **4**. From selective ^{13}C{^{31}P} decoupling experiments it was determined that the carbonyls at 204.6 and 187.5 ppm are bound to the ruthenium centre, while those at 172.4 and 157.7 ppm are iridium-bound.

An X-ray structure determination of **4** confirms an acetyl-bridged formulation as shown in Figure A.1. This structure is of the tetrafluoroborate salt of **4** (**4-(BF$_4$)$_2$**) although it has been established by multinuclear NMR spectroscopy as well as an X-ray determination that the structure of **4** is the same, either as a triflate or tetrafluoroborate salt. Bond lengths and angles are summarized in Table A.3. Each metal has a distorted octahedral geometry with one site on each occupied by a metal-metal bond. Similar to the acetyl-bridged Rh/Os complexes observed in Chapter 4, the major distortion from idealized octahedral geometry in **4** results from the bridging nature of the acetyl group. This results in an acute Ir-Ru-O(5) angle (69.0(1)°) and an obtuse C(4)-Ru-O(5) angle (100.6(2)°). In addition, the P(2)-Ru-P(4) angle (163.50(6)°) is substantially distorted from 180° as a result of the bridging acetyl group and metal-metal bonding. The Ir-Ru distance (2.8599(6) Å) is typical of an Ir-Ru single bond. The metals are bridged by the acetyl group with the acetyl-carbon bound to iridium and the acyl-oxygen coordinated to ruthenium (Ru-O(5) =2.137(4) Å). Both the short Ir-C(5) (Ir-C(5) = 2.060(6) Å) and the long C(5)-O(5) (1.250(8) Å) distances

are consistent with a degree of carbene character. The Ir-acyl distance is comparable to the Ir-CO distances (Ir-C(1), Ir-C(2) = 1.978(7), 1.954(6) Å) for which significant π back-bonding is assumed. Similarly, the C(4)-O(4) distance is substantially longer than observed in normal η^1-acetyl groups and is comparable to that reported by Eisenberg (1.28(2) Å).[9a] The structural parameters for the bridging acetyl group are in support of an oxycarbene formulation although not to the degree of the Rh/Os acetyl complexes reported in Chapter 4.
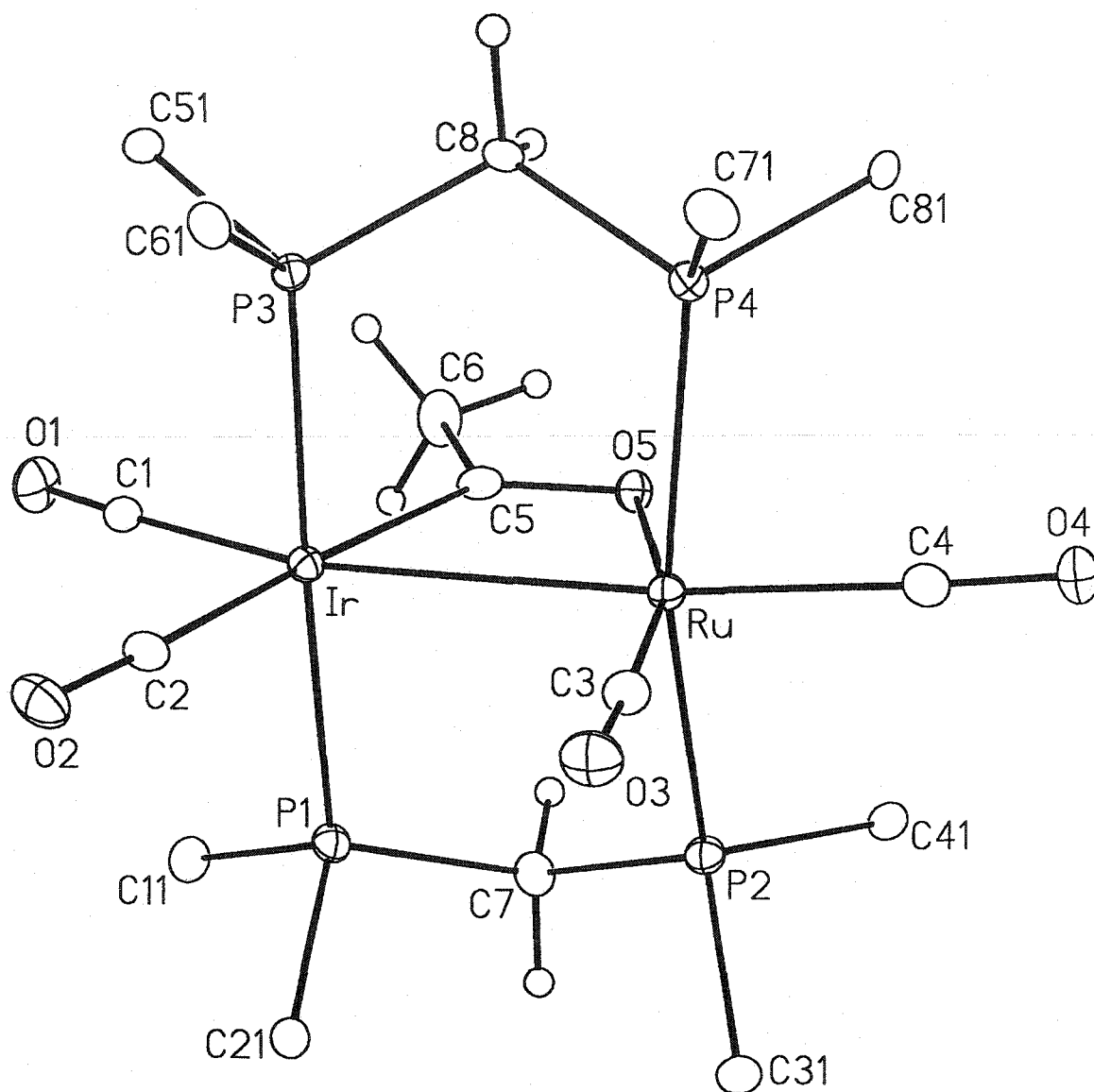
Figure A.1. Perspective view of [IrRu(CO)$_4$(μ-C(O)CH$_3$)(dppm)$_2$] [BF$_4$] (4) showing the atom-labeling scheme. Non-hydrogen atoms are represented by Gaussian ellipsoids at the 20 % probablility level. Hydrogen atoms are shown with arbitrarily small thermal parameters. Only the ipso carbons of the dppm phenyl groups are shown for clarity.
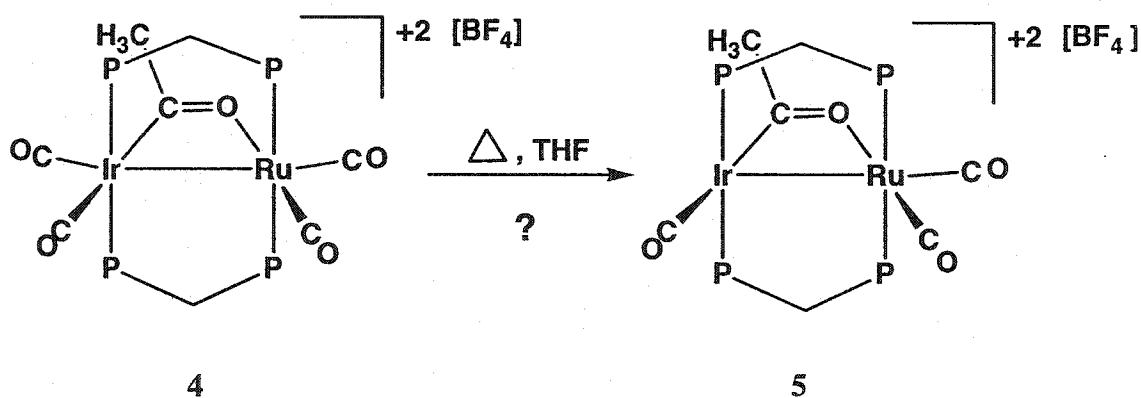
Table A.3 Selected Bond Distances and Angles of [IrRu(CO)₄(μ-C(O)CH₃)]- [BF₄]₂ (4)

Atom 1	Atom 2	Distance (Å)	Atom 1	Atom 2	Atom 3	Angle (°)
Ir	Ru	2.8599(6)	Ru	Ir	C(1)	156.81(18)
Ir	P(1)	2.3707(17)	Ru	Ir	C(2)	107.04(19)
Ir	P(3)	2.3628(16)	Ru	Ir	C(5)	65.68(19)
Ir	C(1)	1.978(7)	P(1)	Ir	P(3)	177.14(6)
Ir	C(2)	1.954(6)	C(1)	Ir	C(2)	96.1(3)
Ir	C(5)	2.060(6)	C(1)	Ir	C(5)	91.1(3)
Ru	P(2)	2.4005(18)	C(2)	Ir	C(5)	172.6(3)
Ru	P(4)	2.3973(18)	Ir	Ru	O(5)	69.0(1)
Ru	O(5)	2.137(4)	Ir	Ru	C(3)	95.6(2)
Ru	C(3)	1.860(7)	Ir	Ru	C(4)	169.4(2)
Ru	C(4)	1.928(7)	P(2)	Ru	P(4)	163.50(6)
O(1)	C(1)	1.138(8)	O(5)	Ru	C(3)	164.5(2)
O(2)	C(2)	1.132(7)	O(5)	Ru	C(4)	100.6(2)
O(3)	C(3)	1.143(7)	C(3)	Ru	C(4)	94.9(3)
O(4)	C(4)	1.126(8)	Ru	O(5)	C(5)	105.6(4)
O(5)	C(5)	1.250(8)	Ir	C(5)	O(5)	119.7(5)
C(5)	C(6)	1.509(9)	Ir	C(5)	C(6)	125.9(5)
			P(1)	C(7)	P(2)	108.4(3)
			P(3)	C(8)	P(4)	110.6(3)

We have also obtained the structures of two other Ir/Ru acetyl compounds however the rational synthesis of these compounds, **5** and **6**, is not yet known. Crystals of both compounds were obtained from the reaction mixtures of $[IrRu(CO)_4(\mu-CH_2)(dppm)_2][X] + HX$ ($X = BF_4^-$, $CF_3SO_3^-$) in CD_2Cl_2, which slowly evaporated in NMR tubes over several weeks. NMR spectroscopic data has not yet been obtained for these compounds. The structure of **5** has been determined by an X-ray analysis and the result shown in Figure A.2. The structure is similar to that of **4** except that the carbonyl of Ir opposite the metal-metal bond has been lost. The Ir-Ru bond distance (2.7949(7) Å) is typical for a single bond and there is again an acetyl group bridging the two metals resulting in distortion of the octahedral geometry of ruthenium (P(2)-Ru-P(4) = 167.74(7)Å). The iridium-carbon (Ir-C(4) = 2.028(8)Å) and ruthenium-oxygen distances (C(4)-O(4) = 1.285(8) Å) suggest a higher degree of carbene character in **5** than **4**.

We are currently attempting to synthesize **5** by removing a carbonyl from **4** by the addition of Me₃NO. However, the result was a mixture of many products. Another attempt at carbonyl removal from **4** by refluxing a THF solution of **4** (Chart A.1) has led to the formation of one major product, however it has not yet been characterized spectroscopically.

Chart A.1

4   5
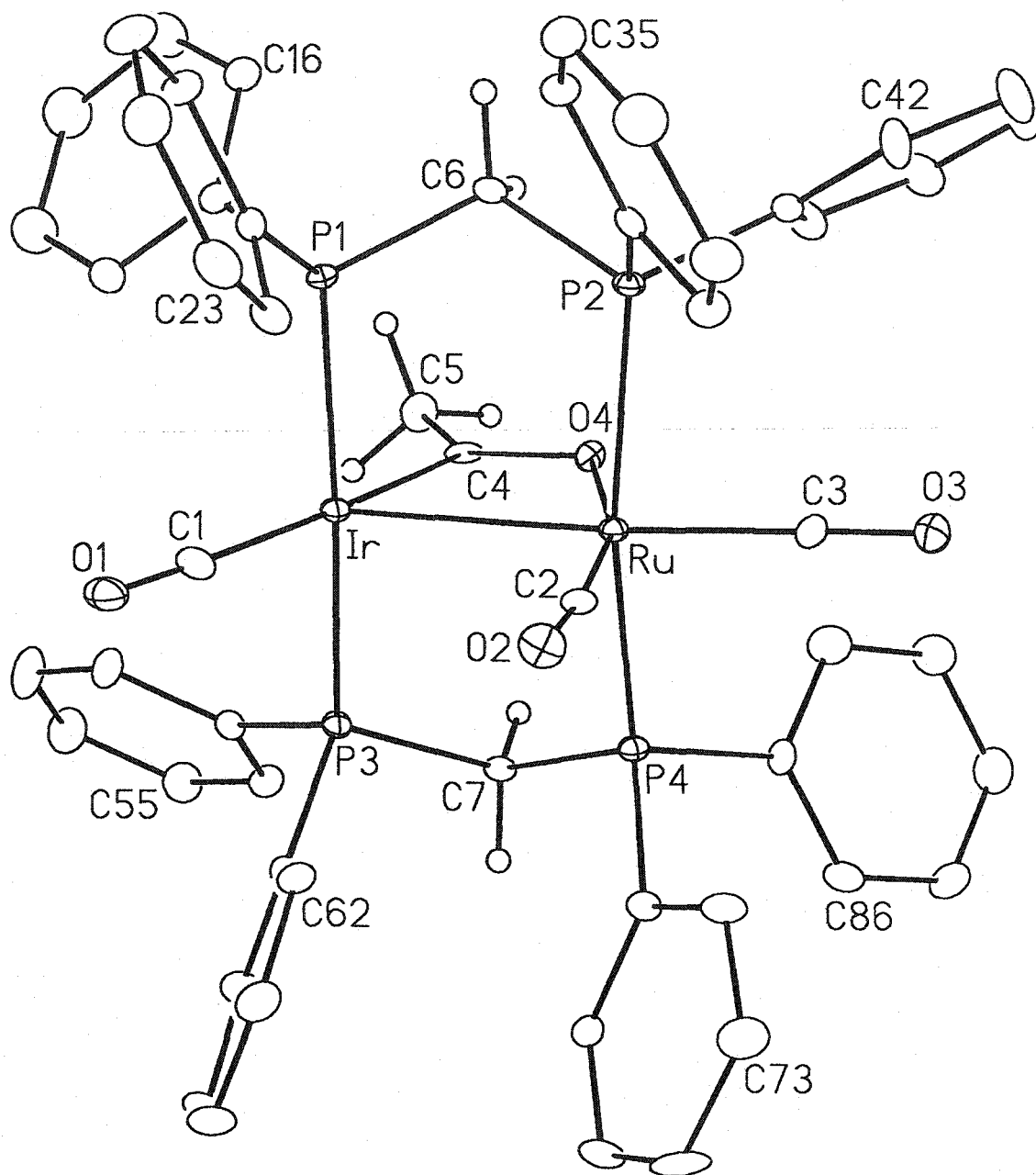
Figure A.2 Perspective view of [IrRu(CO)$_3$(μ-C(O)CH$_3$)(dppm)$_2$][BF$_4$]$_2$ (5) showing the atom-labeling scheme. Non-hydrogen atoms are represented by Gaussian ellipsoids at the 20 % probablility level. Hydrogen atoms are shown with arbitrarily small thermal parameters. The dppm phenyl hydrogens are not shown for clarity.

Table A.4 Selected Bond Distances and Angles of [IrRu(CO)$_3$(μ-C(O)CH$_3$)-(dppm)$_2$][BF$_4$]$_2$ (5)

Atom 1	Atom 2	Distance (Å)	Atom 1	Atom 2	Atom 3	Angle (°)
Ir	Ru	2.7949(7)	Ru	Ir	C(1)	115.8(2)
Ir	P(1)	2.3318(18)	Ru	Ir	C(4)	66.65(18)
Ir	P(3)	2.3356(18)	P(1)	Ir	P(3)	173.74(7)
Ir	C(1)	1.943(8)	C(1)	Ir	C(4)	177.4(3)
Ir	C(4)	2.028(8)	Ir	Ru	O(4)	70.43(13)
Ru	P(2)	2.4125(19)	Ir	Ru	C(2)	93.2(2)
Ru	P(4)	2.4175(19)	Ir	Ru	C(3)	172.9(2)
Ru	O(4)	2.132(5)	P(2)	Ru	P(4)	167.74(7)
Ru	C(2)	1.874(8)	O(4)	Ru	C(2)	163.6(3)
Ru	C(3)	1.884(7)	O(4)	Ru	C(3)	102.5(2)
O(1)	C(1)	1.128(9)	C(2)	Ru	C(3)	93.9(3)
O(2)	C(2)	1.135(9)	Ru	O(4)	C(4)	103.0(4)
O(3)	C(3)	1.148(8)	Ir	C(4)	O(4)	119.9(4)
O(4)	C(4)	1.285(8)	Ir	C(4)	C(5)	123.0(6)
C(4)	C(5)	1.486(9)	O(4)	C(4)	C(5)	117.1(7)
			P(1)	C(6)	P(2)	110.5(4)
			P(3)	C(7)	P(4)	110.3(3)

An X-ray structure determination of **6** has also been carried out. Although the data were of poor quality, the connectivity is clear as shown below. Of particular interest is the coordination mode of the acetyl group which is reversed relative to compounds **4** and **5**, having the acetyl carbon bound to Ru. In addition, coordination of a triflate group to the Group 8 metal (Ru) is unexpected based upon the observed coordination of triflate to the Group 9 metal (Rh) in the analogous dicarbonyl Rh/Os acetyl complex (**6** in Chapter 4). However, we have proposed coordination of the triflate group to Ru in compound **2**.

6
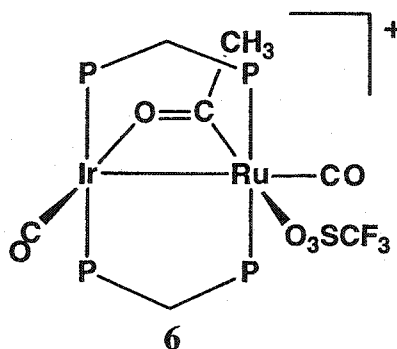
Discussion

Protonation of the methylene-bridged compound [IrRu(CO)$_4$(μ-CH$_2$)-(dppm)$_2$][CF$_3$SO$_3$] with either HBF$_4$ or CF$_3$SO$_3$H at -80°C results in the formation of an iridium-bound methyl complex (**1**). In contrast to the analogous Rh/Os system, the initially observed complex in the Ir/Ru system has the newly-formed methyl group on the Group 9 metal. In the Rh/Os system the first methyl species observed has an osmium-bound methyl group which is also agostically bound to Rh. We assume that this difference arises from the stronger metal-carbon bond involving the third row metal in each case.[10] As a solution of the tetracarbonyl complex (**1**) is warmed to room temperature, two new compounds, the tricarbonyl complex (**2**) and the pentacarbonyl complex (**3**) are observed in a 1:1 ratio. After

several hours a 1:1:1 ratio is established for compounds **1, 2,** and **3.** Why **1** converts to **2** and **3** is unclear. It may be that coordination of the triflate anion to the electrophilic dication is favoured and that the carbonyl that is displaced upon triflate coordination is scavenged by unreacted **1** to yield **3.** At 25°C compound **3** slowly converts to the acetyl species **4** while **2** decomposes into several unidentified products. In order to generate a pure sample of **3,** and subsequently **4,** CO can be added to compound **1** at low temperature, resulting in the sole production of **3.** Addition of CO to a mixture of **1, 2,** and **3** also results in only **3** being formed. Unlike the analogous Rh/Os methyl compound which generates the acetyl compound immediately at room temperature, **3** converts very slowly to the acetyl compound **9;** complete reaction occurs after three days at room temperature. This observation is consistent with the lower tendency of third row metals to undergo migratory insertion, which is presumably a reflection of the stronger Ir-CH_3 versus Rh-CH_3 bond.[10]

As discussed in Chapter 4, a rationale for studying acetyl complexes was the possibility of converting these groups into oxygen-containing substrates *via* reaction with H_2; mimicing another step in the **FT** production of oxygenates. There are two focuses here: first, whether the carbene-like bonding will influence the products of hydrogen transfer and second, whether the two different connectivities (acetyl carbon bound to the Group 8 or 9 metal) will be a factor. Certainly it seems logical that an acyl that is carbon-bound to Ir would likely lead to hydrogen transfer to the acyl or carbene, assuming H_2 addition at iridium. However, **6** has the acetyl oxygen bound to Ir suggesting that hydrogen transfer to oxygen, yielding a hydroxycarbene might occur, followed by hydrogenation of the metal-carbene linkage to give a hydroxy/ethyl group, which may then reductively eliminate ethanol. Unfortunately, these studies have not yet been carried out.

Conclusions

We have observed the formation of several species with bridged acetyl group in the Ir/Ru dppm-bridged system. As anticipated, the Ir/Ru complexes are formed via different intermediates than the Rh/Os system due to the different properties of the metals; in particular, the stronger M-C bonding of Ir compared to Rh, and the greater tendency of Ir to have an 18 electron configuration, whereas Rh prefers a 16 electron configuration.

Unfortunately the two most promising compounds for a hydrogenation study, **5** and **6**, have been obtained by serendipity and have not yet been synthesized rationally. Therefore, the subsequent chemistry of these complexes with H_2 is not yet known.

References and Notes

(1) (a) Vannice, M.A. *J. Catal.* **1975**, *37*, 449. (b) Verkerk, K.A.N.; Jaeger, B.; Finkeldai, C.-H.; Keim, W. *Appl. Catal. A:* **1999**, *186*, 407. (c) Watson, P.R.; Samorjai, G.A. *J. Catal.* **1981**, *72*, 347.

(2) Ichikawa, M.; Fukuoka, A.; Xiao, F. *J. Catal.* **1992**, *138*, 206.

(3) (a) Biloen, P.; Sachtler, W.M.H. *Adv. Catal.* **1981**, *30*, 165. (b) Van der Laan, G.P.; Beenachers, A.A.C.M. *Catal. Rev.-Sci. Eng.* **1999**, *41*, 255. (c) Schulz, H. *Appl. Catal. A.* **1999**, *186*, 3. (d) Maitlis, P.M.; Quyoum, R.; Long, H.C.; Turner, M.L. *Appl. Catal. A.* **1999**, *186*, 363.

(4) Overett, M.J.; Hill, R.O.; Moss, J.R. *Coord. Chem. Rev.* **2000**, *206-207*, 581.

(5) Collman, J.P.; Hegedus, L.S.; Norton, J.R.; Finke, R.G.; *"Principles and Applications of Organotransition Metal Chemistry"*, University Science Books, Mill Valley, CA, 1987, Chapter 6.

(6) Dell'Anna, M.M.; Trepanier, S. J.; McDonald, R.; Cowie, M. *Organometallics* **2001**, *20*, 88.

(7) (a) George, D.S.A.; McDonald, R.; Cowie, M. *Organometallics,* **1998**, *17*, 2553. (b) George, D.S.A.; Hilts, R. W.; McDonald, R.; Cowie, M. *Organometallics,* **1999**, *18*, 5330.

(8) Trepanier, S. J.; McDonald, R.; Cowie, M. *Organometallics* **2002**, accepted.

(9) (a)Shafiq, F.; Kramarz, K.W.; Eisenberg, R. *Inorg. Chim. Acta* **1993**, *213*, 111. (b) Gao, Y.; Jennings, M.C.; Puddephatt, R.J. *Organometallics* **2001**, *20*, 1882. (c)Johnson, K.A.; Gladfelter, W.L. *Organometallics* **1990**, *9*, 2101. (d)Jeffrey, J.C.; Orpen, A.G.; Stone, F.G.A.; Went, M.J. *J. Chem. Soc., Dalton Trans.* **1986**, 173.

(10) (a) Ziegler, T.; Tschinke, V. *Bonding Energetics in Organometallic Compounds*; Marks, T.J., Ed.; American Chemical Society: Washington, DC, 1990; Chapter 19. (b) Ziegler, T.; Tschinke, V.; Urenbach, B. *J. Am. Chem. Soc.* **1987**, *1-0*, 4825. (c) Armentrout, P.B. *Bonding Energetics in Organometallic Compounds*; Marks, T.J., Ed.; American Chemical Society: Washington, DC, 1990; Chaper 2.